# UNIVERSITÉ DE STRASBOURG

*ÉCOLE DOCTORALE SCIENCES DE LA VIE ET SANTÉ*
**UPR 3212 CNRS**

# THÈSE présentée par :

## Dhanasak DHANASOBHON

soutenue le : **24 Octobre 2017**

pour obtenir le grade de : **Docteur de l'Université de Strasbourg**

Discipline/ Spécialité : Neurosciences

---

# Spinal cholinergic system and chronic pain

## Douleur chronique et système cholinergique spinal

---

**THÈSE dirigée par :**
  **Mme. Matilde CORDERO-ERAUSQUIN**     Chargé de recherches CNRS, Université de Strasbourg

**RAPPORTEURS :**
  **Mme. Myriam ANTRI**          Maître de Conférences, Université Clermont Auvergne
  **M. Philippe ASCHER**         Professeur Émérite, Université Paris Diderot

---

**AUTRES MEMBRES DU JURY :**
  **M. Michel Barrot**          Directeur de recherches, Université de Strasbourg

# Acknowledgements

I dedicate this thesis to my family – my parents, brother, and late Aunt – Pa Yam. Thank you for making me who I am today.

# Table of Contents

# Abbreviation list

| | |
|---|---|
| 5-HT | Serotonin |
| ACh | Acetylcholine |
| AChE | Acetylcholinesterase |
| ACSF | Artificial Cerebral Spinal Fluid |
| ALT | Anterior lateral tract |
| AMPA | A-amino-3-hydroxy-5-methylisozazole-4-propionate |
| ATF3 | Activating Transcription Factor 3 |
| ATP | Adenosine triphosphate |
| BDNF | Brain derived growth factor |
| C-LTMR | C–low threshold mechanoreceptors |
| CCI | Chronic constriction injury |
| CCK | Cholecystokinin |
| CFA | Complete Freund's Adjuvant |
| CGRP | Calcitonin gene related peptide |
| ChAT | Choline Acetyltransferase |
| CHT | Choline transporter |
| CNO | Clozapine N-oxide |
| CNS | Central Nervous System |
| Cs | Cesium |
| CSF | Cerobrospinal fluid |
| CsOH | Cesium hydroxide |
| CTb | Cholera toxin B subunit |
| DA | Deep axons |
| DF | Descending facilitation |
| DH | Dorsal horn |
| DHbE | Dihydro-β-erythroidine |
| DI | Descending inhibition |
| DNIC | Interestingly, Diffuse Noxious Inhibitory Controls |
| DR | Dorsal root |
| DREADD | Designer Receptor Exclusively Activated by Designer Drugs |
| DRG | Dorsal Root Ganglia |
| ECl | Chloride reversal potential |
| eGFP | Enhanced green fluorescent protein |
| EM | Electron microscope |
| eRET | early RET |
| GABA | Gamma-Aminobutyric acid |
| GAD | Glutamate decarboxylase |
| GDNF | Glial derived neurotrophic factor |
| GRP | Gastrin-releasin peptide |

| | |
|---|---|
| GSA | General Somatic Afferent |
| GVA | General Visceral Afferent |
| HCN | Hyperpolarization activated cyclic nucleotide gated channels |
| HIV | Human immunodeficiency virus |
| HS | Horizontal slices |
| HT | High-threshold |
| HTMR | High threshold mechanoreceptors |
| IASP | International Association for the Study of Pain |
| IB4 | Isolectin B4 |
| IPSC | Inhibitory post-synaptic currents |
| ISI | Inter-spike intervals |
| KA | Kainate |
| KCC2 | Potassium-chloride cotransporter 2 |
| LA | Local axons |
| LC | Locus Coeruleus |
| LPb | Lateral Parabracial |
| LT | Low-threshold |
| LTMR | Low threshold mechanoreceptors |
| mAChRs | Muscarnic acetylchonile receptor |
| mEPSC | Miniature excitatory postsynaptic currents |
| MH | Mechano-heat |
| MLA | Methyllycaconitine |
| Mrgpr | Mass-related G protein coupled receptors |
| NA | Noradrenaline |
| nAChRs | Nicotinic acetylcholine receptor |
| NDNI | N-n-decylnicotinium iodide |
| NeP | Neuropathic pain |
| NF | Neurofilament |
| NGF | Nerve growth factor |
| NKB | Neurokinin |
| NKCC1 | Sodium-potassium-chloride cotransporters 1 |
| NMDA | N-methyl-D-aspartate |
| NN | Non Nociceptive |
| NS | Nociceptive Specific |
| NSA | Non-Spontaneously Active |
| NSAIDS | Non-steroidal anti-inflammatory drugs |
| NTF4 | Neurotrophin 4 |
| NTF5 | Neurotrophin 5 |
| PAD | Primary afferent depolarization |
| PAG | Periaqueductal gray |
| PB | Parabrachial |
| pChAT | peripheral Choline Acetyltransferase |
| PKCg | Protein kinase gamma |

| | |
|---|---|
| PNS | Peripheral nervous systems |
| PS | Parasagittal |
| PSN | Primary sensory neurons |
| PV | Parvalbumin-expressing |
| RA | Rapid adapting |
| RVM | Rostral Ventromedial Medulla |
| SA | Slowly adapting |
| SA | Spontaneously active neurons |
| SCI | Spinal cord injury |
| SIA | Stress induced analgesia |
| SNI | Spared nerve injury |
| SST | Somatostatin |
| TGs | Trigeminal ganglia |
| TH | Tyrosine hydroxylase |
| TRP | Transient receptor Potential |
| TRPV1 | Transient receptor potential subfamily V member 1 |
| TS | Transverse slices |
| TTX | Tetrodotoxin |
| vAChT | Vesicular acetylcholine transporter |
| VGCC | Voltage-gated calcium channels |
| vGlut3 | Vesicular glutamate transporter type 3 |
| VGSC | Voltage-gated sodium channels |
| Vh | Holding potential |
| WDR | Wide dynamic range |
| WT | Wild type |

# List of figures

# List of tables

# Chapter 1: Introduction

## 1. Pain and the Nervous system

### 1.1.    *Nomenclature and classifications from nociception to pain*

#### 1.1.1. *Pain*

Pain – a "necessary evil" for our survival. Pain is a subjective experience resulting from the transduction, transmission, and the modulation of incoming sensory inputs. The integration of these information is dependent on the individual's genetic background, past learning experience, psychological factors, and sociocultural influences. Amongst individuals, the same noxious stimulus can illicit varied behavioral and emotional responses. Pain is experienced only under conscious state.

Since 1979, the International Association for the Study of Pain (IASP) has defined pain as – "An unpleasant sensory and emotional experience associated with actual or potential tissue damage, or described in terms of such damage", based on the work of Merskey (1964) (Merskey and Bogduk, 1994). Broadly, pain can be decomposed into three components (Garland, 2012):

1. Sensory-discriminative: This component encompasses the encoding of the modality (mechanical, thermal), localization, intensity and duration of the noxious stimulus.
2. Motivational-affective: This component is linked to the aversive nature of pain and rhe desire to disengage from such instigators. This unpleasantness produces powerful emotions (e.g. anger and fear) which in turn act via psychophysiological pathways (autonomic, endocrine and immune systems) to influence pain perception.
3. Cognitive-evaluative: This component represents the cognitive appraisal, based on personal beliefs; i.e. an individual's subjective evaluation of incoming somatosensory inputs, whether it is to be considered harmful or not. Classically, the more the pain is perceived, the lower pain intensity is scored.

Interestingly, the section "described in terms of such damage" highlights the existence of pain in the absence of tissue damage or disease, despite thorough investigation, such as the one experienced by people suffering from fibromyalgia.

Recently a new definition for pain was proposed by Williams and Craig – "Pain is a distressing experience associated with actual or potential tissue damage with sensory, emotional, cognitive,

and social components". A notable addition draws attention to the sociality aspect i.e. how social contexts influence exposure, communication and reaction to pain (Williams and Craig, 2016). [Review of chronic pain in clinical context by (Gatchel et al., 2007)].

Following acute injury, perception of pain originating from the activation of somatic nociceptors in the periphery occurs in two phases: (1) Fast pain – the sharp, prickling sensation (2) Slow pain – an unpleasant, less localized pain that happens after a longer delay. On the other hand, visceral pain has neither fast nor slow components but is experienced as a rather poorly localized, deep and dull sensation (Julius and Basbaum, 2001) [Review on comparing somatic vs. visceral pain (Cervero, 2009)].

Noxious stimuli (i.e. chemical, mechanical or thermal) are transmitted from the periphery along primary afferent fibers called nociceptors, to second-order neurons located in dorsal horn (DH) of the spinal cord. The DH is an important player as incoming noxious signals undergo processing by a complex circuit of excitatory and inhibitory DH interneurons, and are modulated at this level by descending controls from higher brain centers. The output of the DH is transmitted to supra-spinal structures by projection neurons, and, depending on the subcortical or cortical structure reached, this will lead to the sensory-discriminative or emotional, cognitive, and social components of the pain experience (Almeida et al., 2004; Garland, 2012). – Fig. 1.1

The peripherally and centrally neurons involved in the encoding of noxious stimuli have long been studied (Millan, 1999; Basbaum et al., 2009; Todd, 2010), yet several pieces of the puzzle are still missing, or more precisely their exact function is unknown. During my doctoral work, I focused on one of these pieces, located in the spinal cord: the spinal cholinergic system, that has been shown to be implicated in the modulation of sensory information processing. Yet the cellular and circuit basis for this modulation are still unknown, and my thesis aimed at unraveling them.In the following paragraphs, I will introduce the terms and players of noxious information processing, with a special focus on the DH of the spinal cord. Importantly, because of this focus on the spinal cord, we will be talking of nociception rather than of pain (see below).

### 1.1.2. Nociception

While processing in higher brain structures is required for pain perception, nociception (the processing of noxious stimuli) can occur independently (Scholz and Woolf, 2002). Sherrington (1906) described a 'noxious' stimuli as events that cause harm or potential harm to tissues. Such stimuli have the intensity and quality sufficient to activate sensory nerves with specialized endings (nociceptors) ultimately leading to pain sensation. Subsequently, he coined the term nociception as
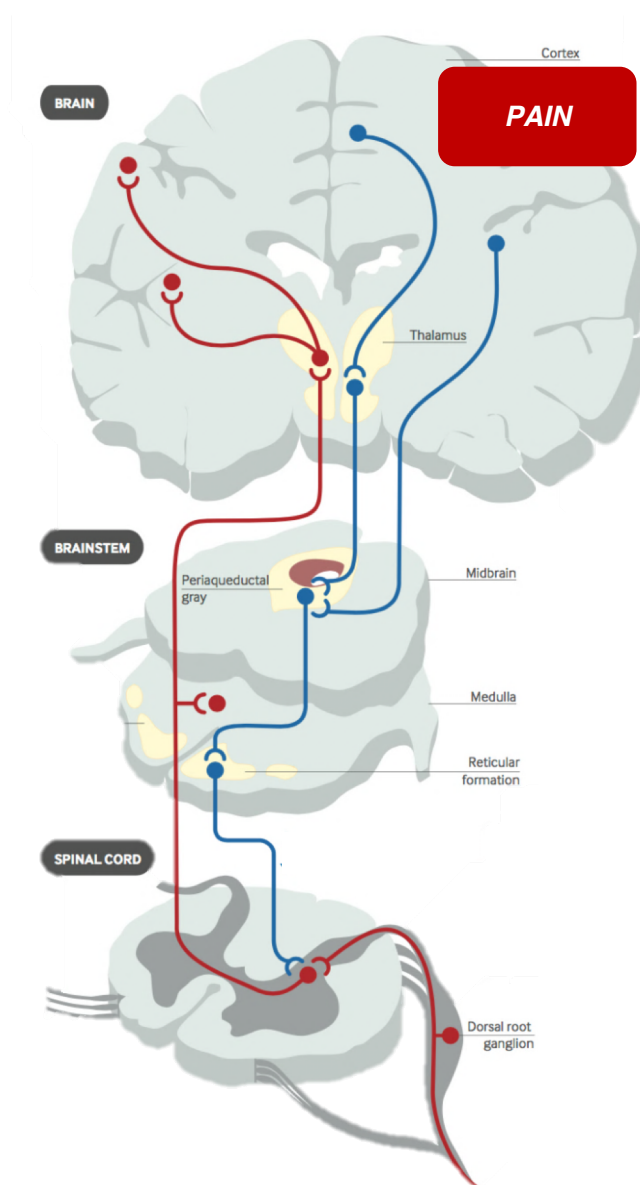
**Figure 1.1:** The physiological pain pathway. The ascending tract (red) brings noxious information arising from the periphery via second order neurons, located in the dorsal horn of the spinal cord, to the supra-spinal areas. Axon collaterals project to the medulla and thalamus. From the thalamus, information is relayed to cortical areas where pain is processed. Descending pathways (blue) from cortical areas in turn activate circuits in the periaqueductal gray and reticular formation responsible in descending controls that in turn modulate the incoming signals. [Modified from Cohen and Mao, 2014]

the signaling and processing of noxious stimulus, arising from external and internal environments, by the peripheral and central nervous system. At the spinal and supra-spinal levels, this information is integrated to provide the sensory-discriminative component of pain. Besides inducing the aversive nature of pain, noxious stimulation can result in withdrawal reflexes and autonomic changes (i.e. increase in heart rate). Notably, these behavioral and physiological changes can occur under condition preventing the experience of pain, i.e. in anesthetized and spinal cord transected animals.

### 1.1.3. Types of Pain

Acute pain: A transient noxious stimulus produces a limited pain sensation via the activation of nociceptors in the skin and other tissues in the body. When tissue injury does not occur, the sensation ends when the body engages into an appropriate motor response to remove the stimulus. This everyday life phenomenon protects individuals from physical damage arising from the environment or overstraining of the body. When the stimulus produces a local injury, this leads to change in responses at the level of the nociceptors, spinal cord and supraspinal structures. This allows the body to commence reparative mechanisms and prevent any further injuries. Although medical care is not required, it can be provided to reduce pain and speed up the healing process by reducing the injury period. The pain can last ranging from a few days to weeks (Loeser and Melzack, 1999).

Chronic pain: While acute (physiological) pain has an important protective function, persistent pain can become a characteristic of pathological conditions such as cancer and chemotherapy (Everdingen et al., 2007); diabetes (Tesfaye and Selvarajah, 2012); and neuropathy for instance. Chronic pain can develop long after the injury has healed and can arise even in the absence of any obvious instigators (Kuner, 2010).

Epidemiological research has shown that chronic pain (broadly described as extended and long-term pain lasting at least 3 months) and chronic recurrent pain (returning episodes of pain alternating with pain-free period lasting over months or years) affects 10 to 20% of adults within the general population (Gatchel et al., 2007). One out of five adult Europeans suffers from mild to severe forms of chronic pain while healthcare and socioeconomic costs associated with chronic pain accounts for 3 to 10% gross domestic product of Europe (Breivik et al., 2006; Breivik et al., 2013). The quality of life experienced by patients is reduced, for instance an estimated of 4,700 million chronic pain days per year were lost in France alone. Its persistence and recurrence leads to depression, reduction in physical and cognitive function, sleep problems and mood alterations (Phillips, 2009). This illustrates how the prevalence and costs of chronic pain are a serious physical

and mental clinical issue to the individual and society. [Review on epidemiology and socioeconomic burdens of pain (Henschke et al., 2015)].

## 1.2. Primary Sensory Neurons of the Somatosensory system

### 1.2.1. General overview

The somatosensory system has three main functions: exteroreceptive and interoreceptive, for our perception and reaction to stimuli originating outside and inside the body, respectively; and proprioceptive function, for the perception and control of body position and balance.

The diverse sensations, arising from innocuous to noxious stimuli, are first detected and encoded by primary sensory neurons (PSN) or first order neurons. The cell bodies of PSN are found in ganglia located at the base of the skull (Trigerminal ganglia or TGs) and along the spinal cord (Dorsal Root Ganglia or DRGs). These neurons are 'pseudo-unipolar' shaped – they have no dendrites but rather a single axon that bifurcates to form one branch extending to the periphery while another project to the Central Nervous System (CNS). The peripheral nerve endings of TGs are distributed throughout the face and neck and they project directly to the brainstem; while the peripheral endings originating from DRGs are spread around the rest of the body and transmit the sensory information to the spinal cord. Depending on the origins of the stimulus, the information travels through the General Somatic Afferent (GSA) or General Visceral Afferent (GVA) fibers. GSA fibers have nerve endings spread throughout the skin, joints, muscles and tendons while GVA fibers originate from internal organs. The characteristics of the primary afferent fibers are discussed below with a specific focus on those encoding stimuli originating from external environments.

### 1.2.2. Anatomical and physiological properties

The primary afferent fibers can be distinguished into 3 types: A$\alpha$/A$\beta$, A$\delta$ and C. This classification is based on the conduction velocity, size of the cell body and axon diameter, and myelination thickness [Fig. 1.2]. The A$\alpha$/A$\beta$- fibers are fast conducting (ranging between 30 to 100 m/s), originating from neurons with a large soma size (>50 µm)/axon diameter (>10 µm), and are highly myelinated. The A$\delta$- fibers are slower conducting than A$\alpha$/A$\beta$ (ranging between 4 to 30 m/s), have intermediate size of cell bodies/axon diameter (2 – 6 µm) and are thinly myelinated. The C-fibers are slow conducting (<2.5 m/s), have small cell bodies/ axon diameter (0.4 - 1.2 µm), and are unmyelinated (Willis and Coggeshall, 1978). In general, the percentage of incoming cutaneous
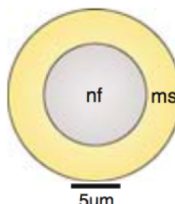
**Figure 1.2:** The mammalian cutaneous primary afferent fibers. The table summarizes information for each fiber providing (left to right): Approximate diameter (measured in cats, ms: myelin sheath); specific fiber type; the modality it encodes; percentage of concerned fiber with respect to total number of cutaneous fibers; von Frey thresholds for respective fiber (mN: milli-Newtons) and thermosensitivity shows when fiber is capable of transducing noxious heat (red)/cold (blue). [Modified from St. John Smith and Lewin, 2009]

fibers are distributed as: 70% of C-fibers, 10% of Aδ-fibers and the remaining 20% of Aβ-fibers (Millan, 1999).

### 1.2.3. Molecular markers for identification

Neurochemical markers and differential gene expressions during development have been used to further delineate primary afferents classification. The myelinated A-fibers contain exclusively a form of phosphorylated neurofilaments with molecular weight of 200 kDa (NF200) (Lawson and Waddell, 1991). Primary afferents can also be differentiated according to the modality they encode as will be developed below [Section 1.2.4]. It is interesting to note that there is a certain overlap between molecular and modality classifications. Aβ-, Aδ (fiber)- low threshold mechanoreceptors (LTMR) express eRET (early) [receptor for glial cell line-derived neurotrophic factor (GDNF)], TrkB (NTRK2) [receptor the brain derived growth factor (BDNF) and neurotrophin (NTF5)] and TrkC (NTRK3) [receptor for neurotrophin 4 (NTF4)]. A subtype of Aβ LTMR are uniquely marked with NPY2R (Li et al., 2011). In contrast, the high threshold Aδ neurons demonstrate early TrkA (NTRK1) [receptor for the nerve growth factor (NGF)] expression; with TrkA being found in all newly formed embryonic nociceptors (Woolf and Ma, 2007; Olson et al., 2016). Moreover, when intact somatic peripheral nerves are injected with Cholera toxin B subunit (CTb), which binds to the GM1 ganglioside, it is taken up and transported mainly by myelinated primary afferents (Hughes et al., 2003).

The unmyelinated C-fibers can be divided into two broad categories: The peptidergic class of C-fibers expresses neuropeptides such as substance P or calcitonin gene related peptide (CGRP) along with TrkA (NTRK1) receptor. The non-peptidergic class of C-fibers contains exclusively TRPC3, ATP gated P2X3 receptor, mass-related G protein coupled receptors (Mrgpr) D and binds to the histological marker isolectin (IB4). Interestingly, MrgprA3 is found to colocalize with both CGRP and IB4; demonstrating the fluidity of the classifications. C-LTMR have been identified with vesicular glutamate transporter type 3 (vGlut3) and tyrosine hydroxylase (TH) whereas MrgprB4 has been used to define tactile C-fibers (Woolf and Ma, 2007; Lallemend and Ernfors, 2012; Le Pichon and Chesler, 2014).

All primary fibers are glutamatergic, but may release other transmitters and/or co-factors such as ATP or substance P.

## *1.2.4. Sensory modalities*

All three types of afferent Aα/β-, Aδ- and C-fibers can transmit non-noxious information. Although Aδ- and C-fibers are usually considered as the nociceptive fibers, a proportion Aβ also transmit noxious stimulus (Djouhri and Lawson, 2004).

**Innocuous information:**

Aα fibers are responsible for the transmission of proprioceptive signals. The muscle spindles are innervated by Ia and some II afferents while those projecting from Golgi tendon organs encompass group Ib and II afferents (Dietz, 2002).

The Aβ-LTMR can be subdivided based on their response to sustained mechanical stimulus. 'Rapidly adapting' (RA) mechanoreceptors fire during the onset, sometimes at the offset and only occasionally or not at all during the applied stimulus. Conversely, the 'Slowly adapting' (SA) mechanoreceptors demonstrate a sustained firing both at the onset and during stimulus. The RA Aβ-LTMRs consist of three types: (1) Meissner's corpuscles (Type I) have small receptive field while responding to low frequency (30 - 40 Hz) vibrations; they are possibly responsible for velocity detectors of skin deformations. (2) Pacinian corpuscles (Type II) have large and less well defined receptive fields. They respond to high frequency vibrations (250 – 300 Hz). (3) Lanceolate endings surround Guard and Awl hair follicles of hairy skin; they potentially function as detectors of hair movement velocity (Willis and Coggeshall, 1978; Olson et al., 2016).

The SA Aβ-LTMR are as follow: (1) associated with Merkel cell, they form complexes (Type I) with small receptive fields on both glabrous and hairy skin. Each complex is known as 'touch spot' and 'touch dome' in glabrous and hairy skin respectively. Touch domes appear to innervate only guard hair follicles (Li et al., 2011). They are tuned for high resolution discrimination of shape and texture (Maricich et al., 2012). (2) Ruffini endings (Type II) have large receptive fields and respond to stretching of the skin (Willis and Coggeshall, 1978).

The Aδ-LTMR, also known as D hair cells, and C-LTMR form palisades of lanceolate endings around zigzag and awl/auchenne hair follicles in hairy skin. They are highly responsive to mechanical touch and respond to rapid cooling (Seal et al., 2009; Li et al., 2011).

Tactile TH+ C-fibers have free nerve endings in hairy skin (Liu et al., 2007). It has been shown these neurons mediate pleasant stroking and light touch (Vrontou et al., 2013).

**Noxious information:**

A-fibers have been classified by their response to mechanical and thermal stimuli, into:

(i)     High threshold mechanoreceptors (A-HTMR) responding to only mechanical stimuli. They have free nerve endings in both glabrous and hairy skin. In rat, 50% of A-HTMR are reported to have Aβ-fiber conduction velocities. The Aδ-HTMR are thought to contribute to first/fast mechanical pain along with contributions by Aβ-HTMR (Djouhri, 2016)

(ii)    Mechano-heat (A-MH) units responding to noxious mechanical and short applications of noxious heat. The A-HM units are sub-classified in type I and II. Type I responds to high heat (>53 ℃) but lower mechanical thresholds (3.7 to 5 bar) whereas type II reacts to lower heat threshold (median 46 ℃) but relatively higher mechanical thresholds. Type I are found on both glabrous and hairy skin whereas type II are only on hairy skin. Interestingly, a third of type I are Aβ-fibers while type II are purely Aδ-fibers. Type I are thought to provide the sharpness sensation to punctate stimuli. Type II appear to mediate mechanically evoked cutaneous pain and the first response of thermal pain (Djouhri and Lawson, 2004; Dubin and Patapoutian, 2010).

The unmyelinated C-fibers terminate as free nerve endings throughout the skin. Glabrous skin is innervated by both CGRP and IB4 expressing fibers whereas hairy skin contains only CGRP+ fibers (Lallemend and Ernfors, 2012). Most C-fibers are polymodal (i.e. respond to chemical, mechanical and thermal noxious stimuli) while the remaining are responsive to purely noxious temperatures or mechanical, some by mechanical with heat and mechanical in combination with cold. A certain fraction (10 – 25%) of C fibers are considered as silent (i.e. do not respond to mechanical and thermal stimuli under physiological conditions) however, they become sensitive to noxious mechanical and thermal stimuli after being sensitized by inflammatory mediators (Dubin and Patapoutian, 2010). Generally, C-fibers are responsible for the second phase of pain (Millan, 1999). Peptidergic C-fibers expressing CGRP are sensitive to noxious heat but neither cold nor mechanical stimuli. Surprisingly, the genetic ablation of these fibers induced an increase in cold sensitivity thus suggesting that CGRP+ fibers may play a role in tonic inhibition on fibers transmitting cold (McCoy et al., 2013). Many non-peptidergic C fibers, binding to IB4, also express MrgprD (>75%). The removal of MrgprD sensory neurons produced a phenotype where noxious mechanical sensitivity is reduced. (Le Pichon and Chesler, 2014)

### 1.2.5. Spinal cord terminations

**Gross anatomy of the spinal cord**

The spinal cord is part of the central nervous system (CNS), extending caudally from the medulla, and protected by the vertebral columns. The grey matter contains neuronal cell bodies while the surrounding white matter contains myelinated fibers [Fig. 1.3]. Initially, the organization of the grey matter, described by Rexed in cats, was divided into ten laminae based on their cytoarchitectonic (Nissl) stainings. This classification was later modified and applied to other mammals including human. The first six laminae arranged one on top of another, from dorsal to ventral plane, form the DH of the spinal cord. The layers VII-IX form the ventral horn while lamina X surrounds the ependymal canal. For functional studies, the laminae are grouped as pairs: LI-II (superficial DH), LIII-IV (nucleus proprius) and laminae V-VI (Deep DH) however, some studies consider LIII-IV as deep DH (Cordero-Erausquin et al., 2016).

**Innocuous information:**

The Aβ RA LTMR main axonal branch enters the spinal cord and bifurcates to send branches in both the rostral and caudal axis in the spinal cord dorsal columns. Most of their ascending projections reach the dorsal column nuclei (Abraira and Ginty, 2013; Niu et al., 2013). The collaterals from axons of each subtype projects differentially onto grey matter of the DH. Meissner's corpuscle afferents arborize medially in Lamina III to V (Shortland and Woolf, 1993). The Pacinian corpuscle neurons innervates two areas in the DH: LIII and small part of LV (Semba et al., 1984). The collaterals from lanceolate endings for "flame shaped" arbors in deeper laminae (Brown, 1982; Woodbury et al., 2001).

As observed with Aβ RA LTMR, the Aβ SA LTMR have similar ascending projections to supraspinal structures and collateral spread into the spinal cord. The collaterals made by Merkel cell – neurite complexes first projects into LIV-V before making a medial C shaped turn to innervate LIII-V. The Ruffini ending neurons initially projects to LIII before branching off to innervate LIII-V (Olson et al., 2016).

The axon of Aδ LTMR runs in the spinal cord in the rostral direction for a few segments, before innervating LIII (dorsal to Aβ LTMR termination region). The axon from either C LTMR and TH+ C tactile fibers also project rostrally for one or two segments. These projections form collaterals that terminate in LII with flame-shaped arborizations (Li et al., 2011; Vrontou et al., 2013).

A
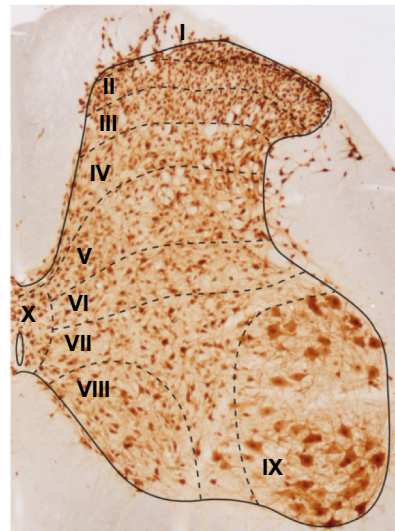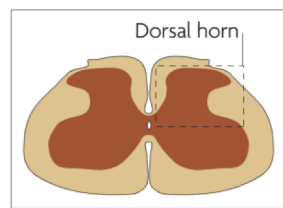


B
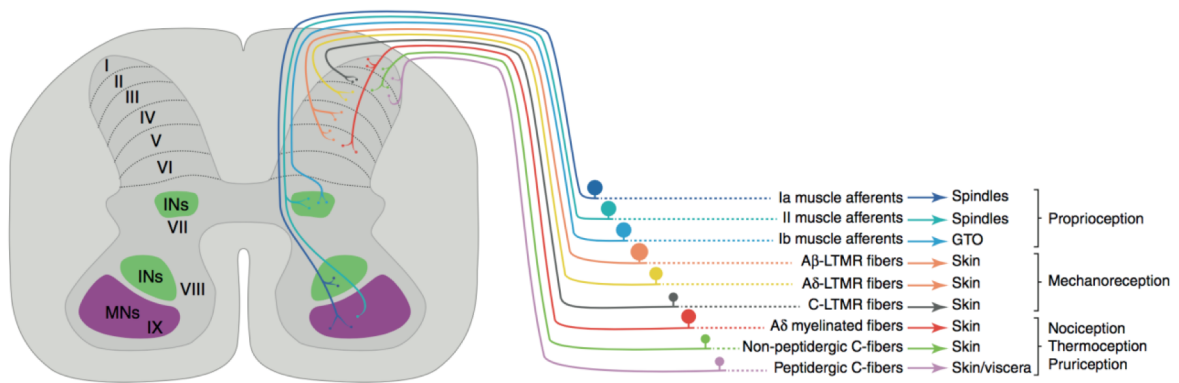


**Figure 1.3:** Rexed divisions of the ten laminae of the spinal cord. **A:** A transverse section of rat mid-lumbar spinal cord that is immunostained using an antibody (NeuN) that specifically labels neurons. Laminar boundaries are shown by the dashed lines. The Dorsal Horn consists of LI-VI [Modified from Todd 2010]. **B:** Termination patterns of primary afferent fibers in the spinal cord. The group Ia and some group II afferents that innervate muscle spindles (spindles) project directly to motor neurons. Group Ib afferents (which innervate golgi tendon organs, GTO, peripherally) as well as group II afferents, connect interneurons at the intermediate zone of the spinal cord, whereas group Ia afferents terminate more ventrally. The C-, A-delta- and A-Beta -low-threshold mechanoreceptors (LTMRs) project to the dorsal horn where they terminate in LIIi; LIIi – LIII; and LIII-V respectively. The A-delta myelinated fibers innervate laminae I and V whereas the peptidergic and non-peptidergic C neurons terminates in laminae I and II. [Modified from Lallemend and Ernfors, 2012]

**Noxious information:**

In general, Aδ-fibers project mostly into lamina I, IIo, and V while Aβ-fibers terminate in superficial laminae of cats and monkeys (Light and Perl, 1979; Djouhri and Lawson, 2004).

Roughly, C-fibers have major terminations in LI, II and some to X (Millan, 1999; Basbaum et al., 2009). Peptidergic fibers (CGRP+) terminate in LI, IIo while non-peptidergic (IB4 and MrgprD+ fibers) terminate in LIIi (Zylka et al., 2005).

As observed, the termination regions of primary afferents appear to be located throughout the DH. However, it is generally accepted that LI-II receives nociceptive inputs whereas LIII and deeper will incorporate both noxious and innocuous information (Cordero-Erausquin et al., 2016).

Understanding the trajectory of primary afferent axons and termination zones in the DH of the spinal cord is vital for analyzing the primary afferent inputs into local interneurons as we did in this doctoral work. Indeed, we were using spinal cord slices in different orientations (i.e. Horizontal, Parasagittal or Transverse) and were electrically stimulating the roots of primary afferents, left intact. Yet, depending on the orientation of the slice, some types of fibers would be truncated, thus preventing the recording of a synaptic response.

### 1.2.6. Detection and transduction of nociceptive information

Nociceptors have specialized sensors on their peripheral terminals to allow the transduction of the various modalities. Several channels/receptors contribute to noxious heat-, cold-, mechanical- and chemical-induced generated potentials [Fig. 1.4]. An important family of such receptors is the family of ionotropic TRP (Transient Receptor Potential), some members of which will be discussed below [For review on other transducer (Basbaum et al., 2009)]. The TRPV1 (TRP cation channel sub-family V member 1), a non-selective cation channel, is the principle detector of noxious heat (>42 °C). Interestingly, TRPV1 knock-out mice have reduced sensitivity to heat while ablation of TRPV1 neurons removes all aversion to noxious heat (40 – 50 °C) (Caterina et al., 2000; Pogorzala et al., 2013). The TRPV1 reporter mice show TRPV1 expression for all unmyelinated, peptidergic DRGs but the reporter protein is mostly absent from IB4+ non-peptidergic C-fibers. This is in contrast with previous observations in rats of TRPV1 immunoreactivity in IB4+ fibers (Guo et al., 1999). Notably, a proportion of TRPV1+ (>20%) are present on Aδ-fibers (Cavanaugh et al., 2011).

TRPM8 (Transient receptor potential subfamily M member 8) is expressed on subsets of small diameter Aδ- and C-fibers, overlapping with some TRPV1 (Dhaka et al., 2008). This non-selective
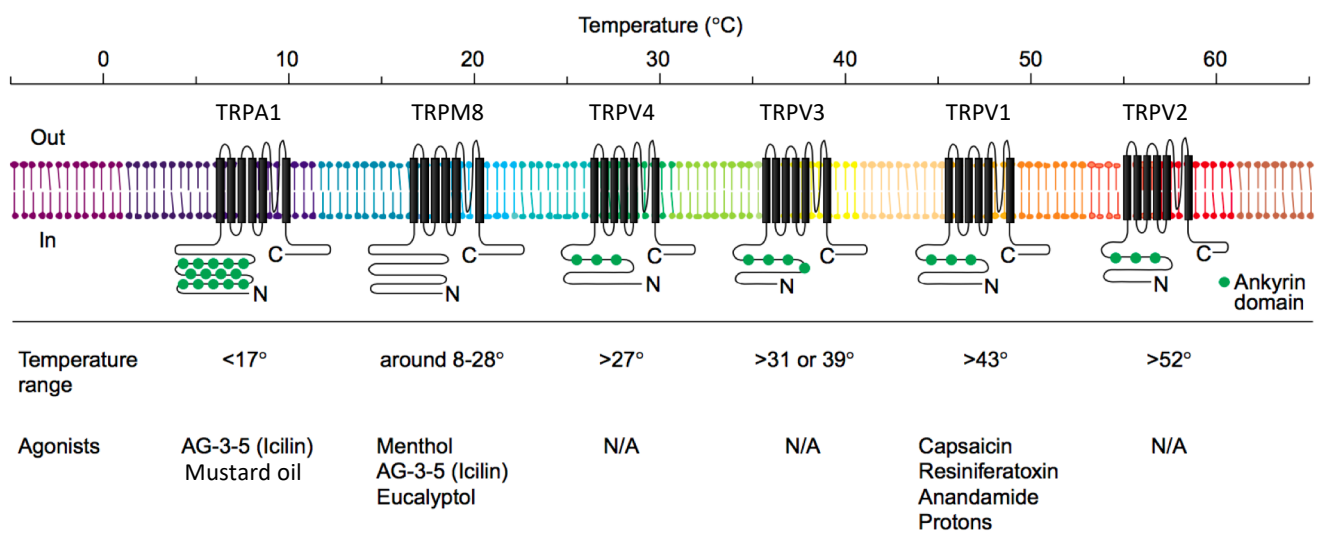
**Figure 1.4:** Different types of TRP thermoreceptors found on sensory neurons. Each channel is presented at their reported thermal threshold along with range of temperatures and agonists to which they respond to. [Modified from Jordt et al., 2003]

cation channel is responsible for the detection of innocuous cooling and noxious cold. TRPM8 knock-out showed deficits in cold sensitivity while complete TRMP8+ cell ablation caused a loss of noxious temperature detection while retaining responses to heat (Pogorzala et al., 2013).

The TRPA1 (Transient receptor potential subfamily A member 1) is found on TRPV1 expressing fibers (30% of all TRPV1+ fibers express TRPA1) (Story et al., 2003). These cationic channels are established sensors for noxious irritating electrophilic compounds while their role as a detector for extreme cold remains controversial (Dubin and Patapoutian, 2010). Interestingly, mice without TRPV1, TRPM8 and TRPA1 demonstrate deficits in the detection of a range of temperatures (5 to 55 °C), chemical irritants and pruritogens (Mishra et al., 2011).

These receptors can be activated pharmacologically with their respective agonists thus providing an essential tool to elucidate their roles on spinal cord slices.

## 1.3. Dorsal Horn of the Spinal cord

### 1.3.1. Cytoarchitecture and functional properties of DH neurons

The Rexed lamination is defined based on the density of cell bodies, their morphology, dendritic arborization and axonal connections (Willis and Coggeshall, 1978). The functional classification of DH neurons is determined through electrophysiological properties and primary afferent inputs based classifications.

**Lamina I:**

The most dorsal lamina covering the tip of the DH, also known as marginal zone of Walderyer, contains low neuronal density. Three types of neurons have been identified: fusiform, multipolar ('flattened' types were annexed) and pyramidal (Lima and Coimbra, 1986; Zhang and Craig, 1997). Most of these neurons have their cell bodies and dendritic arborizations orientated in the rostrocaudal axis, while some have their processes extending along the mediolateral axis (Lima and Coimbra, 1986; Yu et al., 2005). Many neurons have processes restricted locally in LI while a small proportion of neurons have dendritic spread into LII and deeper layers (Almarestani et al., 2007; Cordero-Erausquin et al., 2009). Projection neurons from LI innervate multiple supraspinal structures including thalamus, parabrachial nucleus and periaqueductal gray (PAG) (Todd, 2010). Local LI interneurons demonstrate axon branches protruding into the deep dorsal horn (LIII-IV) but also across several spinal segments (Szucs et al., 2013). Notably, projection neurons appear to

have larger soma (>200μm) compared to local interneuron populations (<200 μm) (Al Ghamdi et al., 2009).

Neurons are often classified according to their electrical properties and particularly their pattern of action potential firing upon depolarization. In Lamina I there is some correlation between electrical properties and morphology. Fusiform neurons have tonic firing; pyramidal types are phasic and multipolar types display single spikes along with delayed onset discharge profile (Prescott and De Koninck, 2002). When recorded in vivo, neurons can also be defined by their function; i.e. the type of sensory information they respond to. There is a certain correlation between the morphologies and function of LI neurons recorded in cats (Han et al., 1998). These functional groups are: (i) Nociceptive-specific neurons responding to noxious heat and mechanical (pinch) stimulus, are morphologically either fusiform or multipolar. (ii) Neurons responding to only innocuous cooling are all pyramidal cells. (iii) The polymodal nociceptive neurons responding to noxious heat and mechanical (pinch) along with non-noxious cold (HPC), are denoted as multipolar shaped (Ribeiro-da-Silva and De Koninck, 2008).

**Lamina II:**

Initially, Rolando described the substantia gelatinosa (or LII) as distinctly more gelatinous and less fibrous in texture compared to other grey matter regions. This is due to the presence of small and closely packed cells. This lamina is further divided into two sections: II outer (LIIo) and II inner (LIIi) for the more dorsal and ventral parts respectively. LII neurons have been divided into four morphological subtypes: central, islet, radial and vertical cells. Most have dendritic arbors around LII however, preferential orientations have been observed. Islet and central cells have their dendrites elongated in the rostrocaudal axis; with 1000 μm extension reported for islet cells. The radial and vertical have dendrites located from LI to deeper laminae (Grudt and Perl, 2002) (Yasaka et al., 2007). Most islet cells are observed to be inhibitory (GABA and glycine) while radial and vertical cells are predominately excitatory (Glutamate). In contrast, central cells contain both excitatory and inhibitory subpopulations (Maxwell et al., 2007; Yasaka et al., 2010). Interestingly, unclassified cell types were found in the studies mentioned above. The axons of LII appear to innervate laminae exterior to LII ranging from LI with some to deeper laminae (Eckert et al., 2003; Braz et al., 2005).

These cell types exhibit various firing patterns (Tonic, Phasic, Single, Delayed) however islet and inhibitory central cells display preferentially tonic firing patterns (Lu and Perl, 2005). Besides the patterns mentioned earlier, LII neurons' morphologies electrical properties, neurochemical

markers are heterogeneous therefore cannot be correlated with their possible functional roles (Yasaka et al., 2010). Furthermore, LII is innervated by both myelinated and unmyelinated primary afferent fibers (Yasaka et al., 2007).

**Lamina III-IV:**

The nucleus proprius is identified based on the increased myelinated, lower neuronal density and presence of larger cells compared to LII. The morphology of LIII-IV neurons are heterogeneous but two main dendritic arborizations patterns have been described: (i) dorsally orientated dendrites spreading throughout LI-III (Littlewood et al., 1995; Naim et al., 1997; Polgar et al., 1999) (ii) rostrocaudally elongated dendrites (Maxwell et al., 1983). A proportion of neurons showing dorsally orientated dendrites are NKr1+ projections neurons, with collaterals in the thalamus and lateral Parabrachial (LPb) (Al-Khater and Todd, 2009). In hamsters, interneurons reported with rostrocaudal morphology were further divided into two types: (i) local axons (LA) and deep axons (DA). DA neurons have a larger dendritic spread in dorso-ventral and medio-lateral orientations compared to LA. The axon territories for LA cells extends rostral caudally within a spinal segment in LIII/IV whereas DA cells axon projects ventrally before bifurcating over several spinal segments in rostral and caudal directions. These axon form branches innervating LIV- VI (Schneider, 1992, 2003). Both classes contain excitatory (vGLUT2) and inhibitory (GAD) markers (Schneider and Lopez, 2002; Schneider and Walker, 2007).

LIII/IV neurons exhibit a heterogeneous firing patterns whereby cell possessing tonic, phasic and delayed-firing patterns accounts for 47%, 38% and 15% of the total population respectively. A correlation between firing pattern and morphology was seen for local axon types who exhibit phasic firing patterns while projection neurons appeared to display tonic firing (Schneider, 2003).

**Lamina V-VI:**

The layers V and VI are called the "neck" and the "base" of the dorsal horn respectively LV forms a sharp medial boundary with the dorsal funiculus, and its lateral boundary has an indistinct reticulated appearance due to the presence of several myelinated fibers (Willis and Coggeshall, 1978). Furthermore, LVI only exits in cervical and lumbosacral enlargements of the spinal cord. In these laminae are found "multi-receptive", or now known as Wide Dynamic Range (WDR) neurons (i.e. receiving both noxious and innocuous information). Some display large dorsoventral spread ranging from LIII-LVII while presenting an extensive mediolateral and rostralcaudal coverage. In addition, their axons appear to ascend in the contralateral ventral white matter without making any collaterals in the Dorsal Horn (Ritz and Greenspan, 1985). Moreover, some LV neurons have

dendrites reaching LII and project to the thalamus (Braz et al., 2005). LVI neurons have dendrites that radiate in dorsoventral and mediolateral planes but with limited extension in longitudinal axis. Thus, they appear as flattened disks with long and relatively unbranched dendrites (Willis and Coggeshall, 1978).

Most deep DH neurons produced a tonic discharge pattern (90%) while the remaining demonstrated plateau potential characterized by an accelerating firing response and a sustained after-discharge (Derjean et al., 2003).

### 1.3.2. Neurochemistry of the spinal cord

**Excitatory transmission:**

L-glutamate is the main excitatory neurotransmitter in the CNS. Glutamate is utilized by both primary afferent fibers and excitatory interneurons in their communication. The detection of glutamatergic cell bodies through conventional immuno-histochemical approaches have not been straightforward due to the presence of glutamate in large quantities in all cells. Therefore, vesicular transporters for glutamate (vGLUT1, vGLUT2 and vGLUT3) have been used for marking axons of glutamatergic neurons. Alternatively, it is considered that non-GABA and/or non-Glycine producing cells are by default glutamatergic in nature (Todd, 2010). The developmental markers of glutamate cell lineage, *Tlx1 and Tlx3*, have been utilized for excitatory neuron detection (Cheng et al., 2004).

The DH has high densities of vGLUT1 immuno-stained varicosities in LIII and LIV whereas vGLUT2 was reported in LI-II (Todd et al., 2003; Alvarez et al., 2004). In addition to DH neurons, these terminals can arise from primary afferents. Indeed, most myelinated afferent fibers injected with cholera toxin B subunit were vGLUT1-immunoreactive. On the other hand, peptidergic primary afferents expressing substance P, and non-peptidergic IB4+ C fibers showed either low levels of vGLUT2-immunoreactivity or were not immune-reactive to vGLUT1 and 2 (Todd et al., 2003). Furthermore, vGLUT3 was detected in unmyelinated, non-petidergic C fibers that terminate in superficial layer (Seal et al., 2009), and can also have a supraspinal origin (Alvarez et al., 2004).

vGLUT1 and vGLUT2 mRNA were detected throughout the DH however, high intensities of vGLUT1 was reported in the superficial DH. The vGLUT3 mRNA levels were weak in deep DH layers (Landry et al., 2004). However, transiently-expressing vGLUT3 interneurons in LIII have been implicated in the development of mechanical allodynia (Peirs et al., 2015). Previously, presumed glutamatergic neurons (i.e. non-GABA/Glycine) were reported to account for 74.2% and 62.4% of cells in LI-II and LIII respectively. Several neurochemical markers have enabled to

distinguish sub- populations of excitatory neurons; for instance, neuropeptides – somatostatin (SST), neurotensin, neurokinin B (NKB), gastrin-releasing peptide (GRP) and calcium binding proteins – calbindin, calretinin and PKCγ (Gutierrez-Mecinas et al., 2016).

Glutamate produces its effects via two classes of receptors: ionotropic and metabotropic receptors. Three ionotropic glutamate receptors have been identified: N-methyl-D-aspartate (NMDA), (R, S)-α-amino-3-hydroxy-5-methylisozazole-4-propionate (AMPA) and kainate (KA) receptors. By in-situ hybridization, subunits of NMDA, AMPA and KA receptors were detected throughout the DH (Tolle et al., 1993). For metabotropic glutamate receptors, mRNA of mGluR1-5 were observed in the DH of adult mice (Berthele et al., 1999). Generally, the binding of glutamate results in excitation of its target. However, it can occasionally result in inhibition. For instance, the activation of presynaptic AMPA and KA receptors on primary afferent terminals reduces the evoked glutamate release (Lee et al., 2004). [For further review (Bardoni, 2013)].

**Inhibitory transmission:**

GABA and Glycine are the two-main fast inhibitory neurotransmitters within the spinal cord. GABA was detected in cells throughout the DH, with uniform levels observed in LI-III both for rats (Todd and Sullivan, 1990) and mice (Polgar et al., 2013a). Alternatively, GABAergic neurons are detected through immunolabeling of glutamate decarboxylase (GAD), the enzyme for GABA synthesis. Two isoforms of this protein have been identified, GAD65 and GAD67, which are encoded by the genes *gad2* and *gad1* respectively (Mackie et al., 2003). Through transgenic GAD67::eGFP mouse (Tamamaki et al., 2003), where enhanced green fluorescent protein eGFP is expressed under the GAD67 promoter, GABAergic cell bodies were observed in the DH, while in-situ hybridization against GAD mRNA confirmed the presence of GABAergic cells in superficial and deep DH layers (Castrolopes et al., 1994). In addition, transcription factors determining GABAergic cell fate (*Lbx1*, *Pax2* and *Lxh1/5*) can also be used to distinguish inhibitory from excitatory interneurons (Pillai et al., 2007; Huang et al., 2008; Larsson, 2017).

Besides the SC, glycine acts as an inhibitory transmitter in other CNS regions such as brainstem, cerebellum and retina. Glycine containing cells were observed in LI-VI, although higher levels were seen in LIII compared to superficial layers (Todd and Sullivan, 1990; Polgar et al., 2013a). The expression of the neuronal glycine transporter (GlyT2) is required for the loading of glycine in presynaptic vesicles, and GlyT2 is considered as a reliable marker for glycinergic axons and their termination areas. The transgenic mice GLYT2::eGFP demonstrated the presence of eGFP+ glycinergic somas in LIII-IV but sparsely in superficial laminae (Zeilhofer et al., 2005).

Interestingly, much of LI-III glycinergic interneurons exhibit also GABA. Notably, pure glycinergic neurons (i.e. non-GABA) are almost non-existent (Todd and Sullivan, 1990; Polgar et al., 2003). Utilizing combined probes for GAD67/GlyT2 mRNA, few labelled neurons were seen is superficial layers whereas marked neurons in the deep dorsal were mostly medium to large in numbers (Hossaini et al., 2010).

Within LI-III, inhibitory interneurons account for an estimated 30.1% and 33.9% of cells in mice and rats respectively (Todd and Sullivan, 1990; Polgar et al., 2003; Polgar et al., 2013a). Four largely non-overlapping populations of inhibitory interneurons were identified by their expression of neuronal markers: NPY, galanin, nNOS and parvalbumin (Polgar et al., 2013b).

GABAergic and glycinergic terminals are found throughout the DH (Spike et al., 1997; Mackie et al., 2003). A fraction of these terminals are GABAergic and glycinergic descending inputs arising from rostral ventromedial medulla (Antal et al., 1996).

The transmission of GABA occurs via two types of receptors: GABA-A and GABA-B. GABA-A are fast-responding, ionotropic channels whereas GABA-B are slow-responding, G- protein coupled receptors (GPCR). In the spinal cord, GABA-A immunoreactivity was observed in high intensities in LII-IV while other laminae had lower detected levels (Coggeshall and Carlton, 1997). A uniform distribution of GABA-A subunits ($\alpha$3, $\beta$2/3 and $\gamma$2) mRNA was found throughout the various laminae of rat DH (Bohlhalter et al., 1996). Interestingly, GABA-B appeared to be more prevalent in the DH compared to GABA-A, especially in LI-IV (Coggeshall and Carlton, 1997). Furthermore, removal of primary afferent terminals, either mechanically or chemically, produced a reduction of GABA-A and GABA-B expression in the DH, thus suggesting their presence on primary afferent fibers (Singer and Placheta, 1980; Price et al., 1987). Furthermore, GABA-A subunit expression has been observed in DRGs and primary afferent fibers (Zeilhofer et al., 2012).

For the DH, strychnine-sensitive glycine receptors are expressed throughout LII-VI but low level detections were noted for LI and the white matter (Coggeshall and Carlton, 1997). In addition, glycine receptors are presumed to be absent from primary afferents, due to unchanged glycine receptor levels in DH following neonatal capsaicin application (Singer and Placheta, 1980). Futhermore, the scaffolding protein Gephyrin, postsynaptic maker for inhibitory synapse, has been demonstrated to co-localize both GABAergic and glycinergic postsynaptic structures (Todd et al., 1995).

Co-transmission of GABA and glycine has been reported in the DH. Lots of evidence support the co-release of GABA and glycine from the same presynaptic vesicles (Bohlhalter et al., 1994; Todd

et al., 1996). The co-detection of these synaptic events was reported in LI (Chery and De Koninck, 1999). Interestingly, the detection of these synaptic events depends on the developmental stage (Keller et al., 2001; Inquimbert et al., 2007). The GABA-A receptors found on the soma and dendrites of intrinsic dorsal horn neurons mediate classical postsynaptic inhibition; but also, presynaptic inhibition of sensory afferents terminals via primary afferent depolarization (PAD).

Primary afferent fibers possess a high intracellular chloride concentration due to high expression of sodium-potassium-chloride cotransporters 1 (NKCC1) and low levels of potassium-chloride cotransporter 2 (KCC2) (Coull et al., 2003). GABA-A are activated by GABAergic interneurons leading to efflux of chloride ions leading to depolarization of primary afferents. Ultimately, synaptic vesicles are not released however, sodium and calcium channels are inactivated via shunting (i.e. prevention of action potential initiation) (Doyon et al., 2016). Different inhibitory interneuron populations were reported to contact unmyelinated and myelinated fibers (Betley et al., 2009). PAD of primary afferent fibers play a role in sensory information processing (Bardoni, 2013). [Review on fast inhibitory transmission in the spinal cord - (Zeilhofer et al., 2012)]

### 1.3.3. Functional connectivity within the dorsal horn circuitry

The basic neuronal components of the DH consist of local interneurons, propriospinal neurons, and projections neurons which form a complex circuit. In 1965, Melzack and Wall proposed the "gate control theory" as a framework for nociceptive processing (Perl, 2011). In the original model, incoming signals via high threshold nociceptors and low threshold mechano-sensitive fibers connect to spinal projection neurons in DH. Moreover, local interneurons connected to these fibers are responsible for either opening or closing the "pain gate". Although some assumptions have been proven incorrect, this mode helped in delineating the roles of various DH interneuron populations in nociceptive information transmission [Review on the gate control theory (Mendell, 2014)].

**Identified DH circuit:**

Connective units between DH elements were uncovered through paired recordings of local neurons and electrical stimulation of primary afferent fibers [Fig. 1.5] (Cordero-Erausquin et al., 2016). A few canonical connections have been identified: (1) inhibitory connection between the islet interneurons and central interneurons (2) an excitatory connection between central interneurons and vertical interneurons (3) Vertical interneurons and potentially LI projections neurons (Lu and Perl, 2003, 2005).
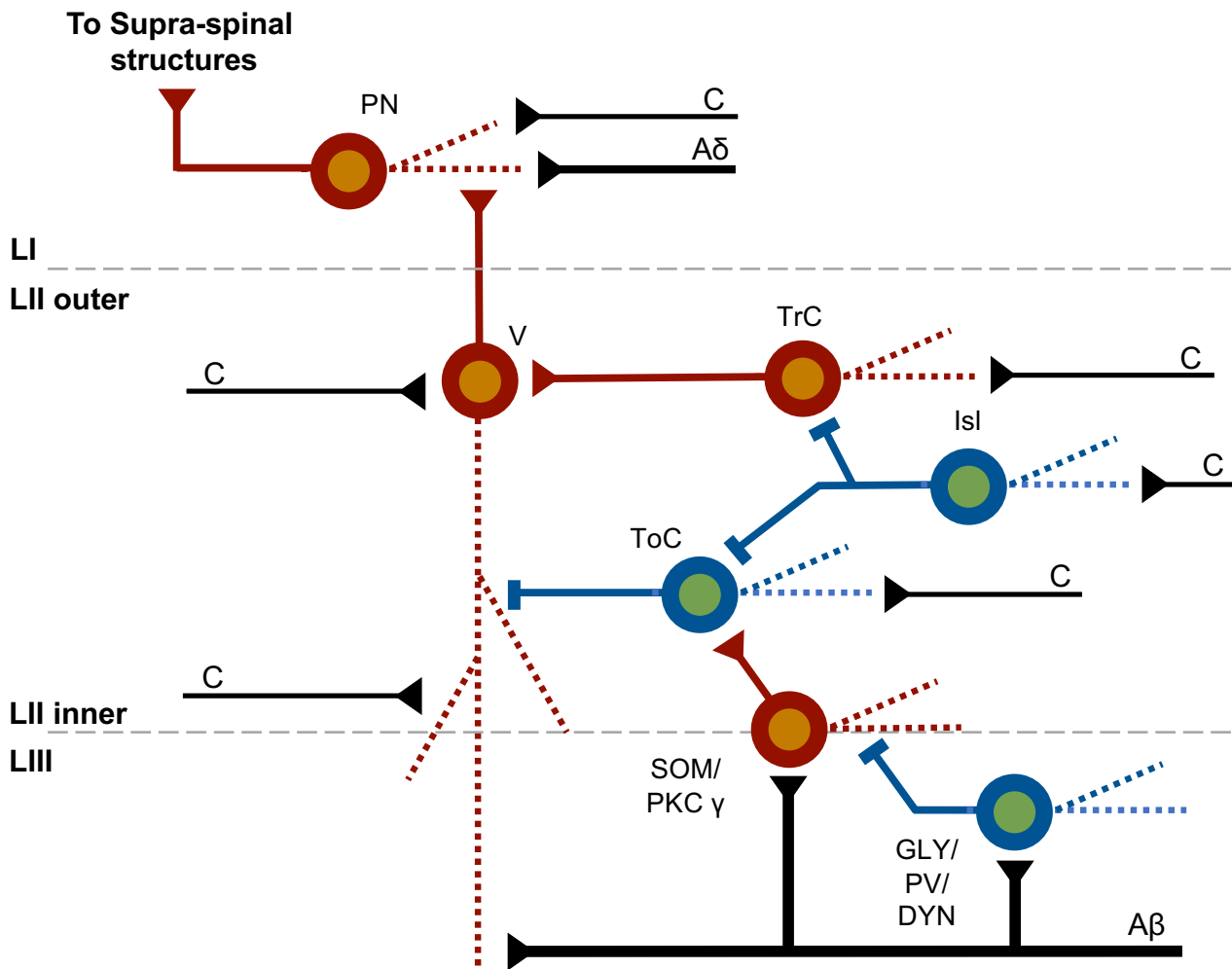
**Figure 1.5:** Simplified circuitry in the superficial dorsal horn circuitry. Lamina I projection neurons (PN) are contacted by C and Aδ primary afferents and vertical cells. Islet cells (Isl) are GABAergic inhibitory interneurons that contact both tonic central cells (ToC) and Vertical (V) cells. Inhibitory central cells display a tonic mode of action potential discharge. Excitatory central cells preferentially display a transient mode of action potential discharge (TrC) and connect to vertical cells. TrC are contacted by Somatostatin (SOM-) and/or PKC γ -expressing excitatory interneurons localized at the border of laminae IIi and III. The LIII inhibitory interneurons Glycine (GLY)/Parvalbumin (PV)/Dynorphin (DYN) form a connection onto SOM and/or PKC γ interneurons and provide feedforward inhibition preventing transmission of non-noxious information (Aβ fibers) into noxious pathway. Neurons in red are excitatory and utilizes glutamate. Neurons in blue are inhibitory and use GABA and/or glycine. [Modified from Cordero-Erausquin et al., 2016]

Similarly, a circuitry connecting Aβ fibers to the superficial layers has been demonstrated. Importantly, this circuit is silenced in control conditions, warranting that superficial layers are mostly (if not exclusively) responding to high threshold inputs. But *in vivo* recordings made with glycine receptor antagonists demonstrated that nociceptive-specific (NS) LI neurons could respond to Aβ fiber inputs. Their results suggest that Protein Kinase C gamma (PKCγ) interneurons are involved in this circuit (Miraucourt et al., 2007; Miraucourt et al., 2009). Indeed, Lu and colleagues later demonstrated a pathway between PKCγ interneurons, transient central cells and vertical cells of LII, the latter projecting to LI neurons. PKCγ receive monosynaptic Aβ synapses, but Aβ stimulation does not result in activation of this population in control situation: this is due to a strong feed forward inhibition they receive, mostly by glycinergic neurons that also receive Aβ monosynaptic inputs (Lu et al., 2013).

Moreover, the recording of NK1+ putative projection neurons in LI showed that they receive monosynaptic high threshold inputs (Aδ and C) but none from low threshold Aβ fibers. However, co-application of GABA-A and glycine receptor antagonists reveals Aβ mediated polysynaptic inputs in these NK1+ LI neurons (Torsney and MacDermott, 2006).

Another pathway involving a subpopulation of excitatory interneurons, expressing somatostatin, was highlighted. Therein, Aβ inputs were observed on both somatostatin/PKCγ populations located at LII/III border and somatostatin positive vertical cells, suggesting two pathways for Aβ fiber mediated information reaching LI neurons. Furthermore, it was proposed that some inhibitory interneurons (including dynorphin expressing neurons), also receiving Aβ inputs, were responsible for gating Aβ input transmission to superficial layers via the somatostatin population. From a behavioral point of view, somatostatin ablated mice presented mechanical allodynia only whereas dynorphin conditional knock-out mice presented mechanical hypersensitivity (Duan et al., 2014). Furthermore, the population transiently-expressing VGLUT3 (that receives Aβ inputs) has been shown to connect to downstream PKCγ and excitatory calretinin populations (Peirs et al., 2015). Moreover, LI projection neurons was shown to receive direct input from low threshold, primary afferent – evoked inhibitory inputs, thus hinting a postsynaptic gate control pathway (Luz et al., 2014).

**Intra-laminae connections**

Within LII, approximately 11% of neurons demonstrate monosynaptic connectivity (Lu and Perl, 2003). Within LI, transsynaptic tracing demonstrated that spino-PB neurons have presynaptic

neurons within LI (Cordero-Erausquin et al., 2009) while paired recording showed that neurons projecting via the anterior lateral tract (ALT) receive excitatory inputs from local LI interneurons (Luz et al., 2010).

For deeper laminae, the probability of finding a pair is 30%, with twice more inhibitory connections compared to excitatory. However, the failure rate of synaptic connections is approximately 44% thus suggesting a low reliability in synaptic transmission between LIII-IV synapses (Schneider, 2008).

**Inter-laminae connections**

Between LI-III, both excitatory and inhibitory neurons in LII made connections with adjacent laminae. The inhibitory LII neurons preferentially contacted LI (53% of recorded inhibitory pairs with a presynaptic LII neuron) rather than LIII (13%) compared to the internal projections within LII (34%) (Santos et al., 2007). On the contrary, the excitatory LII neurons predominantly contacted neurons within their lamina (76%) compared to contacting LI (14%) or LIII (10%). Interestingly, the authors reported a higher probability of finding connections in their more recent study (25% as opposed to 10%) due to improved visibility of cells (Santos et al., 2009).

Functional connections between superficial and deeper laminae were observed with *in vivo* recordings in rats (Biella et al., 1997; Luccarini et al., 2001). In monkey and cats, intracellularly filled LI-LII neurons axons formed collaterals throughout LIII-V (Light and Kavookjian, 1988). Furthermore, glutamate uncaging within spinal cord slices demonstrated synaptic connections between laminae. A subpopulation of neurons between LI-LIIo (with ventrally orientated dendrites) receive excitatory and inhibitory inputs from deeper laminae. These recorded neurons in LIIo potentially correspond to LII neurons with long ventral dendrites which are presynaptic to putative LI projection neurons. Their dendrites are contacted by Aβ fibers in LIII as well as Aδ and C fibers in LII (Yasaka et al., 2010; Yasaka et al., 2014).

Glutamate encaging suggests that superficial laminae receive inputs arising below their cell bodies. Half of LIII/IV neurons receive their excitatory inputs from LIII/IV, while the other half (including neurons with long dorsally oriented dendrites) has excitatory inputs coming from superficial layers (LI-II). Their inhibitory inputs, in contrast, appeared to be more local (Kato et al., 2009; Kato et al., 2013).

Furthermore, a series of recordings performed in our lab suggests the existence of an inhibitory drive to LIII-IV are originating from even deeper laminae (LV-VI). Indeed, the application of

exogenous capsaicin and noradrenaline increased the spontaneous frequency of inhibitory inputs in LIII-IV of rats; however, transection between LIV and LV resulted in a loss of the response. This hints to an inhibitory drive arising from deeper laminae within their respective pathways (Petitjean et al., 2012; Seibt and Schlichter, 2015). Along these lines, loss of LI-II resulted in absence of capsaicin-induced increase of spontaneous excitatory and inhibitory responses in LV. Thus, suggesting a pathway between superficial laminae and LV (Nakatsuka et al., 2002; Cordero-Erausquin et al., 2016).

**Other types of connections**

The communication between different spinal segments is conducted by intrinsic propriospinal interneurons. In de-cerebrated cats, propriospinal neurons originating from other spinal segments could modulate the background activity and noxious heat-evoked response of multi-receptive dorsal horn neurons within lumbar regions (Sandkuhler et al., 1993). From anatomical reports in rats, two cell groups are distinguished based on their axonal spread in rostrocaudal axis: (1) Short axons (2.5mm) have cell bodies in medial part of LI-IV (2) Long axons spread (lumbar enlargement) have their soma in lateral regions of the DH. For mediolateral projections, medial axons terminate in lateral areas of LIIi to IV whereas lateral axons spread from LI-VI. Moreover, commissural propriospinal neurons project from lateral areas of LI-IV that terminate in the contralateral DH; mostly in LIII-IV (Petko and Antal, 2012).

### 1.3.4. Neuronal classification based on sensory afferent inputs

DH neurons play an important role in the integration of somatosensory information. Their firing response to noxious and innocuous stimulation enable to distinguish three neuronal classes: nociceptive specific (NS) neurons, responding exclusively to noxious inputs; wide dynamic range (WDR) neurons responding to both noxious and non-noxious information; and non-nociceptive (NN) neurons, responsive to non-noxious information but not to noxious (Millan, 1999).

NS neurons receive inputs from C and Aδ fibers and are found distributed in LI and LIIo, and more scattered in LV-VI. They have limitations in encoding stimulus intensity but encode stimulation location precisely. WDR neurons receive inputs from the skin, muscles and viscera but are classified based on their cutaneous C, Aδ and Aβ fiber inputs. They are abundant in LV but can also be found in superficial laminae (LI-IIo). These neurons can encode the distinction between noxious and non-noxious information, as nociceptive inputs generate higher firing frequencies comparted to innocuous inputs. In addition, WDR neurons respond in a graded fashion to various noxious stimuli, i.e. they fire more with hotter or sharper objects. Moreover, the sub-modalities

(chemical, mechanical and thermal) can be distinguished based on responses in WDR neurons (Price et al., 2003). NN neurons receive inputs from Aβ fibers and are located between LII-V. This group is responsive to innocuous information and acts as a relay for mechanical information processing (Millan, 1999; Abraira and Ginty, 2013).

### 1.3.5. Ascending tracts

Following the integration of information within the DH, the axons of projection neurons become part of the ascending fascicle after leaving the grey matter. The tract allows the transmission of sensory information (noxious and innocuous) to several supraspinal structures. The rostral transmission of information occurs via two phylogenetically different pathways [Table 1.1]. The first tract, conserved from older species, passes through the medial regions of the brainstem and consists of paleo-spinothalamic, spinoreticular, spinomesencephalic, spinoparabrachial and spinohypothalamic tracts. The latter system, more recent via evolution, is found in the lateral region of the brainstem and consists of neo-spinothalamic, spinocervical and postsynaptic dorsal column bundles (Almeida et al., 2004).

There are several ascending pathways transmitting nociceptive information. Traditionally, the spinothalamic tract is accepted as the main "pain" pathway, however most projection neurons have multiple supraspinal targets: in lamina I most output neurons project to the parabrachial nucleus (PB), but have also collaterals to the thalamus (Hylden et al., 1989), while in deeper laminae a fraction of spino-thalamic neurons neurons also project to the periaqueducal grey matter (PAG), the reticular formation, the cerebellum, or the mesencephalon (Lu and Willis, 1999; Hunt and Mantyh, 2001) .

Projection neurons in the DH are mostly found in LI however, they have been observed in other laminae as well. These axons enter the anterolateral tract (also called ventrolateral) in the ipsilateral side of the spinal cord. They soon decussate to the contralateral side; generally, within the same spinal segment before the axons travelling along the ventrolateral quadrant of the white matter (Todd, 2010).

LI projection neurons terminate in two main regions in supraspinal structures. (1) In the pons, dense projections were observed in the lateral PB nucleus and, to a fewer extent, in the ventrolateral PAG. PB neurons respond to a range of stimuli, including mechanical and thermal noxious stimuli but also cooling. The nociceptive PB regions project to two areas: (i) Amygdala which is implicated in fear and anxiety behaviors, and (ii) hypothalamic ventromedial nucleus – this area is involved in defensive/aggressive behaviors and energy metabolism. The ventrolateral PAG area is responsible

| Tract | Laminae of origin | Cell types | Tissue input | Possible roles |
|---|---|---|---|---|
| Spinothalamic tract | I<br>II (few)<br>IV<br>V/VI<br>VII/VIII<br>LSN | NS<br>WDR<br>Non-N (few) | Skin<br>Viscera<br>Joints/muscle | Discriminative-sensory<br><br>Motivational-affective<br>Descending inhibition |
| Spinoreticular tract | I<br>V/VI<br>VII/VIII<br>X (few) | NS (most)<br>WDR<br>Non-N (few) | Skin<br>Viscera<br>Muscle | Motivational-affective?<br>Descending inhibition |
| Spinomesence-phalic tract | I–II<br>IV/V<br>VII<br>X<br>LSN | NS (I)<br>WDR<br>Non-N | Skin<br>Viscera<br>Joints/muscle | Motivational-affective.<br>Autonomic, motor |
| Spinoparabrachio-amygdaloid tract | I<br>II (few) | NS | Skin<br>Viscera<br>Joints/muscle | Motivational-affective.<br>Autonomic |
| Spinoparabrachio-hypothalamic tract | I<br>II (few) | NS | Skin<br>Viscera<br>Joints/muscle | Motivational-affective.<br>Endocrine |
| Spinohypothalamic (spinotelencephalic) tract | I<br>V<br>X<br>LSN | NS<br>WDR<br>Non-N (few) | Skin<br>Viscera | Sleep, autonomic and endocrine function<br>Thermoregulation |
| Spinocervical tract | I (few)<br>III/IV (most)<br>V | WDR<br>Non-N (most) | Skin<br>Joints/muscle | Discriminative-sensory<br>Motivational affective<br>Autonomic? |
| Postsynaptic dorsal column (ML) pathway | III–V (most)<br>VI<br>VII | NS<br>WDR<br>Non-N | Skin<br>Viscera<br>Joints/muscle | Discriminative-sensory<br><br>Motivational-affective |

**Table 1.1:** Ascending tracts. The pathways are named based on their origins and their targets. NS: Nociceptive-specific; WDR: Wide dynamic range; Non-N: Non-nociceptive. [Modified from Millan 1999]

for anti-nociceptive and defensive reactions. The LI-PAG pathway provides a feedback loop observed in autonomic and anti-nociceptive response to strong noxious stimuli, via descending controls into the DH of the spinal cord (see below). (2) Ventral posterior nucleus of the thalamus that projects to the primary somatosensory cortex. This provides the discriminative aspect of nociceptive processing in rats. Furthermore, this area receives tactile input from dorsal column neurons. For deep laminae projection neurons, several brainstem reticular areas have dense innervations. The medullary reticular formation has been implicated as a relay for nociceptive signals since anterolateral quadrant tracts project here. Moreover, the direct spinal projections to the medial thalamus are conveyed to prefrontal and anterior cingulate cortices; thus, providing emotional aspects of pain (Gauriau and Bernard, 2002; Villanueva et al., 2006).

### 1.3.6. Descending controls

Descending projections play a crucial role on spinal nociceptive information processing for both acute and chronic pain [Fig. 1.6]. These descending pathways can engage in both inhibition and facilitation of nociceptive information transmission. Descending controls are toniccaly active, as blocking brainstem-spinal pathways predominantly resulted in facilitation of heat-evoked spinal reflexes. Response variations exist between location (i.e. tail vs hind-paw) and sub-modality of test stimulation (i.e. noxious heat vs mechanical) (Kauppila et al., 1998).

While some descending inputs are tonically active, the balance between descending inhibition (DI) or facilitation (DF) is dynamic. This balance can be modified by various behavioral, emotional and pathological states (Millan, 2002). In physiological conditions, inhibitory mechanisms reduce the excessive sensitivity to noxious stimuli via a negative feedback loop, i.e. the noxious stimulus activates brainstem nuclei involved in DI and reduces the response to incoming signals. For example, it is involved in stress-induced analgesia (SIA), a phenomenon that involves activation of endogenous analgesia (or anti-nociception) by states of extreme stress or fear (Butler and Finn, 2009). In addition, DI sharpens the signal to noise ratio for incoming noxious signals between stimulus site and surrounding areas (Le Bars, 2002). However DI can shift to DF and contribute to hyperalgesia following inflammation, nerve injuries and chronic opioid application (Heinricher et al., 2009). DF is required for the maintenance, but not the induction, of nerve induced injuries (Vera-Portocarrero et al., 2006).

Interestingly, Diffuse Noxious Inhibitory Controls (DNIC), simply put 'pain inhibiting pain', describes the phenomena where painful stimulation inhibits other pain information produced from another stimulation site to allow sharpening of the sensory system to the most potentially harmful stimulus. Early observations described how peripheral noxious stimuli (electrical activation of C

Hypothalamaus

Amygdala

Periaqueductal
grey

Locus
coeruleus

A5
nucleus

A7 nucleus

Rostroventral
medial
medulla

• Noradrenaline pathway

• Pain suppression pathways
  • Serotonin
  • GABA

• Pain facilitation pathway
  • Serotonin
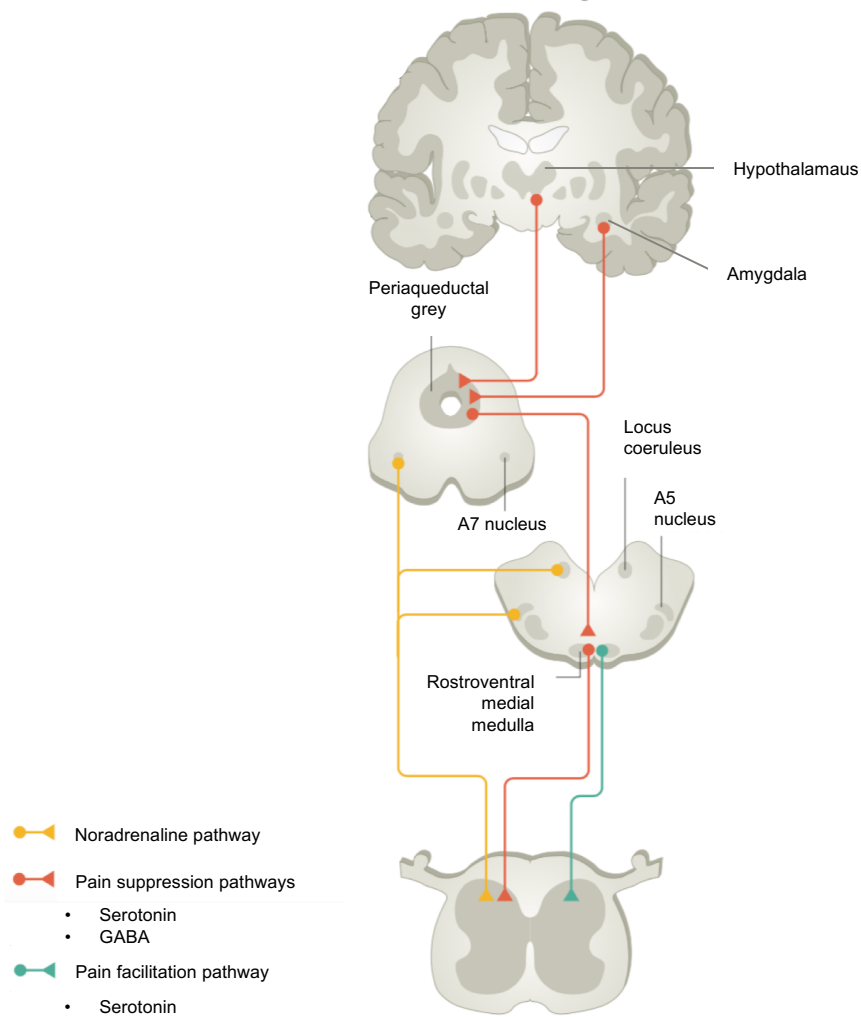
**Figure 1.6:** Simplified descending controls. Several supraspinal structures such as brainstem, thalamus, hypothalamus, amygdala and cortex regions suppress pain through descending projections to the spinal dorsal horn, and in most cases their descending pain suppressive effect is relayed through the periaqueductal gray (PAG)–rostral ventromedial medulla (RVM). [Adapted from Colloca et al. (2017)]

fibers or heat) reduced the responses in WDR neurons. This inhibition was observed when the WDR-activating noxious stimulus was applied to different regions in the body, hence it being 'diffuse' in nature. Interestingly, it was observed that only WDR neurons are susceptible to DNIC, as opposed to neurons responding only to noxious, innocuous or proprioceptive inputs (Le Bars et al., 1979b; Le Bars et al., 1979a). The dorsal reticular nucleus of the medulla has been implicated in DNIC (Bouhassira et al., 1992). Although DNIC results in DI, it has been proposed that the global effect is to promote pain perception by the most threatening stimulus (Pertovaara and Almeida, 2006).

Descending pathways can modulate nociception via several elements in the DH: (1) the terminals of the primary afferents; (2) Projection neurons; (3) local excitatory and inhibitory interneurons; and (4) Terminals of other descending pathways. The DI pathway may involve the reduction of release of pro-nociceptive molecules from noxious encoding fibers, and directly or indirectly (via interneurons) reduce the excitability of projection neurons. In contrast, DF operates via (i) descending inputs utilizing different neurotransmitter (ii) analogous neurotransmitters targeting a receptor coupled to another secondary messenger pathway (iii) target cell with alternate neurochemistry (Millan, 2002).

Furthermore, descending controls have differential effects on C- and A-fibers modulating spinal nociception in physiological conditions: for example, C-fiber evoked activity is greatly reduced whereas A fiber responses remains untouched following PAG activation. This suggests an important survival adaptation in which potentially distracting C fiber information are suppressed while maintaining sensory-discriminative information from A fibers (Heinricher et al., 2009).

The DI and DF pathways have overlapping supraspinal structures of origin: Brainstem – Rostral Ventrolateral Medulla (RVM), Nucleus Raphe Magnus (NRM), Locus Coeruleus (LC); and Hypothalamus. Aforementioned areas have direct projections to the spinal cord via dorsolateral and ventrolateral funiculi; these tracts are involved in both DI and DF processes (Millan, 2002).

The RVM receives information from the PAG and is generally considered as the final relay area before the spinal cord. This structure is implicated in both DF and DI: local applications of opioid in the RVM produces analgesia whereas the neuropeptide cholecystokinin induces hyperalgesia (Fang et al., 1989; Kovelowski et al., 2000). The RVM circuitry was elucidated through correlating neuronal activity with noxious elicited behavior (i.e. tail flick response to noxious heat). Three neuronal populations have been reported: (i) "on-cells" are those that increase fire before tail-flick response (ii) "off-cells" have reduced firing prior to the noxious reflex and (iii) "neutral" cells have

no correlation with noxious behavior (Fields et al., 1983; Heinricher et al., 1989; Potrebic et al., 1995). Both "on-cells" and "off-cells" have been shown to project to the DH. Two-thirds of each three types of neurons express GAD (Winkler et al., 2006). Moreover, local opioid peptide application resulted in elevated firing of "off-cell" following disinhibition (Fang et al., 1989). Recently, GABAergic RVM neurons projecting spinally have been shown to modulate noxious mechanical inputs via spinal enkephalin positive interneurons and GABA mediated presynaptic inhibition (Francois et al., 2017).

The NRM is the principle source of serotonin (5-HT) in the DH of the spinal cord, yet some spinally projecting serotoninergic neurons are also found in the nucleus paragigantocellularis and the ventral part of nucleus gigantocellularis (Kwiat and Basbaum, 1992). 5-HT has a bifunctional role in nociceptive information processing, depending on the receptor subtype. Analgesia from microinjection of opioids in the RVM was blocked by antagonist of 5-HT7 while 5-HT7 agonist reduced capsaicin-induced mechanical hypersensitivity. In contrast, 5HT3 antagonist blocked the hyperalgesia response produced by local cholecystokinin (CCK) supply in the RVM. [Review on role of 5-HT in DF (Suzuki et al., 2004a)].

The source of noradrenaline (NA) to the spinal cord includes the A5 (Locus coeruleus), A6 and A7 (Köl-linker-Füser) nuclei (Bruinstroop et al., 2012). NA projections produce DI effects via inhibiting the presynaptic and postsynaptic transmission of nociceptive information; commonly by adrenergic 2 receptors ($\alpha$2R) (Howe et al., 1983; Wolff et al., 2007). [Review on noradrenergic system (Llorca-Torralba et al., 2016)].

Other neurotransmitters and neuropeptides are implicated in descending controls into the DH: Oxytocin (Paraventricular nucleus of the hypothalamus) (Eliava et al., 2016); Dopamine (A11 nuclei in hypothalamus); and controversially acetylcholine (RVM) (Stornetta et al., 2013).

## 1.4.    Conclusion: Overview of the spinal cord

The DH of the spinal cord plays an important role in nociceptive information processing. Through intricate interactions between local network of excitatory and inhibitory interneurons along with descending controls, the incoming information from the periphery is modulated. The ascending tract transmits this information to supraspinal structures for the perception of pain. Here, the circuit has been described in its naïve state; thus, the next section shall detail the changes of these players following damage to the nervous system.

# 2. Neuropathic pain

Chronic pain can be induced by various causes [cf. Section 1.1.3.], amongst those include neuropathy. The special interest group "Neuropathic Pain" of IASP has proposed a new definition for neuropathic pain (NeP); it states: "the pain initiated or caused by lesion or disease of the somatosensory system" (Jensen et al., 2011). This may result from traumatic lesions, inflammation, infections, cancer and consequences of pharmacological interventions (i.e. chemotherapy or anti-viral treatments) (Dworkin et al., 2003).

Along with NeP, inflammatory pain can arise following injury. However, inflammatory pain resolves in parallel with the resolution of injury (i.e. healing). Moreover, non-steroidal anti-inflammatory drugs (NSAIDS) are effective as a treatment (Dickenson, 2010). [Review comparing NeP vs inflammatory pain (Xu and Yaksh, 2011)].

NeP is characterized by the following symptoms: hyperalgesia (an amplified response to a given painful stimuli), allodynia (an exaggerated response to usually non-noxious stimuli), paresthesia (tickling, 'pins and needles', numb sensations), dysesthesia (abnormal tactile sensations) and spontaneous pain in the absence of external stimuli, which manifests as ongoing burning or paroxysmal electric shock-like sensations (Kuner, 2010; Truini et al., 2013) [Primer on NeP (Colloca et al., 2017)].

## 2.1.1. Animal models

Animal models have been used to uncover the neurobiological changes underlying neuropathic pain and identify new therapeutic compounds for 'mechanism based' treatments. Notwithstanding, certain drawbacks exist that need to be considered while using these models. Firstly, a common factor to all animal models is the difficulty to appreciate the animal's perception, especially due to the subjectivity of pain. Secondly, the procedures to induce neuropathy are standardized thus producing robust phenotypes such as allodynia and hyperalgesia. In contrast, nerve injuries do not always result in NeP while in cases that they do, 'normal' observed symptoms are highly variable (Attal et al., 2008). Finally, for ethical reasons, animals cannot be kept for extensive periods, however, in patients, chronic or recurrent pain lasts over years (Bridges et al., 2001; Henschke et al., 2015).

Another issue concerns the appropriateness of nociceptive assessments made on these models. Classically, the latency or stimulus threshold of evoked avoidance behavior (i.e. withdrawal of hindpaw or tail) was measured. However, most patients suffer from ongoing, spontaneous pain

and sensory loss. Nevertheless, new assessment paradigms have been developed to try to assess pain, rather than nociceptive reflexes; i.e. conditional place aversion to noxious stimulus or the "grimace scale" for painful expressions (Barrot, 2012).

Different types of animals models have been introduced to accommodate the diverse etiology and consequences of the neuropathy that include peripheral nerve injury, spinal cord injury (SCI), cancer and HIV induced pain, or diabetes-induced models [Review on other models (Colleoni and Sacerdote, 2010; Jaggi et al., 2011)]. The common models for peripheral nerve injury are discussed below.

**CCI model:**

The most commonly used model of peripheral neuropathy is the one developed by Bennett and Xie (Bennett and Xie, 1988), that corresponds to a lesion of the rat sciatic nerve. It was later adapted to mice: a proportion of the common sciatic branch is exposed at mid-thigh level, proximal to the sciatic trifurcation; and three loose ligations are made with chromic gut sutures (Sacerdote et al., 2008). Due to the presence of the constrictive ligatures, it combines focal ischemia with Wallerian degeneration and an epineural inflammatory lesion. Spontaneous pain is observed along with behavioral changes including thermal and mechanical hyperalgesia, cold allodynia after one week post-surgery (De Vry et al., 2004). These changes last up to at least 7 weeks (Dowdall et al., 2005). Moreover, a reduction in nerve conduction combined with histopathological studies suggests greater damage to myelinated than non-myelinated axons (Carlton et al., 1991). Furthermore, both A- and C-fibers become sensitized following partial nerve damage (Gabay and Tal, 2004).

**SNI model:**

Decosterd and Woolf (Decosterd and Woolf, 2000) initially described the procedure in rats but it was later adapted to mice with minor alterations (Shields et al., 2003). The sciatic nerve and its three terminal branches (sural, the common peroneal and tibial nerves) are exposed without stretching the structures. Both tibial and common peroneal are axotomized while the sural nerve is spared. Mechanical and thermal hyperalgesia and allodynia are reported to occur within 4 days post-surgery and lasts up to 6 months (Bourquin et al., 2006).

**Cuff model:**

In this model, neuropathy is induced by implanting a polyethylene cuff (2 mm in length) around the common branch of the sciatic nerve of rats (Pitcher et al., 1999); it was later implemented in mice (Benbouzid et al., 2008b). This model provided calibrated, standardized sciatic nerve

constriction with low inter-individual variability (Yalcin et al., 2014). The induced neuropathy leads to long lasting allodynia (2 months) while thermal hyperalgesia lasts up to three weeks. This model showed minor changes in spontaneous pain (Benbouzid et al., 2008c). In rats, alterations in peripheral nerves were observed, with a transient decrease in number of unmyelinated and small myelinated axons, and a sustained decrease in large myelinated axons. Moreover, Wallerian degeneration combined with inflammatory reactions were observed. Interestingly, this was very similar to the morphological and behavioral changes observed with CCI model (Mosconi and Kruger, 1996).

Functional changes following cuff implantation has been studied in rats. Cuff surgery lead to glial activation and hyperexcitation of LI spinal neuron activities due to a shift in anion gradient (Coull et al., 2003; Coull et al., 2005). Moreover, knockdown of glutamate receptors in the spinal cord resulted in reduction of heat hyperalgesia and mechanical allodynia in cuff rats (Fundytus et al., 2001). Moreover, the cuff models respond to gabapentinoids and antidepressants, as is the case of neuropathic pain in the clinics (Benbouzid et al., 2008a; Kremer et al., 2016). In addition, the cuff animals demonstrated anxiety-like behavior 6 weeks post-surgery and depressive-like behavior following 8 weeks (Yalcin et al., 2011).

### 2.1.2. Peripheral changes following nerve injury

**Tissue damage and peripheral sensitization:**

After tissue damage or inflammation, an immune response at the peripheral terminal causes the release of active factors from the blood, mobility of local and migrating inflammatory cells. These substances include prostanoids, bradykinin, and adenosine triphosphate (ATP). Peripheral sensitization results in reduced activation threshold, increase in membrane excitability and an amplified magnitude of response to noxious stimuli (Bessou and Perl, 1969). Furthermore, ectopic discharge of fibers are observed (Kuner, 2010). The peripheral sensitization and ongoing activation leads to continuous input to the SC; leading to central sensitization.

**Ectopic activity in afferent fibers:**

Following nerve damage, ectopic discharges are generated across many sites: from around the terminal of injury site (neuroma) and the DRG of the injured axons (Amir et al., 2005); additionally, from adjacent intact fibers (Wu et al., 2002). Expression of different voltage-gated sodium channels (VGSC) have been implicated in ectopic discharge generation: locally-applied non-selective sodium channel blockers produced an inhibitory effect. Nav1.3 and Nav1.8 VGSC are upregulated in the DRG following nerve injury (He et al., 2010). Interestingly, knockdown of Nav1.8 through small

interfering RNA (although not specific to the DRGs) suggests that this channel has a role in the development of NeP (Dong et al., 2007; Schmalhofer et al., 2008). In contrast, knock-outs Nav1.3, 1.7 and 1.8 had no effect on NeP (Nassar et al., 2005; Nassar et al., 2006).

It has been suggested that other voltage-gated channels expressed in the DRGs, in particular calcium channels (VGCC) and potassium ones, are involved in NeP. Both Cav2.2 (N-type VGCC) and their auxiliary subunits α2δ1 are upregulated in DRGs following peripheral nerve damage (Newton et al., 2001; Cizkova et al., 2002). The deletion of Cav2.2 (also called α1β) reduced NeP associated behavior (Saegusa et al., 2001). Interestingly, in vitro experiments demonstrate that the VGCC auxiliary subunits α2δ1 interact with gabapentin and pregabalin, the first line treatments for NeP, to reduce the expression Cav1 and Cav2 in cultured DRG neurons (Hendrich et al., 2008). Concerning potassium channels, the HCN (for hyperpolarization activated cyclic nucleotide gated channels) that generates pacemaker I(h) currents, is involved in spontaneous activity in DRGs: indeed specific HCN blockers reduced ectopic discharges (Chaplan et al., 2003; Luo et al., 2007).

**Phenotype switch:**

Nerve transection causes propagation of calcium waves to the soma (Wall et al., 1974); which are important for the two retrograde signaling complexes: mitogen activated protein kinases (Zrouri et al., 2004) and nuclear signaling molecules such as importins (Hanz et al., 2003). These signals are transported to the soma by dynein motors thus leading to changes in gene transcription (Michaelevski et al., 2010) including altered regulation of ionic channels and their associated subunits (Costigan et al., 2009). Furthermore, Activating Transcription Factor 3 (ATF3) is upregulated, which has been shown to promotes neurite outgrowth in culture DRGs (Seijffers et al., 2006), and is considered as a marker for nerve damage (Tsujino et al., 2000). Changes in gene expression can affect excitability, in addition to transduction and transmission properties of fibers (Cohen and Mao, 2014).

**Sprouting of nerve fibers:**

Following injury in the peripheral nerve, loss of sensation may arise, or paradoxicaly hyperalgesia and increased pain (de-afferentation pain). These ongoing sensations arise from distal sprouting of the injured DRG axons in response to local release of nerve growth factors (Cohen and Mao, 2014). Furthermore, sprouting of the central terminals of Aβ fibers from deeper laminae into LII was reported (Woolf et al., 1992). However, this study is now controversial, as it used CTb injections to label A fibers: it was later demonstrated that, after injury, the tracing is not specific to

A fibers (Shehab et al., 2003). More specific approaches have failed to identify sprouting of low threshold Aβ fibers in LII following axotomy (Woodbury et al., 2008). Sprouting has been observed in the DRG, arising from sympathic nerves and illustrating the interaction between the sympathetic nervous system and somatosensory nerves (Xie et al., 2007).

**Change in peripheral excitatory / inhibitory balance:**

Following nerve injury, it should be noted that presynaptic GABA-A activation was not sufficient to produce presynaptic excitation, albeit having a reduced inhibitory effect (Guo and Hu, 2014). Upregulation of NKCC1 was reported in both mice and rats DRGs (Chen et al., 2014a; Modol et al., 2014). Similarly, a shift in chloride reversal potential on primary afferents were recorded in vitro (Pieraut et al., 2007) and in vivo (Chen et al., 2014a). Recordings of trigeminal complexes with voltage-dyes demonstrated that GABA-A agonists were unable to reduce the primary afferent terminal currents in nerve-injured animals (i.e. loss of presynaptic inhibitory effect); however, this was reversed with NKCC1 antagonists such as bumetanide (Wei et al., 2013). However, blocking BDNF prevented change in GABA-A receptor conductance and induction of neuropathic behavior – thus suggesting a role of BDNF in modulation of presynaptic inhibition (Chen et al., 2014a).

Furthermore, the excitatory drive to inhibitory interneurons was impaired following to injury. The study observed a reduction in miniature EPSC, and a change in paired pulse ratio suggesting a decrease in primary afferent transmitter release probability. Furthermore, no change in morphology, density nor number of excitatory contacts on inhibitory neurons were observed; thus, suggesting a presynaptic effect of primary afferent release (Leitner et al., 2013).

### 2.1.3. Central changes following nerve injury

**Central sensitization:**

The ongoing input from primary afferents contributes to the activity-dependent plasticity within the spinal cord. In 1983, Woolf demonstrated that a repeated peripheral noxious heat stimulus, enough to produce mild inflammation of hind paw, resulted in an increased excitability of flexor muscles and reduced withdrawal reflex threshold (Woolf, 1983). Subsequently, it was shown that intense C fiber input produced an increase in the size of receptive field combined with new responses to innocuous inputs in DH neurons (Cook et al., 1987). This phenomenon of C-fiber activity-evoked plasticity is known as central sensitization. The induction of C sensitization requires intense, repeated and sustained noxious inputs. Two distinct temporal phases, each including

unique sets of molecular mechanisms, have been described for central sensitization. The early phase is phosphorylation-dependent and transcription independent, and involves glutamate receptors and other ion channels. The late phase involves gene transcription and the synthesis of new proteins responsible for maintenance of central sensitization (Woolf and Salter, 2000; Latremoliere and Woolf, 2009).

**Change in central excitatory / inhibitory balance:**

Plasticity of the spinal inhibitory system has long been proposed to play a role in central sensitization. A reduction in GABA and GAD65/67 expression is reported in the DH after injury (Castrolopes et al., 1993; Ibuki et al., 1997; Moore et al., 2002). Interestingly, a reduction of presumed inhibitory terminals with GAD65 has been shown to correlate spatially and temporally with disappearance of IB4+ primary afferents (Lorenzo et al., 2014). Whether this reduction is linked to a loss of GABAergic neurons is controversial. Some studies have suggested apoptosis of inhibitory neurons, (Scholz et al., 2005; Meisner et al., 2010), while other report that apoptotic markers are rather co-localized with microglia as opposed to neurons (Polgar et al., 2005). This latter group has also found no loss in GABA-A β3 subunits and GABAergic boutons following nerve injury (Polgar and Todd, 2008), as well as no loss in total number of neurons in LI-III (Polgar et al., 2004; Polgar et al., 2005) and unchanged numbers of GABAergic neurons (Polgar et al., 2003). Measuring the indirect inhibitory post-synaptic currents (IPSC) evoked in the DH by stimulation of primary afferents is a mean to evaluate the weight of inhibitory signaling. This indirect IPSC is reduced in its incidence, magnitude and duration in injured animals (Moore et al., 2002; Scholz et al., 2005). Moreover, long lasting polysynaptic excitatory responses to Aβ, Aδ and C fibers are revealed in LII in presence of GABA-A antagonists in naïve mice. However, such antagonists induced minimal changes in LII neurons in SNI animals thus suggesting a reduced GABAergic tone (Baba et al., 2003) (see also below).

Analysis of miniature IPSCs suggested a reduction in GABA release. This is also supported by the observed reduction in GABA secretion from stimulated spinal cord slices (Lever et al., 2003). A tonic GABAergic current has been reported by some authors, due to persistent activation of specific extra-synaptic GABA-A receptors, containing the δ subunit; such tonic current was reduced in neuropathic animals (Moore et al., 2002; Iura et al., 2016). In addition, the α5 subunit of GABBA-A has been shown to contribute to a tonic conductance in DH. In α5 k/o mice, the sensitization recovery duration was extended in Complete Freund's Adjuvant (CFA) models thus, suggesting continuously activated currents hasten recovery from hyperalgesia (Perez-Sanchez et al.,

2017). A reduced inhibitory tone, as well as more generally disinhibition, can be explained by a depolarizing shift in chloride equilibrium in DH neurons (Coull et al., 2003). This depolarizing shift is due to a reduction in the expression of the potassium-chloride-co-transporter 2 (KCC2). In consequence, GABAergic and glycinergic inputs have less inhibitory effect and may even occasionally result in a net excitatory effect. This phenomenon involves activation of microglia after nerve damage and BDNF signaling. Initially, the release of cytokine CCL2 from damaged nerves activates microglia in the DH, and induces the upregulation of the purinergic receptor P2X4 (Zhang and De Koninck, 2006; Thacker et al., 2009). ATP, also released following tissue damage, acts on P2X4 receptors on activated microglia thus leading to release of BDNF (Tsuda et al., 2003). The BDNF in turns binds to trkB receptors on DH neurons, thus leading to downregulation of KCC2 (Coull et al., 2005). Interestingly, there appears to be a sex difference concerning this mechanism (Mapplebeck et al., 2016).

**Circuit unmasking:**

In rats with neuropathy, stimulation of Aβ primary afferents evoked an increase in calcium signals in LII and LIII-IV, while changes were observed only in LIII-IV in naïve rats (Schoffnegger et al., 2008). This can be related to the excitatory feedforward circuit that exists between Aβ fiber terminals in deeper laminae and superficial layers of DH, which is under inhibitory control in naïve states (see section 1.3.3). The feedforward inhibition impinging onto PKCγ neurons appears to be perturbed following nerve injury: Indeed, glycinergic inputs to PKCγ interneurons were weaken after neuropathy (Lu et al., 2013). Moreover, the number of appositions from parvalbumin-expressing (PV) neurons (an inhibitory population) onto PKCγ interneurons was reduced after neuropathy (Petitjean et al., 2015); PV neurons also receive Aβ inputs. Interestingly, mechanical allodynia phenotype during injury was transiently rescued by activating either glycine-expressing neurons; parvalbumin or transient-VGLUT3 populations (Foster et al., 2015; Peirs et al., 2015; Petitjean et al., 2015). These results indicate that Aβ inputs gain access to LI projection neurons through loss of multiple feedforward inhibitory circuits following nerve injury.

As mentioned in section 1.3.3., somatostatin and dynorphin interneurons are also implicated in circuits linking Aβ terminals in the deep DH with LI neurons. Interestingly, the ablation of somatostatin population in the DH results in loss of mechanical hypersensitivity following neuropathy. In contrary, the removal of local dynorphin populations did not exacerbate the mechanical allodynia observed after injury (Duan et al., 2014).

**Glial activation:**

Microglia cells becomes activated within a day, followed by astrocytes, with their activation lasting up to 12 weeks after injury. Moreover, the depletion of spinal microglia in neuropathic rats has demonstrated their role in enhancing central sensitization through the release of proinflammatory cytokines/chemokines (early phase) whereas the microglia requires trophic factor brain-derived neurotrophic factor (BDNF) to prolong pain hypersensitivity (late phase) (Echeverry et al., 2017). In neuropathic states, the glial cells undergo morphological and functional changes. Astrocytes release several pro-nociceptive mediators including cytokines, excitatory amino acids and prostaglandins (Mika et al., 2013).

**Ascending pathway:**

As described within the previous sub-headings, LI projection neurons appear to receive low-threshold inputs following to injury; this could underlie mechanical allodynia. Indeed, in neuropathic rats, spino-parabrachial LI projection neurons were observed to respond to innocuous stimulus, gain spontaneous firing and had amplified output to noxious inputs (Keller et al., 2007).

Functional alterations were also reported, such as hyper-excitability to a range of stimuli (Tan et al., 2011), as well as increased spontaneous activity, reduced C fiber threshold, increased C fiber response and enlarged receptive fields in WDR neurons (Liu et al., 2011). In contrast, the threshold for innocuous tactile information was altered for the NS neurons but not for WDR neurons after peripheral nerve injury. Therefore, the mechanical allodynia is suggested to be due to switch in modality specificity within naïve nociceptive-specific spinal relay neurons rather than a change in gain within a projecting WDR (Lavertu et al., 2014).

**Descending pathways:**

Alongside spinal plastic events, the descending controls undergo changes that are implicated in central sensitization during neuropathy. In the RVM, the nociceptive modulatory neurons undergo changes following to continued noxious inputs (Morgan and Fields, 1994). This has been proposed to play a role in the development of central sensitization (Urban and Gebhart, 1999). DF mechanisms have been implicated in exacerbating allodynia/hyperalgesia through enhanced excitatory 5HT pathway involving 5-HT3 receptors (Suzuki et al., 2004b). Interestingly, the efficacy of gabapentin requires the upregulation of 5HT3 mediated DF (Suzuki et al., 2005).

Similarly, the DI controls via noradrenergic pathways may undergo plasticity as observed with upregulation of α2R and elevated NA levels (Satoh and Omote, 1996) along with increased efficacy of local α2R agonists (Mansikka and Pertovaara, 1995).

## 2.2. Conclusion: The changes during neuropathic states

After nervous system damage, several peripheral and central adaptations occur. Each component in the nociceptive processing network undergoes their respective changes which interact to facilitate the amplification of nociceptive information and blurring the limitations of different modalities contributing to the pain experience. Within the spinal cord, an excitatory and inhibitory balance maintains these nociceptive thresholds which become aberrant after damage. Amongst several neurotransmitters involved, the cholinergic system is a key player for this maintenance.

# 3. Spinal cholinergic system

The cholinergic system has several roles in the nervous system from locomotion, memory, attention and pain modulation. In the following section, the cholinergic system regarding nociceptive information processing shall be discussed.

## 3.1. Overview of cholinergic system

### 3.1.1. The synthesis of acetylcholine

In 1942, the first neurotransmitter to be described in the literature was Acetylcholine (ACh) (Loewi, 1921) and subsequently the enzyme response for its synthesis : the Choline Acetyltransferase (ChAT) (Nachmansohn and Machado, 1943). This enzyme mediates the transfer of the acetyl group from acetyl coenzyme A to choline. ACh governs several biological processes including motor, memory, sleep-wake cycles, and nociception (Miwa et al., 2011).

ChAT is produced in the soma and transported by both fast and slow axonal transport systems to the nerve terminals (Oda, 1999). In cholinergic nerve terminals, ChAT exists as both membrane bound and soluble forms (Gabrielle et al., 2003). In rats, the gene encoding ChAT consists of 15 exons (a single 5' non-coding exon followed by 14 coding exons) (Eiden, 1998). Following transcription, the transcript is spliced and translated into the ChAT protein (640 amino acids or 67 kDa) (Hahn et al., 1992). ChAT mRNA is subjected to alternative splicing: alongside the 'common' form of cChAT, there is a splice variant produced due to exon skipping: pChAT. Due to its prevalence in the peripheral tissues, it has been coined 'peripheral type of ChAT' or pChAT (Bellier

and Kimura, 2011). For continuity, the 'common' or 'central' ChAT shall be referred to as ChAT, unless stated otherwise.

Another mRNA splice variant encodes for the vesicular acetylcholine transporter (vAChT). Interestingly, the entire vAChT gene is in the first intron of the ChAT gene (Erickson et al., 1994). After synthesis, ACh is transported into synaptic vesicles via vAChT.

The released ACh is broken down by the Acetylcholinesterase (AChE). Different types of AChE exist due to many slice variants. Two major types of AChE subunits in mammals are AChE-H and AChE-T, that differ in their targeting and functional anchoring at extracellular sites (Massoulie, 2002). The enzyme is distributed in the CNS and Peripheral Nervous System (PNS) with variability in different vertebrates. In addition, it has been reported on non-neuronal and glial cells (Tripathi and Srivastava, 2010). However, AChE is not used as a marker for cholinergic cells due to existence of non-cholinergic "cholinoceptive" neurons. Therefore, ChAT is considered as an ideal marker for cholinergic cells (Anglade and Larabi-Godinot, 2010).

Following the hydrolysis of acetylcholine, the acetate might be recycled at the cholinergic presynaptic terminal (Corthay et al., 1985). For choline, it is recaptured by the high affinity choline transporter (CHT) found on the membrane of cholinergic cells' terminals. Notably, choline recapture is the rate-limiting step for the synthesis of ACh (Ferguson and Blakely, 2004) [Fig. 1.7].

### 3.1.2. Distribution of the Cholinergic neurons

Analysis of ChAT immunolabeling led to the definition of 5 groups of cholinergic neurons, from the dorsal to the ventral horn of the spinal cord (Barber et al., 1984; Borges and Iversen, 1986):

(i)    Somatic motor neurons located in VII-IX
(ii)   Partition cells located in V-VII having a dispersion between LX and the inter-mediolateral column
(iii)  Autonomic neurons (sympathetic preganglionic neurons in the thoracic region, parasympathetic preganglionic neurons in the sacral parts
(iv)   Central canal neurons present in LX
(v)    Sparse cholinergic interneurons in LIII-IV of the DH

However, the exact role of these DH cholinergic interneurons in nociceptive processing remains elusive. Thus, characterizing this population is one of the aims of this thesis.

Some reports suggest the existence of non-spinal cholinergic populations projecting to the spinal cord: some DRGs neurons, for example, have been reported to express pChAT and co-localizes
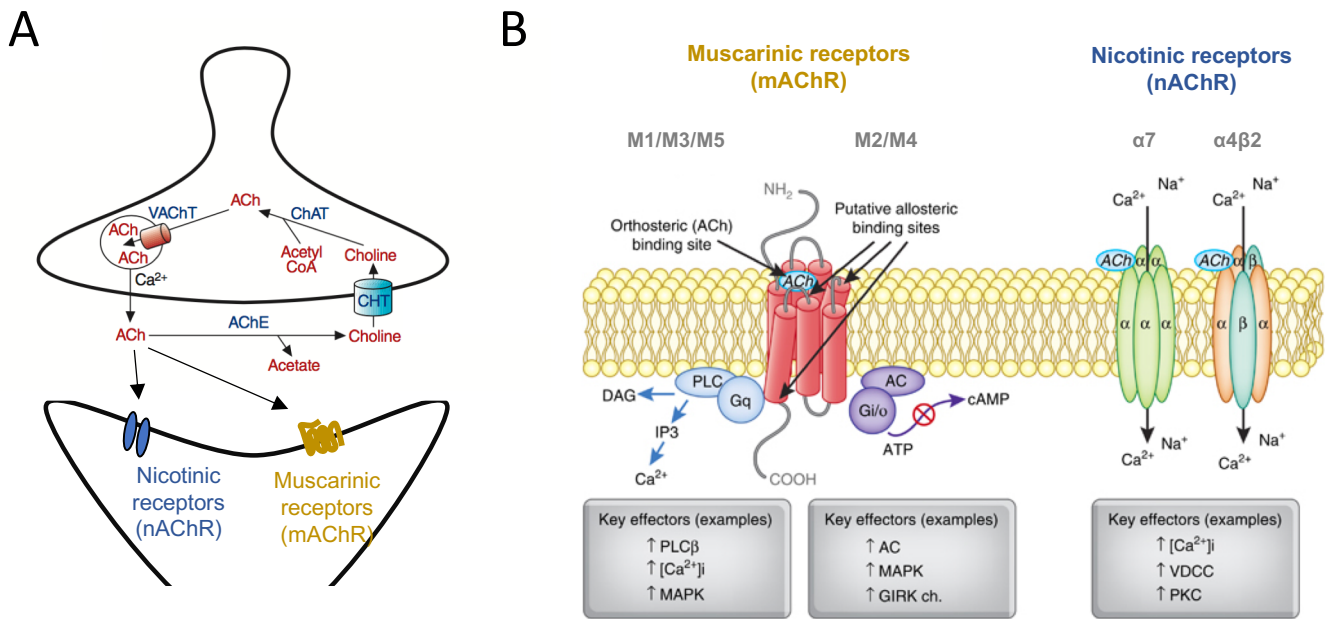
**Figure 1.7:** Cholinergic synapse. **A:** The acetylcholine is produced from Cholineacetyltransferase (ChAT) and stored into vesicles by vesicular acetylcholine transporter (VAT). The released acetylcholine in the synaptic cleft acts on metabotropic muscarinic acetylcholine receptors (mAChR) and ionotropic nicotinic acetylcholine receptors (nAChR). The acetylcholinesterase breaks down the ACh into choline and acetic acid. The high affinity choline transporter (CHT) takes up the choline from the cleft and brings it back to the neuron and into the cycle. [Modified from Ferguson and Blakely, 2004] **B:** The signaling pathway of AChR. The 7 transmembrane mAChR are divided into two groups based on G protein coupling: (1) M1/M3/M5 mAChR are coupled to Gq/G11- G protein. This activates phospholipase Cβ (PLCβ) thus generating inositol-1,4,5-trisphosphate (IP3) and 1,2-diacylglycerol (DAG) ultimately increasing Ca+ levels (2) M2/M4 mAChR are coupled to Gi/Go type. The inhibition of adenylate cyclase reduces intracellular levels of cAMP and enhances opening of K+ channels. Neuronal nAChR are pentameric ligand gated ion channels, commonly found with α4, β2, and α7 subunits, are permeable to Ca2+ and Na+. The heteromeric α4β2 receptor subtypes have different Ca2+ permeability: (α4)2(β2)3 receptors have low whereas (α4)3(β2)2 receptors have high permeability. However, homomeric α7 nAChR shows high Ca2+ permeability. Activation of α4β2 nAChRs can increase intracellular levels of Ca2+ by secondary activation of Voltage Gated Calcium Channels (VDCC), whereas α7 nAChRs preferentially elevate Ca2+ release from ryanodine-sensitive intercellular stores through Calcium induced Calcium Release. [Modified from Jones et al., 2011]

with unmyelinated C fibers and myelinated A fibers (Matsumoto et al., 2007). In supraspinal structures, several cholinergic cell bodies are confined to the striatum and basal forebrain. ChAT cells are commonly widespread in other regions including amygdala, globus pallidus and the entopeduncular nucleus (Woolf, 1991). Interestingly, within the medial part of the RVM lies a population of cholinergic cells which appear to be neither parasympathetic preganglionic neurons nor motor neurons. These have been reported to form projections to the DH of the spinal cord (Stornetta et al., 2013).

Another aspect to this thesis is to determine the contribution of these different potential sources of ACh to contributing to the local ACh pool within the spinal cord.

### 3.1.3. Cholinergic receptors in the Dorsal Horn of the Spinal Cord

There are two types of ACh receptors: nicotinic (nAChRs) and muscarinic (mAChRs) receptors, respectively ligand-gated cation channels and GTP protein coupled receptors (GPCR) (McCormick, 1989). The nAChR consists either a hetero- or a homo-pentamer. The subunits composing the nAChRs found on neurons are among: alpha ($\alpha$2-7, $\alpha$9 and $\alpha$10) and beta ($\beta$1-4). nAChRs conduct small monovalent and divalent cations such as $Na^+$, $K^+$ and $Ca^{2+}$ (Dani, 2015). The mAChR consists of five subtypes (M1-M5) which are divided into two categories: those coupled with $G_q$/11 (i.e. M1, M3 and M5) or those with $G_i$/$G_o$ (i.e. M2 and M4) (Brown, 2010). [Further information on cholinergic receptors (Jones et al., 2012)]

**Nicotinic acetylcholine receptors:**

The binding of [$^3$H]-epibatidine, a nAChR agonist, demonstrates the presence of nAChRs throughout the spinal cord, with greater density in the superficial layers of the rat DH (Khan et al., 2003). The in-situ hybridization studies have demonstrated the presence of subunits $\alpha$3, $\alpha$4 and $\beta$2 (Wada et al., 1989), $\alpha$5 (Wada et al., 1990) and $\alpha$7 (Seguela et al., 1993) in rat DH. RT-PCR at the single level demonstrated expression of $\alpha$4, $\alpha$6 and $\beta$2 subunits in inhibitory interneurons whereas $\alpha$3, $\alpha$7 and $\beta$2 were expressed in excitatory interneurons along with NK1+ projection neurons in juvenile mice (Cordero-Erausquin et al., 2004). In addition to the spinal parenchyma, $\alpha$3, $\alpha$4, $\alpha$5, $\alpha$6, $\alpha$7, $\beta$2 and $\beta$4 nAChR subunit transcripts were observed in DRGs (Haberberger et al., 2003; Khan et al., 2003; Shelukhina et al., 2009; Wieskopf et al., 2015). Most nAChR antibodies have been demonstrated non-specific, thus interpretation of immuno-localization studies should be made with caution (Moser et al., 2007).

**Muscarinic acetylcholine receptors:**

The binding of [³H]-N-methylscopolamine, a mAChR antagonist, suggests the presence of M2, M3 and/or M4 mAChRs in the superficial regions of the DH (Hoglund and Baghdoyan, 1997); RT-PCR led to similar results, including M5 (Wei et al., 1994). Moreover, M2 immunoreactivity was detected in superficial layers of rat DH (Li et al., 2002). Similarly, M2, M3 and M4 were detected in both rat DH cells and DRGs (Cai et al., 2009).

## 3.2. Cholinergic system and Pain Behavior

### 3.2.1. Elevating Acetylcholine Levels

**Acetylcholine esterase inhibitors:**

Epidural administration of Neostigmine, an acetylcholinesterase (AChE) inhibitor provides pain relief during childbirth and post-operative pain in clinics (Eisenach, 2009). In post-operative patients, the epidural administration of neostigmine provided a mild reduction in pain score. However, it amplified the analgesia of systemically administered α2 adrenoceptor agonist and local anesthetics, as well as the effect of morphine provided epidurally. However, for laboring patients, the analgesia effect was more the resultant of conjunction between neostigmine and other drugs (i.e. clonidine, local anesthetic). This suggests that ACh can modulate pain perception through an action at the spinal cord level and be a potentially interesting source for alternative pain therapy.

AChE inhibitors have also been applied locally in the spinal cord of rodents (intrathecal injections, or i.t.) to produce analgesia; other administration routes have also been employed, that will be discussed later. Neostigmine is analgesic when injected i.t. prior to thermal noxious stimulation in rats (Hartvig et al., 1989; Naguib and Yaksh, 1994; Chen and Pan, 2003). Furthermore, neostigmine increased the analgesic score in animals injected with acetic acid intraperitoneally (Miranda et al., 2002). During a thermal test, neostigmine (i.t.) produced analgesia differently between male and female rats. Notably, neostigmine was more potent in females compared to males; and the effects was blocked by atropine in both sexes whereas mecamylamine proved effective only in females (Chiari et al., 1999). This demonstrates that increasing the levels of spinal ACh is analgesic in rodent models of acute thermal nociceptive information processing and that the underlying mechanism is sex-dependent.

The effect of AChE inhibitors has also been investigated in chronic pain models. In neuropathic rats, neostigmine resulted in an increase of paw withdrawal thresholds (Lavand'homme et al., 1998; Hwang et al., 1999; Hwang et al., 2000). Neostigmine produced an anti-allodynic effect with more efficacy in female than male rats. Moreover, atropine was completely effective in blocking its action for both sexes whereas mecamylamine resulted in a partial reduction in analgesia (Lavand'homme and Eisenach, 1999). Another example is in the formalin model, which consists in the injection of formalin (a noxious chemical stimulus) in the paw of rats. The intrathecal application of the AChE inhibitor physostigmine reduces flinching, the nociceptive response involving flexing and withdrawing of the paw injected with formalin (Yoon et al., 2003). Similarly, neostigmine produced anti-inflammatory effect in a zymosan induced inflammatory model (Yoon et al., 2005). These data suggest that it is possible to recruit the spinal cholinergic system to relieve chronic pain-related behaviors.

In addition AChE inhibitors have been injected through other routes, potentially activating cholinergic receptors in supraspinal structures to induce anti-allodynia. However the local (spinal) application of antagonists suggest the contribution of spinal ACh to this effect: in neuropathic rats, donepezil administered orally produced analgesia which was blocked by atropine administered intrathecally but not mecamylamine (Clayton et al., 2007). Also, intraperitoneal injections of donepezil resulted in anti-hyperalgesia however, it was completely blocked by intrathecal administration of atropine while mecamylamine produced a partial block (Kimura et al., 2013). Interestingly, the dose used was effective to produce analgesia in injured animals but not analgesia in controls, suggesting changes in the function of AChE and/or the downstream receptors.

**Other substances:**

Beyond AChE inhibitors, other substances that induce an increase in spinal ACh levels also produce analgesia. Elevated levels of ACh was observed following intrathecal application of epibatidine (nAChR agonist) and oxotremorine (mAChR agonist) (Hoglund et al., 2000).

Morphine and clonidine are two widely used analgesic drugs. Clonidine induces a release of ACh in the spinal cord of rats (DeKock and Meert, 1997; Abelson and Hoglund, 2004) and humans (Detweiler et al., 1993; DeKock et al., 1997). Morphine elevated ACh levels in both rats (Zhu et al., 2008) and monkeys (Gage et al., 2001) in the trigeminal nuclear complex and spinal cord respectively.

In rats, the analgesic effect of these drugs has been shown to involve nAChRs and mAChRs activation. For morphine, the intravenous application elevates thermal PWT in naïve conditions.

Its analgesic effect was blocked by both mecamylamine and atropine applied intrathecally. This suggests that the effect of systemic morphine requires a spinal cholinergic component (Chen and Pan, 2001).

The anti-nociceptive effects on mechanical PWT of clonidine were also blocked by intrathecal injections of atropine in rats and mice (Honda et al., 2002; Paqueron et al., 2003). In a diabetic mouse model, the analgesic effect of clonidine on PWT was abolished with co-treatment of intrathecal atropine (Koga et al., 2004). After SNI, the analgesic effect of clonidine in rats was completely blocked with atropine while partially maintained in mecamylamine. The contributions of different receptors following neuropathy in clonidine induced analgesia may therefore vary as a function of the pathology model and species under study. In addition, spinal ACh release has been reported during noxious stimulation via cerebrospinal fluid (CSF) sampling (Eisenach et al., 1996). Altogether, these experiments demonstrate that an increase of ACh levels in the spinal cord is principally associated with analgesia.

### 3.2.2. Inhibiting the cholinergic tone

**Pharmacological blocking of cholinergic receptors:**

The spinal injection of cholinergic receptors antagonists has demonstrated the existence of an endogenous cholinergic tone. Indeed, mechanical and thermal nociceptive thresholds appear to be under the control of tonically activated nAChRs, while the contribution of mAChRs is controversial ((Honda et al., 2002; Paqueron et al., 2003) but see (Zhuo and Gebhart, 1991)).

For nAChRs in rats, a reduction in mechanical thresholds was observed after i.t. delivery of antagonists with different pharmacological profile: mecamylamine or hexamethonium (non-specific nicotinic antagonist), Dihydro-β-erythroidine (DHβE, that inhibits mostly non-a3b4 nAChRs), α-conotoxin MII and N-n-decylnicotinium iodide (NDNI - α4β2 antagonist), α-conotoxin MII (α3β2/α6β2 antagonist), while data are controversial for methyllycaconitine (MLA, selective for a7* nAChRs) (Rashid et al., 2006; Young et al., 2008b; Young et al., 2008a; Yalcin et al., 2011). In contrast, i.t. mecamylamine, DHβE or MLA had no effect on thermal withdrawal responses in rats (Khan et al., 1998; Rueter et al., 2000). However, in mice, i.t. application of mecamylamine, DHβE (but not MLA) induced thermal hyperalgesia (Rashid and Ueda, 2002; Rashid et al., 2006). This suggest the presence of cholinergic tone involving nAChR for mechanical nociceptive thresholds although their role for thermal threshold differs.

Cholinergic antagonists have also been injected i.t. in chronic pain models. Mechanical allodynia in neuropathic rats was not altered by i.t. mecamylamine, DHβE, MLA nor α-conotoxin MII (Lavand'homme and Eisenach, 1999; Young et al., 2008b; Young et al., 2008a). Atropine i.t. was also without effect on mechanical thresholds in rats with spared nerve ligation (Lavand'homme and Eisenach, 1999; Paqueron et al., 2003), or diabetic mice (Koga et al., 2004). Concerning the thermal hyperalgesia observed in neuropathic mice, it was unchanged after i.t. application of mecamylamine (Rashid and Ueda, 2002); atropine was also without effect on thermal hyperalgesia in rats (Paqueron et al., 2003). These data suggest the disappearance of the spinal cholinergic tone in neuropathic animals.

**Removing elements within the cholinergic system:**

Locally decreasing ACh levels through either inhibition of its synthesizing enzyme ChAT or ablation of cholinergic neurons has been performed. Intrathecal administration of the cholino-toxin AF64A (Ethylcholine mustard aziridinium ion) reduces the number of cholinergic neurons in the spinal cord. In naïve rats, the thermal withdrawal threshold remains unchanged after treatment however, the analgesic effect produced by morphine is reduced (Chen and Pan, 2001). In neuropathic rats, AF64A did not exacerbate the mechanical allodynia. However, the analgesic effect of clonidine was completely abolished with 15nmol treatment with AF64A (Paqueron et al., 2001). Inactivation of ChAT with an antisense strategy induces a reduction of both thermal and mechanical nociceptive thresholds in mice (Matsumoto et al., 2007). The induced loss of cholinergic tone appeared to affect both mechanical and thermal nociceptive thresholds in mice but rats remained unaffected.

The alteration in the level of expression of cholinergic receptors perturbs nociceptive thresholds in mice. β2 subunit nAChR knock-out mice (β2 KO) have a reduced mechanical threshold, i.e. they are allodynic compared to wild types (WTs). The nicotinic antagonist hexamethonium becomes ineffective. Moreover, β2 KOs have thermal hyperalgesia on dynamic hot plate but not with (constant temperature) hot plate or in the Hargreaves test (Marubio et al., 1999; Yalcin et al., 2011). The knock-down of α4 nAChR in the spinal cord (through an antisense strategy) similarly produced thermal and mechanical hyperalgesia (Rashid et al., 2006). This demonstrate that α4* and β2* nAChRs are necessary for the normal encoding of mechanical and thermal nociceptive responses in mice, and the anti-sense data suggest that the spinal cord is a key player in this effect.

Following neuropathy, β2 KOs, as well as α6 KOs developed more intense allodynia compared to WTs, while α5 KOs exhibited a weaker allodynia (Vincler and Eisenach, 2005; Yalcin et al., 2011;

Wieskopf et al., 2015). The expression of α6 nAChR in murine DRGs were demonstrated to correlate with mechanical allodynia produced after neuropathy (Wieskopf et al., 2015). As observed with antagonists, lowering the expression of M2/M3 and M4 subtype (through small interfering RNA) did not alter the thermal threshold for injected rats (Cai et al., 2009). Following neuropathy, nAChR influences the development and maintenance of these conditions.

These studies therefore suggest the presence of a spinal cholinergic tone that modulates nociceptive processing. An aim of this thesis is to better characterize the spinal cholinergic tone both in control and neuropathic animals to help identifying the origin of this plasticity.

## 3.3.    Cholinergic system and spinal nociceptive circuits

In addition to the above mentioned behavioral experiments, electrophysiological recording have been performed in the DH of the spinal cord to try and identify the underlying mechanisms of cholinergic analgesia.

**Role of mAChR**

The application of mAChR agonist resulted in an increase in inhibitory transmission in LII in rats, implicating the M2, M3 and M4 mAChR subtypes (Baba et al., 1998; Zhang et al., 2005) In contrast, non-specific muscarinic agonists induced a decrease in inhibitory transmission in mice. Activation of the different muscarinic subtypes appear to have opposite effects: M2 and M4 subtype activation results in a decrease in the frequency of GABAergic IPSCs (possibly due to the disinhibition of other inhibitory interneurons) whereas M3 subtype activation facilitated them (Zhang et al., 2006; Pan et al., 2008). Activation of the M3 subtype also facilitated glycinergic transmission, both in rats and mice (Wang et al., 2006; Zhang et al., 2007b).

Excitatory transmission was also influenced by muscarinic activation. In mice, two-thirds of LII neurons increased frequency of sEPSCs after oxotremorine application (Chen et al., 2010) whereas in rats it resulted in inhibition (Zhang et al., 2007a).

The role of mAChR on primary afferent transmission in the DH was also explored. The amplitude of primary afferent evoked EPSC was reduced after application of muscarinic agonists in rats, and it was proposed that this effect is mediated by M2 mAChRs present on presynaptic terminals of primary afferent fibers. In mice, oxotremorine similarly induced an inhibitory effect on evoked EPSC. It was reported that M2, M4 and M5 subtypes were located on the primary afferents. To explain the global effect by oxotremorine, the authors suggested that the increased release of

glutamate, via M5 activation, acts on group II/III mGluR thus attenuating primary afferent input (Chen et al., 2014a).

Because in vitro recordings are usually performed on unidentified neurons, it is difficult to infer the global effect of the applied drugs on the nociceptive circuit. In vivo recordings enable to go one step further, in particular when they are performed on identified supraspinally projecting neurons, i.e. the output of the circuit. Such recordings were performed in rats, where the authors analysed the firing frequency of the projection neurons following noxious and innocuous peripheral stimulations. Locally-applied muscarine, a non-specific mAChR agonist, reduced the action potential firing in response to both types of inputs. Therefore, this demonstrates that spinal mAChRs can modulate the incoming signals into the DH. In addition, the effect of muscarine was reduced in the presence of GABA-B antagonists thus, implicating their role in the pathway (Chen and Pan, 2004).

**Role of nAChR:**

In vitro experiments demonstrated that nicotine induced an increase in the frequency of both spontaneous and miniature IPSCs in the LII neurons of neonatal rats (Kiyosawa et al., 2001; Takeda et al., 2003; Genzen and McGehee, 2005; Takeda et al., 2007). There might be a developmental shift in type of nAChRs involved in this effect: $\alpha4\beta2^*$ nAChRs appear to be involved in neonatal rats (Kiyosawa et al., 2001; Genzen and McGehee, 2005), while however, the elevated IPSCs frequency was reported to be $\alpha4\beta2$ independent in adult rats (Takeda et al., 2003). Moreover, a contribution of non-$\alpha4\beta2^*$ nAChRs on the effect of nicotine on inhibitory transmission has been suggested in young rats (Genzen and McGehee, 2005; Takeda et al., 2007; Gao et al., 2010). Although most studies focus on LII, an $\alpha7$ nAChRs-mediated effect was found on inhibitory transmission in LV neurons (Takeda et al., 2007). In addition, nicotine, as well as a partial $\alpha4\beta2$ agonist, also produced an increase in frequency of spontaneous and miniature EPSC (Genzen and McGehee, 2003; Takeda et al., 2003).

In vitro recording also enabled to gain information of nAChR located in the somato-dendritic compartment, leading to so-called post-synaptic responses (Takeda et al., 2003; Cordero-Erausquin et al., 2004; Takeda et al., 2007). Single cell RT-PCR performed on you mice suggest that excitatory neurons express $\alpha3\beta2\alpha7^*$ while the inhibitory neurons demonstrate $\alpha4\alpha6\beta2^*$ nAChRs (Cordero-Erausquin et al., 2004). Application of selective antagonists suggest that superficial laminae contain non-$\alpha4\beta2$ (Takeda et al., 2003) whereas LV express $\alpha4\beta2^*$ nAChRs (Takeda et al., 2007).

There is functional evidence supporting the presence of nAChR on DRGs and primary afferent fibers. In DRGs of neonate rats, 4 types of response were observed: α7-like, α3β4-like, α4β2-like and unclassified receptor types (Genzen et al., 2001). Moreover, nicotine increased primary afferent evoked responses, via α7 receptors, which increased the probability of LTP in DH cells of young rats (Genzen and McGehee, 2003). In cultured DRG neurons from adult rats, they observed three nicotine evoked responses: the slow decaying currents were attributed to α3β4*; the fast decaying responses mediated by α7; and simultaneous fast and slow decaying currents by heteromeric nAChR (Fucile et al., 2005). The expression of nAChRs was studied more specifically on nociceptors. The capsaicin-sensitive, unmyelinated fibers expressed α7 and other nAChRs while other nociceptors expressed α3β4 and α3β4α5 subtypes (Rau et al., 2005). Moreover, α6β4* nAChRs was observed in the PNS (Smith et al., 2013). The expression of these nAChR subtypes can explain the pro-nociceptive behavioral effect of nicotine.

Moreover, the nAChR have been implicated in PAD [cf section 1.3.2]. nAChR antagonists were reported to reduce dorsal root potential amplitude, through α9 receptors nAChRs (Hochman et al., 2010). This can occur by activation of GABAergic interneurons by an upstream cholinergic component or by direct activation of the fibers. ACh released can act directly on the primary afferents via bicuculline-sensitive nAChR (i.e nAChR antagonized by classical GABA-A antagonists) such as α9 and α10 nAChR (Shreckengost et al., 2010).

It has been reported that nAChRs modulate descending controls via the PAG-RVM pathways. Presynaptic nAChR may temporarily regulate the excitability of PAG neurons but not overexcite them, thus modulating the PAG output (Nakamura and Jang, 2010). Recently, it was described that two-thirds of PAG-RVM projection neurons expressed α7 receptors and that presynaptic nAChR increased glutamatergic inputs to PAG-RVM projection neurons (Umana et al., 2017) .

**Role of AChE:**

In vitro on spinal slices from adult rats, application of neostigmine (AChE inhibitor) resulted in an increase in the frequency of GABAergic IPSCs that is blocked by atropine, a non-specific mAChR antagonist (Baba et al., 1998). Similarly, neostigmine increased the frequency of spontaneous IPSCs in LII neurons; which was blocked by mecamylamine and DHβE (Rashid et al., 2006). In neonate rats, Methamidophos or neostigmine (AChE antagonists) along with atropine resulted in an increase in the frequency of miniature EPSCs and subsequently blocked by MLA (Genzen and McGehee, 2003). In the trigeminal nerve of young rats, physostigmine (AChE antagonist) reduced

the amplitude of primary afferent evoked EPSCs (Jeong et al., 2013). In general, ACh plays an important role in modulating excitatory and inhibitory transmission in the spinal cord.

**Endogeneous cholinergic tone**

The endogenous spinal cholinergic tone revealed by behavioral experiments proved more difficult to identify in vitro; and only a nicotinic component was observed. The primary afferent evoked EPSCs demonstrated no difference in the presence of M2, M4 and M2/M4 subtypes antagonists for both rats (Zhang et al., 2007a) and mice (Zhang et al., 2006). However, in the presence of mecamylamine, a general nAChR antagonist, spontaneous EPSCs were unaffected but different responses were noted for spontaneous IPSCs of adult mice. Approximately one-third of neurons had a reduction in frequency of spontaneous IPSCs while a small fraction had an increase. The DHβE reduced the frequencies for both GABAergic and glycinergic IPSCs; unlike MLA, an α7 nAChR antagonist, which resulted in reduction in one-sixth of mecamylamine-sensitive cells (Rashid et al., 2006). This suggests a tonic activation of heteromeric nAChRs in inhibitory interneurons. Futhermore, tonic activation of cholinergic tone has been described with descending 5HT pathway; whereby DHβE increased the basal release of serotonin (Cordero-Erausquin and Changeux, 2001). These electrophysiological data exemplify the diversity of the cholinergic system in the spinal cord, primary afferents and descending structures. [Review on role of cholinergic modulation of Pain (Naser and Kuner, 2017)]

## 3.4.    Potential sources of spinal acetylcholine

While preclinical and clinical behavior data have demonstrated the potential of spinal ACh to modulate nociceptive responses, the cellular source of this ACh was until recently controversial. Immunohistochemistry experiments with anti-ChAT antibodies demonstrate the presence of a dense plexus of cholinergic processes in DH laminae II-III (Barber et al., 1984; Olave et al., 2002). These processes, comprising both dendrites and axons, are therefore located in the same laminae where nociceptive and non-nociceptive primary afferents terminate. Moreover, they interact in a synaptic and reciprocal way with primary afferents. Indeed, cholinergic axons form pre-synaptic connections to unmyelinated and low threshold primary afferent fibers while these afferent fibers make synaptic contacts onto cholinergic dendrites (Ribeiro-da-Silva and Cuello, 1990). The interconnected and reciprocal interaction between primary afferents and cholinergic processes in laminae II/III appears to be the most probable substrate for cholinergic analgesia.

An ongoing debate continues regarding the source of the cholinergic processes observed in laminae II/III of the DH. Indeed the only local population of cholinergic interneurons, with cell bodies in laminae III/IV, is extremely scarce (Barber et al., 1984). However, there was a consensus on the absence of descending cholinergic controls into the DH (Kanazawa et al., 1979; Sherriff et al., 1991), until the recent description of cholinergic fibers in LIII coming from cell bodies located in the medial aspect of the RVM (Stornetta et al., 2013).

Moreover, the expression of pChAT has been reported on A- and unmyelinated C-fibers (Matsumoto et al., 2007). The combination of Electron microscope (EM) studies (Ribeiro-da-Silva and Cuello, 1990) and immunostaining in the Dorsal Root Ganglia (DRG) and spinal cord performed by our team has recently ruled out the primary afferent fibers as a major origin of cholinergic terminals in the DH (Mesnage et al., 2011). The EM data showed that the cholinergic fibers within the plexus are part of glomeruli. These glomeruli consist of primary afferent fiber, post-synaptic dendrite and presynaptic axon. The last two components arise from the DH and expresses ChAT, but no ChAT expression was observed in the incoming peripheral fiber. Furthermore, Mesnage and colleagues demonstrated that the cholinergic plexus was stained with cChAT whereas the DRGs remained unstained.

Our working hypothesis was therefore that the rare DH cholinergic interneurons are the main source of endogenous ACh at this level. Through EM, this population has been reported to receive contacts from both CTb and IB4+ expressing primary afferent fibers (Olave et al., 2002). This population has been reported in LIII/IV as a subpopulation of GABAergic neurons and co-localizes with NADPH diaphorase (Todd, 1991; Laing et al., 1994).

In a recent study by our team, these neurons were fully characterized though utilizing transgenic mice expressing the enhanced green fluorescent protein (EGFP) under the control of the ChAT promoter (ChAT::EGFP mice) (von Engelhardt et al., 2007; Mesnage et al., 2011). This allowed identifying these rare neurons in living tissue and filling them with a tracer to provide a detailed characterization of their morphology [Fig. 1.8]. They demonstrated dorsally orientated processes, highly elongated in the rostro-caudal direction. Their scarcity seems therefore balanced by an important dendritic and axonal territory (Mesnage et al., 2011). Interestingly, these cholinergic interneurons also express ACh, GABA and nitric oxide (Mesnage et al., 2011). Moreover, a large proportion of this population fires tonically. Although a similar population was thought to be absent from the spinal cord of primates, our team recently demonstrated the presence of a cholinergic interneuronal population in the DH of macaque monkeys, with similar densities with the one observed in rodents. Furthermore, an EM analysis demonstrated that, in the monkey too,
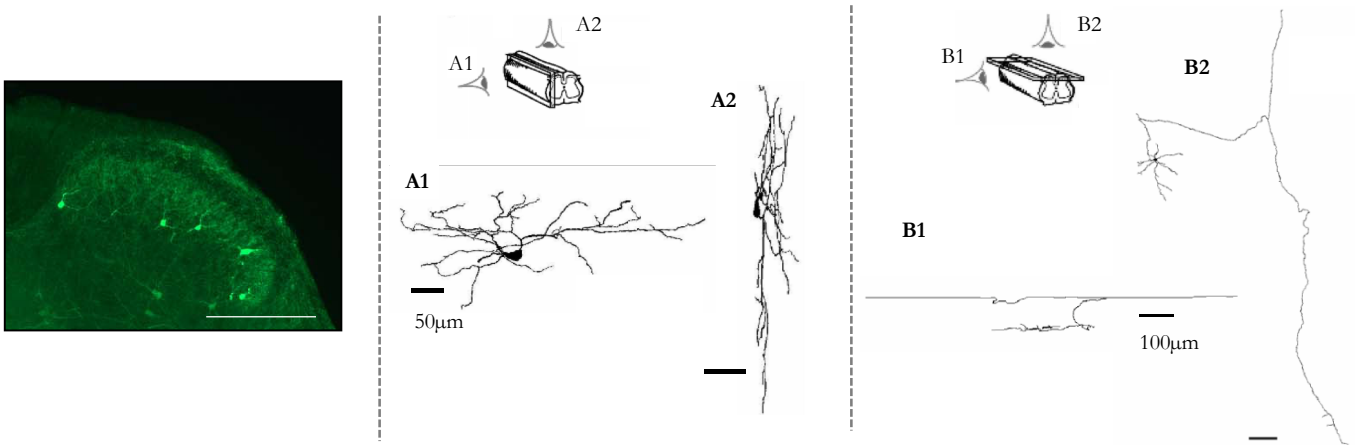
**Figure 1.8:** Anatomical and morphological aspects of Lamina III – IV cholinergic interneurons of the spinal cord. The distribution of cholinergic interneurons in the DH of ChAT::EGFP+ mice (Scale = 200 μm) (left). The morphology of this population is unique in that they have processes orientating towards the dorsal axis (middle) and very elongated in the rostrocaudal axis (right). [Modified from Mesnage et al , 2011]

cholinergic boutons are presynaptic to DH neurons as well as to the terminals of sensory primary afferents; therefore suggesting that they are likely to modulate incoming somatosensory information (Pawlowski et al., 2013b). The similarities observed between primates and rodents validates the interest of a mouse model, and our research endeavor continues with the goal of understanding how such a sparse neuronal population achieves a major control of nociception.

## 3.5. Conclusion: Spinal cholinergic tone and modulation of nociception

In naïve rodents, a spinal cholinergic tone maintaining nociceptive thresholds is reported through manipulating elements of the cholinergic system; i.e. ChAT, AChE and receptors (nAChR and mAChR). However, the role of this endogenous tone remains unclear following neuropathy.

A promising source for the spinal cholinergic tone is the DH cholinergic interneurons due to their unique morphology and localization within the DH network. Ultimately, the interplay of this sparse cholinergic population with surrounding nociceptive network can provide insights into understanding pain processing.

# Thesis objectives

My thesis aimed to improve our understanding of the spinal cholinergic system that is involved in nociceptive information processing, in naïve and neuropathic states. Two main objectives have been addressed:

1. To characterize the spinal cholinergic tone involved in establishing mechanical threshold, in naïve and nerve injured mice
2. To characterize the sparse population of dorsal horn cholinergic interneurons and their role in nociceptive information processing, in naïve and nerve injured mice

The first objective can be divided into 2 parts:

- Assessing the effect of the cholinergic system onto mechanical nociceptive threshold and responses of DH neurons to peripheral stimulation in vivo
- To determine the potential source(s) of ACh contributing to establishing this threshold

The second objective is divided into three parts:

- Study the dorsal horn and peripheral inputs to spinal cholinergic interneurons, to identify the conditions of their recruitment
- Characterize their electrophysiological and membrane properties, to identify their encoding properties
- Identify the downstream targets to the population, to elucidate the neurons responding to the cholinergic system and ultimately leading to the observed behavior.

# Chapter 2: Materials and methods

## 1. Animals

In general, our studies have utilized wild-type and transgenic CD1 and C57BL/6 mice between 3 – 10 weeks. Mice were born and raised in the animal facility of the Institute de Physiologie et Chimie Biologique (from 2013-2014) and the Chronobitron of the Neurochemistry building (from 2014 onwards). The animal facilities Chronobiotron UMS3415 are registered for animal experimentation under the Animal House Agreement A67-2018-38. In addition, supplementary wild type CD1 have been purchased from Charles River Labaratories for behavioral studies. Three different transgenic lines have been used:

(1) ChAT::EGFP CD1 mice were used to identify the sparse cholinergic population in the DH (von Engelhardt et al., 2007).

(2) Transgenic knock-in ChAT-Cre CD1 mouse line was utilized to allow specific expression of channels/receptors within cholinergic populations following virus injections. The C57BL/6J line was obtained from Jackson laboratories (Stock 006410, B6;129S6-Chat<tm2(cre)Lowl>/J), and backcrossed for more than 10 generations onto CD1 background.

(3) The β2*-nAChR knock-out C57BL/6J mice were used as controls to assess the interaction between high doses of cholinergic drugs and the β2*-nAChR receptors (Yalcin et al., 2011).

Male mice have been utilized in priority, except for β2*-nAChR knock-out control experiments, for which female mice was used for a single drug group. The animals were group-housed between two to six animals per cage and maintained on a 12-hour light/dark cycles with food and water provided *ad libitum*. All protocols were approved by the "Comité d'Ethique en Matière d'Expérimentation Animale de Strasbourg" (CREMEAS, CEEA35).

## 2. Cuff surgery

The cuff model is used to induce neuropathic pain in mice (Yalcin et al., 2011). The surgery was carried out under a mixed solution of drugs (10μl/g of animal). The mix (1 ml) solution contained: Ketamine (100 μl - Imalgene1000, Merial); Azepromazin (60 μl - Calmivet, Vetoquinol); Medetomidin (118 μl - Domitor, Orion pharma/Elanco) and NaCl 0.9% (722 μl). Following shaving around the surgical area, the right common sciatic nerve was exposed via blunt dissection

and then maintained by using wooden picks. A 2 mm section of split PE-20 polyethylene tubing (Harvard apparatus, Les Ulis, France) was placed around the right common branch of sciatic nerve in the cuff mice group. Sham-operated mice underwent the same surgical procedure without cuff implantation. The shaved skin was closed via suture. After the surgery, Atipamezol chlorhydrate (Antisedan, Orion pharma/Vetoquinol) mix (10 µl/g of animal), an antidote to medetomidin, was provided to speed up the recovery from the anesthesia. After one week recovery period after surgery, the neuropathic phenotype was assessed with von Frey tests (see below).

# 3. Spinal cord dissection for *in vitro* electrophysiology

## 3.1 Spinal cord extraction

The ChAT::EGFP or ChAT-Cre CD1 mice were anesthetized with Ketamine (200mg/kg - Imalgene 1000, Merial)/Xylazine (20 mg/kg - Rompun 2%, Bayer) mix via intraperitoneal injections (75 µl/ 25g). Older or virus-injected animals tend to be more susceptible to dissection therefore transcardiac perfusion was made following to anesthesia. The animals were perfused for approximately 3 minutes (until the liver becomes pale due to blood loss) with sucrose Artificial Cerebral Spinal Fluid (ACSF) (detailed in Table 2.1). It is crucial to maintain the solution at ice-cold temperatures (1-4°C) and continuously bubbled with carbogen (95% $O_2$/ 5% $CO_2$). The NaCl is replaced by sucrose to reduce neuronal firing and the massive release of glutamate which would result in excitotoxicity. Furthermore, the addition of kynurenic acid (2mM), a glutamate receptor antagonist, in sucrose ACSF aids in reducing excitotoxicity.

The spinal cord can be extracted via two approaches:

(1) Hydraulic extrusion of the spinal cord (Chery and De Koninck, 1999): The skin was incised parallel to the spinal column prior to decapitation. The vertebral column was cut at the thoracic (a few millimeters rostral to the last rib) and sacral levels (before the pelvic bone). A 200-mL pipette tip adapted onto a 10-mL syringe was filled up with ice cold sucrose ACSF solution. The pipette tip was inserted into the sacral opening of the column and extruded onto a petri dish (surrounded by ice) containing sucrose ACSF. The dorsal roots and the meninges (in part) were removed due to the rapid and forceful nature of the injected liquid. This dissection yield better results for younger animals (< 26 days) and was not appropriate for experiments requiring the attachment of dorsal roots to the spinal cord.

(2) In vitro laminectomy (Flynn et al., 2011): The animals were quickly decapitated and 4 incisions were made to extract the torso. Two cuts were made rostral and caudal to the

**Table 2.1: Extracellular solution used for *in vitro* electrophysiology**

| Substances | Sucrose aCSF (mM) | aCSF (mM) |
|---|---|---|
| Sucrose | 252 | - |
| NaCl | - | 126 |
| KCl | 2.5 | 2.5 |
| $CaCl_2$ | 2 | 2 |
| $MgCl_2$ | 2 | 2 |
| Glucose | 10 | 10 |
| $NaHCO_3$ | 26 | 26 |
| $NaH_2PO_4$ | 1.25 | 1.25 |

**Table 2.2: Intracellular solution used for *in vitro* electrophysiology**

| Substances | $K^+$ based intra-solution (mM) | $Cs^{2+}$ based intra-solution (mM) |
|---|---|---|
| $CH_3KO_3S$ | 136 | - |
| KCl | - | 5 |
| $MgCl_2$ | 2 | 2 |
| $Cs_2SO_4$ | - | 80 |
| HEPES | 10 | 10 |
| Biocytin | 10 | 10 |

vertebral column (described above) followed by 2 more on sides flanking the vertebral columns. The internal organs were removed before placing the entire vertebral column into a petri-dish filled with ice-cold sucrose ACSF. From the ventral side, the connective tissue surrounding the spinal column was removed to allow clear visualization of the vertebral bodies. The micro-scissor was inserted from the rostral opening and the vertebral bodies were removed successively. After exposing the spinal cord in the vertebral column, it was extracted from the caudal end with precautions made to preserve the dorsal roots. The vertebral column/spinal cord always remained in solution except for brief moments during exposure and/or transfer of spinal cord from vertebral column.

## 3.2    Slicing in various orientations

After extraction, the spinal cord was transected around the lumbar enlargement while unnecessary roots were removed (i.e. ventral roots). Depending on the slice type, the spinal cord was prepared in several orientation (Fig. 2.1).

- Horizontal slices (HS): The spinal cord was transferred to a square piece of paraffin where it was carefully dried. A small pliable rectangular paper piece was used to transfer the ventral side of the spinal cord into cyanoacrylate glue (Loctite, Henkel France) on a cutting platform. The blade ran along the spinal cord surface and brought down to the dorsal surface of the lumbar segment (in the center of the enlargement). A single slice was made between $200 - 300\mu m$ depending on the size and age of the spinal cord. The blade speed was at $0.03 - 0.04$ mm/s. This first slice was experimented on as it contains the first four laminae of the DH.

- Parasagittal (PS) slices: In this case the lateral edge of the spinal cord was glued onto cyanoacrylate glue. The blade was brought down to the lateral surface of the spinal cord. The first $100 - 150$ $\mu m$ thick slice was discarded (presumed to contain mostly white matter) and at least two $300 - 350$ $\mu m$ thick slices were subsequently made. These slices were cut at 0.03-0.04 mm/s. These slices contain the 6 laminae of the DH but with reduced medio-lateral spread.

- Transverse slices (TS): Prior to the dissection, a groove was performed in a 5% agarose block: its width and depth was approximately the one of the spinal cord, to maintain it in place during the blade movement. The piece of spinal cord was transferred into the groove, and the agarose block was transferred and secured onto the cutting platform with cyanoacrylate glue. $350 - 400\mu m$ thick slices were made at 0.2 mm/s moving blade.

**A**
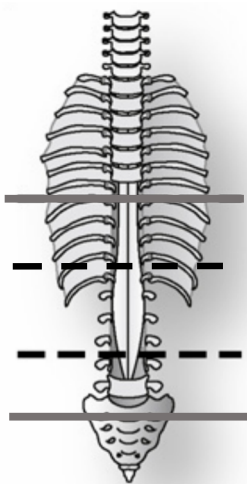
**B**
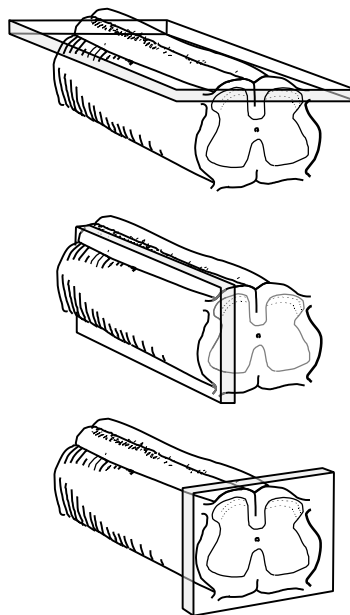
**Horizontal**

**Parasagittal**

**Transverse**

Modified from Flynn et al., 2011

**Figure 2.1:** Spinal cord dissection for in vitro electrophysiology. **9A:** The extraction of the spinal cord. The vertebral column was cut between T13 – S2 for hydraulic extrusion approach (Dashed black lines) and T9 – S6 for the in vivo laminectomy (Full grey lines) **9B:** Spinal cord preparation in three slice orientations. The slices are made from the lumbar segments of the spinal cord. Horizontal slices (HS, Top) contains the first four laminae of the dorsal horn (DH) of the spinal cord. Parasagittal slices (PS, Middle) has the DH although has a restricted rostro-caudal spread. Transverse slices (TS, Bottom) display all ten laminae of the spinal cord. The HS and PS have large rostro-caudal spread (> 1 mm) whereas the TS are restricted longitudinally.

The cutting platform was transferred in the slicing chamber of a sliding vibratome (Leica VT1200S) containing ice-cold sucrose ACSF. The slices were transferred onto a nylon mesh within a stocking chamber filler with ACSF (Table 2.1) bubbled with carbogen at room temperature. The slices were allowed a one hour recovery period prior to recording.

# 4. Electrophysiological recordings

Prior to performing whole cell configuration on target cells, several technical considerations must be optimized to achieve a successful patch.

## 4.1    Patch pipettes

The patch pipettes were made from borosilicate capillaries (CC120F-10 model; external diameter = 1.2 mm, internal diameter = 0.69 mm; Harvard Apparatus) and pulled either with a horizontal laser P-2000 or filament P-1000 puller (Sutter Instrument Co., Novato, California, USA). The final pipette resistance (i.e. when the pipette with intracellular solution was placed in ACSF bath) ranged between $4 - 6.5$ M$\Omega$.

## 4.2    Solutions

During recordings, the extracellular medium was ACSF solution (Table 2.1) similarly used to maintain slices in the stocking chamber.

Two intracellular solutions have been used to perform voltage and current clamp recordings. For voltage clamp, a cesium (Cs) based intracellular solution (Table 2.2) was used. The pH was fixed to 7.3 with Cesium hydroxide (CsOH) and the osmolarity was adjusted to $300 \pm 10$ mOsm with sucrose. The reversal potential of cations ($E_{cat}$) is at 0 mV while the chloride reversal potential ($E_{Cl}$) is set to -90 mV. During recordings of excitatory currents, the holding potential (Vh) was maintained at -60 mV and currents appeared as negative value with inward deflection (inward currents). For inhibitory currents recording, the Vh was held at 0 mV and these currents possessed positive values with outward deflection (outward currents). In addition, Cs ions are potassium (K) channel blockers (due to its larger size compared to K) when used as internal solution and prevents depolarization; thus, allowing recordings at 0 mV.

For current clamp recordings, the K-based intracellular solution allows the recordings of action potentials. The pH was fixed to 7.3 with potassium hydroxide and the osmolarity was verified to be $300 \pm 10$ mOsm. Regarding the extracellular and K intracellular solution, the reversal potential

of cations ($E_{cat}$) is at 0 mV while the chloride reversal potential ($E_{Cl}$) is set to -60 mV. For both intracellular solutions, biocytin diffused throughout the cells during recording thus allowing post-hoc morphological and neurochemical revelation.

Furthermore, a silver electrode was coated with AgCl used during recordings. For both intracellular solutions, the liquid junction potential was not corrected.

## 4.3 Visual patch recordings

We performed patch recordings where the slices were visualized with an upright microscope (Axio Examiner A1, Zeiss). The slices were observed through either the eye-piece or a digital camera (WAT-902H Ultimate, Watec) relaying the image onto a screen. The slice was orientated at a lower magnification (x10 objective) and subsequently the magnification was increased (x40 objective) to target and patch cells. To improve optics viewed on a screen, an infrared filter was added to reduce the scattering of light.

The electrophysiological experiments were performed on ChAT::EGFP animals. The cholinergic neurons were identified by the presence of green fluorescent protein produced under the ChAT promoter. Through an LED light source (Prixmatix) and appropriate filters, the green cells were identified prior to patching. A confirmation for patching a green cholinergic cell was made by either noticing a slight change in shape of the green cell when the pipette was placed on the membrane and/or observing a green piece of membrane within the pipette tip.

In general, the naïve cells were recorded through the lumbar segments. For sham and cuff animal groups, recorded cells were in the area corresponding to termination of the sciatic nerve (end of L3 – L6 spinal segments). The L4 segment was first identified due to the largest nerve corresponding to L4 nerve. Other spinal segments were identified in accordance to their respective spinal nerves while considering the L4 nerve. The different laminae were identified based on anatomical aspects of the spinal cord and/or the spinal cholinergic system. LII was identified utilizing the translucent crescent (for TS) or longitudinal (for PS) band due to reduced myelination. In addition, the dense cholinergic plexus in LII inner confirmed this lamina. In HS, the LIII/IV was determined by the few ChAT::EGFP neurons located on the surface of the first slice; these correspond to the sparse cholinergic interneurons of the DH. For PS and TS, LIII/IV was determined as the region below LII coupled with the presence of the sparse DH cholinergic interneurons. A band of white matter, corresponding to lateral funiculus, on PS (long longitudinal band) and TS (invagination into the grey matter) was used to assess the beginning of LV.

## 4.4    In vitro electrophysiology

The recording chamber was continuously perfused with ACSF solution via gravity. Different pharmacological substances were relayed into the recording chamber through a multi-tap system. In turn, the waste from the bath was removed by a peristaltic pump (Minipuls 2, Gilson). The reference (connected to the head-stage) was continuously immersed in the ACSF bath while a patch pipette approached an acute slice with micro-manipulators (MPC-200, Sutter Instruments).

A positive pressure was applied into the pipette prior to entering the bath for two reasons (1) to prevent the clogging of the pipette tip (2) to "clean" the surrounding area of the targeted cell. Simultaneously, a – 5 mV (20 ms) voltage step was imposed on the pipette at 50 Hz. The injected current to maintain this voltage step is used to assess the pipette resistance. Once the pipette tip was slightly touching the cell membrane, the pipette was further moved diagonally onto the cell until pipette resistance increased between 0.5 – 0.9 MΩ. Subsequently, the pressure was quickly removed and a tight junction was formed between the cell membrane and pipette. A Giga-seal (pipette resistance to the order of $10^9\,\Omega$) was established and the cell was in cell-attached mode.

To proceed into whole cell mode, the piece of membrane was broken due to slight aspirations applied to the pipette tip. Two transient capacitive currents were formed at the beginning and end of the voltage step; thus, indicating whole cell mode. These large currents were compensated by internal rectification within the amplifier.

## 4.5    Data acquisition

The recordings were made through the Axopatch 200A (Axon instruments) and the Multiclamp 700A (Molecular devices) in voltage and current clamp. The current traces were first filtered at 5 kHz, digitalized via a digitizer (BNC-2110, National Instruments) at 20 kHz and subsequently stored in hard disk of a computer unit. The long duration recordings were made with WinEDR software (Strathclyde Electrophysiology Software V3.6.6, John Dempster, University of Strathclyde, Glasgow, UK). For short voltage and current clamp recordings (i.e. electrical stimulations or repetitive current pulses with stepwise amplitude increase) were made on WinWCP program (Strathclyde Electrophysiology Software V5.1.3, John Dempster, University of Strathclyde, Glasgow, UK).

## 4.6 Baseline recordings

The spontaneous and miniature excitatory (EPSC) and inhibitory (IPSC) post-synaptic currents were recorded over a 5-minute period in voltage clamp mode. The miniature events were recorded in the presence of Tetrodotoxin (TTX) 0.5 μM (Table 2.3). In naïve animals, recordings were performed in HS, PS and TS. However, only HS and TS were utilized for sham- and neuropathic-animals because of the difficulty in obtaining parasagittal slices from the ipsi- and contra-lateral side (for comparison) from the same animal.

## 4.7 Active and passive membrane properties

In current clamp, the following parameters were studied: Resting membrane potential ($V_{rest}$) membrane input resistance ($R_{in}$), membrane capacitance ($C_m$), rheobase and firing patterns. These parameters were determined with repeated hyperpolarizing currents (-90 to -30 pA) and repetitive depolarizing current pulses (30 to 600 pA) with increasing amplitudes (30 pA increments with 700 ms duration). These current steps were injected in the soma from resting potential and the membrane potential ($V_m$) change was recorded. To prevent cell damage, the protocol was terminated when it appeared the action potential discharge was trailing off following the injected current.

## 4.8 Pharmacology

The various pharmacological substances were relayed in different tubes merging into a common pipette into the bath chamber. The perfusion rate is 3.5 mL/min which remained unaltered for the whole experiment. For each recording, a baseline recording was made 3 minutes prior to drug application. These substances were stored at stock concentrations in aliquots at -20 °C. The drugs were diluted to their final concentrations with ACSF just prior to the experiment. The different substances are summarized in Table 2.3.

## 4.9 Electrical stimulations

A suction electrode (stimulation electrode) was placed at the most distal region, relative to the spinal cord, of the dorsal root. A stimulation electrode was connected to an external stimulator (Isostim A320, World Precision Instruments).The recordings were made at both – 60 mV (mono- or poly-synaptic evoked EPSC) and 0 mV (polysynaptic IPSC) to assess the afferent induced responses. Various intensity ranges were tested (pulse duration 0.1 – 0.2 ms) to observe an afferent-induced response, either by Aβ, Aδ and/or C fibers, within the recorded cell. The stimulus

**Table 2.3: Pharmacological substances used for *in vitro* electrophysiology**

| Common name | Technical name | Supplier | Final concentration | Pharmacological target | Solvent | Storage |
|---|---|---|---|---|---|---|
| Capsaicin | Capsaicin | Toctris, | 5 µM | TRPV1 receptor agonist | Ethanol | 4 °C |
| Mustard Oil | Allyl isothiocyanate (AITC) | Sigma-Aldrich | 100 µM | TRPA1 receptor agonist | Milli-Q $H_2O$ | -20 °C |
| Menthol | (-) Menthol | Sigma-Aldrich | 500 µM | TRPM8 receptor agonist | Ethanol | 4 °C |
| TTX | Tetrodotoxin | Latoxan, Valence | 0.5 µM | Blockers of $Na^+$ voltage gated channels | Milli-Q $H_2O$ | -20 °C |

threshold of each evoked response is considered as the minimum current intensity to elicit at least one evoked current. A minimum of five stimulations were made for each intensity. To assess the fiber (Aβ, Aδ and C) nature of these responses, we performed a train of electric stimulation at frequencies of 1, 5, 10 and 20 Hz, as high-threshold C fibers are known not to follow at high stimulation intensity (Daniele and MacDermott, 2009)

Another variable to distinguish the afferent-mediated responses is the conduction velocity of afferent fibers. This is calculated from the response on-set latency (with respect to the stimulation artifact) of each response (see below) and the distance between the stimulation electrode and the recoding pipette. This was assessed in either of two ways: (1) After the recording, the approximate distance was calculated thanks to the images that were taken by a camera fitted over the eye-piece of the microscope. (2) The micromanipulator reports the exact co-ordinates of the patch pipette in the x, y and z dimensions. After recordings, the patch pipette was moved close to stimulation electrode tip and the total displacement was calculated from these two sets of co-ordinates. The combination of conduction velocity, synaptic connectivity (mono- or poly-) and fidelity of the evoked response to increasing frequency trains provides information on the fibers origin of these evoked responses.

## 4.10  Data analysis

<u>Voltage clamp</u>

The synaptic events were detected with the threshold search method with WinEDR software. The threshold was set, for miniature and spontaneous EPSCs, to amplitudes $\geq$ 2 pA and a duration $\geq$ 1.25 ms. For miniature and spontaneous IPSCs, the thresholds were set to amplitudes $\geq$ 3 pA and a duration $\geq$ 1.75 ms. A baseline track-time of 5 ms was implemented prior to each event. Following the automatic detection by the software, all captured events were inspected individually, and only events that possessed a quick rise followed by an exponential decay were kept. The absolute frequency is calculated as the number of events over the total duration of the recording. The peak amplitudes were measured for accepted events via semi-automated procedures in WinWCP. However, individual events were excluded if they contained overlapping events or had an unstable baseline. The frequency and amplitude of currents were analyzed over a 5-minute duration.

<u>Current clamp</u>

A program written in Labview (National Instrument) allowed the measurement of $R_m$ and $C_m$ during cell hyperpolarization steps. As previously described (Mesnage et al., 2011), the membrane

potential ($V_m$) change was recorded following injected current steps. The $R_{in}$ was calculated from the maximal membrane potential change ($\Delta V_m$) over the injected current step (I). The $\Delta V_m$ is given by $\Delta V_m = V_m - V_{rest}$, where $V_{rest}$ is the stable voltage phase before current injection. Assuming an isopotential cell, the cell membrane resistance ($R_m$) is equivalent to the $R_{in}$. Moreover, a membrane potential change is characterized by a single exponential with the time constant ($\tau$): this means that $\tau$ seconds following the application of the current step, the voltage of the membrane will be at $(1-e^{-1}) \approx 63.2$ percent of the maximum voltage drop (observed at the end of the current step). $\tau$ was therefore determined as the time needed to reach 63.2 percent of final voltage drop. The total membrane capacitance ($C_m$) was calculated as $C_m = \tau / R_m$. The $C_m$ and $R_m$ provide information on the number of open channels and cell size respectively. The rheobase current was determined as the smallest step current to produce at least one action potential. In some neurons, injection of hyperpolarizing currents induced a sag potential, characterized by a minimum reached within the first 50 ms and then a partial repolarization. This was quantified by calculating the percentage of minimum negative voltage within the last 50 ms, compared to the voltage drop at the end of the hyperpolarizing steps.

The software provided quantification of number of spikes with each injected depolarization currents and the time of inter-spike intervals (ISI). The spikes elicited by the injected step-current were detected using a derivative threshold method. The instantaneous frequency of spikes was calculated as the reciprocal of the ISI. The firing patterns were classified as previously reported (Gassner et al., 2013).

<u>Assessment of pharmacological responses</u>

For each neuron that has undergone pharmacological treatment, the cumulative number (N) of synaptic events was expressed as a function over time. Two best-fit line equations were applied to the cumulative events:

$$N = f_0 \times t + a \qquad\qquad for\ t < t_c \quad (1)$$
$$N = f_c \times t + (f_0 - f_c) \times t_c + a \qquad for\ t \geq t_c \quad (2)$$

In these equation, $t_c$ corresponds to the intersection point between the two best-fit lines and denotes the possible time in which the pharmacological agent produces its effect. The slope $f_0$ represents the average frequency before $t_c$ (i.e. the average frequency of baseline period) whereas the slope $f_c$ accounts the average frequency after $t_c$ (the average frequency during application). The constant 'a' is equivalent to y intercept of equation (1). We considered a neuron was responding to the drug if it had time-locked alterations (i.e. $t_c$ occurs within the drug application period) and had

a change in frequency of synaptic events greater than 20% of the baseline frequency of the recorded cell. This change in frequency was calculated as follows:

$$Change\ in\ frequency\ (\%) = \frac{[f_c - f_0]}{f_0} \times 100$$

<u>Electrical stimulation</u>

The recordings were analyzed using the clampfit software (version 10.7, Molecular Devices). The evoked afferent responses were screened utilizing the threshold search. Due to difficulties to determine the event latencies for superimposed events, only the first detected events were kept for this thesis. The jitter time was determined as the standard deviation of latency times of events evoked by a stimulation intensity. The conduction velocity was calculated as the total distance between the pipette tip and stimulation electrode over the averaged event latency.

# 5. Biocytin revelation

Following the recordings, the slices were stored in paraformaldehyde 4% (Original stock 32%, Electron Microscopy Science) diluted in sucrose ACSF to fix the tissues at 4 °C. At the time of writing this manuscript, we didn't have the time to perform the biocytin revelation and immuno-histochemical markers.

# 6. In vivo electrophysiology

All in vivo recordings were performed by Maria-Carmen Medrano. The methods employed can be found in her previous publication (Medrano et al., 2016). Briefly, adult CD1 males were anesthetized with urethane (2.5 g/ kg, i.p.) and the trachea was cannulated. A laminectomy was performed to expose L3-L5 segments of the spinal cord, and a small chamber (approximately 0.1 ml) was created with 2% agar around the exposed lumbar spinal cord; the drugs were directly applied in this chamber. Table 2.4 summarizes the drugs used for this study. Single-unit extracellular recordings were made with glass electrodes from dorsal horn neurons responding to mechanical stimulation of the ipsilateral hind-paw. The 10-s long stimulation was performed with: a camel's hair brush (for light touch stimulus), or small serrated forceps (for pinch stimulus).

**Table 2.4: Pharmacological substances used for *in vivo* electrophysiology**

| Common name | Technical name | Supplier | Final concentration | Pharmacological target | Solvent | Storage |
|---|---|---|---|---|---|---|
| Atropine | Atropine | Sigma | 10 µM | Muscarinic AChR antagonist | Milli-Q $H_2O$ | -20 °C |
| Mecamylamine hydrochloride | Mecamylamine hydrochloride | Sigma | 100 µM | Nicotinic AChR antagonist | Milli-Q $H_2O$ | -20 °C |
| Bicuculline | Bicuculline | Sigma | 10 µM | GABA-A receptor antagonist | Milli-Q $H_2O$ | -20 °C |
| PMBA | Phenylbenzene ω-phosphono-α-amino acid | Sigma | 10 µM | Glycine receptor antagonist | Milli-Q $H_2O$ | -20 °C |

**Table 2.5: Pharmacological substances used for behaviour**

| Common name | Technical name | Supplier | Final concentration | Pharmacological target | Solvent | Drug application route |
|---|---|---|---|---|---|---|
| Atropine sulphate | Atropine sulphate | Sigma | 1, 5, 10 and 15 nmol/10µl | Muscarinic AChR antagonist | Saline 0.9% | Intrathecal |
| Mecamylamine hydrochloride | Mecamylamine hydrochloride | Sigma | 10, 20, 100, 400 nmol/10µl | Nicotinic AChR antagonist | Saline 0.9% | Intrathecal |
| Scopolamine hydrobromide | Scopolamine hydrobromide | Sigma-Aldrich | 1, 5 and 10 nmol/10µl | Muscarinic AChR antagonist | Saline 0.9% | Intrathecal |
| Neostigmine bromide | Neostigmine bromide | Sigma-Aldrich | 10 nmol/10µl | Acetylcholinesterase inhibitors | Saline 0.9% | Intrathecal |
| Physostimine/ Eserine | Physostimine/ Eserine | Sigma | 1.5, 7.5 and 15 nmol/10µl | Acetylcholinesterase inhibitors | Saline 0.9% | Intrathecal |
| CNO | Clozapine N-Oxide | Carbo-synth | 10 mg/kg | Activator of hM4D$_i$ receptors (DREAD) | Milli-Q $H_2O$ | Intraperitoneal |

# 7. Behavior experiments

## 7.1 Drug injections

Intrathecal (i.t.) injections were performed under gaseous anaesthesia (3% Isoflurane for induction and 2% for maintenance). The animal was placed in a prone position (hunched-back) and the hair on their back was clipped. The caudal lumbar part, just above the iliac crests, was held rightly by the thumb and middle finger. The index finger was placed on the tip of the sixth lumber (L6) spinous process. A 33-gauge needle connected to a 50µl Hamilton syringe was inserted into the space between L5 and L6 vertebrae, and 10µl of the drug solution (Table 2.5), freshly dissolved, was injected. Solution was injected at approximately 1 µl/s. The needle was left in position for at least 30 s to prevent reflux of the solution. Each animal received a single dose of a single drug. For simplification, i.t. doses shall be denoted by their moles.

Clozapine N-oxide was administrated intraperitoneally All drugs used for behavior experiments are summarized in Table 2.5.

## 7.2 Nociceptive test: Mechanical sensitivity

We assessed the role of spinal cholinergic modulation on mechanical transmission in naïve and neuropathic CD1 mice. The mechanical threshold for hind-paw withdrawal was assessed with von Frey filaments (Bioseb, Chaille, France) with calibrated bending force. Mice were habituated for 15 minutes in clear Plexiglas boxes (7cm x 9 cm x 7 cm) on an elevated mesh screen. Filaments were slowly brought to the plantar surface of each hind paw and removed after a slight bent. The mechanical threshold is determined as three or more withdrawals observed among five consecutive trials. The filaments used in the study were labeled as: 0.01, 0.04, 0.07, 0.16, 0.4, 0.6, 1, 1.4, 2, 4, 6, 8, 10 and 15 grams. The results were expressed in grams. For naïve animals, the left and right paw data were averaged for each time point. The mice were tested prior to injection or surgery to establish the baselines. A minimum of three tests were performed over 3 to 7 days to determine the mechanical withdrawal threshold.

# 8. Virus injections via manual pressure

Injection of viruses had two objectives: (1) To determine the source(s) of spinal cholinergic tone either from local spinal and/or descending and/or peripheral ChAT populations. (2) To study the downstream neurons to ChAT interneurons in the DH.

## 8.1 Pipette and virus preparation

Borosilicate glass capillaries (1.2 mm OD, 0.69 mm ID, 100 mm L, Harvard Apparatus) were pulled with a horizontal puller to produce pipettes with long tapers (6-8 mm) and small tips. Under binoculars, these pipettes were recut by eye and could be resized until pipette is loaded with the virus. Aliquots (2.5 – 5 μl) of virus were stored at -80 °C and unfrozen prior to the experiment. A droplet of virus was placed on a paraffin strip and aspirated in the pipette via negative pressure. A 1 ml syringe connected to the end of the pipette through small tubing provided this negative pressure. The virus-filled pipettes were stored away from light at 4 °C prior to virus injections.

Two different sets of viral constructs have been used: (1) AAV8- hSYN-Flex-hM$_4$D$_i$-mCherry (Neurophotonics centre, Quebec) or AAV9-hSYN-Flex-hM$_4$D$_i$-mCherry (Neurophotonics centre, Quebec) (2) AAV2-CBA-Flex-WGA (Neurophotonics centre, Quebec).

## 8.2 Spinal cord injections

ChAT-Cre animals (≥ 3.5 weeks old) were anesthetized with gaseous anaesthesia (4% Isoflurane for induction and 2% for maintenance). After shaving the back, betadine 10% (Meda Pharma) was applied for 3 minutes to sterilize the area. The skin was incised with 24mm blade to reveal the vertebral column surrounded by connective tissue. We targeted L3-L5 spinal segments which are located between the T13- L1 vertebral space. The last rib was traced and marked on the muscles above the T13 vertebra. The vertebral column was exposed from surrounding muscles and was suspended with spinal clampers. The mouse was placed in a prone position revealing the intra-vertebral space. The exposed spinal cord had its dura matter removed with a bent 33 gauge syringe. This successful removal can be confirmed by loss of shiny surface combined with the leakage of cerebrospinal fluid.

For the injection, the pipette was zeroed at the surface on the midline of the spinal cord. The pipette was moved 400 μm laterally and 250 μm deep. A total volume of 180 to 270 nl of virus was injected via manual pressure into the spinal cord. The rate of injection was 90 nL/10s. The pipette was removed after 7 minutes (to prevent reflux of virus) and the opening was closed with metallic staples. Each mouse received 3 substances post-injection: (1) Metacam 2mg/ml (i.p. Boehringer Ingelheim) to treat post-surgery pain (2) Mannitol 12.5% (i.p) to improve virus infection (3) Saline 0.9% to rehydrate the mouse.

### 8.3  RVM injection

Similarly, adult ChAT-Cre animals have been used for RVM injections. The surgery was performed under gaseous anesthesia and mice were head-fixed with skull-flat stereotaxic configuration which aligns the bregma-lambda plane horizontally. After shaving and sterilizing the surface, the pipette was brought approximately 0.7 mm lateral to midline, and 1.2 mm caudal to lambda (Stornetta et al., 2013). The target position was marked with a pen on the skull. Subsequently, the pipette was retracted and an electric driller was used to perform a hole in the skull at the marked area. The pipette was brought back in the right position, at the surface of the brain and then down 6 mm. The virus was injected as previously described and the pipette removed only after 7 minutes. The skin was closed and mice received similar post-injection treatment as described above.

### 8.4  Dorsal root ganglia infection

To infect the DRGs, P5 ChAT-Cre heterozygous pups were bred from homozygous parents pairing. All pups were transferred into a separate new cage; leaving the parents in their home cage. The virus was drawn up into a 30 gauge needle connected to a Hamilton syringe (filled with mineral oil). The pup's body and hindpaw were held steadily while the syringe was inserted onto the plantar area of the hinpaw. Subsquently, 5 μl of virus was injected subcutaneously and the syringe maintained for at least 10 seconds. After all pups were injected, the whole litter was returned to the home-cage.

## 9. Tissue fixing and slicing preparations

The animals were transcardially perfused under pentobarbital (Ceva Sante Animal, 54.7mg/ml, i.p. injection) with 0.1M phosphate buffer (PB, pH 7.4) followed by 4% Paraformaldehyde (PFA) in PB for 15 minutes. For spinal cord and DRG extraction, the sciatic nerve was traced thus preserving the L3, L4, L5 and L6 (if present) DRG and roots attached to the spinal cord. However, in vitro laminectomy was performed when only the spinal cord was kept. Moreover, the brain was quickly extracted. All removed tissue was postfixed overnight in 4% PFA in PB 0.1M and stored in Phosphate Buffer Solution (PBS) at 4°C. 50μm-thick transverse or parasagittal sections were produced with a vibrating blade microtome (VT 1000S, Leica, Rueil-Malmaison, France) and were serially collected in wells. The tissues were stored away from light at 4 °C.

# 10. Staining

Two immunohistochemistry protocols were implemented. For sole ChAT revelation, the sections were washed three times with PBS and saturated with PBS/ 0.5% Triton X-100/ 5% donkey serum at room temperature for 45 minutes. The sections were incubated at room temperature overnight in PBS/ 0.5% Triton X-100/ 1% donkey serum with goat polyclonal ChAT antibodies (1:500 dilution, Chemicon Millipore, AB 144P). After three PBS washes, the slides were incubated with CY3 anti-goat antibodies (1:400 dilution, Jackson Immunoresearch) for 2 hr. The sections were finally washed three times with PBS and mounted with fluorescent mounting media (Dako, Les Ulis, France).

For WGA and ChAT revelation, the sections were washed three times with PBS/ 0.3% Triton X-100 and saturated with PBS/ 0.3% Triton X-100/ 5% donkey serum at room temperature for 45 donkey serum with goat polyclonal ChAT antibodies (1:250 dilution, Chemicon Millipore, AB 144P) and rabbit polyclonal anti-WGA (Sigma-Aldrich). After three PBS/ 0.3% Triton X-100 washes, the slides were incubated with CY3 anti-goat antibodies (1:400 dilution, Jackson Immunoresearch, 705-165-147) and Alexa anti-rabbit (1:400 dilution, Invitrogen, A21206 ) for 2 hr. The sections were washed three times with PBS, placed in serial order and mounted with mounting media. All slides were examined under fluorescence using a microscope (Leica) and cell counting was made.

# 11. Statistics

The statistical analysis was performed with the statistical software R (version 3.4.1) in conjunction with Graphpad software (Prism 7 for Mac, GraphPad Software, Inc., San Diego, CA, USA). Similarly, the graphical illustrations were made with Graphpad software.

For in vitro data, almost all statistical comparisons for frequency, amplitude and cell properties, considering the various dependent variables, were made with the ANOVA function. The original or transformed (log or inverse function) datasets were verified to show a normal distribution (Shapiro-Wilk normality test). For post-hoc comparisons, interactions with only one or two variables were made with TukeyHSD (honest significant difference) test. However, Dunnett test for multiple comparisons were made for interactions involving 3 or more variables. For non-normalized dataset (i.e. Rheobase), we used the Kruskal-Wallis test. The Fisher's exact test was used to compare proportion of contingency tables for pharmacological experiments. A more

complex 3x3x3 contingency table was performed online at http://vassarstats.net/abc.html for firing pattern and rebound spike observations.

For in vivo data, statistical evaluation was carried out with non-parametric tests because most of the data did not show a normal distribution (Shapiro-Wilk normality test). In addition, the paired-samples Wilcoxon test signed-rank was performed to compare the effects before and after drug application within the same cell. The two-sample Wilcoxon-Mann-Whitney rank-sum test was performed to compare independent groups.

For behavioral data, the significance of the data was measured using non-parametric tests due to its non-continuous nature. The statistical software R-based plug-in "nparLD" (Noguchi et al., 2012) provided an ANOVA type multiple-factor analysis taking into account a longitudinal variable (time) along with multiple dependent (right vs left paw) and independent (surgery; drug treatment) variables. nparLD was also used for posthoc comparisons against baseline (Time 0).

The significance level was set at $P < 0.05$ and data were expressed as mean $\pm$ SEM for graphs.

# Chapter 3: Plasticity of the spinal cholinergic tone after neuropathy

## 1. Context and objectives

Endogenous acetylcholine (ACh) is an important modulator of nociceptive sensory processing in the spinal cord. Epidural administration of neostigmine, an acetylcholinesterase inhibitor - preventing ACh degradation thus increasing its levels, provides pain relief for child birth and post-operation pain in clinics (Eisenach, 2009). In rodents, antagonizing nicotinic and muscarinic ACh receptors in the spinal cord leads to hyperalgesia and/or allodynia (Honda et al., 2002; Rashid et al., 2006). This suggests that a basal tone of spinal ACh modulates the threshold for nociceptive responses. This tone appears to be disrupted in neuropathic animals (Rashid and Ueda, 2002), however, the details of the plasticity of the spinal cholinergic system observed during neuropathy remains elusive.

Besides well-documented evidence on the cholinergic tone, the source contributing to spinal ACh remains controversial. Three groups of cholinergic neurons, expressing Choline Acetyltransferase (ChAT), the synthesizing enzyme for ACh, potentially terminate within the Dorsal Horn (DH) of the spinal cord. They are located in the Dorsal Root Ganglia (DRG) (Matsumoto et al., 2007), Rostral Ventromedial Medulla (RVM) (Stornetta et al., 2013) and Spinal Cord (SC). Herein, the last structure contains a potential local source: diverse cholinergic interneuron populations have been described within the SC (Barber et al., 1984).

To improve our understanding of spinal cholinergic analgesia, this section contains two main objectives:

- To characterize the cholinergic tone modulating mechanical nociceptive responses and its plasticity after peripheral nerve injury in *in vivo* conditions
- To elucidate the potential source(s) contributing to the spinal cholinergic analgesia

# 2. Characterization of the spinal cholinergic tone in naïve mice

## 2.1. Behavioral characterization

### 2.1.1. General overview

Prior to the pharmacological assessment, male CD1 mice (ChAT::EGFP mice or their wild-type littermates, 5-9 weeks old) were tested over 3 to 7 days for their mechanical withdrawal threshold (Von Frey test) to ensure that their threshold was stable (at least three measures, the last one being on the experiment day). The value at time "0" corresponds to the last measurement made on the experiment day.

Since ChAT::EGFP mice are BAC transgenic strains, the random and multiple integration of the transgene in the genome could impact the behavior. Therefore, the paw withdrawal threshold (PWT) of ChAT::EGFP mice (Mean = 3.919 ±0.087, N = 62) and of their wild-type (WT) littermates (Mean = 4.081 ±0.098, N = 74) in naïve conditions were compared; with no significance found (p = 0.2658; Mann-Whitney test; results not shown). Subsequently, the two groups of animals were pooled for all the behavioral study.

*Interpretation-discussion:* No differences in the PWT were observed between ChAT::EGFP animals and their WT littermate. This suggests that the multiple insertion of the BAC transgene does not influence the behavior under study (PWT).

### 2.1.2. Nicotinic antagonist: mecamylamine

Mice were injected i.t. with the non-specific nicotinic antagonist mecamylamine (10-100 nmol) or with saline (0.9% NaCl), and tested at different time points after the injection (Fig. 3.1A). Mecamylamine induced a dose-dependent reduction in the mechanical withdrawal threshold that was visible as soon as 5min post-injection and lasted more than two hours for higher doses. 100 nmol mecamylamine did not have a more pronounced effect than 20 nmol, although its effect lasted longer: the mice still had a withdrawal threshold of 1.42 g at 150 min after the 100 nmol injection, while their threshold was back to 2.94 g after the 20 nmol injection.

*Interpretation-discussion:* We confirmed the observation that i.t. nicotinic antagonists produce mechanical allodynia, in another mouse line than ddY (Rashid et al., 2006). In addition, we have performed a full dose-response curve of this effect. The pharmacological effect of an antagonist suggests the existence of a spinal cholinergic tone, acting via nicotinic receptors, participating in the control of mechanical threshold.
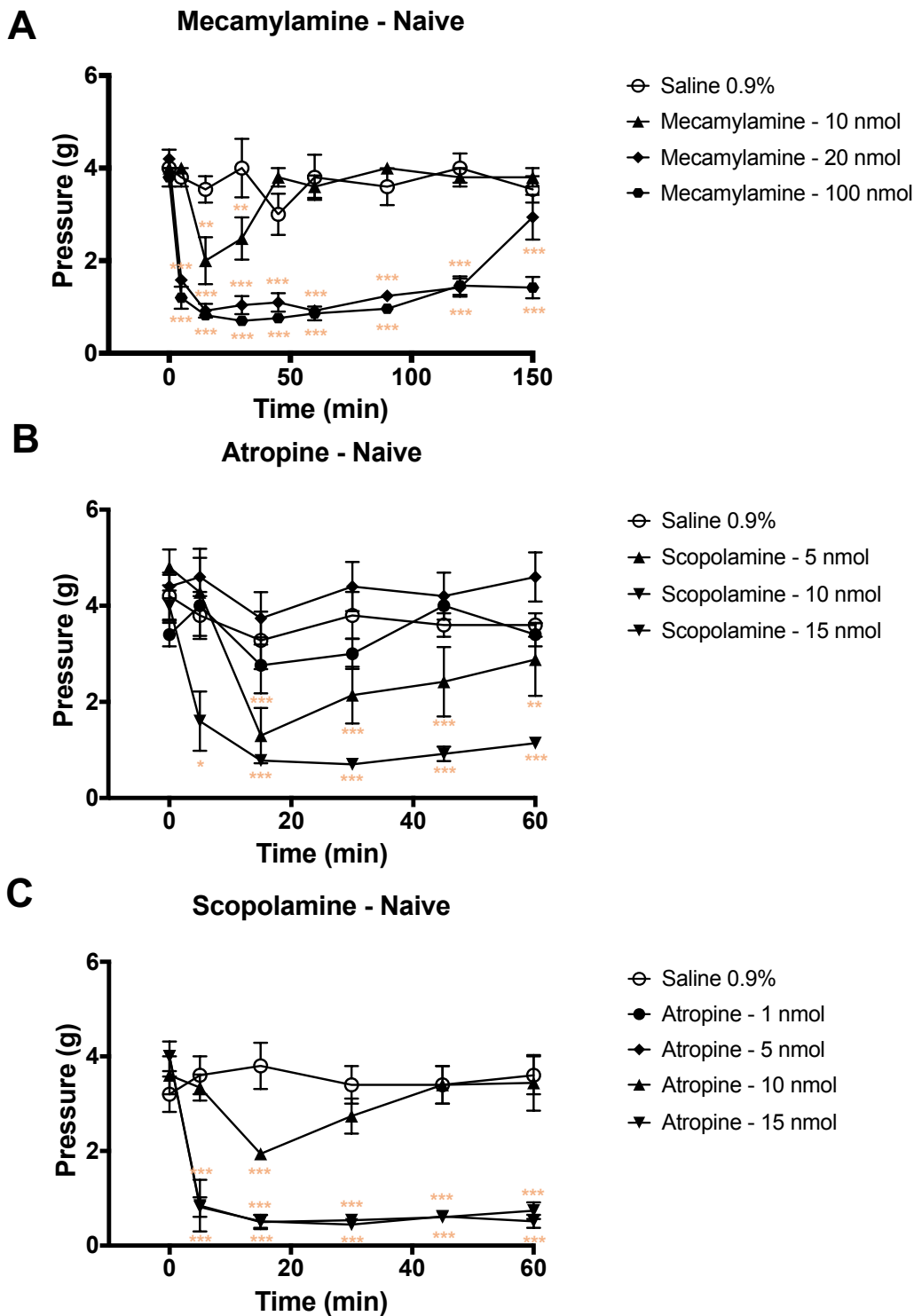
**Figure 3.1:** Time course of the effect of intrathecal mecamylamine (nicotinic antagonist -Top; 3.1A), and atropine and scopolamine (muscarinic antagonists – Middle and Bottom; 3.1B,C), antagonists on mechanical threshold of naïve Cd1 mice [Groups n = 5 - 6]. **3.1A:** Mecamylamine induced mechanical hyperalgesia at 10, 20 and 100 nmol (Drug-Time interaction: $p < 0.001$, post-hoc: TukeyHSD). **3.1B:** Atropine induced mechanical hyperalgesia at 10 and 15 nmol (Drug-time interaction: $p < 0.01$, post-hoc: TukeyHSD). **3.1C:** Scopolamine reduced mechanical threshold at 5, 10 and 15 nmol (Drug-time interaction: $p < 0.001$, post-hoc: TukeyHSD). *** $p < 0.001$ vs baseline, ** $p < 0.01$, * $p < 0.05$.

The effect we observed with 10 nmol mecamylamine was slightly shorter than the one observed by Rashid and authors, as they reported a mechanical allodynia lasting up to 90 min while we observed return to baseline after 45 – 60 min.

### 2.1.3. *Muscarinic antagonist: atropine and scopolamine*

We similarly tested the mice with i.t. injections of two non-specific muscarinic antagonists: atropine (1-15 nmol), or scopolamine (5-15 nmol); and with saline (0.9% NaCl). Both atropine and scopolamine produced a dose-dependent reduction in the mechanical withdrawal threshold (Fig. 3.1B and C). Like for mecamylamine, this effect was visible as soon as 5 minutes post-injection although it reached its peak effect at 15min post-injection. It lasted more than an hour (and up to 4 hours for the higher doses of scopolamine, result not shown).

*Interpretation-discussion:* The spinal cholinergic tone is also acting via muscarinic receptors to modulate the mechanical threshold. The contribution of muscarinic receptors had only been demonstrated to date in rats, where hyperalgesia was observed following to mechanical stimulation on their tails (Zhuo and Gebhart, 1991). The literature reported no change in mechanical PWT in mice following intrathecal application of Atropine (273 pmol); the M1 type antagonist Pirenzepine (50 nmol); the M3 type antagonist 4-DAMP (30 nmol) and the M2 type antagonist Methoctramine (15 nmol) (Honda et al., 2002). Similarly, atropine (30 μg) produced no alterations to the mechanical PWT of rats (Paqueron et al., 2003). In contrary, we observed a change in the PWT potentially due to higher doses studied.

While nicotinic receptors are ionotropic and lead to depolarization thus excitation of the neurons, muscarinic receptors can produce either excitation or inhibition of the neurons depending on their subtype. In order to explain the similar behavioral effect of nicotinic and muscarinic antagonists in these experiments, there are two working hypotheses: i) the involved muscarinic receptors are of the M1-3-5 type, linked to Gq (with an excitatory output) and could be expressed by the same neurons expressing the nicotinic receptors, or ii) they are of the M2-4 type, linked to Gi/o, but are expressed by neurons having an opposite effect on the final behavior.

### 2.1.4. *Control experiments in β2 knock-out mice*

In order to obtain the dose-response curve, we had to use relatively high concentrations of cholinergic antagonists with potential non-specific effects. We even increased the dose of mecamylamine in experiments on neuropathic animals (see below). We had at our disposal β2 nicotinic knock-out mice (β2 K/O) that enabled us to test whether these high doses of
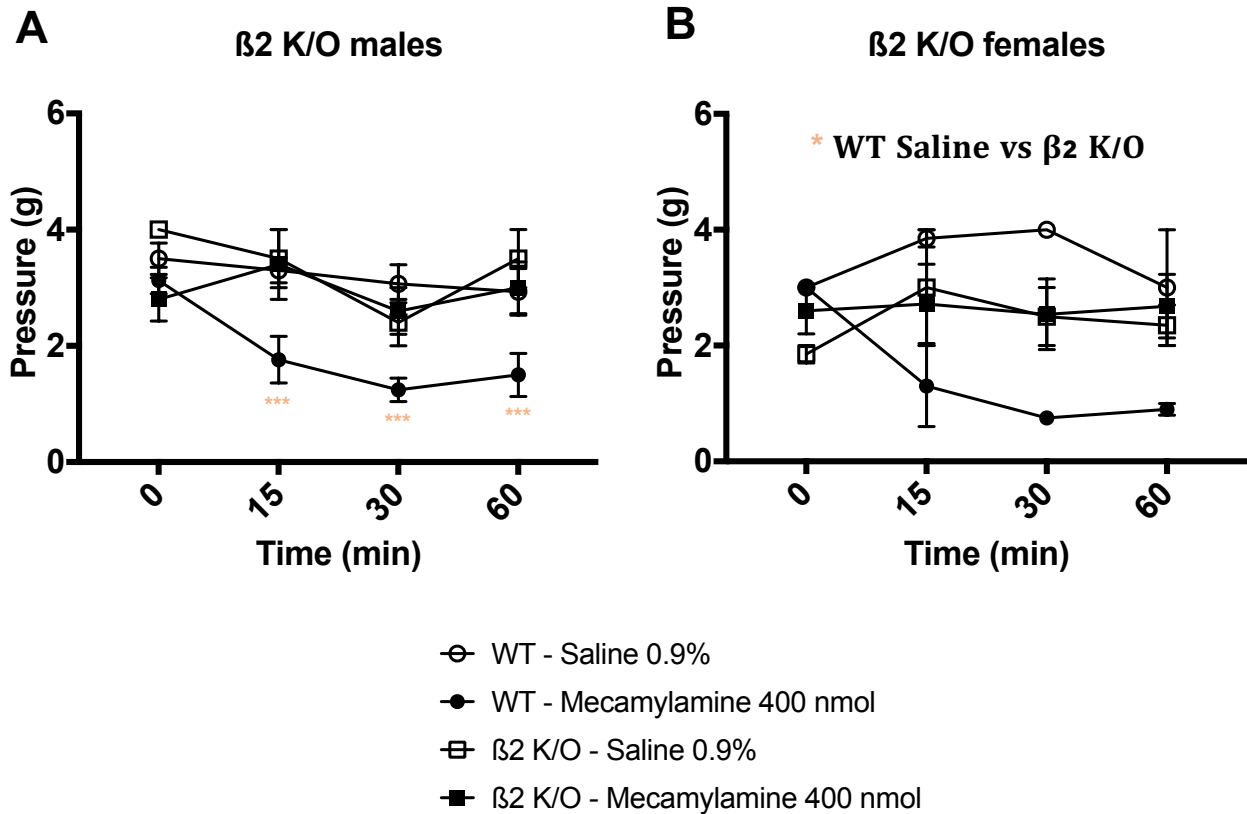
**Figure 3.2:** Time course of the effect of intrathecal mecamylamine (nicotinic antagonist) on mechanical threshold of naïve males (Fig. 3.2A) and female (Fig. 3.2B) WT and β2* nAChR knock-out (β2 K/O) C57BL/6 mice [Groups n = 2 - 10]. **3.2A:** Mecamylamine induced mechanical allodynia at 400 nmol in WT males but not β2 K/O (Animal:Time:Drug interaction: $p < 0.05$, post-hoc: Dunnett's multiple comparisons). **3.2B:** Mecamylamine induced mechanical allodynia at 400 nmol in WT females but not β2 K/O groups (not individual time points) (Animal:Drug interaction: $p < 0.001$, post-hoc: Dunnett's multiple comparisons) *** $p < 0.001$, ** $p < 0.01$, * $p < 0.05$.

mecamylamine was specific to nAChR receptors. Due to the low-success of breeding and limited amount of β2 K/O animals available, we used both males and females for this experiment.

While 400 nmol i.t. mecamylamine induced a marked reduction of the mechanical withdrawal threshold in WT animals, it produced no effect on β2 K/O mice (Fig. 3.2).

*Interpretation-discussion:* The β2 subunit of nicotinic receptors, in conjunction with α4 subunit - thus α4β2* nAChRs, are the most common subunit found in the CNS (Wu and Lukas, 2011). There is a massive reduction in nicotinic binding in β2 K/O mice (Marubio et al., 1999). In addition, these mice have been reported to have reduced mechanical and thermal thresholds (Yalcin et al., 2011); we surprisingly did not reproduce this observation. Admittedly, the mechanical PWT for wild type male animals in the Yalcin study was on average around 6 g, while we measured 3.5±0.18g (n = 18). For the β2 K/O mice, the study reported approximately 2g whereas we observed 3.1±0.34g (n = 7). These differences could be explained by a bias due to the experimenter, or to some environmental (stress?) or genetic (drift?) factors.

Importantly, we reproduced the effect of i.t. injection of a non-specific nicotinic antagonist in the wild-type littermates, while the effect of 400nmol mecamylamine was completely lost in β2 K/O mice. This strongly suggests that this antagonist acts specifically through β2*-nAChRs to control mechanical thresholds. In a similar fashion, the non-specific nAChR antagonist Hexamethonium lost its effects in β2 K/O mice thus reaffirming the requirement of β2* nAChR in establishing nociceptive thresholds at the spinal level (Yalcin et al., 2011).

## 2.2.    *In vivo electrophysiological characterization*

The effect of cholinergic antagonists on dorsal horn neurons was recorded in vivo by Dr. Maria-Carmen Medrano, a post-doctoral fellow in our team. I summarize her results here as they will be of interest for the discussion of my results (and part of the manuscript we are preparing).

In the 2016 paper, Medrano demonstrated that there are spontaneously and non-spontaneously active neurons in the DH, and she studied them separately. However, she also demonstrated that some of these neurons change "phenotype" by becoming spontaneously active after neuropathy, blurring the borders between these two populations. We therefore decided to analyze them as a single population in the present study.
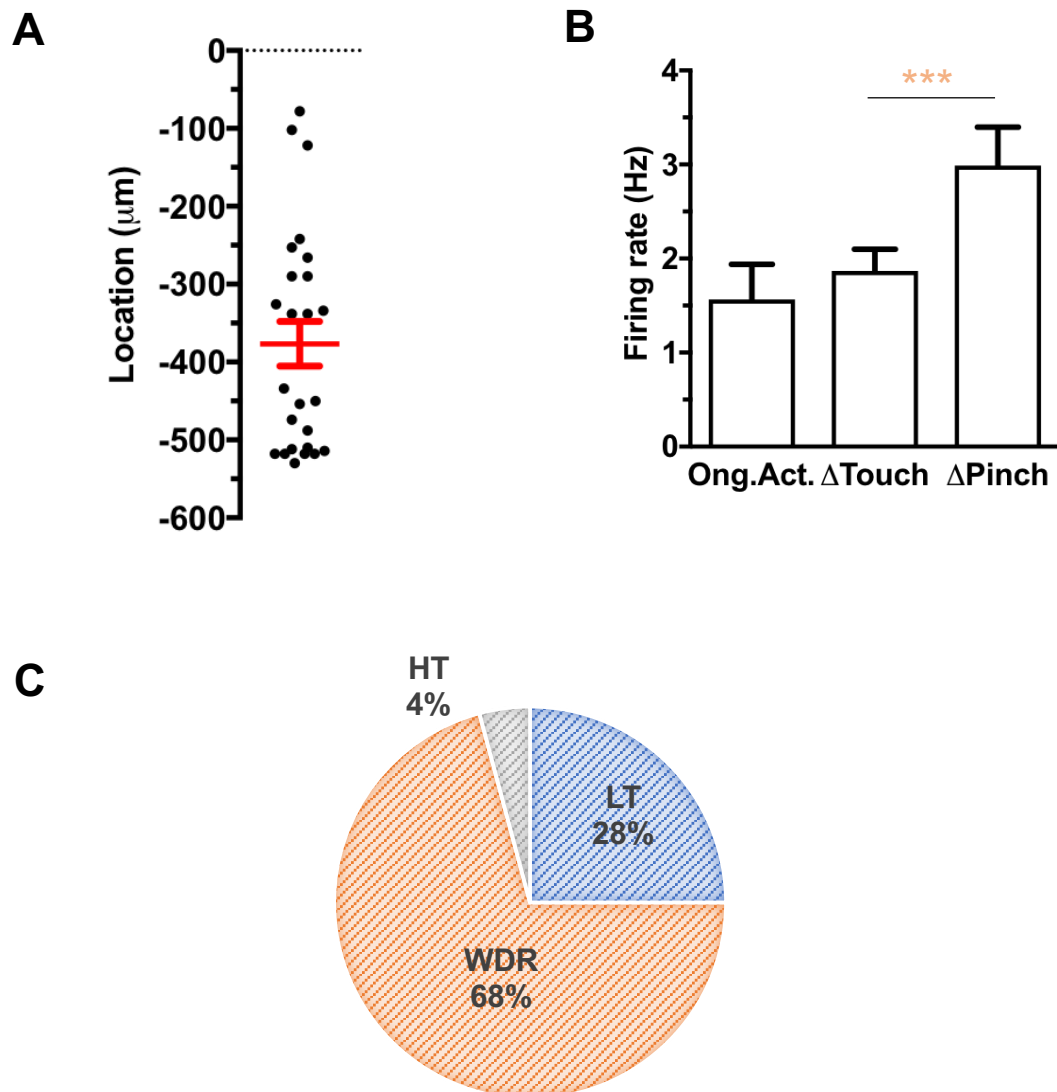
**Figure 3.3:** The characterization of recorded neurons in the DH. **3.3A**: Location of the recorded DH neurons (N = 24). Symbols are the individual cells and red lines are the mean ± S.E.M of neurons. **3.3B**: The effect produced by touch and pinch on neurons in naïve mice. Increase of firing rate induced pinch was greater than in touch. Bars represent the mean ± S.E.M of the increase of firing rate during touch and pinch application (10 s); ***p < 0.001 touch vs. pinch (Paired-samples Wilcoxon test). **3.4C:** The percentages of Low Threshold (LT), Wide Dynamic Range (WDR) and High Threshold (HT) neurons. LT, WDR and HT classification is based on the ratio between the effect of touch and pinch.

### 2.2.1. Properties of recorded neurons

Recorded neurons were distributed along the dorsal horn, with an average depth of 370.8 μm ± 29.23 μm (range: 78, 530 μm) (Fig. 3.3A). All the selected neurons responded to mechanical stimulation of the paw with an increase in firing rate; the increase was higher after pinch compared to touch (Fig. 3.3B) (N = 24, p < 0.001 for Δtouch vs Δpinch, Paired-samples Wilcoxon test).

Three types of neurons could be distinguished based on their differential response to touch *vs.* pinch: i) low-threshold (LT) neurons responded equally or more to non-noxious touch than to noxious pinch; ii) wide dynamic range (WDR) neurons responded more to pinch than to touch; and iii) high-threshold (HT) neurons responded only to pinch, or at least ten times more to pinch than to touch. The large majority of recorded neurons were WDR (Fig. 3.3C).

*Interpretation-discussion:* The recorded neurons had properties similar to the one already published (Medrano et al., 2016).

### 2.2.2. Nicotinic antagonist: mecamylamine

The nicotinic antagonist mecamylamine (100 μM) was applied locally at the surface of the spinal cord. It produced an elevation in the ongoing activity of the neurons. On top of this increased ongoing activity, touch and pinch also induced larger responses in the presence of mecamylamine (Fig. 3.4A) (N= 12, p <0.05 for ongoing activity and pinch & p < 0.01 for touch with drug vs control, Paired-samples Wilcoxon test).

*Interpretation-discussion:* The effect of the nicotinic antagonist on DH neurons firing demonstrates that they are under the control of a cholinergic tone acting through nAChRs. Although we do not infer a causal link, such increase in ongoing activity is also observed in DH neurons after neuropathy (Medrano et al., 2016).

In addition, these recordings demonstrate that the spinal cholinergic tone also tunes the intensity of DH neurons response to hindpaw mechanical stimulation. Although the neurochemical nature and the role of recorded neurons in nociceptive circuits is not known, it is tempting to relate their increased response to a peripheral input with the observed mechanical allodynia after i.t. mecamylamine in behaving animals.

### 2.2.3. Muscarinic antagonist: atropine

Maria Medrano similarly applied the muscarinic antagonist atropine (10 μM) locally at the surface of the spinal cord. This also produced an elevation in the ongoing activity of DH neurons, as well
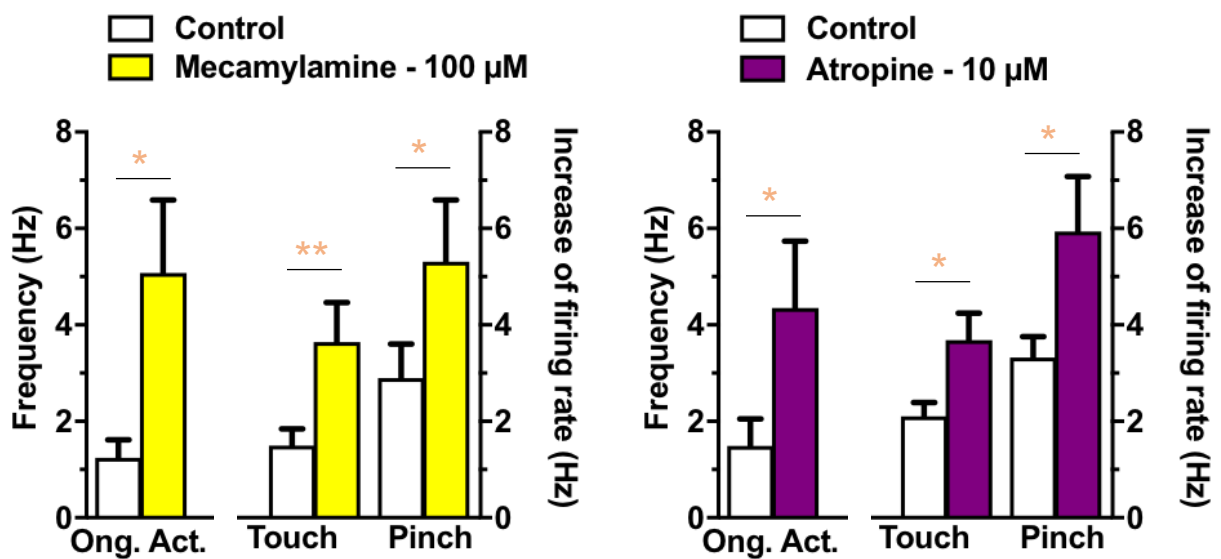
**Figure 3.4:** The effect of cholinergic drugs on touch and pinch response in DH recorded neurons. **3.4A**: Effect of mecamylamine (non-specific nAChR antagonist) on touch and pinch responses animals (N = 12). Mecamylamine increased the ongoing activity and responses to touch and pinch. **3.4B**: The effect of atropine (non-specific mAChR antagonist) in touch and pinch on neurons in naive mice (N= 12). Similarly, the ongoing activity, responses touch and pinch was elevated in the presence of atropine during sham. However atropine lost all its effects in cuff animals. Bars represent the mean ± S.E.M of the increase of firing rate during touch and pinch application (10 s); ** p < 0.01; *p < 0.05 touch or pinch with drug vs control (Paired-samples Wilcoxon test).

as an increase in their response to touch and pinch (Fig. 3.4B) (N= 12, p <0.05 for ongoing activity touch and pinch with drug vs control, Paired-samples Wilcoxon test).

*Interpretation-discussion:* Again, these recordings demonstrate that the spinal cholinergic tone controlling DH neurons acts not only through nAChRs, but also through mAChRs. On average, the effect of atropine goes in the same direction as the effect of mecamylamine, as was observed after i.t. injections in behaving animals. The discussion about the direction of this effect is similar to one we proposed after the behavior experiments in 2.1.2.

# 3. Plasticity of the spinal cholinergic tone in neuropathic conditions

In order to investigate plasticity after nerve injury in mice, we chose the cuff model due to its reliability and the fact that it is mastered by our collaborator in charge of performing the surgeries (Dr. Ipek Yalcin) (Fig. 3.5A).

## 3.1. Behavioral characterization

### 3.1.1. Mechanical allodynia observed after peripheral nerve injury

The PWT was measured before and one week after the surgery (Fig. 3.5B). We compared the PWT between ChAT::GFP and WT groups in neuropathic conditions. There was a significant difference between Animal (Sham vs Cuff., p = 1.58e-50), Paw (Left vs Right, p = 3.23e-112) but not Type (GFP+ vs WT, p = 1.75e-01). The Animal:Foot interaction was significantly (p = 9.50e-92) which was due to reduced PWT in cuff right paw (Mean = 1.053 ± 0.0177, N = 62) compared to cuff left paw (Mean = 3.97 ± 0.0975, N = 62,  p < 0.001, Kruskal-Wallis test) or sham right paw (Mean = 3.871 ± 0.09, N = 62, p < 0.001, Kruskal-Wallis test). There was no significant Animal:Type:Paw interactions (p = 1.08e-01). Like the naïve, the GFP+ and WT animals were thus pooled for all the behavioral study.

We used a non-parametric multiple comparison test (nparLD, see Methods) to compare the PWT between animals (Sham vs Cuff), paws (Left vs Right) and days (days after surgery: -2, -1, +7, +8, +9). There was a significant difference between the Animals (p =7.62e-05), Paws (p =9.18e-19) and Days (p = 5.83e-10). There was in addition a significant interaction Animal:Paw (p = 3.13e-21). as sham animals showed no difference in their PWT after the surgery, while cuff mice showed a marked reduction in their PWT of their right hindpaw (Fig. 3.5). Post-hoc analysis demonstrated

**A**



Benbouzid et al. 2008

**B**
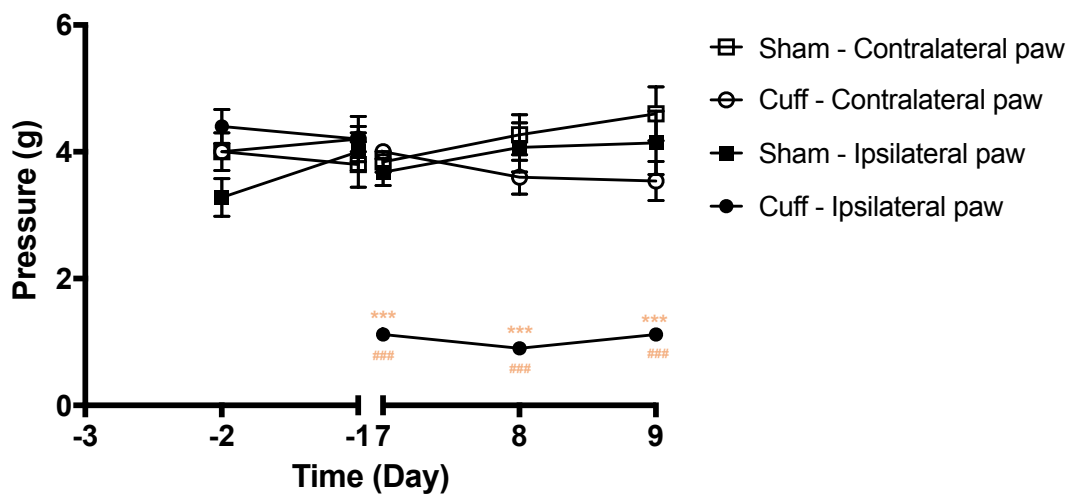


**Figure 3.5:** The cuff model to induce peripheral neuropathy in mice. **3.5A:** The surgery was performed on > 3 week old animals. The sciatic nerve of the anesthetized animal was exposed using wooden picks (Left panel). The cuff animals have a 2mm polyethene cuff placed on the right sciatic nerve (Right panel) whereas the sham undergoes the same surgery but without a cuff being placed (Middle panel). **3.5B:** Following one week post-surgery, the mechanical paw withdrawal threshold demonstrated was unchanged in sham whereas a reduction was observed in right paw of cuff mice versus their left paw and right paw of sham mice (Animal: Day: Paw p = 9.47e-16, post-hoc: TukeyHSD). This reduction observed is the mechanical allodynia . *** p < 0.001 vs baseline, ** p < 0.01, * p < 0.05.

that the ipsilateral PWT in cuff mice was significantly different than ipsilateral in sham and contralateral in cuff.

*Interpretation-discussion:* As previously published (Yalcin et al., 2014), cuff animals develop a robust and reliable mechanical allodynia in the ipsilateral paw after the surgery.

### 3.1.2. *Nicotinic antagonist: mecamylamine*

As for naïve animals, drugs were injected only after a stable PWT was determined. Sham and cuff mice were injected i.t. with mecamylamine (10-400 nmol) or with saline (0.9% NaCl), and tested at different time points after the injection; the threshold at 15 and 150 min after injection is presented in Fig. 3.6 A,B. For either the ipsilateral or the contralateral paw, we used a non-parametric multiple comparison test (nparLD, see Methods) to compare the PWT between animals (Sham vs Cuff), Drug (saline, 10-400 nM mecamylamine) and Time (0, 15 and 150 min post i.t. injection). There was a significant effect of Animals and Time (p =6.2e-01), as well as a significant interaction between Drug and Time (p=1.04e-19). There was a significant interaction between Animal, Time and Drug (p = 4.60E-002).

Mecamylamine induced a dose-dependent reduction in the mechanical withdrawal threshold of the contralateral hindpaw in sham and cuff mice. For the ipsilateral hindpaw, 10 nmol was ineffective in cuff as opposed to sham groups. The mechanical allodynia is exacerbated when higher doses were injected within cuff animals. However, there was a shift in the dose-response after neuropathy, with higher doses being necessary to obtain a significant effect (Fig. 3.6 C). Interestingly, unlike 100 and 400 nmol mecamylamine that maintained its effect in both animal groups for 150 min; the PWT returned to baselines for 20 nmol mecamylamine in cuff animals.

*Interpretation-discussion:* We are the first to demonstrate the presence of a spinal cholinergic tone in mice after peripheral neuropathy. In a study using a different neuropathy model (partial nerve ligation) and a different strain of mice (ddY), Rashid and co-authors had demonstrated that a 10 nmol mecamylamine dose after neuropathy did not affect the thermal PWT.

We decided to further investigate this point by performing a dose-response curve. Interestingly, we started to see an exacerbation of the allodynia with 20 nmol mecamylamine. The effect was even stronger with increasing doses. This led us to the conclusion that the spinal cholinergic tone was still present in cuff animals, involving nAChRs and affecting mechanical responses.

Because baseline PWT are very different between cuff and sham mice, it was difficult to directly compare the "potency" of mecamylamine effect between these two groups. We thus decided to
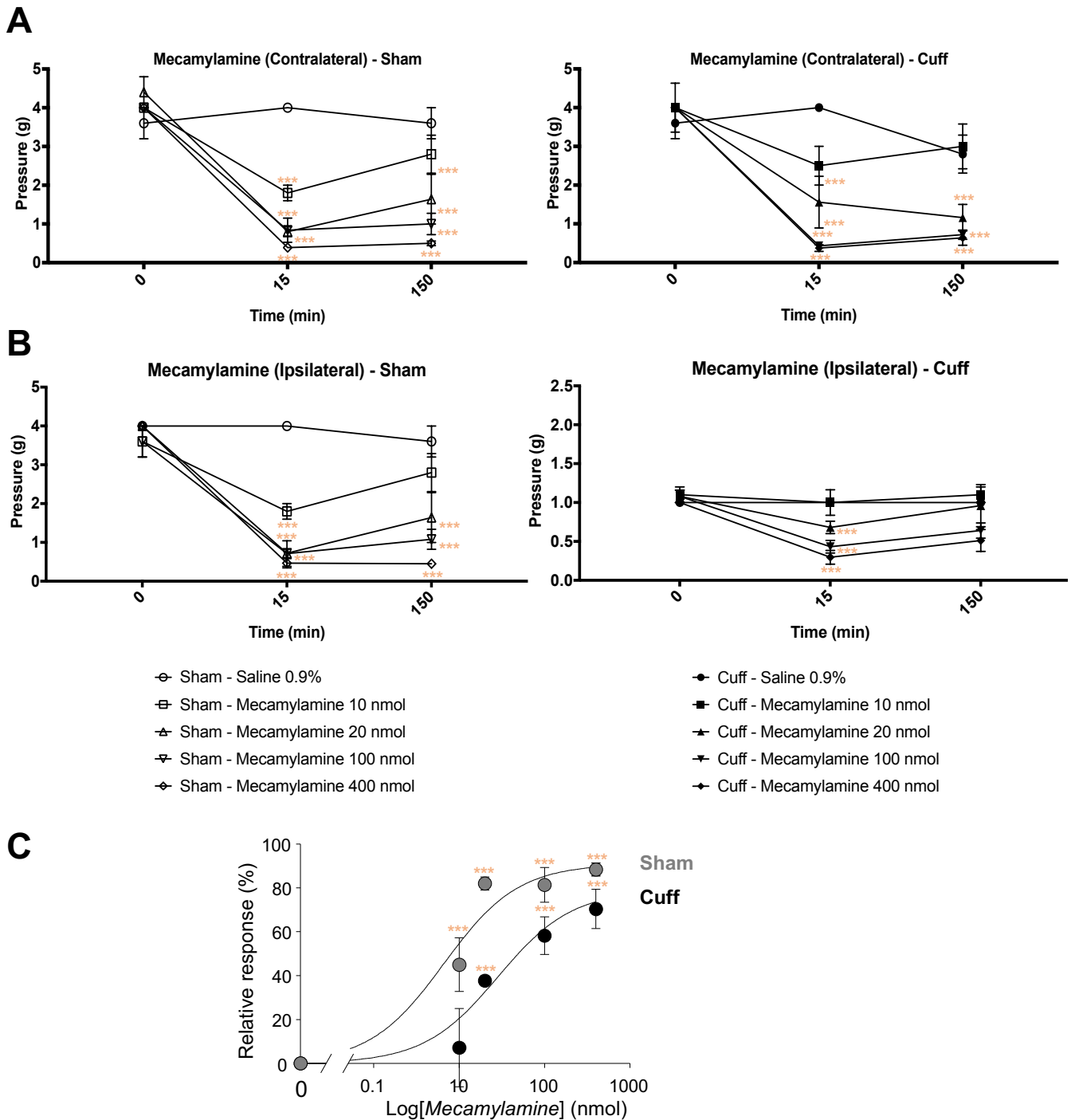
**Figure 3.6:** Time course of the effect of intrathecal mecamylamine (nicotinic antagonist) on mechanical paw withdrawal threshold [PWT] of neuropathic Cd1 mice [Groups n = 4 - 5]. **3.6A,B**: Treatment with 10 nmol mecamylamine did not intensify mechanical allodynia (lowering of PWT) in ipsilateral paw of cuff mice. The mechanical allodynia in the ipsilateral paw was further potentiated when treated with 20, 100 and 400 nmol mecamylamine (bottom right) (Animal -Drug-Time interaction: p < 0.001). **3.6C**: Dose response curve for mecamylamine at 15 min post-injection for the ipsilateral paw of sham and cuff mice. (Animal - Drug-Time interaction: p < 0.001). The relative response for time point (t) = $\frac{(PWT_t - PWT_0)}{100} \times 100$. *** p < 0.001 vs baseline, *p < 0.05 vs Time 0

express the drug effect as a relative response (see legend of Fig. 3.6 C). It then became evident that there was, in cuff mice, a shift to the right in the dose-response curve for mecamylamine, suggesting that a plasticity took place in the spinal cholinergic system.

### 3.1.3. *Muscarinic antagonist: atropine and scopolamine*

Atropine (15-30 nmol) or Scopolamine (10-20 nmol) was similarly injected i.t. in cuff and sham mice. For either drugs, and either the ipsilateral or the contralateral paw, we used a non-parametric multiple comparison test (nparLD, see Methods) to compare the PWT between animals (Sham vs Cuff), Drug (saline, 15-30 nmol atropine or 10-20 nmol scopolamine) and Time (0, 15 and 60 min post i.t. injection).

It produced dose dependent reduction in PWT in sham mice as observed in the naïve animals. In cuff mice, 15 and 30 nmol atropine had no effect on mechanical PWT in cuff ipsilateral paw but remains effective for both hind-paws in sham and contralateral paw of cuff group (Fig. 3.7A). In contrary, we observed a further decrease in the mechanical PWT with Scopolamine (10 – 20 nmol).

*Interpretation-discussion:* The presence of a muscarinic component of the spinal cholinergic tone had never been investigated in mice after peripheral neuropathy. The scopolamine data suggest the presence of a cholinergic tone acting via mAChR even after peripheral neuropathy. Somehow surprisingly, we did a different observation with atropine. In general, both atropine and scopolamine are non-selective antagonists to mAChR. Both compounds have been reported to cross the blood brain barrier. They have similar structures except for scopolamine that has an additional epoxide group that reduces its basic strength thus allowing it to penetrate the CNS more readily (Crespo et al., 2010). However, we did not observe any difference in the onset of reduction of PWT in both sham and naïve groups which could be due to the more direct drug administration via it. injections. Furthermore, the affinities to different subtypes of (human) mAChRs are similar between atropine (Peralta et al., 1987; Buckley et al., 1989) and scopolamine (Huang et al., 2001). Yet, these two drugs have different CNS-depressive effects such as drowsiness, amnesia, fatigue and dreamless sleep (Corallo et al., 2009). Although difficult to explain from a mechanistic point of view, the different effect of scopolamine vs. atropine in cuff mice is therefore not completely unexpected.

Atropine was tested in diabetic neuropathic models yet did not alter the mechanical withdrawal threshold (Koga et al., 2004). In rats, atropine was also ineffective in altering the nociceptive mechanical thresholds following peripheral neuropathy (Lavand'homme and Eisenach, 1999; Paqueron et al., 2003).
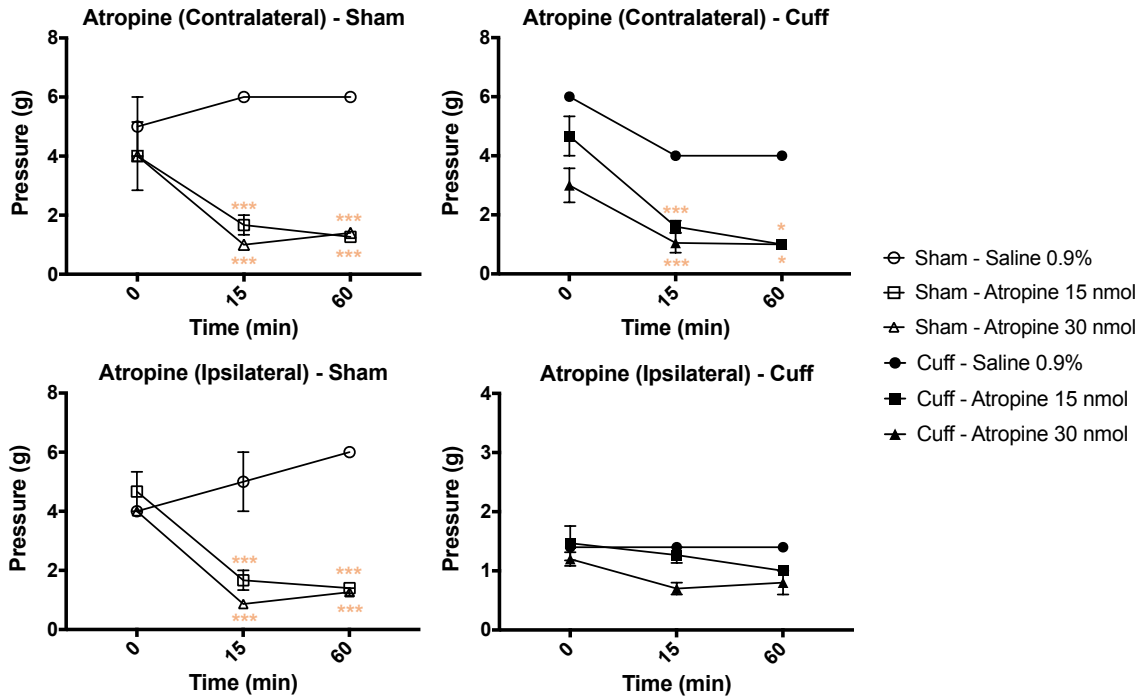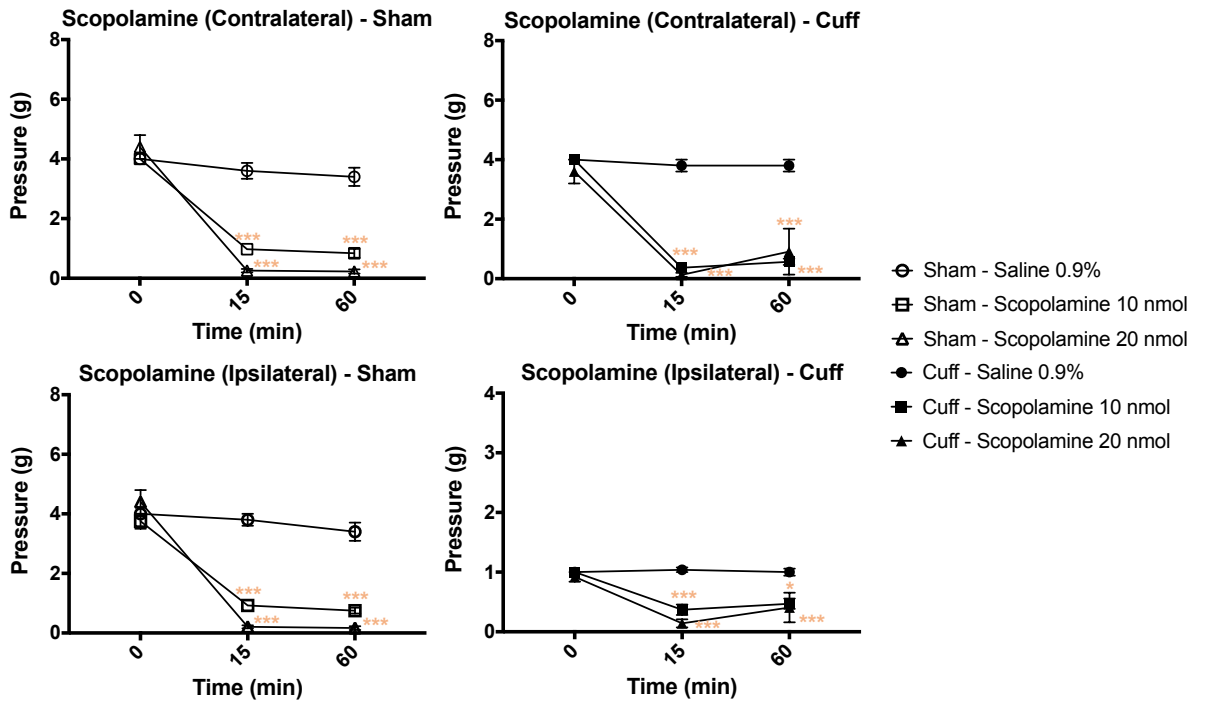
**Figure 3.7:** Time course of the effect of intrathecal atropine and scopolamine (muscarinic antagonist) on mechanical paw withdrawal threshold [PWT] of neuropathic Cd1 mice [Groups n = 3 - 10]. **3.7A**: Treatment with 15 and 30 nmol atropine did not intensify mechanical allodynia (lowering of PWT) in ipsilateral paw of cuff mice (bottom right) but did in sham (bottom left) animals. (Drug-Time interaction: $p < 0.01$). **3.7B**: Treatment with 10 and 20 nmol scopolamine intensified mechanical allodynia in sham and cuff mice. (Contralateral: Drug-Time interaction: $p < 0.01$; Ipsilateral: Animal: Drug: Time $p < 0.01$) *** $p < 0.001$ vs baseline, *$p < 0.05$ vs Time 0

## 3.2. *In vivo electrophysiological characterization*

### 3.2.1. *Properties of recorded neurons*

DH neurons were recorded from both sham (N = 46) and cuff mice (N = 32). Recorded neurons had in sham were more superficial compared to cuff groups (Fig. 3.8A) (# $p < 0.05$, paired-sample Wilcoxon test). The neurons recoded in sham were distributed along the dorsal horn, with an average depth of 316.1 μm ± 21.21 μm (range: 30, 622 μm) whereas with the cuff animals – the average depth was at 394.5 μm ± 23.06 μm (range: 89, 602 μm). There was no change in the touch and pinch, but the response to mean ongoing activity was increased in cuff animals compared to sham ones (Fig. 3.8B) (* $p < 0.05$, paired-sample Wilcoxon test). The basal ongoing activity has increased in cuff compared to sham animals (## $p < 0.01$, two-sample Wilcoxon test). The proportion of neurons remained similar between sham and cuff groups (Fig. 3.8C).

*Interpretation-discussion:* The previously published study (Medrano et al., 2016) distinguished spontaneously and non-spontaneously active neurons (SA and NSA); the reported ratio was 1SA:1NSA in sham vs. 4SA:1NSA in cuff. On average, the firing property of SA neurons was unchanged after neuropathy. But taking into account the reduced number of "silent" NSA neurons in cuff mice, we observe a rise in global ongoing activity (including all SA and NSA neurons).

As SA neurons accounts for 80% of the recorded neurons in cuff, we do not observe an increased response to touch in these animals as previously reported in SA neuron in cuff animals. In addition, the larger number of WDR neurons sampled in our cuff group could introduce a bias towards neurons responding less to touch.

### 3.2.2. *Nicotinic antagonist: mecamylamine*

Neurons recorded in sham-operated mice responded to the local application of 100 μM mecamylamine as the ones recorded in naïve mice, i.e. by an increased ongoing firing as well as an increased response to touch and pinch (Fig. 3.9A) (N = 14, $p < 0.05$ ongoing activity, touch and pinch with drug vs control, Paired-samples Wilcoxon test). In contrast, mecamylamine had no effect on the ongoing activity of DH neurons recorded from cuff mice, neither on their response to pinch. It only induced an increased response to touch (N = 11, $p < 0.05$ touch with drug vs control, Paired-samples Wilcoxon test).

*Interpretation-discussion:* The nicotinic antagonist still has an effect on the response of DH neurons to touch in cuff animals, demonstrating that there is a spinal cholinergic tone present in these neuropathic animals, acting through nicotinic receptors. However, the absence of effect on the
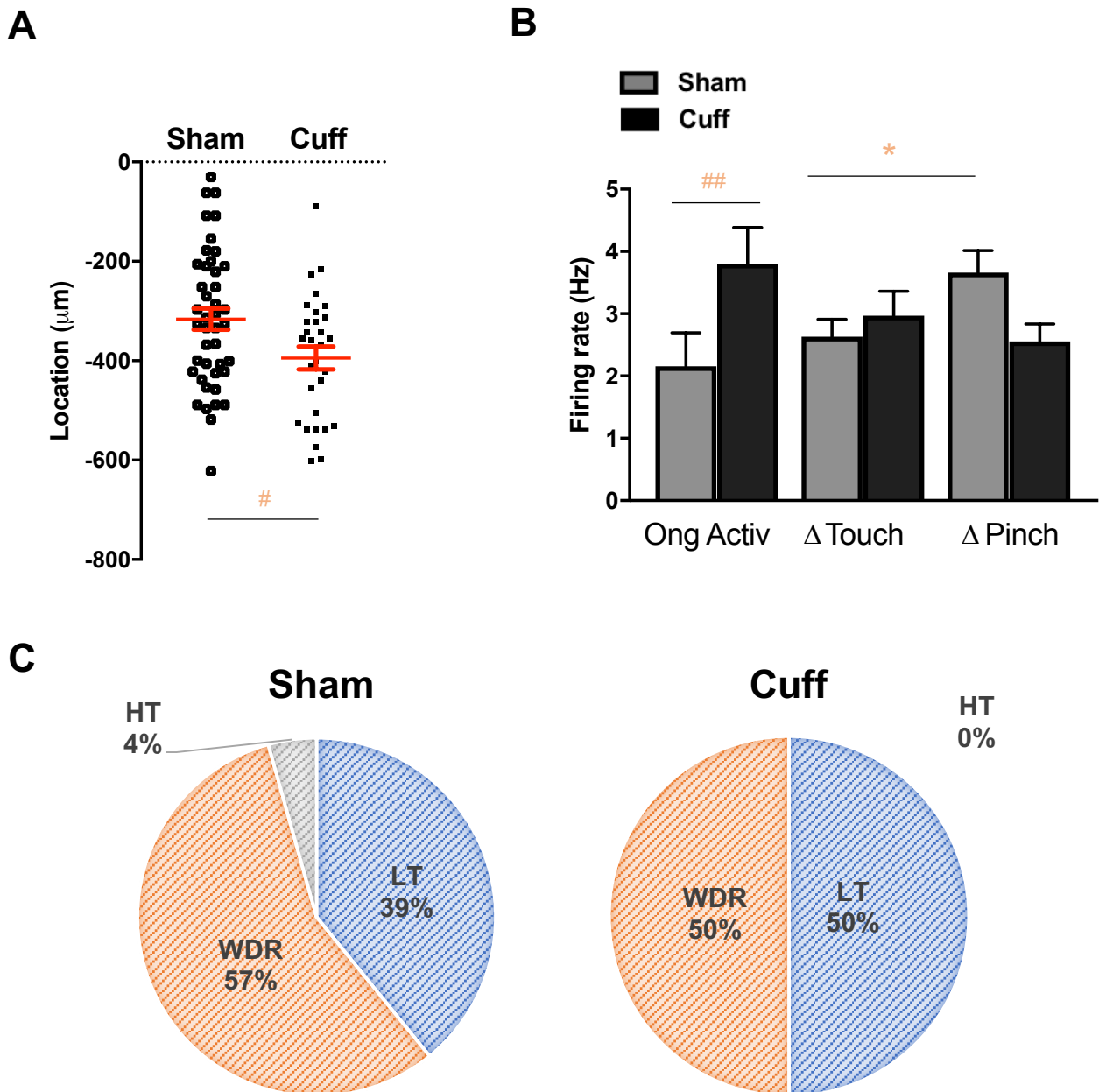
**Figure 3.8:** The characterization of recorded DH neurons after peripheral neuropathy. **3.8A**: The localization of the recorded DH neurons in sham (N = 46) and cuff (N = 32 ) animals. Symbols are the individual cells and red lines are the mean ± S.E.M of neurons (# p < 0.05, paired-sample Wilcoxon test). **3.4B**: The effect produced by touch and pinch on neurons in neuropathic mice. Higher firing rate induced by pinch compared to touch was observed in sham but not cuff mice (* p < 0.05, paired-sample Wilcoxon test). The basal ongoing activity has increased in cuff compared to sham animals (## p < 0.01, two-sample Wilcoxon test). Bars represent the mean ± S.E.M of the increase of firing rate during touch and pinch application (10 s). **3.4C:** The percentages of Low Threshold (LT), Wide Dynamic Range (WDR) and High Threshold (HT) neurons in sham and cuff animals.

ongoing activity or on the response to pinch suggests that the spinal cholinergic system (or the circuit up- or down-stream to it) has undergone plasticity. Interestingly, this plasticity appears to affect differentially non-nociceptive and nociceptive circuits.

### 3.2.3. *Muscarinic antagonist: atropine*

Similarly, neurons recorded in sham-operated mice responded to the local application of 10 μM atropine as the ones recorded in naïve mice, i.e. by an increased ongoing firing as well as an increased response to touch and pinch (Fig. 3.9B) (N = 13, p < 0.05 ongoing activity, touch and pinch with drug vs control, Paired-samples Wilcoxon test). In contrast, atropine had no effect on any of the investigated properties of DH neurons recorded from cuff mice (N = 9).

*Interpretation-discussion:* Recordings in the presence of 10 μM atropine in cuff mice suggest that the spinal cholinergic tone is not acting through muscarinic receptors after neuropathy. However, we cannot exclude that higher doses of atropine (or more specific antagonists acting only on the M1-M3-M5 or M2-M4 subtypes of mAChRs) could reveal the presence of a muscarinic component of the cholinergic tone in cuff mice. In all cases, our data strengthen the demonstration of a plasticity of the spinal cholinergic system after neuropathy.

### 3.2.4. *Interplay with the inhibitory circuits*

In order to further investigate the interplay between the spinal cholinergic system and spinal inhibitory circuits, Maria Medrano repeated the previous experiments in the presence (or absence) of antagonists for GABA-A and glycine receptors, respectively bicuculline (10 μM), and Phenylbenzene O-phosphono-A-amino acid (PMBA) (10 μM). The combination of these antagonists is hereafter called inhAnt.

In sham mice, the application of inhAnt induced an increased response to touch and pinch (Mecamylamine: N = 10, p< 0.05 Pinch, p < 0.001 Touch with drug group vs control, Paired-samples Wilcoxon test & Atropine: N = 10, p < 0.01 Touch and Pinch with drug group vs control, Paired-samples Wilcoxon test). The subsequent application of 100 μM mecamylamine or of 10 μM atropine (on top of the inhAnta) had no further effect (Right - Fig. 3.10 A and Fig. 3.10 B).

As previously published, the application of inhAnt in neurons recorded in cuff mice did not have any effect. Moreover, the subsequent application of 100 μM mecamylamine or of 10 μM atropine (on top of the inhAnta) had no further effect (Right - Fig. 3.10 A and Fig. 3.10 B) (Mecamylamine: N = 11 & Atropine N = 9).
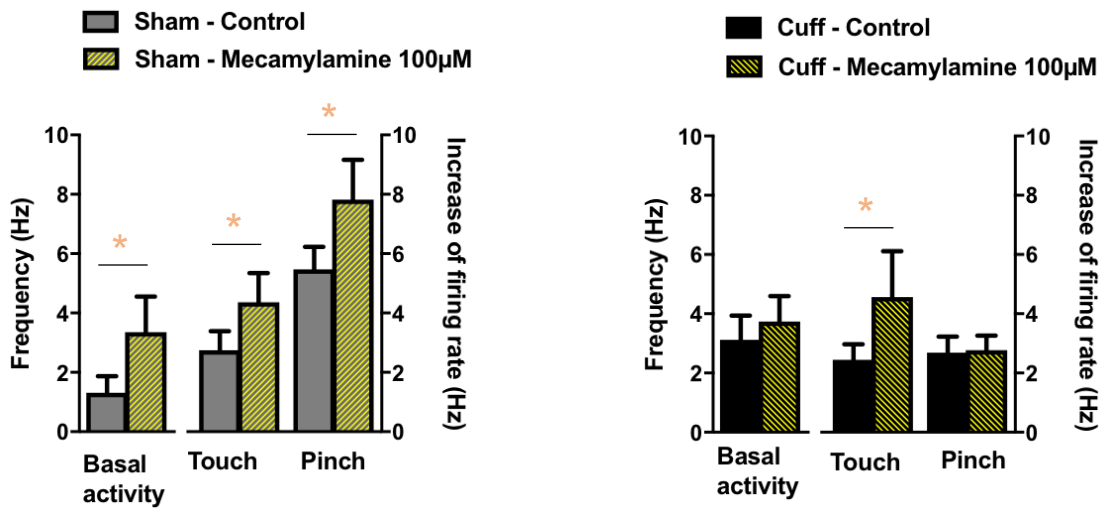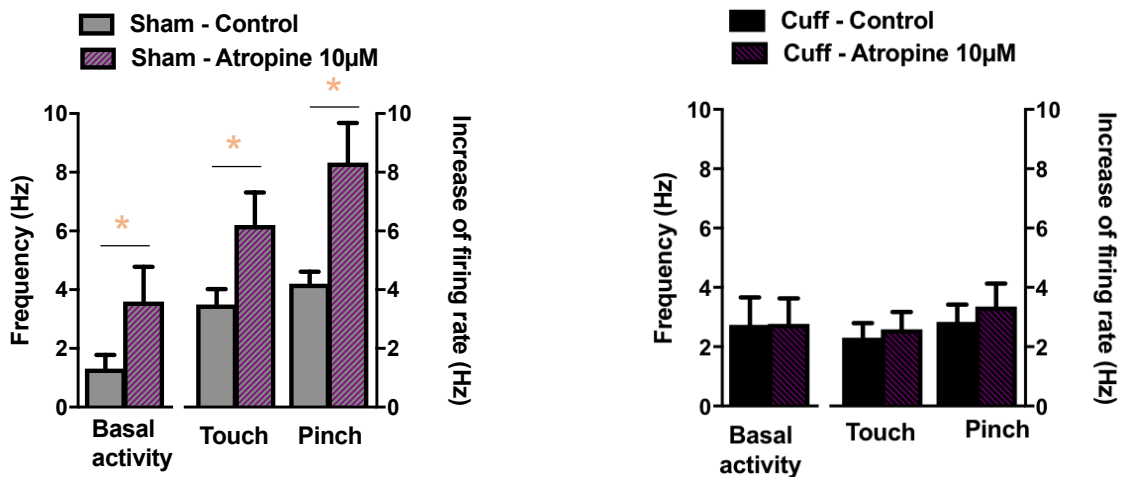
**Figure 3.9:** The effect of cholinergic drugs on touch and pinch response in DH recorded neurons following peripheral neuropathy. **3.9A**: Effect of mecamylamine (non-specific nAChR antagonist) on touch and pinch responses of sham (Left, N = 14) and cuff (Right, N = 11) animals. Mecamylamine increased the ongoing activity and responses to touch and pinch. However, only an increase in firing after touch was observed after neuropathy. **3.9B**: The effect of atropine (non-specific mAChR antagonist) in touch and pinch on neurons in sham (Left, N = 13) and cuff (Right, N = 9) mice. Similarly, the ongoing activity, responses touch and pinch was elevated in the presence of atropine during sham. However atropine lost all its effects in cuff animals. Bars represent the mean ± S.E.M of the increase of firing rate during touch and pinch application (10 s); *p < 0.05 ongoing activity or touch or pinch with drug vs control (Paired-samples Wilcoxon test).

*Interpretation-discussion:* In the previous publication, Medrano and authors observed that the application of InhAnt induced the development of ongoing activity in previously "silent" neurons (NSA neurons), and increased the ongoing activity of SA recorded in sham mice. We were therefore expecting an increased ongoing activity in our sham sample, which we did not observe. A possible explanation is the smaller number of recorded neurons in the present study. We however confirmed the increased response to touch and pinch observed in the study. This indicates that DH neurons are submitted to an inhibitory tone that controls their response to peripheral mechanical stimulation.

In sham mice, mecamylamine and atropine have no effect when applied on top of inhAnta, suggesting the involvement of inhibitory neurons in the effect of cholinergic antagonists. Potential circuits will be discussed below.

Medrano previously demonstrated that the net effect of the inhibitory tone was entirely lost in cuff mice, and we confirmed this observation with the present sample. Like in sham mice, the effect of cholinergic antagonists was lost in the presence of inhAnt; however, in cuff mice, the only effect of cholinergic antagonists was the effect of mecamylamine on the response to touch (Fig. 3.9 A - Right). Therefore, the inhAnt experiment suggests that this effect is mediated by inhibitory neurons.

The most straightforward hypothesis would be that cholinergic receptors (tonically activated in sham) are expressed by inhibitory neurons impinging onto the recorded cell: in the presence of inhAnt, even though the presynaptic neuron is less active because of antagonism of the cholinergic tone by mecamylamine, this has no effect on the recorded neuron as inhibitory transmission is silenced. Of course, more complex circuits are conceivable, with the intervention of excitatory neurons.

## 4. In search for the source of the spinal cholinergic tone

The following section entails a joint work with Dr. Yunuen Moreno-Lopez, a post-doc within our team where she has optimized the virus injection technique in adult mice. Several potential sources of the spinal cholinergic innervation have been described (see introduction section 3.4). We aimed to unravel the contributing of each of these cholinergic populations to the modulation of nociceptive processing by utilizing a DREADD approach. We induced expression of hM4Di receptors, that are modified muscarinic receptors. When activated by a specific ligand – Clozapine N-oxide (CNO), they induce inhibition of the neuron. In our experimental paradigm, we injected adult ChAT::Cre mice with Cre-inducible recombinant AAV vectors: AAV8-hSYN-FLEX-
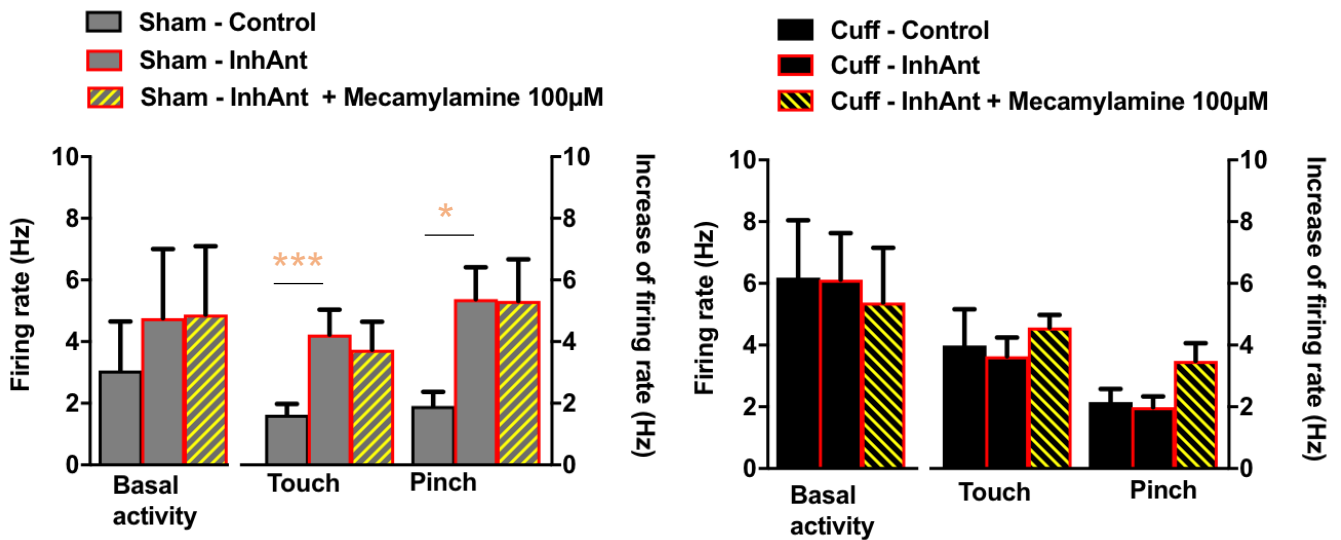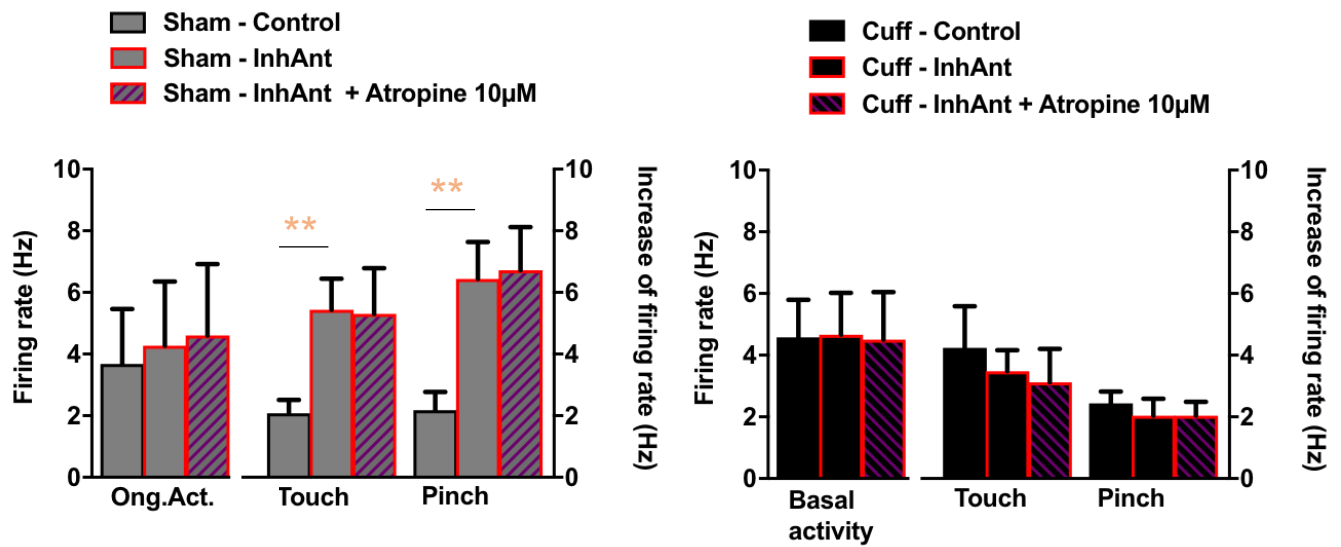
**Figure 3.10:** The pharmacological induced disinhibition of the spinal cord in sham and cuff animals. The inhibitory antagonists (InhAnt) added were non-specific GABA-A antagonist, bicuculline (10μM) and non-specific glycinergic receptor antagonist, PMBA (10μM). **3.10A**: Effect of mecamylamine (non-specific nAChR antagonist) with InhAnt on touch and pinch responses of sham (Left, N = 10) and cuff (Right, N = 6) animals. InhAnt increased the responses to touch and pinch but not in cuff. Moreover, mecamylamine with InhAnt had no effects in sham and cuff animals. **3.10B**: The effect of atropine on touch and pinch responses of neurons in sham (Left, N = 9) and cuff (Right, N = 5) mice. Similarly, the responses to touch and pinch was elevated in the presence of InhANT during sham but not cuff mice. However, atropine with InhAnt lost all its effects in sham and cuff animals. Bars represent the mean ± S.E.M of the increase of firing rate during touch and pinch application (10 s); (* p< 0.05, ** p < 0.01, *** p < 0.001, drug group vs control, Paired-samples Wilcoxon test).

hM4Di-mCfherry (AAV8-hM4Di) and AAV9-hSYN-FLEX-hM4Di-mCherry (AAV9-hM4Di). The different candidate structures are the spinal cord, RVM and DRG. Following the injections, the animals are tested with the von Frey test to identify the populations contributing to the spinal cholinergic tone involved in establishing mechanical nociceptive threshold.

## 4.1. *ChAT-Cre animals*

As a control for the expression, we crossed ChAT-Cre animals with a reporter line, ROSA-26 tdTomato. Surprisingly, we observed expression of the tdTomato reporter protein (red) in a large quantity of non-ChAT expressing cells in adult reporter mice (N = 3, Fig. 3.11).

*Interpretation-discussion:* The different techniques used to produce transgenic mice are differently prone to non-specific expression. Indeed, the level of expression of BAC transgenic mice is highly dependent on the site(s) of insertion of transgene. However the ChAT-Cre mice that we use are knock-in animals: we therefore expected a pattern of expression strictly identical to the endogenous ChAT. However by crossing these mice with a mouse expressing a floxed-version of tdTomato, we have no control over the moment where the recombination occurs. We suspect that the non-ChAT tdTOM+ neurons were ChAT expressing cells at some point before adulthood. The Cre-recombinase enzyme present during younger developmental stages may have permanently enabled the transcription of the tdTomato construct thus allowing these neurons to remain tdTOM+.

Our project mostly involved injection of Cre-dependent viruses in adult mice, and was therefore not impacted by this developmental issue. Only DRG-targeting injections were performed in neonatal mice (see Methods) and deserved particular control for specificity of expression.

## 4.2. *Expression of the viral construct*

Following a minimum of three weeks for recovery and sufficient time for expression of viral constructs (or to reach adulthood for DRG targeted mice), the mechanical PWT of these animals were assessed, in control conditions and after injection of CNO. After their behavioral assessment, the histological experiments were performed to verify the reporter protein expression (mCherry), colocalization with ChAT and their location in the different structures.

### 4.2.1. *Spinal injection*

A total of 14 adult ChAT-Cre animals were injected with both AAV8- and AA9- hM4Di viral constructs (Median injected volume = 540 µl; range 90 to 764 µl). The co-ordinates ranged from 150 – 250 µm in depth and 350 – 400 µm laterally from the midline of the spinal cord. In our

**ChAT**  **Endogenous tdTOM**  **Merged**
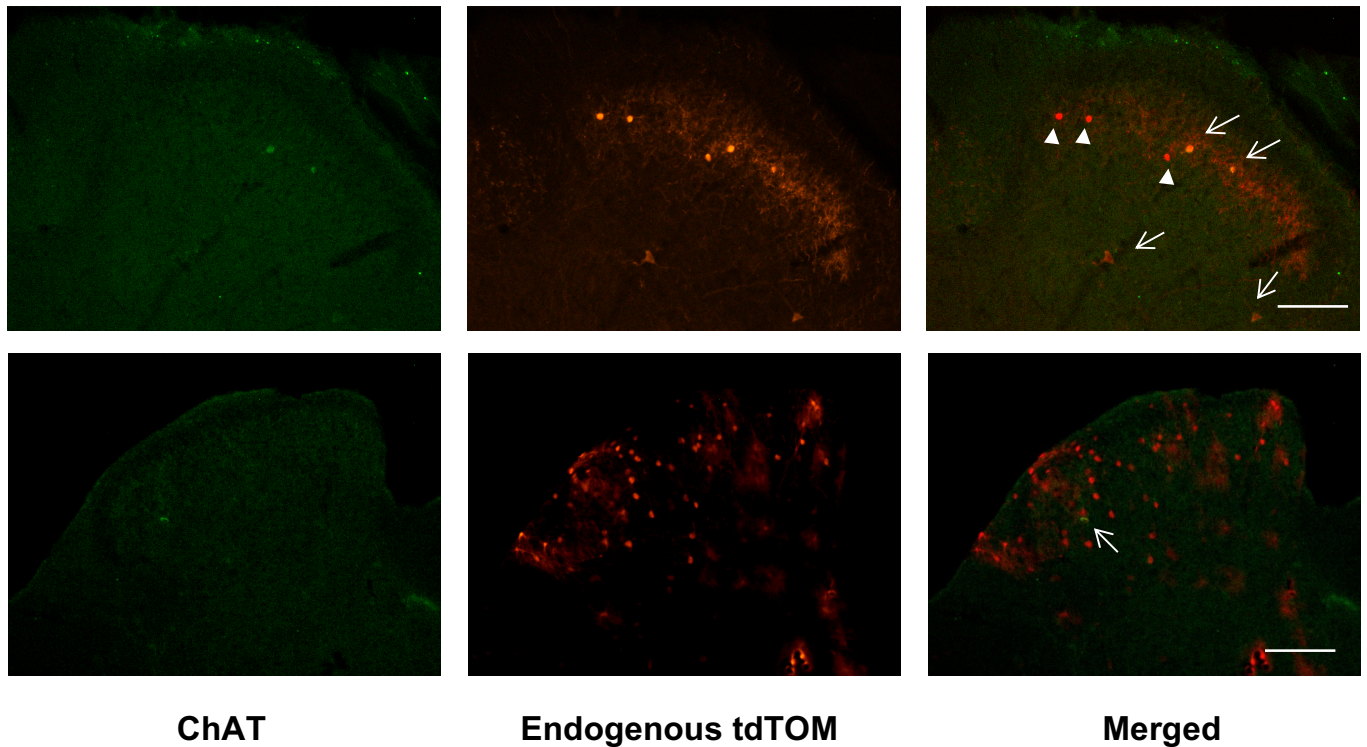
**Figure 3.11:** Expression of tdTomato reporter protein in ChAT-Cre x ROSA26-tdTomato adult mice. Immunoreactivity against Choline acetylcholinetranferase (ChAT) (Green, Left panel) to verify the expression of reporter protein (Red, Middle panel) in cholinergic neurons (N = 3). In the merged images (Yellow, Right panel), a number of cells colocalized with both ChAT and tdTomato (arrows) however, a large proportion of cells were expressed in potentially non-ChAT cells (arrowheads). (Scale = 100 μm)

preliminary experiments, we directly mounted the perfused tissue for verification (without ChAT immunohistochemistry). These two injected mice (injected volume = 630 μl) contained large infections in the DH, central canal and even some motor neuron populations in the ipsilateral side of the spinal cord (Fig. 3.12A). Herein, infected neurons ranged from L3 – L6 spinal segments. We subsequently reduced the injected volumes (< 540 μl) to prevent at least the infection of autonomic and motor cholinergic pools; preliminary data demonstrated that this enabled to restrict the infection to the dorsal horn. Baseline PWT were undistinguishable from those of CD1 mice (personal observation). We tested the effect of CNO on the animals injected with these lower volumes (see below); they now await for histological analysis that can confirm hM4Di receptor expression in cholinergic cells and the exact spread of this expression.

Two spinally injected mice (and two mice injected in the spinal cord and RVM, see below) demonstrated a reduction in PWT with 10 mg/kg CNO (Fig. 3.13). This reduction was profound, robust and reproducible: it could be observed on different testing days, and the same animals did not respond to saline. However the other spinally-injected mice showed no response to CNO.

***Interpretation-discussion:*** In preliminary experiments, a successful expression of viral constructs was observed in the spinal cord. Unsurprisingly, the larger volume of virus resulted in wider expression observed in the dorsal, central and ventral regions of the spinal cord. The response to CNO was extremely variable amongst injected mice, as most did not respond while 4 responded robustly. We are analyzing all variables (quality and freshness of CNO aliquot, conditions of solubilization) that could explain such difference, without a clear lead. The analysis of the spread of infection might provide insight.

### 4.2.2. RVM injection

We have performed a total of 9 injections to target the descending cholinergic populations in the RVM (Median injected volume = 540 μl, ranging from 450 – 810 μl). The current targets co-ordinates are approximately 0.7 mm lateral to midline, 5.2 mm caudal to Bregma and 5 mm ventral to the cerebellar surface. Similarly, to the spinal cord injections, the injection sites were verified in preliminary experiments. We observed expression of mCherry reporter protein that localizes with a proportion of ChAT neurons in the RVM of a mouse (Fig. 3.12B).

Baseline PWT were undistinguishable from those of CD1 mice (personal observation). As mentioned above, two animals injected in the RVM that were also injected spinally, demonstrated reduction in PWT with 10 mg/kg CNO (Fig. 3.13). The other animals did not respond to CNO. All animals have been perfused and await histological verification.
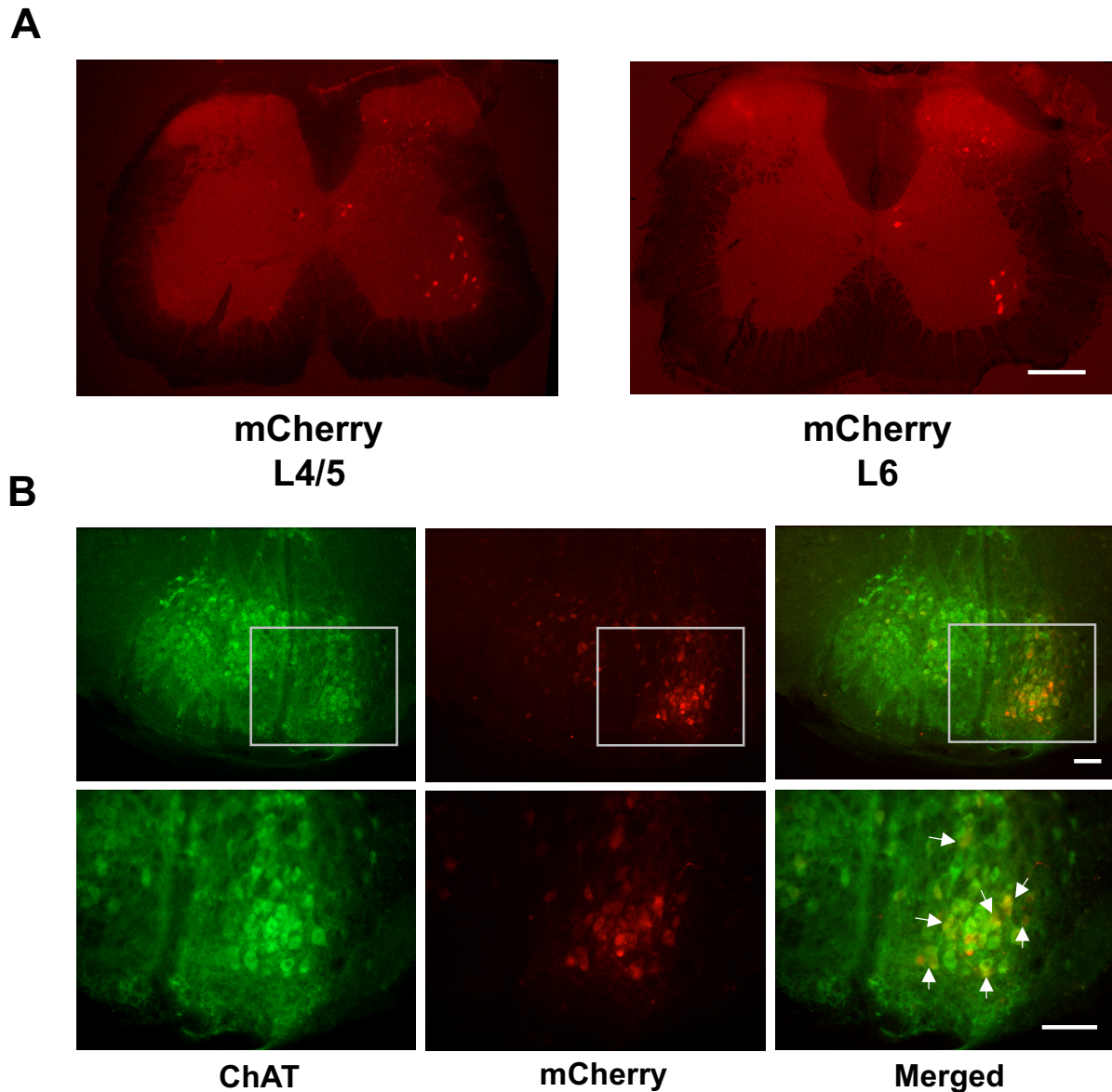
**Figure 3.12:** Expression of hM4Di - mCherry reporter protein in spinal cord and RVM of ChAT Cre animals. **3.12A:** The spinal injected ChAT Cre mice expressed (N = 2) endogenous mCherry coupled to hM4Di in potentially ChAT neurons located in the Dorsal, Intermediate and Ventral regions of the spinal cord (Scale = 200 μm). **3.12B:** The ChAT Cre mouse injected in the Rostral Ventromedial Medulla (RVM) (N = 1). Immunoreactivity against Choline acetylcholinetranferase (ChAT) (Green, Left panel) to verify the expression of mCherry reporter protein (Red, Middle panel) in cholinergic neurons. In the merged images (Yellow, Right panel), a number of cells colocalized with both ChAT and mCherry (arrows) (Scale = 100 μm).
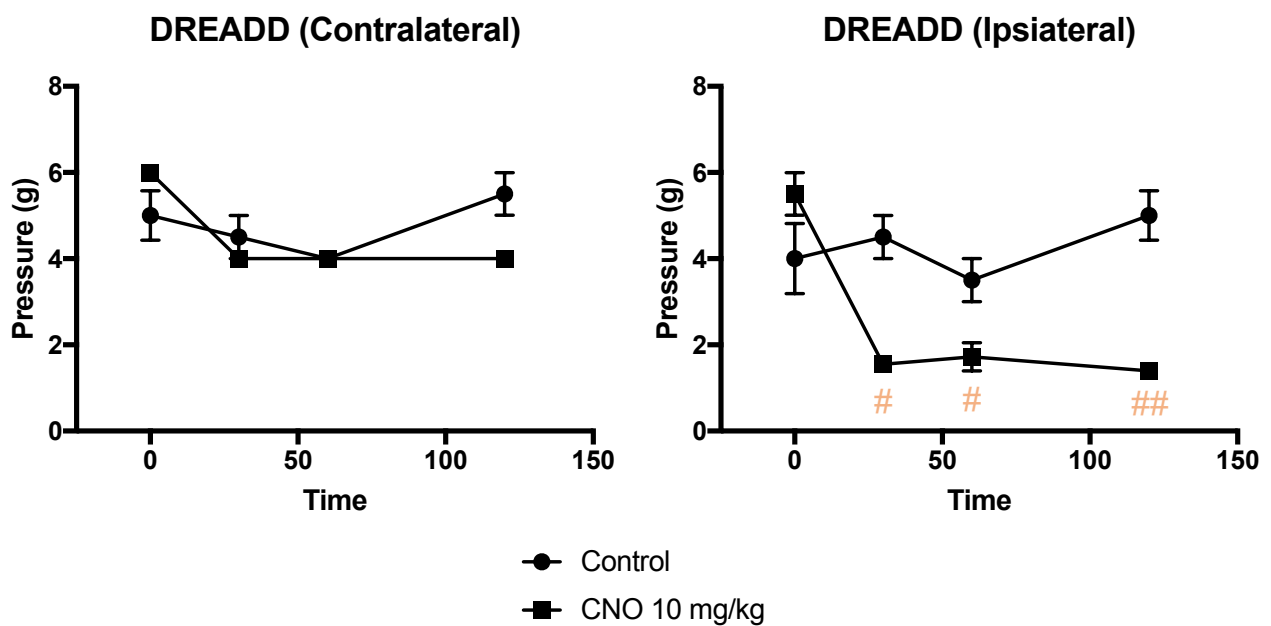
**Figure 3.13:** Time course of the effect of intraperitoneal Clozapine N-oxide (CNO) in ChAT Cre animals injected with AAV8-hSYN-hM4Di-mCherry and AAV9-hSYN-hM4Di-mCherry [N: Spinal cord only = 2, Spinal cord +RVM = 2]. The same animals were tested over several days. For control experiments, the mice received i.p. injection of MilliQ water. After 5 days, CNO (10 mg.kg) induced mechanical allodynia in injected animals. (Ipsilateral side: Drug:Time interaction: $p < 0.01$; post-hoc: Dunnett's multiple comparisons) ## $p < 0.01$, #$p < 0.05$ vs Time 0

*Interpretation-discussion:* Because the two responder mice were also injected in the spinal cord, we hypothesize that their response is due to the expression of hM4Di in the spinal cord. However we need to wait for histological analysis. For RVM injection, two technical points needs to be addressed. First, as the target area is ventrally located thus implicating a long travel route for the pipette. This potentially allows damage to the intermediate structures. In consequence, the pipettes were adapted to possess a thin long taper. Secondly, other cholinergic populations (i.e. autonomic and motor neurons) are located within these areas (Stornetta et al., 2013). We might need to adjust the injected volumes and improved precision in co-ordinates to prevent infection of undesired populations, and thus potential side effects of CNO application.

### 4.2.3. *DRG injection*

We performed two batches of injection aiming at silencing potential cholinergic neurons in the DRG. For this, we performed a unilateral s.c. injection in the hindpaw of P5-P8 animals, and waited for 3 weeks. This procedure has been shown to induce expression of the viral construct in DRG neurons. Similarly as for silencing DH and RVM neurons, we used a floxed version of the DREADD receptors injected in ChAT::Cre mice. The animals are awaiting pharmacological assessment prior to histological control. Although with completed behavioral data for spinal cord and RVM groups, we are unable to form constructive interpretation until histological experiments are performed to confirm the location and the nature of the infected cells. Nevertheless, our preliminary data suggests that the DREADD approach is working by producing mechanical allodynia in infected animals.

# 5. Discussion

In this chapter, we have demonstrated the presence of a spinal cholinergic tone modulating mechanical nociceptive threshold in naïve adult mice. In addition, we have shown that this tone was altered after a surgery inducing peripheral nerve injury.

## 5.1. *Spinal cholinergic tone*

The "cholinergic tone" was defined from pharmacological experiments, either at the behavior level or the circuit level (in vivo recordings). For both experimental approaches, selective antagonists for nAChRs and mAChRs (mecamylamine and atropine) were used and demonstrated that their respective receptors where endogenously activated under basal conditions, and that their activation controlled the way the mice (or the DH neurons) responded to mechanical stimulation.

The term "tone" might be misleading because it is of the same family than "tonic", commonly used to describe an effect that occurs repetitively (i.e. "tonic firing"). The existence of a "pharmacological tone" does not require "tonic" release of ACh: ACh could actually be released phasically as a consequence of the mechanical stimulation. Only the effect of the antagonists on the ongoing firing activity of DH neurons suggests some kind of "ambient level" of ACh in basal conditions.

We only used a general nicotinic antagonist, mecamylamine, but previous papers have shown similar effect using the $\alpha4\beta2$ nAChR antagonist, DH$\beta$E (1-10 nmol) in mice (Rashid et al., 2006). The $\alpha7$ nAChR antagonistMLA (10 nmol) had no effet, suggesting that mechanical PWT is dependent on $\alpha4\beta2$ nAChR but not $\alpha7$ nAChR in mice (Rashid et al., 2006). Interestingly, the $\alpha3\beta2*/\alpha6\beta2*$ nAChR antagonist, $\alpha$-CTX-MII (0.03 – 0.1 pmol) reduced the paw withdrawal thresholds in naïve rats (Young et al., 2008b). This suggests that an endogenous spinal cholinergic tone acts to inhibit the transmission of nociceptive mechanical stimuli via various subtypes of nAChR in rodents.

## 5.2. *Technical considerations*

Certain considerations shall be made for the technical approaches used within our study. For the behavior, we have utilized the von Frey test to determine the PWT of animals. Although the animals are unrestricted during tests, the changes in the behavioral state (deep sleep, light sleep, resting, grooming and alert) can modulate the outcome of the mechanical threshold assessment. Interestingly, animals undergoing grooming appear to be hypoalgesic (reduced sensitivity to pain stimulus) even in nerve injured animals (Callahan et al., 2008). There was certain variability in the baseline responses of animals, which we related to these different behavioral states. Other mechanical tests exist for rats such as the Randall Selitto test in which a blunt point is exerted on the fixed paw of the rats to determine their PWT (Randall and Selitto, 1957). Moreover, calibrated forceps have been described as a quick and reliable manner to determine the mechanical threshold comparted to classical von Frey tests in rats (Luis-Delgado et al., 2006). Although they have been used to assess tail withdrawal threshold of mice (Kashiwadani et al., 2017), they are not yet adapted to study paw withdrawal. von Frey testing remains the most well-established and robust technique to assess mechanical paw thresholds in mice with models of peripheral neuropathy.

Intrathecal injections have been suggested to directly deliver drugs into the subarachnoid space and eventually joining the cerebral spinal fluid. However, this can potentially act on both the central (spinal) and peripheral (PNS) nervous systems. Cholinergic receptors are expressed on primary

afferents (see Introduction section 3.3), and their potential contribution to the observed effects will be discussed below.

It has been reported that non-specific interaction of cholinergic drugs may occur at higher concentrations used. Although we are unaware of unspecific interaction for mecamylamine, given the high concentration used, we decided to perform a control on β2* nAChR K/O mice. This demonstrated that β2* nAChR are the receptors involved in the observed behavior. Atropine and scopolamine have reported non-specific binding. In the presence 1μM atropine, nicotinic inward currents were either inhibited (α3β2, α3β4), less inhibited (α2β4, α7), or potentiated (α4β2, α4β4) (Zwart and Vijverberg, 1997). Although these interactions do not all involve β2* nAChR, we plan to test the effect of atropine in β2 K/O mice to at least rule out some of these non-specific effects. Furthermore, the 5 HT-3 serotonin receptor responses were inhibited by both scopolamine (IC50 = 2.09μM) and atropine (IC50 = 1.74 μM) in xenopus oocytes (Lochner and Thompson, 2016). Some nicotinic antagonists, such as hexamethonium, have been reported to interact with M2 and M3 mAChR subtypes in vitro at concentrations at 0.1 to 10mM respectively (Eglen et al., 1989 ). Similarly to β2 K/O mice, we test the antagonists with their respective knock-out mice (i.e. nicotinic antagonist with nAChR subunit knock-out mice. Alternatively, we can test the same drug in the proposed knock-out version of the proposed receptor (for hexamethonium – using an M2 or M3 mAChR K/O mice). This could provide some clarity concerning the specificity.

We observed differences between the effect of atropine and scopolamine however, their pharmacokinetics appear similar:  Atropine (pKi): M1 = 8.5 – 9.6; M2 = 7.8 – 9.2; M3 = 8.9 – 9.8; M4 = 8.7 – 9. 5; M5 = 9.3 – 9.7. Scopolamine (pKi): M1 = 9.0, M2 = 8.7; M3 = 9.4; M4 = 9.5

DREADD experiments (using hM3D receptors) have been successfully used to elucidate the functional role of two spinal populations in the nociceptive circuit (Peirs et al., 2015; Petitjean et al., 2015). Interestingly, the number of hM3D-mCherry expressing neurons within the population of interest (PV neurons) was very sparse (c.f. Supplementary S6), yet CNO-induced behavior effect was still observed. This drove us to expect a significant effect of CNO beside the modest size of targeted cholinergic populations.

Recently, it has been reported clozapine, an antipsychotic drug, may presumably bind to the CNS expressed DREADD receptors. Following systemic injection, CNO is degraded into clozapine that readily crosses the BBB unlike CNO. This is raising caution in the experimental design and conclusions drawn from DREADD experiments (Gomez et al., 2017).

## 5.3.    *Plasticity of the spinal cholinergic tone and potential underlying circuits*

In naïve (and sham) mice, our experiments demonstrated the presence of a cholinergic tone pacing the on-going spiking activity of DH neurons, as well as their response to touch and pinch; in behaving animals the global output of the tone is antinociceptive (for mechanical PWT).

*Peripheral component to the tone:* As mentioned above, intrathecal administrations potentially impact the peripheral nervous system. Cholinergic receptors are present on primary afferents (see Introduction). For example, $\alpha3\alpha5\beta4*$ nAChR subtypes have been detected in unmyelinated C fibers. Nicotinic activation induces axonal excitability, an effect blocked by mecamylamine. This indicates a pro-nociceptive effect of these nAChRs (Lang et al., 2003). This conclusion is reinforced by the observation that the knockdown in $\alpha5$ nAChR alleviates mechanical allodynia after peripheral injury (Vincler and Eisenach, 2005). Such components go in the opposite direction (pro-nociceptive) to our observations, and therefore do not contribute predominantly to them. However, there is an anti-nociceptive peripheral non-$\beta2*$ nAChR component, that was revealed by the administration of a nicotinic antagonist that does not cross the BBB. In $\beta2$ K/O mice, intrathecal hexamethanonium did not produce any effect; however i.p. injections reduced the mechanical thresholds in WT and $\beta2$ K/O littermates. This suggests that there is a peripheral (but not spinal) nicotinic anti-nociceptive component acting on non-$\beta2*$ nAChR (Yalcin et al., 2011).

Muscarinic receptors are also present on primary afferents. In rat skin nerve preparation, muscarine induced a marked decrease in the response to mechanical and heat stimuli which is blocked by scopolamine and the M2 subtype specific antagonist, gallamine (Bernardini et al., 2001). The anti-nociceptive effect produced by muscarine was lost in M2 K/O mice but was not significantly altered in M4 K/O mice in isolated skin preparations. This reinforces the role of peripheral M2 receptors in anti-nociception (Bernardini et al., 2002). Potentially, our intrathecal application of mAChR antagonists could be blocking these M2 receptors thus leading to a reduction of mechanical PWT.

*Plasticity of the tone:* Our data also indicate that this cholinergic tone is still present in neuropathic mice, and globally acting in the same direction. But several observations demonstrate that it has undergone a profound plasticity. From a behavioral point of view, higher concentrations of nicotinic antagonist are required to obtain an observable effect in cuff animals, suggesting a change in either the number, composition or localization of endogenously activated nAChRs, or alterations

in the up-stream or down-stream network. This plasticity also involves mAChRs, although the maintained effect of scopolamine (in contrast with the loss of effect of atropine) suggests the existence of diverse muscarinic components modulating nociceptive processing.

In vivo recordings of DH neurons give further insight into possible mechanisms and underlying circuits. We found an in vivo correlate of the "cholinergic tone" observed in behaving animals. DH neurons responding to mechanical stimulation were under a cholinergic control, impacting their ongoing firing and their response to mechanical stimulation (nociceptive or non-nociceptive). With the single dose tested in vivo in cuff animals, we could detect only a remnant nicotinic effect on the neurons response to touch. Admittedly, only a single dose of atropine was tested in vivo; similar experiments with scopolamine would be needed to unravel a potential remnant muscarinic component (as observed in behaving mice).

*Putative underling circuit:* Experiments with InhAnT (bicuculline and PMBA –GABA-A and glycinergic receptor antagonists) in conjunction with the cholinergic drugs has allowed further dissection of the spinal circuit involved in the cholinergic modulation of mechanical information transmission. A potential minimal circuit is presented in Fig. 3.14. For naïve and sham mice (Fig. 3.14A), the model proposes the cholinergic tone either activate (via $\beta 2^*$ nAChR or M1/M3/M5 mAChR subtype) or disinhibit (via an inhibitory neuron expressing M2/M4 mAChR subtype) an inhibitory interneuron, which is presynaptic to the recorded DH neuron. In the presence of InhAnt, the pharmacological disinhibition of the spinal circuit blocks the output of presynaptic inhibitory interneurons thus increasing the firing activity directly (disinhibit cell) or via primary afferents (disinhibit incoming fiber). In neuropathic conditions (Fig. 3.14b), a change in spinal GABA/glycine system and dorsal horn network takes place thus InhAnt loses its disinhibition effect on the recoded neuron. However, touch responses continue to be mediated via nAChR.

In conclusion, we have demonstrated the role of a spinal cholinergic tone in establishing mechanical nociceptive thresholds. In the spinal cord, the cholinergic tone has been shown to involve both nAChR and mAChR in naïve and sham mice. Following peripheral nerve injury, the animals appeared to have an altered cholinergic system acting partially through nAChRs.
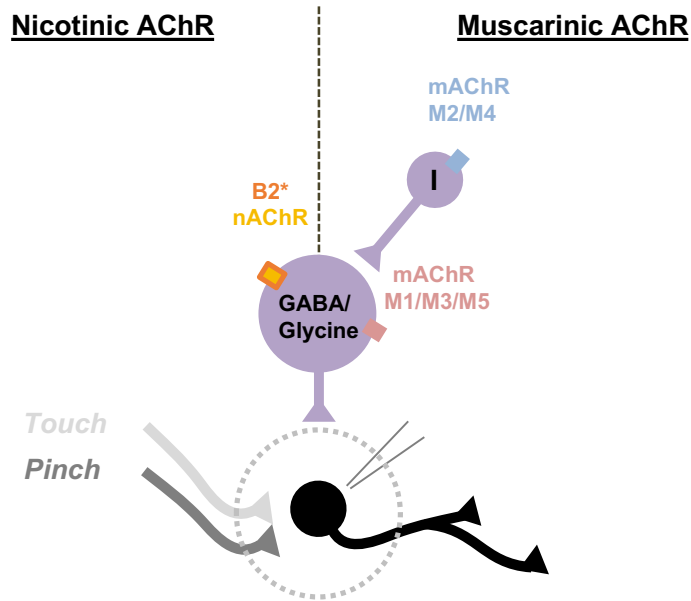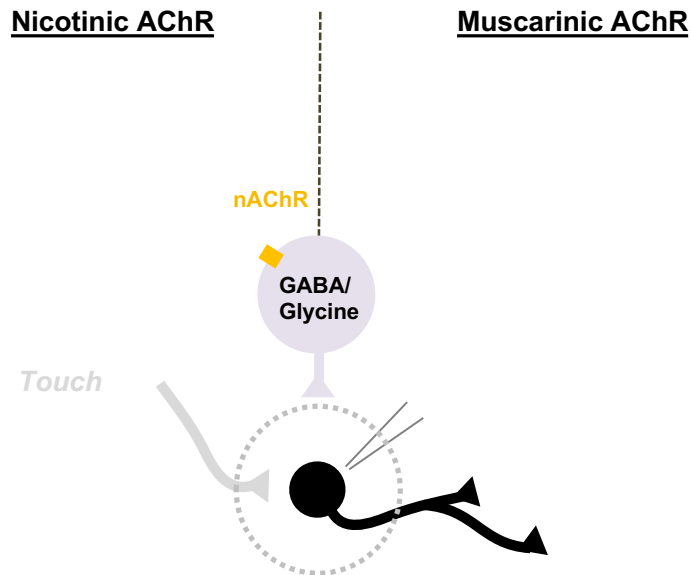
**Figure 3.14:** The proposed spinal circuit in the DH of the spinal cord in naive/sham and cuff mice. **3.14A:** In naïve/sham animals, the presynaptic GABA-/Glycinergic interneuron, to the recorded DH neuron, is activated [via β2* nicotinic acetylcholine receptors (nAChR) or M1/M3/M5 muscarinic acetylcholine receptors (mAChR)] or disinhibited (via an inhibitory (I) interneuron with M2/M4 mAChR) by the cholinergic tone during application of touch or pinch. In the presence of their respective antagonist, the nAChR and mAChR are blocked thus inhibiting the presynaptic neurons and increasing the activity in the recorded cell via disinhibition or direct activation of primary afferent fibers (in turn disinhibited). **3.14B:** In neuropathic conditions, the GABA/Glycinergic system has undergone changes as observed (decolorization of presynaptic cell) however, it is activated by nAChR by cholinergic tone during touch.

# Chapter 4: Dorsal horn cholinergic interneurons: the dual language of a minority population

## **1.** Context and objectives

A dense plexus of cholinergic processes (comprising both cholinergic dendrites and axons) lies in laminae (L) II-III of the DH of rodents (Barber et al., 1984; Mesnage et al., 2011). Within this plexus, cholinergic fibers interact in a synaptic and reciprocal way with incoming sensory afferents (Ribeiro-da-Silva and Cuello, 1990; Olave et al., 2002). This interaction appears to be the most probable substrate for cholinergic analgesia.

Our team has characterized DH cholinergic interneurons (Mesnage et al., 2011) utilizing transgenic mice expressing the enhanced green fluorescent protein (EGFP) under the control of the ChAT promoter (ChAT::EGFP mice) (von Engelhardt et al., 2007). Interestingly, this sparse cholinergic population (< 25 cells/ spinal segment) also express GABA and n-NOS. Their unique morphology demonstrates dorsally orientated processes with large elongation in the rostro- caudal axis. Their scarcity seems therefore balanced by an important dendritic and axonal territory. In addition, our team reported a similar population in the DH of macaque monkeys, with similar densities as in rodents. Cholinergic boutons are presynaptic to terminals of sensory primary afferents in both rodents and primates (Pawlowski et al., 2013a). These findings suggest a role for cholinergic interneurons in the modulation of incoming somatosensory information. Therefore, our objective is to understand the role of cholinergic interneurons within the spinal nociceptive network of naïve mice.

## **2.** Characterization of the spinal cholinergic DH neurons

We recorded from ChAT::EGFP neurons in spinal cord slices, as well as from non-fluorescent neurons located in the vicinity of ChAT::EGFP neurons. This latter LIII/IV non-cholinergic population will be called Non-ChAT. Recordings were performed in slices with three different orientations: transverse (or coronal, TS), parasagittal (PS) and horizontal (HS) (see Methods and Fig. 2.1).

**A**



**B**
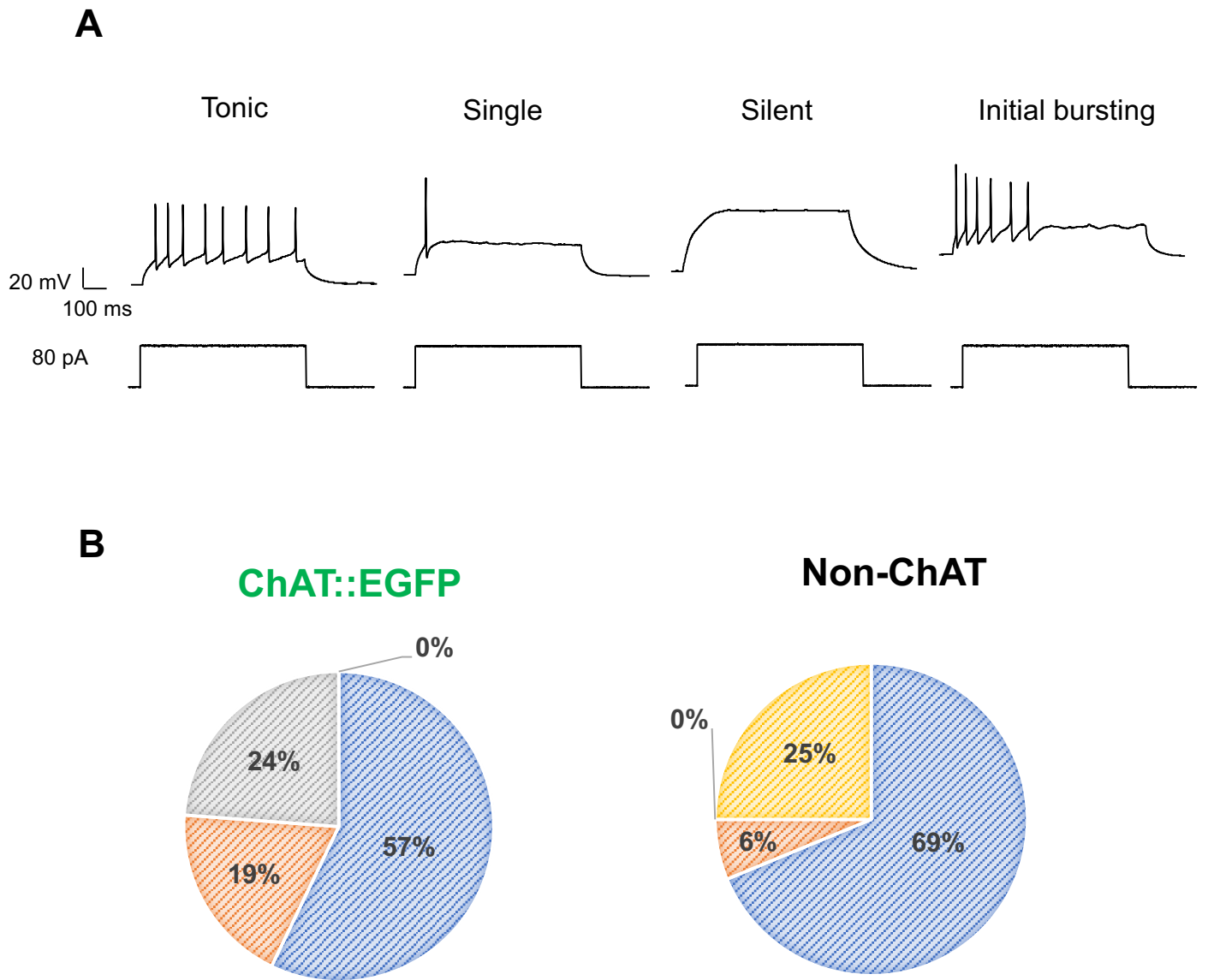


**Figure 4.1:** Firing patterns of ChAT::EGFP and Non-ChAT neurons in LIII/IV of the spinal cord **4.1A:** Recording illustrating of the 4 different types of firing patterns: Tonic; Single; Initial burst and reluctant firing or silent in ChAT::EGFP. **4.1B:** The distribution of different firing patterns in the two neuron groups. The ChAT::EGFP were recorded in horizontal, parasagittal and transverse slices whereas the non-ChAT were not recoded in from parasagittal plane.

## 2.1.   *Firing pattern*

After obtaining a stable whole-cell recording, we switched to the current-clamp mode. A very low fraction of recorded neurons presented spontaneous ongoing firing at rest: 3 out of 21 (14%) ChAT::EGFP neurons, and 4 out of 16 (25%) Non-ChAT neurons (Fig. 4.2). There was no statistically significant difference between the two populations (Fisher's exact test: p = 0.4373). We then applied pulses (700 ms) of positive currents (20 up to 600 pA) to investigate the firing pattern of the cells.

ChAT::EGFP neurons presented different types of firing patterns (Fig. 4.1A,B): tonic (57.1% of neurons), initial burst (19%), or single spike (23.8%) (n= 21 neurons recorded from HS, PS and TS). Among Non-ChAT neurons (n= 16 neurons recorded in HS and TS), 68.8% were tonic, 6.3% single spike. In addition, three neurons (25%) were classified as "silent" or reluctant firing, as they did not fire action potentials after application of depolarizing current of 180 pA. To compare these observations in different slice orientation, firing patterns and neuron types, we have used three-way contingency table. However there was no statistical difference between ChAT::EGFP and Non-ChAT neurons (for HS and TS only) concerning the proportions of the different firing patterns (3x3x3 contingency tables, p = 0.693). We only recorded ChAT::EGFP neurons in PS; the distribution of these neurons amongst the different firing patterns was not different in PS compared to TS and HS (Fisher's exact test, p = 0.2982). Similarly, there was no significant differences between slices for non-ChAT cells (Fisher's exact test, p =0.281) (Table 4.1). There also was no statistical difference in the rheobase for these two populations in different slice orientations (Kruskal Wallis test, p = 0.6427) (Table 4.2).

***Interpretation-discussion:*** A previous publication of our team analyzed the firing pattern of ChAT::EGFP neurons in parasagittal and horizontal slices, and reported 67% of tonic firing pattern, as well as 27% of neurons with ongoing firing activity (Mesnage et al., 2011). These proportions were not significantly different to our observations (chi-square, p=0.56 and p=0.35). Interestingly, in the previous study as well as in the present one, neurons with ongoing activity were of the "tonic" firing type. ChAT::EGFP neurons also presented other firing patterns, and there was no specific feature to this population.

## 2.2.   *Passive properties*

We also injected negative currents (-30 to -90 pA) to investigate the membrane properties of recorded neurons. In particular, we measured the input resistance, the cell capacitance, and the amplitude of a (potential) sag current (see Methods). ChAT::EGFP neurons were recorded in the

**A**

| Firing patterns | Horizontal | | Parasagittal | Transverse | |
| --- | --- | --- | --- | --- | --- |
| | ChAT::EGFP | Non-ChAT | ChAT::EGFP | ChAT::EGFP | Non-ChAT |
| Tonic Firing | 85.7 | 87.5 | 28.6 | 57.1 | 50.0 |
| Single Firing | 0.0 | 0.0 | 28.6 | 28.6 | 12.5 |
| Initial burst Firing | 14.3 | 0.0 | 42.9 | 14.3 | 0.0 |
| Silent | 0.0 | 12.5 | 0.0 | 0.0 | 37.5 |
| Total N | 7 | 8 | 7 | 7 | 8 |

**Table 4.1:** Percentage of observed firing patterns in ChAT::EGFP+ and Non-ChAT cells in three slice orientations of naïve mice.

**B**
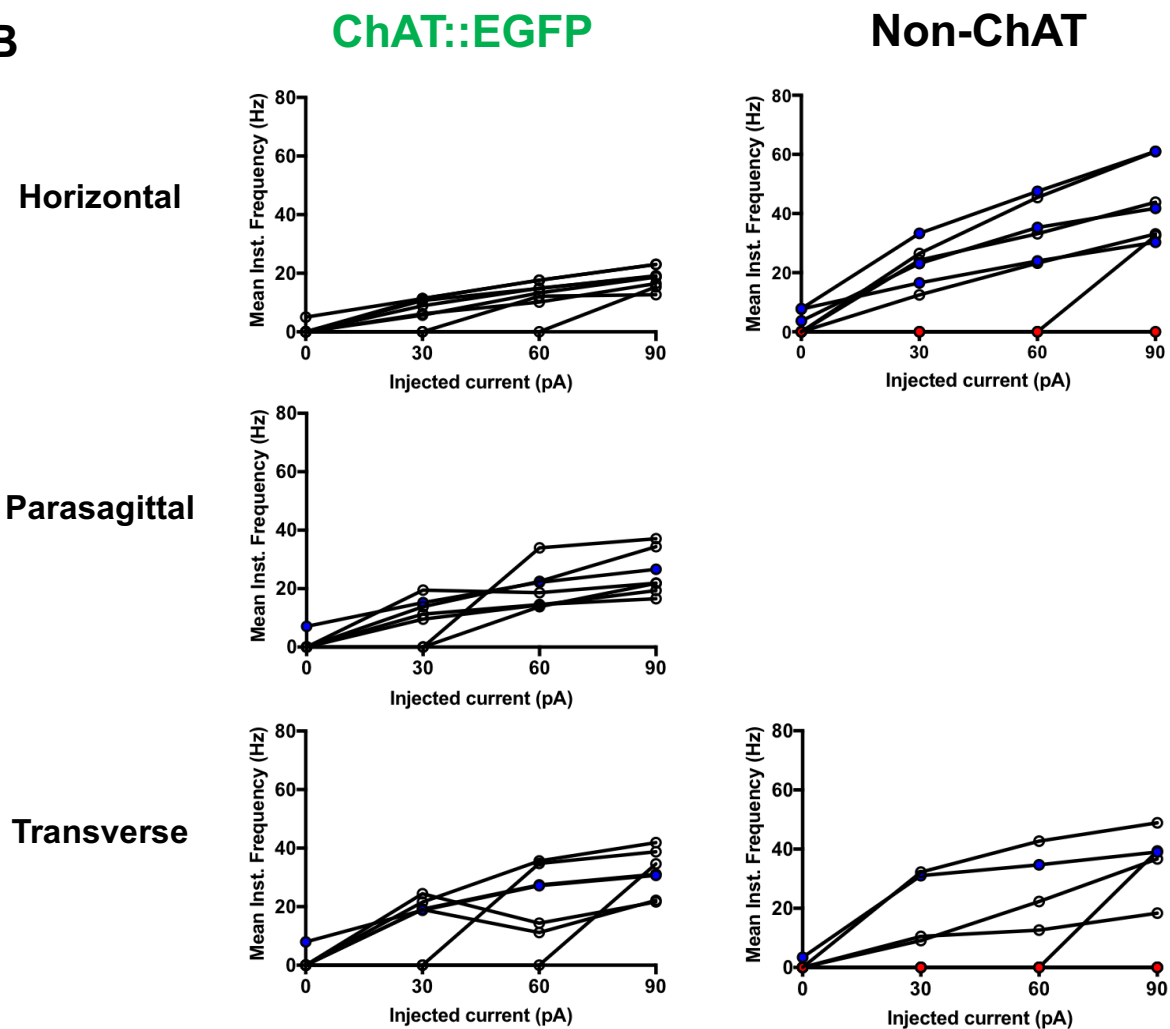


**Figure 4.2:** Mean Instantaneous frequencies for ChAT::EGFP and Non-ChAT cells in three slice orientations. Spontaneously firing cells (blue dots) at rest are present in both populations. The reluctant firing cells (red dots) were present uniquely in Non-ChAT recorded cells.

three slice orientations, while Non-ChAT neurons were recorded in horizontal and transverse slices (Table 4.2). There was no difference in the resting potential (ANOVA, p = 0.69), input resistance (ANOVA: p = 0.3651) or amplitude of sag current (Scheirer-Ray-Hare test: p =0.98511), between these two cell groups, or between slice orientations. However, a difference in cell capacitance was observed between cell groups on different slices (ANOVA: p = 6.5E -003). The capacitance of ChAT::EGFP neurons recorded in transverse and parasagittal slices was statistically smaller than the one recorded in horizontal slices (Table 4.2) (TukeyHSD: respectively p = 8.7E -004 and p = 0.006). Furthermore, the cell capacitance of Non-ChAT cells were smaller compared to ChAT::EGFP cells on horizontal slices (TukeyHSD: p = 8.6E -004).

*Interpretation-discussion:* There was no passive property specific to ChAT::EGFP neurons. The fact that these neurons had lower cell capacitance in transverse slices could be explained by the morphology of the dendritic arbor: the team has indeed previously reported that cholinergic interneurons have an extended dendritic arbor in the rostrocaudal direction, mainly dorsal to the cell body (Mesnage et al., 2011). They are therefore potentially profoundly truncated in transverse slices. On the other hand, they are fully preserved in horizontal slices, and their average larger cell capacitance demonstrates that they are amongst the larger neurons in laminae III-IV.

## 2.3. *Rebound spiking*

The majority (85.7%) of ChAT::EGFP neurons presented a rebound spike upon the end of the hyperpolarizing pulse (Fig. 4.3). This was independent of the slice orientation. In contrast, only 2 out of 13 Non-ChAT neurons (15.4%) presented such a rebound spike. There was a statistical difference between the two populations, when recorded in HS and TS, concerning this feature (Fisher's exact test: p = 0.0004). The proportion of ChAT::EGFP neurons presenting a rebound spike was independent of the slice orientation (HS, PS and TS) (Fisher's exact test: p = 0.7421).

*Interpretation-discussion:* The team previously reported the existence of rebound spikes in half ChAT::EGFP neurons (Mesnage et al., 2011). We observed a higher proportion of such rebound spiking neurons (chi-square, p=0,03), which even can be considered as a specific feature of the cholinergic interneurons in our dataset.
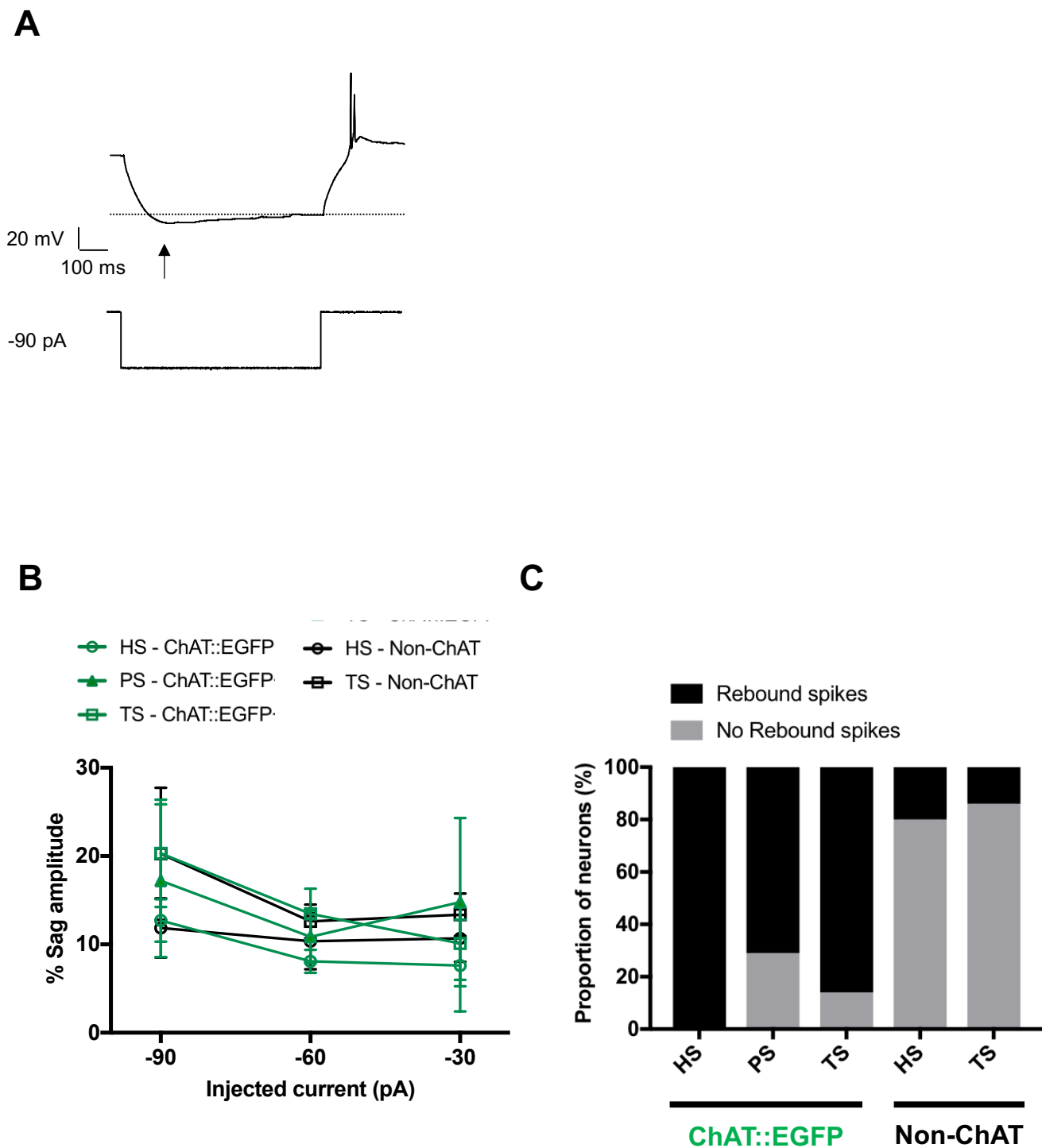
**Figure 4.3:** Electrophysiological properties of for ChAT::EGFP and Non-ChAT cells on horizontal (HS), parasagittal (PS) and transverse (TS) slice in naive mice. **4.3A** Voltage responses to hyperpolarizing current steps. Post-IR: post-inhibitory rebound. Arrow: hyperpolarizing "sag." **4.3B** % sag amplitude. There was no observable differences in the sag amplitudes. **Fig. 4.3C** Proportion of cells demonstrating rebound spikes after hyperpolarization pulses. The rebound spikes appear to be a unique feature of ChAT::EGFP neurons

| Slice | N | | RMP (mV) | | Input Resistance (TΩ) | | Capacitance (pF) | | Rheobase (pA) | |
| | | | ChAT::EGFP | Non-ChAT | ChAT::EGFP | Non-ChAT | ChAT::EGFP | Non-ChAT | ChAT::EGFP | Non-ChAT |
|---|---|---|---|---|---|---|---|---|---|---|
| HS | ChAT::EGFP (7) | Mean | -50.84 | -57.85 | 0.74 | 0.77 | **87.89** | **46.81 \*\*\*** | 42.86 | 25.71 |
| | Non-ChAT (8) | SEM | 4.44 | 3.07 | 0.12 | 0.11 | 7.92 | 3.69 | 8.92 | 11.34 |
| PS | ChAT::EGFP (7) | Mean | -63.35 | N/A | 0.94 | N/A | **52.16 ###** | N/A | 34.29 | N/A |
| | Non-ChAT (N/A) | SEM | 7.12 | N/A | 0.34 | N/A | 6.32 | N/A | 7.82 | N/A |
| TS | ChAT::EGFP (7) | Mean | -56.95 | -60.36 | 0.74 | 0.67 | **45.50 ###** | 41.28 | 38.57 | 36.00 |
| | Non-ChAT (8) | SEM | 2.88 | 4.39 | 0.10 | 0.21 | 8.16 | 5.54 | 10.79 | 11.62 |

**Table 4.2:** Electrophysiological properties of ChAT::EGFP and Non-ChAT cells in horizontal (HS), parasagittal (PS) and transverse (TS) slices of naïve mice. ### $p < 0.001$ comparing capacitance of slice vs HS; post-hoc: TukeyHSD \*\*\* $p < 0.001$ comparing capacitance between ChAT::EGFP+ vs Non-ChAT.

# 3. Spontaneous and miniature excitatory synaptic inputs onto DH ChAT::EGFP neurons

## 3.1. *Frequency of excitatory currents*

We recorded spontaneous and miniature EPSCs (for miniature in TTX 0.5 µM) from ChAT::EGFP and Non-ChAT neurons in horizontal, parasagittal and transverse slices. The individual traces and frequencies of each subsets are illustrated in Fig. 4.4A-B. We first performed a global analysis of the variance of all the data point obtained, in order to establish the validity of subsequent group comparisons (see Methods).

The data being non-normal, their log10 was taken to perform the ANOVA. There was a significant effect of the type of currents (spontaneous vs. miniatures; p=0.0002), the of type of neurons (ChAT::EGFP vs. Non-ChAT; p=0.023) and the slice orientations (p=0.003). In addition, there was a significant association between the type of neurons, currents and the slice orientation (p = 0.029).

To analyze the specific pairings, we performed Tukey post-hoc tests. The frequency of miniatures was significantly lower than the frequency of spontaneous currents (TukeyHSD: p=0.000387; Mean spontaneous: 1.05 ± 0.16 Hz vs Mean miniature: 0.53 ± 0.09 Hz). Post-hoc analysis confirmed a difference between ChAT::EGFP and Non-ChAT cells (TukeyHSD: p=0.031). Finally, the frequency of synaptic currents was significantly lower in transverse slices (0.534 ± 0.09 Hz) compared to parasagittal slices (1.02 ± 0.22 Hz) (TukeyHSD: p=0.00995) and horizontal slices (1.02 ± 0.2 Hz)

As for the interaction between the type of neurons, currents and the slice orientation, ChAT::EGFP neurons received significantly less sEPSCs in transverse slices (0.198 ± 0.04 Hz) compared to horizontal (1.38 ± 0.56 Hz) and parasagittal (0.79 ± 0.153 Hz) (Dunn's test: respectively p= 0.0340 and p = 0.0499). Also, ChAT::EGFP neurons in transverse slices received significantly less sEPSCs than non-ChAT neurons (Dunn's test: p=0.0045; Non-ChAT: 1.04 ± 0.17 Hz vs ChAT::EGFP: 0.63 ± 0.11 Hz).

*Interpretation-discussion:* In transverse slices, the frequency of sEPSCs in ChAT::EGFP neurons is particularly low. The simplest explanation for this observation would be that the majority of excitatory inputs to these neurons are not present in transverse section, i.e. are located more distally

in the rostro-caudal directions. However, a more conservative view is to consider that only the excitatory drive, i.e. what is necessary for presynaptic excitatory neurons to be active, is missing from the slice. Interestingly, the excitatory drive for Non-ChAT neurons is not affected in transverse slices. The localization of its excitatory drive, distally in the rostro-caudal axis, appears thus to be a unique feature of ChAT::EGFP neurons.

We however have to keep in mind that the Non-ChAT population is certainly heterogeneous. This could explain that, on average, there is no difference depending on the slice orientation.

It has been demonstrated that slice orientation can affect the frequency of miniature events (Staley and Mody, 1991). In our study, however, we found no such effect. The frequency of mEPSCs depends on the number of synaptic contacts as well as on their release probability. Our data suggest that the overall number and basal activity of excitatory synapses in LIII-IV is the same in all slices.

It is interesting to compare the frequencies of sEPSCs and mEPSCs. The frequency of sEPSCs in transverse sections is so low that it is very similar to the one of mEPSCs. This suggests that the currents recorded in the absence of TTX, in transverse slices, are actually miniature currents and that the presynaptic excitatory neuron is not present in the slice. This relies on the hypothesis that axons sectioned by the slicing do not fire spontaneously.

We should however mention that, although significantly higher than in transverse, the frequency of sEPSCs in horizontal and parasagittal slices is not significantly different from the frequency of mEPSCs in these slices. Admittedly, we have been using an ANOVA and post-hoc tests taking into account all multiple comparisons (Bonferroni correction), to prevent type-1 error. In this experiment, we have 24 pair-comparisons, which decreases the chances of reaching significance. However, the lack of difference between sEPSCs and mEPSCs in horizontal and parasagittal slices obviously weakens the conclusion of the previous paragraph.

## 3.2.    *Amplitudes of excitatory currents*

We also compared the amplitude of mEPSCs in the different neurons, slice orientation and animals (Fig. 4.4C). After normalization of the data (through log10), the ANOVA demonstrated no significant association between the "neurons" and "slice" factors (p= 0.2715).

*Interpretation-discussion:* There is no difference in the amplitude of mEPSCs linked to the slice orientation or neuron type.
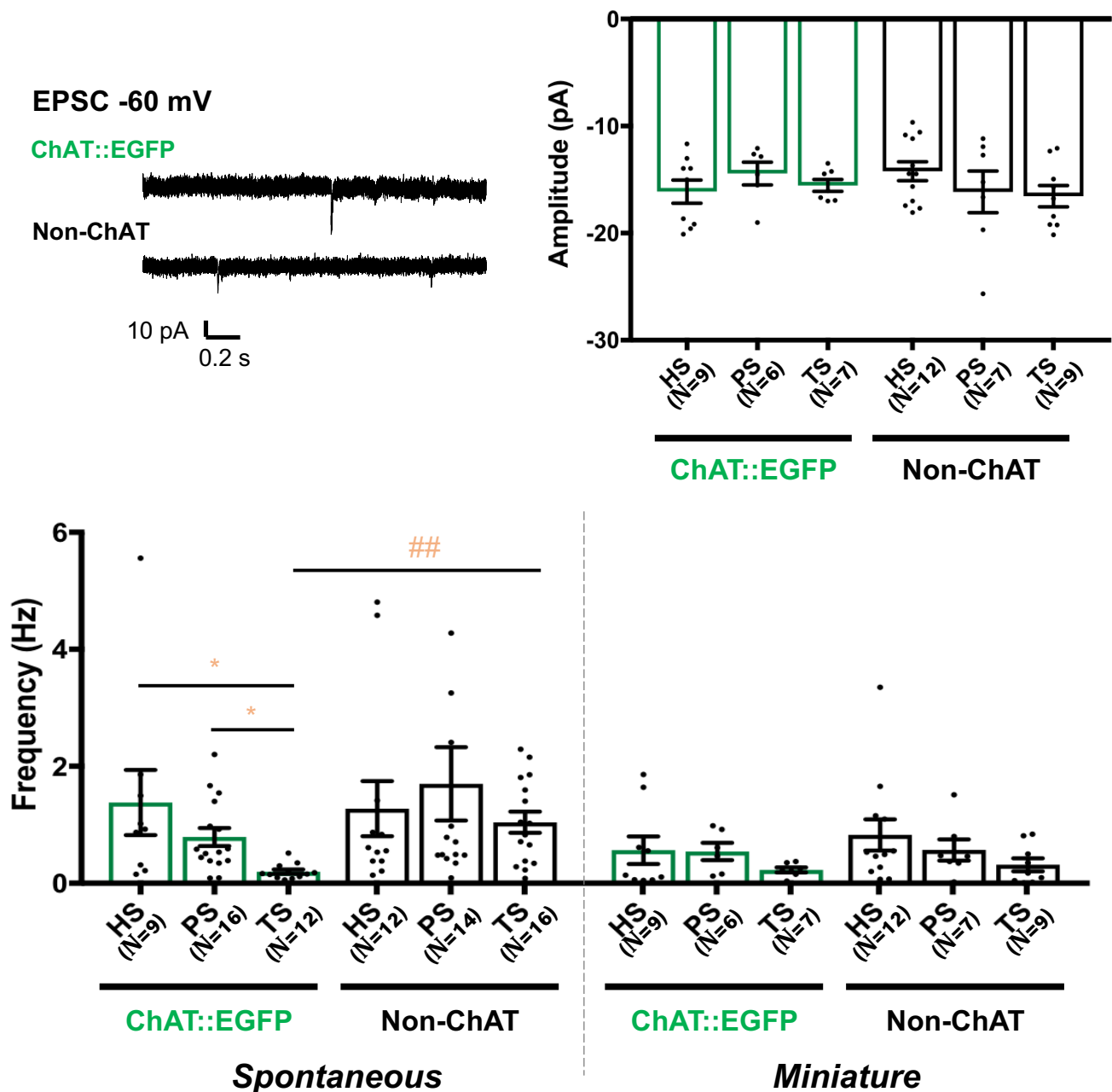
**Figure 4.4:** The frequencies and amplitudes for spontaneous and miniature excitatory post-synaptic currents (EPSC) in ChAT::EGFP and Non-ChAT cells in horizontal (HS), parasagittal (PS) and transverse (TS) slices of naïve mice. **4.4A** Representative traces of spontaneous and miniature EPSC recorded in ChAT::EGFP (left) and non-ChAT (Right) cells. **4.4B** Frequencies of spontaneous and miniature EPSCs. The frequencies of ChAT::EGFP on TS was significantly lower to those in PS and HS in addition Non-ChAT cells on the same slice. ### $p < 0.001$ comparing capacitance of slice vs HS; post-hoc: Dunnett's multiple comparisons * $p < 0.05$; ## $p < 0.01$; * comparing average between between slices and # compare averages within the same slice. **4.4C** The amplitudes of miniature EPSCs of ChAT::EGFP and Non-ChAT. No observable differences in measured amplitudes were reported between neuron type or slices.

# 4. Spontaneous and miniature inhibitory synaptic inputs onto DH ChAT::EGFP neurons

## 4.1. *Frequency of inhibitory currents*

The mean frequencies of inhibitory currents are illustrated in Fig. 4.5A-B. We first performed a global analysis of the variance of all the data point obtained, in order to establish the validity of subsequent group comparisons. As with the excitatory currents, the data being non-normal, log10 was taken to perform the ANOVA. There was a significant effect of type of currents (spontaneous vs. miniatures; p=0.0005), and of type of neuron (ChAT::EGFP vs. Non-ChAT; p=4.73e-5).

We simplified the model to take into account only those parameters that were proven meaningful, and then performed Tukey post-hoc tests. As expected, the frequency of mIPSCs (0.294 ± 0.08 Hz) was statistically lower than the frequency of sIPSCs (0.748 ± 0.16 Hz) (TukeyHSD: p = 0.00072). ChAT::EGFPs neurons had statistically lower frequency of inhibitory currents (0.29 ± 0.08 Hz) than Non-ChAT neurons (0.81 ± 0.17 Hz) (TukeyHSD: p = 5.79e-05).

*Interpretation-discussion:* ChAT::EGFP neurons appear to have lower frequency of inhibitory currents compared to Non-ChAT. Since there is no significant difference in the slice orientation, we can only suggest that the synaptic strength of inhibitory drive may be lower in cholinergic cells.

## 4.2. *Amplitude of inhibitory currents*

We compared with a similar approach the amplitude of mIPSCs in the different neurons and slice orientations (Fig. 4.5C). After normalization of the data (through log), the ANOVA concluded on a significant effect of the "slice" factor (p= 0.0359). LIII/IV neurons had mIPSCs of lower amplitude in parasagittal (22.44 ± 2.21 pA) compared to transverse slice (35.17 ± 5.28 pA) (TukeyHSD: p = 0.0432).

*Interpretation-discussion:* The mIPSCs recorded in parasagittal slices were smaller than those in Non-ChAT neurons. This difference could suggest another control of inhibitory inputs to transverse cells compared to parasagittal.
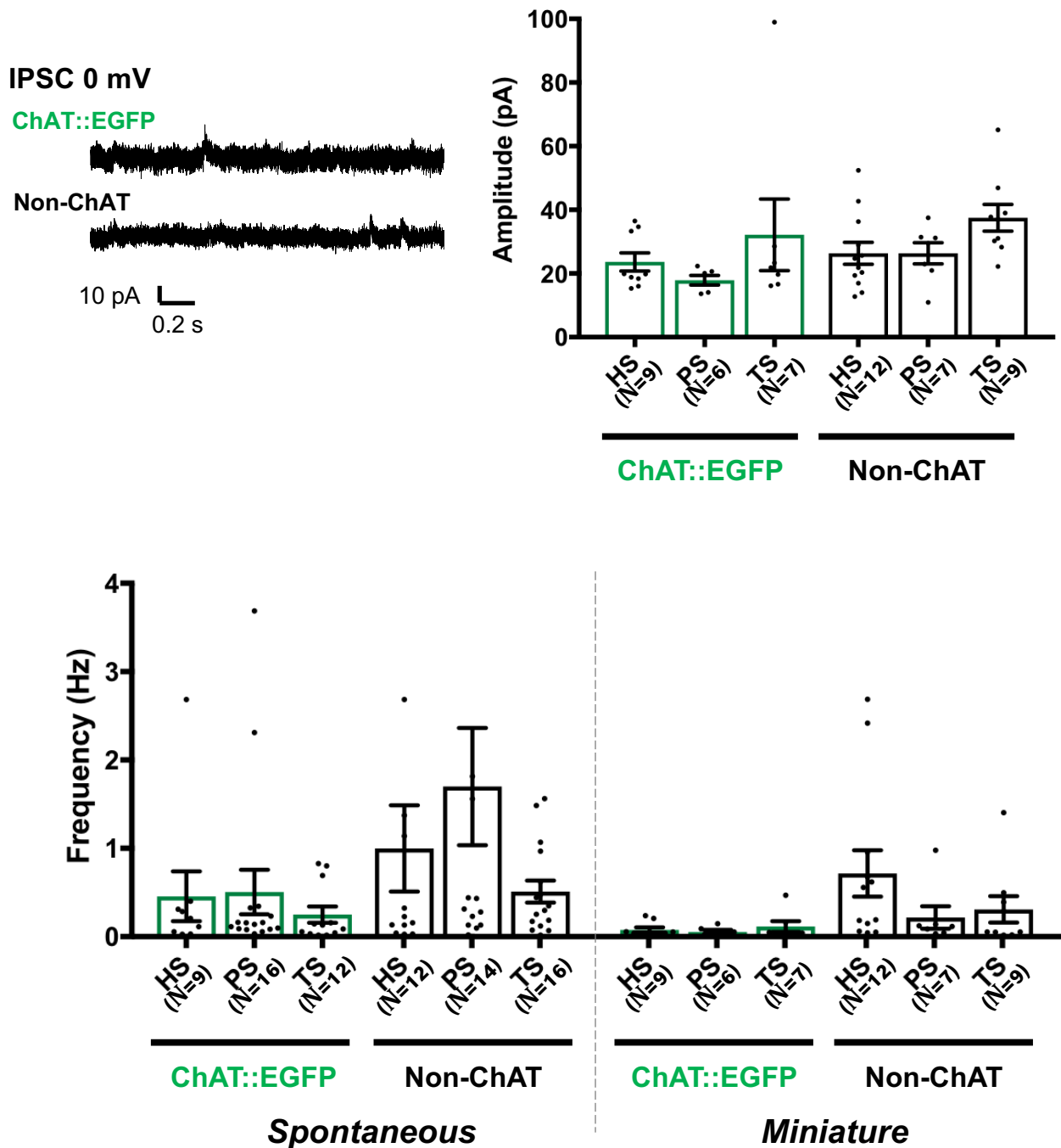
**Figure 4.5:** The frequencies and amplitudes of spontaneous and miniature inhibitory post-synaptic currents (IPSC) ChAT::EGFP and Non-ChAT cells in horizontal (HS), parasagittal (PS) and transverse (TS) slices of naïve mice. **4.5A** Representative traces of miniature IPSCs recorded in ChAT::EGFP (top) and non-ChAT (bottom) cells. **4.5B** The frequencies of excitatory and IPSCs. The inhibitory currents remained constant irrespective of slice or neuron types. **4.5C:** The amplitudes of miniature IPSCs of ChAT::EGFP and Non-ChAT cells. No significant difference has been reported for the amplitudes of inhibitory currents across all groups.

## 5. Excitatory/inhibitory ratio onto DH LIII-IV neurons

The frequencies of excitatory and inhibitory currents were analyzed separately in the previous sections, as we considered them to be two independent features of the recorded neurons. However, because we actually have both excitatory and inhibitory currents recorded on each individual cell, we decided to analyze the ratio between their frequencies (E/I) in a separate analysis.

The E/I ratio was calculated in ChAT::EGFP and Non-ChAT neurons in horizontal, parasagittal and transverse slices. The log10 of the ratios was used to normalize the data (shapiro-wilk test: p = 0.0032); we proceeded with ANOVA due to appropriate sized dataset. We first performed a global analysis of the variance of all the data point obtained, in order to establish the validity of subsequent group comparisons.

There was a significant effect of the type of neuron (ChAT::EGFP vs. Non-ChAT; p = 0.0276). We simplified the model to take into account only those parameters that were proven meaningful, and then performed Tukey post-hoc tests (Fig. 4.6). The E/I ratio in ChAT::EGFP neurons (6.75 ± 0.83) was significantly higher than in non-ChAT neurons (5.34 ± 0.91) (TukeyHSD: p = 0.029).

*Interpretation-discussion:* We observed a small difference in the E/I ratio between ChAT::EGFP and Non-ChAT. We previously reported that the frequency of inhibitory currents was particularly low in ChAT::EGFP neurons. This is the most probable source of high E/I ratio in these neurons compared to Non-ChAT neurons. Moreover, the cumulative charge of EPSC or IPSC from each cell should be taken into account while determining its E/I ratio.

## 6. Primary afferent inputs to DH ChAT::EGFP neurons

### 6.1. *Pharmacological stimulation*

Part of the excitatory currents recorded in DH neurons most likely corresponds to synapses formed by primary afferents. Indeed, immuno-histochemical data suggest that ChAT::EGFP neurons receive contacts from myelinated and non-myelinated fibers (Ribeiro-da-Silva and Cuello, 1990; Olave et al., 2002). We thus decided to more specifically study the peripheral innervation of cholinergic interneurons.

A classical approach to do so is to take advantage from receptors expressed by specific subsets of primary afferents (e.g. TRPV1): applying their agonist (in this case capsaicin) in slices enables to specifically depolarize these fibers. As primary afferents are glutamatergic, their post-synaptic neurons should see an increase in frequency of glutamatergic currents.
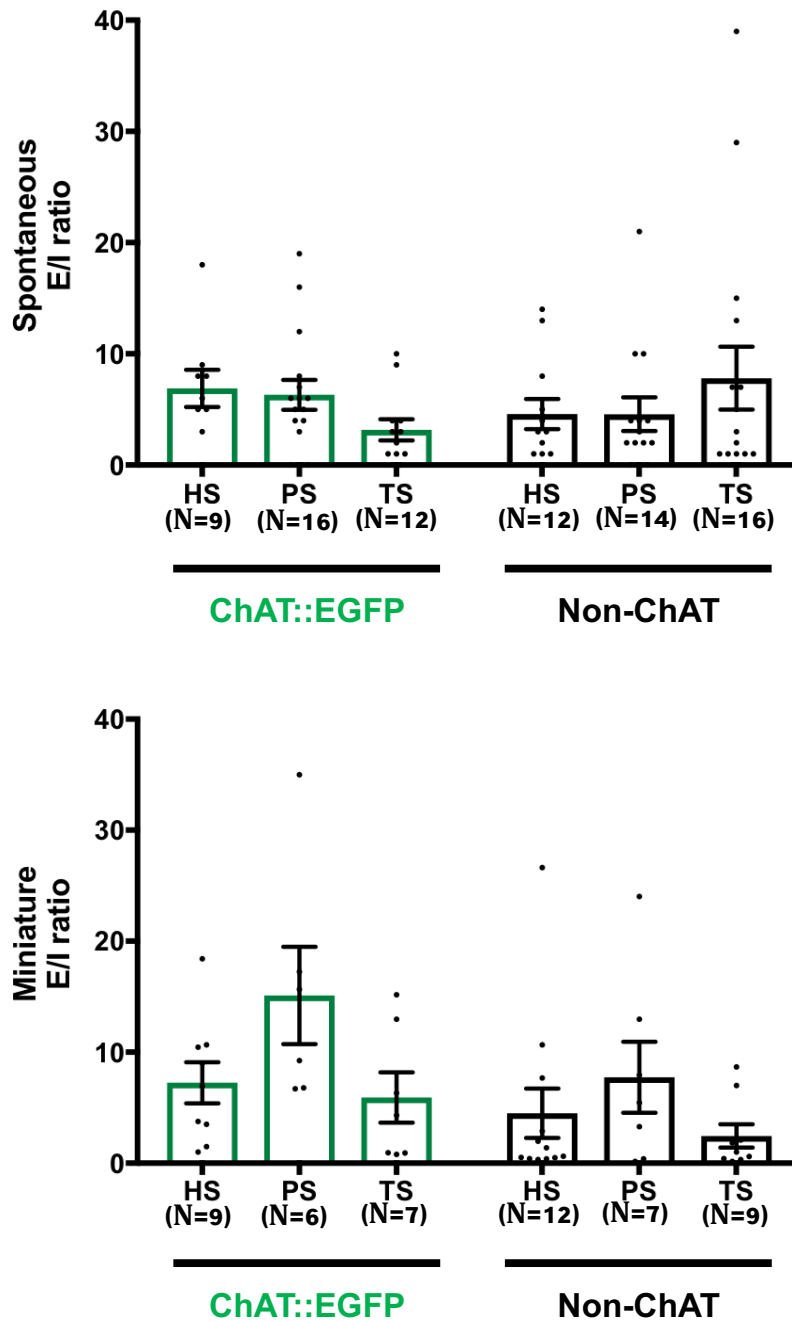
**Figure 4.6:** The ratio between the frequency (f) of spontaneous (top) and miniature (bottom) excitatory (EPSC) over inhibitory (IPSC) post-synaptic currents (f.EPSC/f.IPSC) of ChAT::EGFP and Non-ChAT cells in horizontal (HS) and transverse (TS) slices of naïve, sham and cuff mice. No significant differences were detected at interactions between the Animal (Naïve, Sham, Cuff) * Neuron (ChAT::EGFP or Non-ChAT) * Slice (HS or TS) * Current (Spontaneous or Miniature). However, there were detectable differences observed with fewer interactions (see text).

### 6.1.1. *Capsaicin-responsive primary afferents*

Capsaicin (5 μM), a specific agonist of TRPV1 receptors was bath-applied during 90 s on horizontal spinal slices. This occasionally led to an increase in the frequency of sEPSCs (Fig. 4.7A-B). A cumulative plot of the events number over time enabled to quantify this increase (Fig. 4.7A): in such a plot, the slope of the curve corresponds to the frequency of events. A significant break in the curve (see Methods) demonstrates a response to the drug application.

71,4% of ChAT::EGFP neurons responded to the application of capsaicin with an increase in the frequency of sEPSCs. This however was never observed when TTX was present in the slice (none of the 5 tested neurons showed an increase in frequency of mEPSCs). Half of ChAT::EGFP neurons demonstrated an increase in frequency in sIPSCs after application of capsaicin. None of the ChAT::EGFP neurons tested in TTX responded to capsaicin with an increased frequency of mIPSCs.

Concerning Non-ChAT::EGFP neurons, a third of the neurons responded to capsaicin with an increase in the frequency of sEPSCs; similarly almost a third responded with an increase in the frequency of mEPSCs, or with an increase in the frequency of sIPSCs (different groups of neurons). None responded with an increase in frequency of mIPSCs.

*Interpretation-discussion:* Capsaicin is an agonist for TRPV1 receptor, which is expressed in a subset of primary afferents. There is a controversial article mentioning the existence of TRPV1 expressing GABAergic neurons in the mouse DH (Kim et al., 2012). If true, this could complicate the interpretation of the present experiment, as an increase in IPSCs could be due to activation of these DH neurons, as well as to activation of a pathway initiated by activation of primary afferents. Our data do not favor the existence of TRVP1+ receptors on terminals of neurons impinging onto LIII-IV neurons (ChAT::EGFP or non-ChAT neurons), as we observed no increase of the frequency of mIPSCs in response to capsaicin application. We cannot rule out the potential expression of TRVP1 receptors on DH cell bodies, however the responses we observe to capsaicin most probably largely involve TRPV1-expressing primary afferents.

The absence of response to capsaicin in ChAT::EGFP neurons in presence of TTX suggests that these neurons are not directly post-synaptic to primary afferents expressing the TRPV1 receptor. In contrast, a proportion of non-ChAT neurons appear to be post-synaptic to TRPV1-expressing primary afferents.

However, we observe an increase in the frequency of spontaneous EPSCs and IPSCs in ChAT::EGFP neurons in response to capsaicin. This suggests that this population is downstream
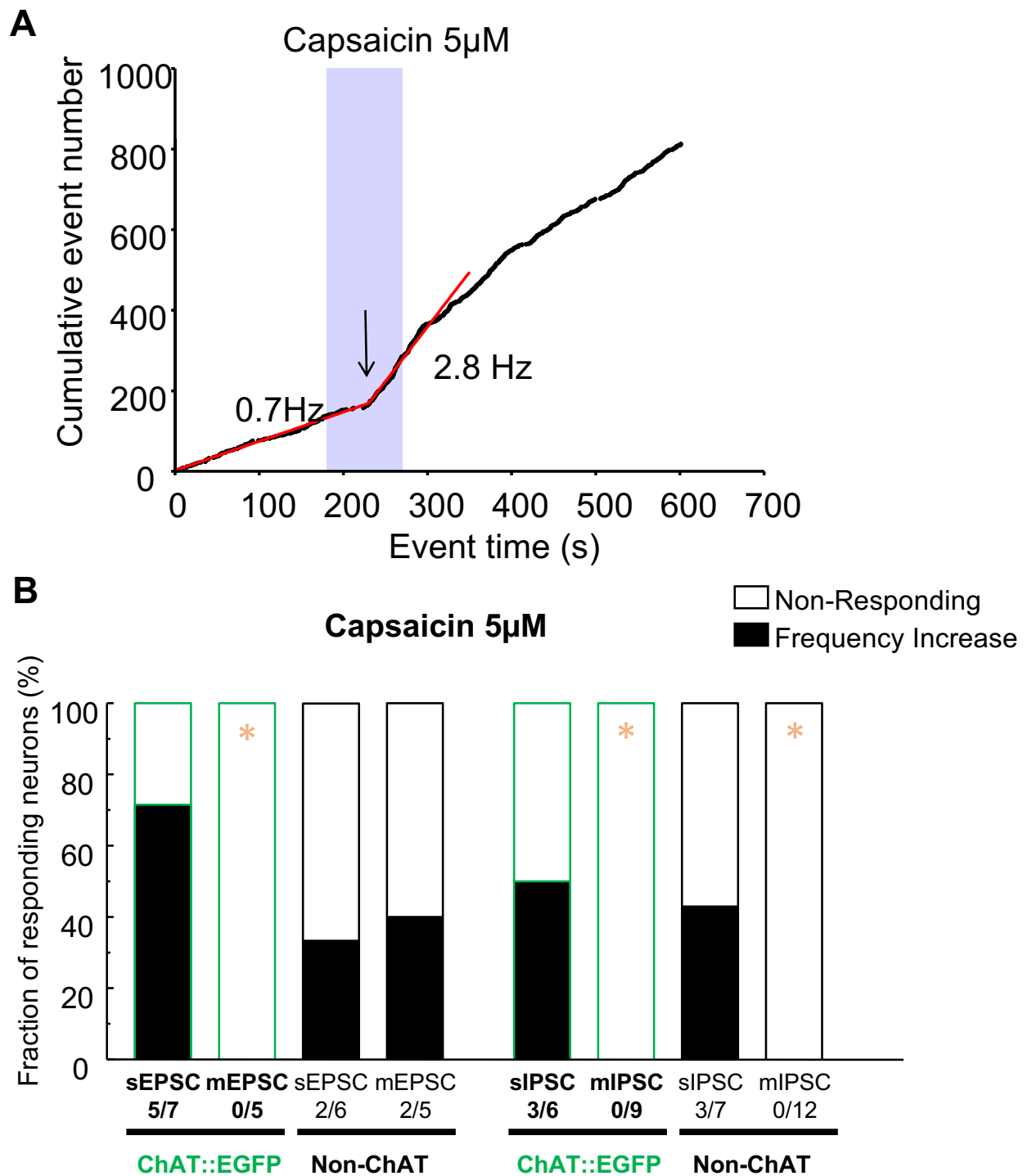
**Figure 4.7:** Effect of Capsaicin on the excitatory and inhibitory synaptic transmission. **4.7A** A representative cumulative frequency histogram of spontaneous EPSC in ChAT::EGPF neurons. The two red lines are best-fit segments fitted on the cumulative synaptic events. This allows the estimation of the frequencies prior and during a capsaicin bath application. The black arrow indicates the time where the frequency change occurs. **4.7B** Summary histogram on the effect of capsaicin 5 μM on spontaneous and miniature EPSCs (Left four bars) and IPSCs (Right four bars) in ChAT::EGFP and Non-ChAT neurons. Miniature synaptic currents were recorded in the presence of TTX 0.5 μM. Fisher's exact test; *P < 0.05

of TRPV1-expressing primary afferents, in a pathway involving an intermediate excitatory or inhibitory interneuron. This is also the case of some non-ChAT neurons.

### 6.1.2. *Mustard-oil responsive primary afferents*

We similarly applied Mustard oil (100 mM), an agonist for TRPA1 receptors, during 180 s in the bath of parasagittal slices (Fig. 4.8A). None of the ChAT::EGFP or non-ChAT neurons responded to this application of Mustard oil with an increase in the frequency of sEPSCs. One non-ChAT neuron (out of 9 tested), but no ChAT::EGFP neuron, responded with an increase in frequency of sIPSCs.

We performed a control experiment on lamina II neuron, as a proportion of LII neurons has been reported to respond to Mustard oil with an increase in the frequency of sEPSCs. We indeed found that 4 out of 5 tested LII neurons responded in that way.

*Interpretation-discussion:* The absence of response to Mustard oil in ChAT::EGFP neurons suggests that these neurons are not located downstream to primary afferents expressing the TRPA1 receptor. This is also the case for most non-ChAT neurons; only one appeared to be indirectly connected to these primary afferents through an inhibitory neuron.

In contrast, as previously reported (Kardon et al., 2014), a large proportion of LII neurons are downstream to TRPA1-expressing primary afferents.

### 6.1.3. *Menthol-responsive primary afferents*

Finally, we also looked for responses to bath-application of Menthol (500 mM), an agonist for TRPM8 receptors, during 180 s onto parasagittal slices (Fig. 4.8B). None of the ChAT::EGFP or non-ChAT neurons responded to this application of menthol with an increase in the frequency of sEPSCs. Two non-ChAT neurons (out of 8 tested), but no ChAT::EGFP neuron, responded with an increase in frequency of sIPSCs.

We performed a control experiment on lamina II neuron, as a proportion of LII neurons has been reported to respond to menthol with an increase in the frequency of sEPSCs. We indeed found that 2 out of 3 tested LII neurons responded in that way.

*Interpretation-discussion:* The absence of response to menthol in ChAT::EGFP neurons suggests that these neurons are not located downstream to primary afferents expressing the TRPM8 receptor. This is also the case for most non-ChAT neurons; only two appeared to be indirectly connected to these primary afferents through an inhibitory neuron.
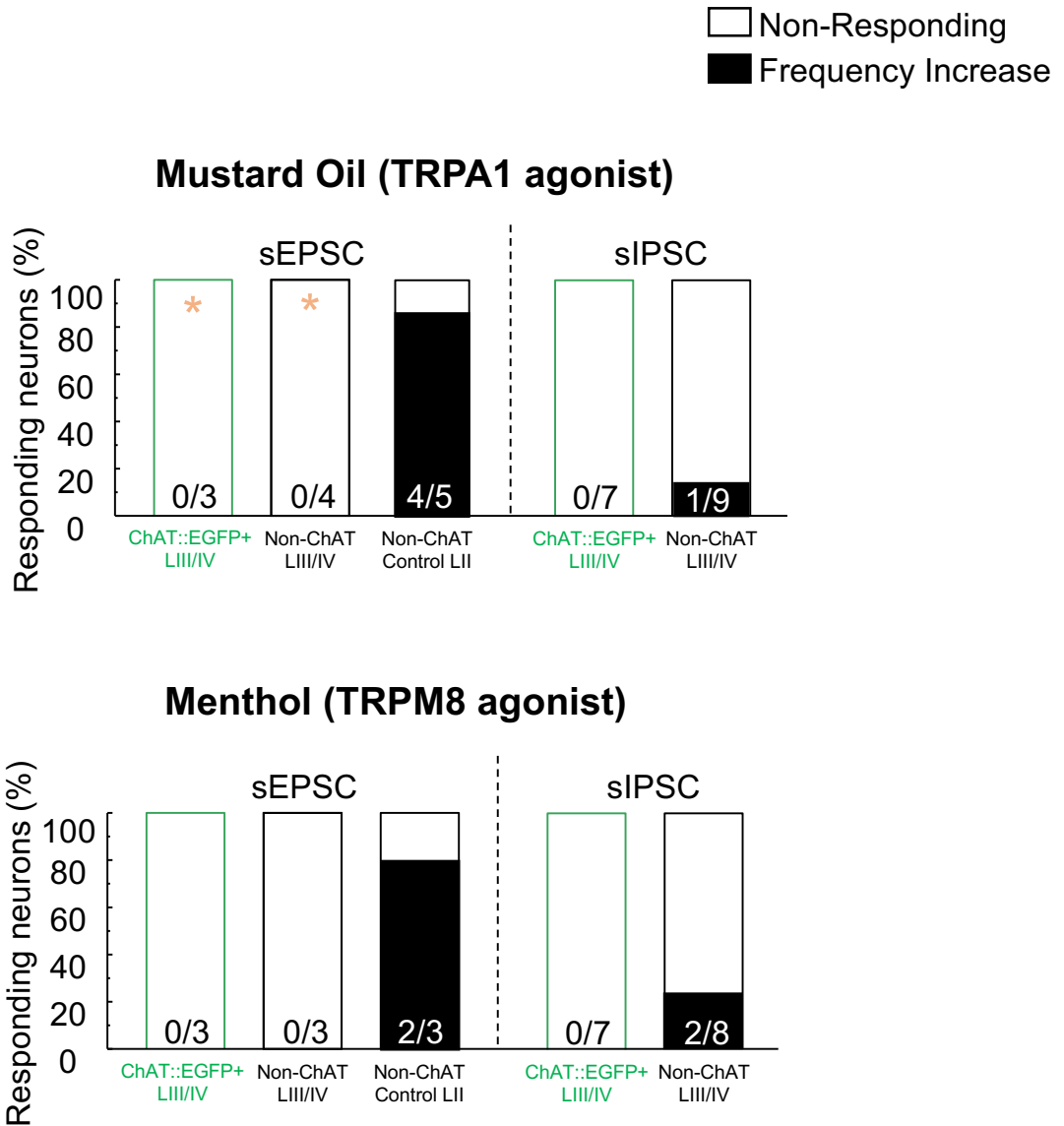
**Figure 4.8:** Effect of menthol and mustard oil on the excitatory and inhibitory synaptic transmission. **4.8A** Summary histogram on the effect of 100 µM on spontaneous EPSCs (Left three bars) and IPSCs (Right two bars) in ChAT::EGFP and Non-ChAT neurons. Mustard oil did not change the EPSCs frequencies of ChAT::EGFP cell. Similarly, the frequencies of EPSCs in LII cells and IPSCs in a fraction of Non-ChAT cells were increased. Fisher's exact test; *P < 0.05  between LIII/IV cells to LII controls. **4.8B** Summary histogram on the effect of Menthol 500 µM on spontaneous EPSCs (Left three bars) and IPSCs (Right two bars) in ChAT::EGFP+ and Non-ChAT neurons. Menthol did not alter the EPSCs frequencies of ChAT::EGFP+ cell. However, it elevated the frequencies of EPSCs in LII cells and IPSCs in a fraction of Non-ChAT cells.

In contrast, as previously reported (Kardon et al., 2014), a large proportion of LII neurons are downstream to TRPM8-expressing primary afferents.

## 6.2. *Electrical stimulation of dorsal root*

From anatomical studies, the DH cholinergic interneurons have been demonstrated to be downstream both myelinated and unmyelinated fibers (Ribeiro-da-Silva and Cuello, 1990; Olave et al., 2002). To examine the functional connection between primary afferents and ChAT::EGFP neurons, we recorded these neurons (and Non-ChAT ones for comparison) while stimulating electrically the attached dorsal root (DR), on horizontal slices (Fig. 4.9). The stimulation of DR inputs resulted in evoked EPSC and IPSC (eEPSC and eIPSC) in both populations. For eEPSCs, we classified the responses as single-(i.e. only one response observed when stimulation intensity was increased) or multi-component (contained eEPSCs with different latencies) responses. We observed a single-component eEPSC in 10% of ChAT::EGFP neurons, while 70% of neurons presented multi-component responses. Similarly, 20% of non-ChAT neurons presented a single-component eEPSC, while 60% presented multi-component responses. The stimulation amplitude required to evoke excitatory responses started at 0.005 mA and went up to 0.1 mA and 0.5 mA for single- and multi-component responses respectively.

Almost half of the recorded ChAT::EGFP and Non-ChAT cells received eIPSCs following DR stimulation. Interestingly, no cells exhibited eIPSCs without the presence of an eEPSC response. The threshold of eIPSC responses ranged from 0.01 up to 0.6 mA.

*Interpretation-discussion:* We have demonstrated that both ChAT::EGFP and Non-ChAT cells receive excitatory and inhibitory inputs following activation of DRs. From the stimulation threshold reported throughout the literature (Nakatsuka et al., 1999; Daniele and MacDermott, 2009; Ganley et al., 2015), the eEPSCs responses may result from activation of low-threshold and/or high threshold primary afferent fibers. In contrast, the detected eIPSCs were in consequence of high threshold activation. Since detected eIPSCs always occurred with eEPSCs, this could suggest that exclusively di-synaptic connection (with an intermediate inhibitory interneuron) with primary afferents does not exist for LIII/IV interneurons.

**A**



Mono-eEPSC        Poly-eEPSC        eIPSC
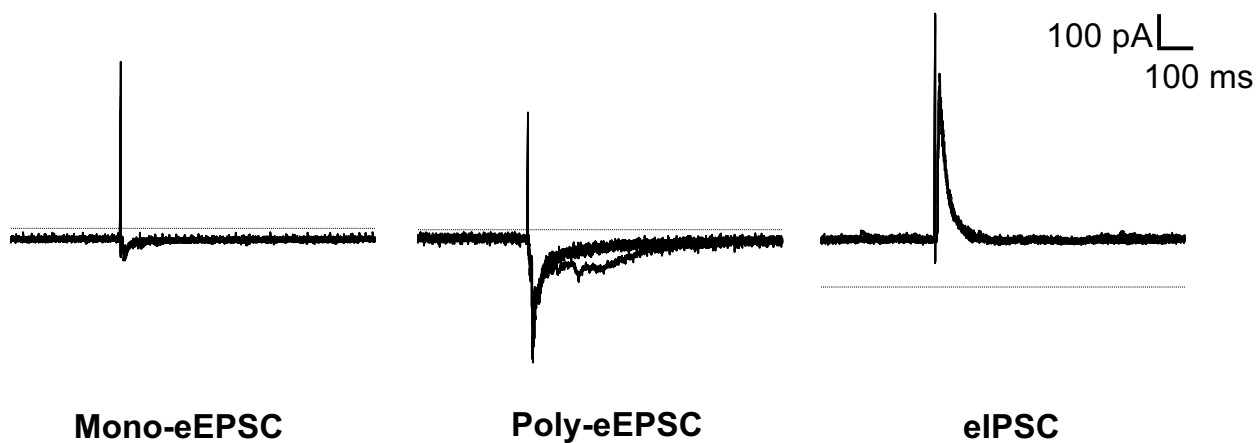
**B**
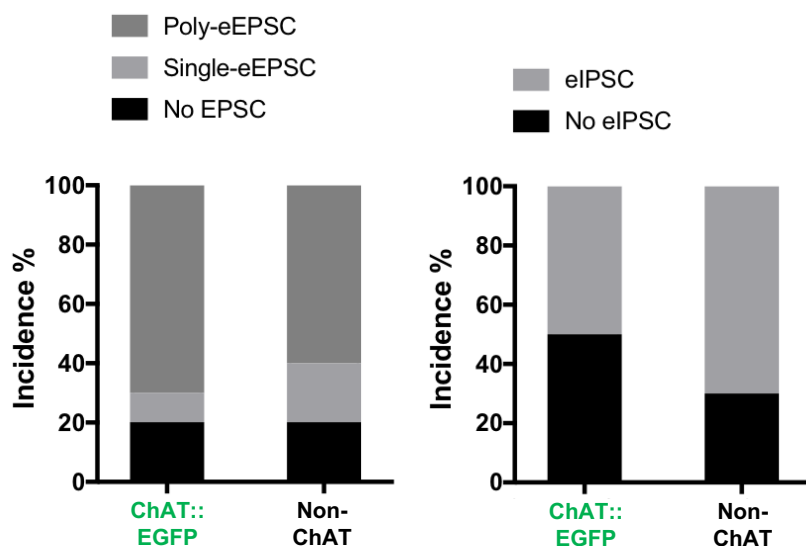


**Figure 4.9:** The evoked excitatory (left) and inhibitory (right) post-synaptic currents in ChAT::EGFP and Non-ChAT cells in horizontal slices of naïve mice after dorsal root (DR) stimulation. (N=10 in each group). **4.9A** Representative traces demonstrating single- (left) and poly- (middle) synaptic eEPSCs and IPSCs (right) in ChAT::EGFP. **4.9B** Incidence of eEPSC and eIPSC observed in both populations.

# 7. Downstream targets of ChAT::EGFP neurons

## 7.1. *Transynaptic tracing*

To investigate the downstream targets of cholinergic interneurons, we have used the trans-synaptic anterograde tracer wheat germ agglutinin (WGA). We injected an AAV encoding for a Cre-dependent form of WGA in the DH of the spinal cord of ChAT-Cre animals: this allows WGA to be expressed in ChAT cell expressing the Cre-recombinase enzyme. Once expressed, the WGA can in theory jump unlimitedly number of synapses; thus, we have perfused the animals at specific time points post-injection. These include: 1.5, 3, 4.5 and 6+ weeks post-injection. The spinal cords await analysis.

In our preliminary results, two ChAT-Cre adult mice have been injected with an AAV2-Flex-WGA virus at 6 weeks' post-injection (Fig. 4.10). We observed expression of WGA neurons throughout in the ipsilateral side of the spinal cord. WGA infected cells were in the DH, intermediate zones and ventral horn. For the DH, we observed co-localization between the WGA expressing cells and ChAT immunoreactivity; these cells are potentially the (first) virus infected cell or downstream cells to other cholinergic neurons.

*Interpretation-discussion:* Our preliminary experiments demonstrate the feasibility of the approach, as we observed WGA expression in DH ChAT::EGFP neurons as well as in non-ChAT-IR ones. This strongly suggests that the WGA initially expressed in ChAT neurons has been transported to its targets. Only a detailed analysis of the time course of WGA spread will enable us to gain information on the post-synaptic targets of DH cholinergic interneurons. It remains hard to confirm exactly which populations were the originally infected cells. Potentially, it is feasible to inject a floxed non-trans-synaptic AAV- expressing a reporter protein in addition to AAV-Flex-WGA. This approach was performed in search of the downstream targets to enkephalinergic neurons. The authors injected both AAV-FLEx-WGA and AAV-FLEx-YFP into the DH of Penk-Cre mice. The downstream targets were identified to be mostly LII inner glutamatergic neurons (Francois et al., 2017).

## 7.2. *Photostimulation of cholinergic neurons*

Throughout the course of my doctoral work, we have tried to obtain channelrhodopsin (ChR2) expression in DH cholinergic interneurons by different means. Although we were unsuccessful in our attempts, we collaborated with Dr. Brett Graham (Newcastle University, Australia) who obtained mice appropriated for an optogenetic approach. This was achieved by crossing ChAT::Cre

| WGA | ChAT | Merged |
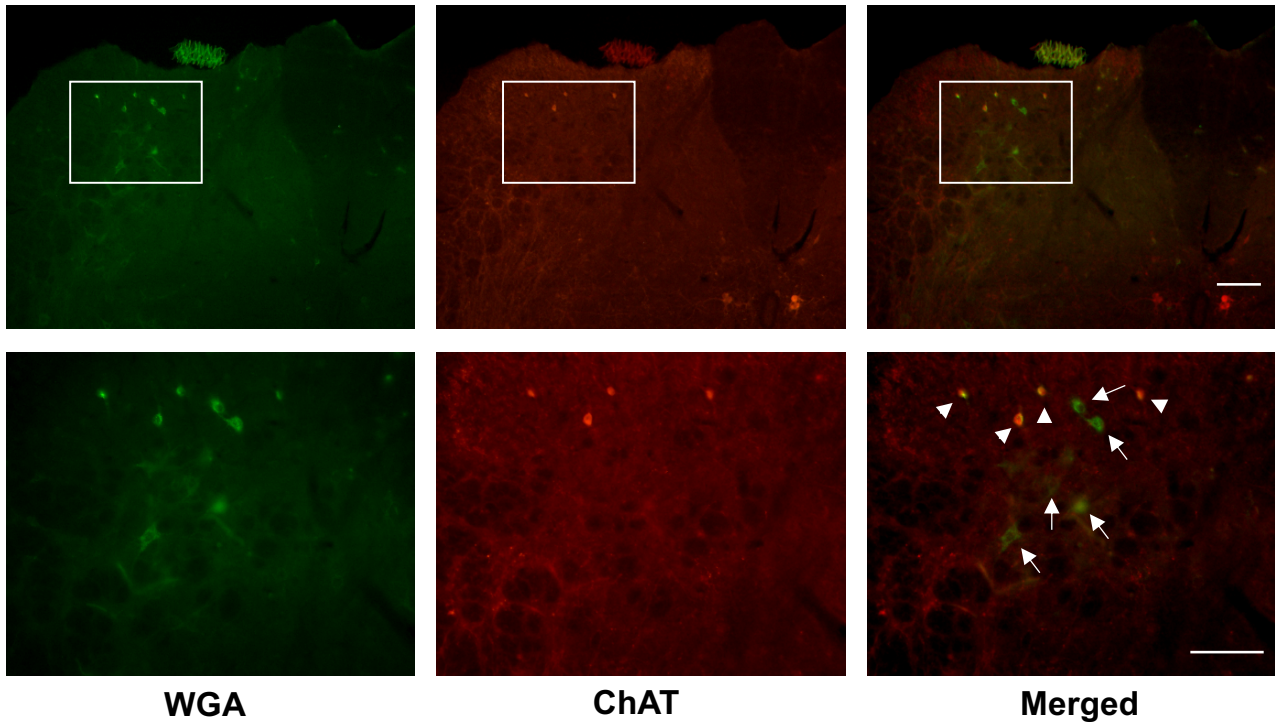
**Figure 4.10:** Expression of trans-synaptic anterograde tracer what germ agglutinin (WGA) in the Dorsal Horn of ChAT Cre animals [N = 2]. Immunoreactivity against Choline acetylcholinetranferase (ChAT) (Red, Middle panel) to determine cholinergic interneurons (or potential first infected cell) and the expression of WGA identified with anti-WGA antibodies (Green, Left panel). In the merged images (Yellow, Right panel), a number of cells colocalized with both ChAT and WGA (arrowheads) while the downstream cells expressing WGA are detected throughout the DH (arrows) (Scale = 100 μm).

mice with mice expressing ChR2 in a cre-dependent manner. We are briefly reporting here their preliminary results, as they will be part of the manuscript in preparation and useful for the discussion of our data.

DH cholinergic neurons are known to also express GABA in mice and rats, but were reported to be non-glycinergic in rat ((Todd, 1991; Mesnage et al., 2011). However, after photo-activation (single pulse) of cholinergic interneurons on DH network, they observed in LII neurons mono-synaptic current consisting of 75% glycinergic and 25% GABAergic component. Amongst non-ChAT LII neurons, 3.2% (1/31) presented a monosynaptic only response, 38.7% (12/31) a polysynaptic only response, and 54.8% (17/31) mono- and poly-synaptic responses while 3.2% (1/31) were non-responding. They also recorded cholinergic interneurons in lamina III-IV, and found that 18.2% (4/22) had a monosynaptic only response, 18.2% (4/22) a polysynaptic only response, 45.5% (10/22) mono- and poly-synaptic responses while 18.18% (4/22) were non-responding. These results indicate that DH cholinergic interneurons are very well connected with LII and amongst themselves.

A single pulse of photostimulation only produced GABA/Glycine responses. To investigate the cholinergic component, they performed a photo-stimulation train of 20 pulses at 20 Hz. The downstream LII neurons reported: 18.2% (4/22) nicotinic, 18.18% (4/22) muscarinic, 45.5% (10/22) nicotinic and muscarinic responses and 18.18% (4/22) non-responsive. This suggest that the cholinergic transmission was less likely observed compared to GABA/Glycinergic IPSCs.

## 8. Discussion

Our results demonstrate that DH cholinergic interneurons are well-integrated in the spinal network. From recordings in various slice orientations, we propose that these cholinergic cells receive excitatory drive arising from distant spinal segments within LI-IV. In contrast, the inhibitory inputs are possibly localized within the same spinal segment and first four laminae of the DH. In addition, they receive (directly or indirectly) information from primary afferents (including nociceptive ones), and appear to project throughout the dorsal horn.

### 8.1. *Synaptic inputs*

**Excitatory inputs:** Synaptic inputs to LIII-IV DH neurons have been studied before in different species. Glutamate uncaging experiments have shown that rat LIII/IV neurons with long upward projecting dendrites receive excitatory and inhibitory inputs from superficial layers; in contrast more ventral LIII/IV cells received only excitatory inputs above LII/III border (Kato et al., 2013).

In hamsters, the local LIII/IV connections are generally inhibitory although with low reliability (Schneider, 2008). Because all our slices comprised LI/IV, we could not specifically interrogate the precise localization of the synaptic drive within these laminae (LI/IIo vs. LIIi/III for example). However our data suggest that presynaptic excitatory neurons connect ChAT::EGFP neurons quite distally in the rostrocaudal axis. This can be related to the extended rostral-caudal dendritic spread of LIII-IV cholinergic interneurons (Mesnage et al., 2011). In contrast, the excitatory and inhibitory inputs to Non-ChAT cells remained constant regardless of slice orientations; thus, suggesting the recorded cells may receive functional inputs arising locally.

**Inhibitory inputs:** It has been proposed that the control of inhibitory transmission in rat LIII/IV implicates deeper laminae (LV –VI) (Petitjean et al., 2012; Seibt and Schlichter, 2015). In our hand, whatever the different slice orientations, we did not observe any change in the DH inhibitory inputs to LIII/IV neurons. One discrepancy between our approaches is that the above-mentioned studies recorded inhibitory inputs driven by application of exogenous substances, while we recorded spontaneous events. Also, these studies were performed in rat while we recorded mouse tissue.

## 8.2.     *Primary afferents inputs*

**Types of inputs:** LIII/IV cholinergic interneurons appear to be downstream to incoming peripheral inputs. These inputs range from low threshold (potentially myelinated) and high-threshold (unmyelinated fibers). Traditionally, LIII/IV neurons are known to receive non-nociceptive information via myelinated fibers. For example, the neurons transiently expressing vGLUT3, glycinergic, paravalbumin and/or dynorphin interneurons receive direct inputs from Aβ fibers (Lu et al., 2013; Duan et al., 2014; Peirs et al., 2015; Petitjean et al., 2015). There are also LIII/IV neurons receiving high-threshold inputs: NK1+ neurons with dorsally projecting dendrites to LII receive direct inputs from TRPV1 expressing fibers in neonatal rats (Labrakakis and MacDermott, 2003). Anatomical information was available for DH cholinergic interneurons in rats: they were known to receive inputs from both type I and type II glomeruli, with IB4 and CtB expressing contacts (Ribeiro-da-Silva and Cuello, 1990; Olave et al., 2002). Our preliminary data confirms connections with both types of fibers, however further analysis is required to determine the type (mono- or poly- synaptic) or nature (Aβ, Aδ or C fiber) these connections.

**TRPV1 expressing primary afferents:** Through pharmacological intervention, we investigated the specific modalities of these incoming fibers. We showed that the LIII-IV cholinergic interneurons are indirectly connected by TRPV1 expressing fibers, through excitatory and inhibitory interneurons. This was also the case of non-ChAT neurons, also a proportion of them

was also directly postsynaptic to TRPV1+ fibers. In rats, the TRPV1 agonist capsaicin has been reported to increase both excitatory and inhibitory responses in LIII/IV, although only indirect responses were observed (Petitjean et al., 2012). In addition, the mechanical transection between LIII/IV and deeper laminae in rat transverse slices reduced the number of responding cells with inhibitory current facilitation from 60% to < 10% (Petitjean et al., 2012). Our recordings were performed in horizontal slices, devoid of deep laminae (below LIV); we were therefore expecting a lower proportion of capsaicin-induced increase in the frequency of inhibitory currents. As this was not the case (we observed about half the neurons responding), our results suggest that the inhibitory control downstream to TRPV1+ fibers may be different between rats and mice.

In our voltage clamp recordings, we looked specifically at either excitatory or inhibitory inputs and did not study the integrated output, i.e. the firing of the cell following dorsal root stimulation by capsaicin. In rats, bath application of capsaicin (300 nM – 1 μM) between 8 – 10 minutes on spinal slices did not alter the detected acetylcholine levels (Dussor et al., 2005), suggesting that stimulation of TRPV1+ primary afferent does not lead to net excitation of cholinergic neurons. However, this could also result from the lower concentrations used as opposed to our study (Capsaicin 5 μM). Interestingly, neonatal treatment of capsaicin (to pharmacologically mimic de-afferentation) resulted in reduced high-potassium-induced release of ACh, confirming a link between TRPV1+ fibers and spinal cholinergic neurons (Dussor et al., 2005). In behavioral experiments in β2 nAChR knock-out mice, the effects of a normally sub-threshold dose of capsaicin applied to the paw surface resulted in mechanical allodynia, and the effect of a supra-threshold dose was prolonged compared to WT mice (Yalcin et al., 2011). This again highly suggests the implication of the spinal cholinergic system in the processing of nociceptive information encoded by TRPV1+ primary afferents.

**TRPM8 and TRPA1 expressing primary afferents:** In contrast, none of ChAT::EGFP cells were downstream to TRPM8 and TRPA1 expressing fibers. While it is known that TRMP8 is absent from TRPV1 fibers, TRPA1-expressing fibers are considered a subset of TRPV1-expressing ones (Kobayashi et al., 2005). This suggest that the fibers upstream to cholinergic cells are a unique subset of TRPV1 expressing fibers (not expressing TRPA1). TRPA1 receptors are suggested to be involved in noxious cold or chemical induced allodynia while TRPM8 receptors contribute to encoding cold sensations (Dubin and Patapoutian, 2010). Interestingly, intrathecal mecamylamine (10 μg) and atropine (10 μg) did not alter the flinching responses observed in phase 1 or 2 in the formalin test(Hama and Menzaghi, 2001), suggesting again that spinal cholinergic neurons are not involved in the processing of chemical inflammation. On the other hand, the cholinergic system

has been implicated in mechanism of electro-acupuncture relieving cold allodynia following neuropathy (Park et al., 2009); as our results suggest that cholinergic interneurons are not downstream TRPM8 fibers, we can hypothesize that other fibers might be implicated, or the link between these fibers and ChAT neurons is too faint to be detected using our approach. High concentrations icillin (100 μM), activators of TRPA1 and TRPM8, have been shown to increase the frequency of miniature EPSCs in LI-III neurons of young male rats (Wrigley et al., 2009). We did not record miniature EPSCs but rather spontaneous ones, and similarly found responses to the activation of TRPA1+ et TRPM8+ fibers in lamina II, but not in lamina III-IV.

## 8.3. *Targets*

Our preliminary transynaptic labeling experiments suggest that the potential downstream targets to cholinergic interneurons are throughout the DH. Electron Microscopy (EM) studies have demonstrated a direct cholinergic innervation of LI neurons (Ribeiro-da-Silva and Cuello, 1990). DH cholinergic interneurons are shown to have axons that travel first dorsally and then rostro-caudally up to 2 mm (Mesnage et al., 2011); this suggests that LII interneurons are also potential targets. Finally, DH cholinergic neurons could be presynaptic to primary afferents. Both nicotinic and muscarinic receptors are located on primary afferent fibers and the application of exogenous cholinergic agonists modulate the responses observed in DH neurons following peripheral nerve stimulation (Li et al., 2002; Genzen and McGehee, 2003; Zhang et al., 2007a). In corroboration with these functional data, EM studies have shown that cholinergic boutons are pre-synaptic to primary afferent fibers found in LIIi, thus suggesting that cholinergic neurons may produce similar effects with endogenous ACh.

The work of our collaborator B. Graham has demonstrated that cholinergic interneurons are presynaptic to LII neurons as well as to other LIII-IV ChAT::EGFP cells. Moreover, they communicate using GABA, Glycine and Acetylcholine (via nAChR and mAChR). Interestingly, such a dual mode of communication for cholinergic neurons has been described previously in the brain. For example, when optogenetics were used to study cholinergic neurons from the Habenula projecting to the interpeduncular nucleus (Ren et al., 2011). A brief light pulse resulted in a fast-excitatory synaptic current mediated exclusively by glutamatergic receptors, while a tetanic stimulation produced slow inward currents which were largely mediated by nAChR, thus suggesting volume transmission of ACh. Our collaborators similarly employed a barrage of light stimulations in order to detect cholinergic responses in LII cells.

## 8.4.    *Functional role*

To improve our understanding in the role of DH cholinergic interneurons at the behavior level, si-RNA and genetic tools have been used. An antisense anti-ChAT were injected intrathecally in adult mice, which resulted in the reduction of thermal and mechanical PWT in treated mice (Matsumoto et al., 2007). In contrast, injection of cholino-toxin AF64A did not alter the thermal PWT in naïve rats (Chen and Pan, 2001). Recently, ChAT-Cre mice were crossed with Tau-Diphtheria Toxin Receptor (DTR) and Lbx1-Flpo mice to drive DTR expression exclusively in DH ChAT neurons. Subsequently, DTR-expressing neurons were ablated upon intraperitoneal injection with diphtheria toxin (DTX). Following 10 – 14 weeks after ablation, the population-ablated animals demonstrated no differences in mechanical, thermal nor cold PWT (Duan et al., 2014). With knock-down and cholino-toxin studies, these substances were delivered via intrathecal injections thus could potentially act on other cholinergic sources (peripheral, descending fibers) in addition to DH cholinergic interneurons. The more recent study has implemented a genetic approach thus allowing the precise removal of a specific population. Their conclusions weaken the argument for the role of DH cholinergic interneurons as a key player in nociceptive information processing. However, one has to keep in mind that they have performed their behavioral studies 10 weeks after DTX injection which could imply compensatory mechanisms or potentially redundant systems coming into play. Ultimately, with only few studies made on this population the exact contribution of this population to spinal nociceptive network remains highly controversial.

We have demonstrated the LIII/IV cholinergic interneurons are receive both excitatory and inhibitory inputs from the DH network and periphery. From local network, the control of excitatory inputs is located more distally compared to the inhibitory ones. Potentially low and high threshold fibers are upstream to these populations and they are indirectly connected to TRPV1+ but not TRPM8 or TRPA1 fibers. Their downstream targets consist of LII and other cholinergic interneurons whereby they communicate with GABA, Glycine and ACh.

# Chapter 5: Characterization of the DH cholinergic interneurons following peripheral nerve injury

## 1. Context and objectives

Endogenous acetylcholine (ACh) is an important modulator of nociceptive sensory processing in the spinal cord. While a basal tone of spinal ACh seems to modulate the threshold for nociceptive responses, this tone appears to be disrupted in neuropathic animals (Rashid and Ueda, 2002). A population of cholinergic interneurons identified in the spinal dorsal horn (DH) of rodents and primates (Barber et al., 1984; Mesnage et al., 2011; Pawlowski et al., 2013a) is a potential source contributing to the spinal cholinergic tone. The previous chapter (Chapter 4) identified the features that enable this sparse neuronal population to achieve such a major control over pain processing by elucidating the interplay of DH cholinergic interneurons with the surrounding naïve nociceptive network.

Following peripheral neuropathy, several aberrant alterations at a molecular (Coull et al., 2003), circuit (Moore et al., 2002) and behavioral levels (Kuner, 2010) have been reported. Herein, to improve our understanding of changes occurring in the spinal circuit and cholinergic system following nerve injury, we have studied the DH cholinergic interneurons and LIII-IV network in a model of peripheral neuropathy.

## 2. Behavioral and electrophysiological investigation of cuff mice

### 2.1.    *Mechanical allodynia*

After establishing stable baselines, the ChAT::EGFP+ Cd1 mice went through cuff surgery (c.f. methods). All animals were allowed to recover at least 7 days prior to behavior assessment (Fig. 5.1A). The sensitivity to the mechanical stimulation in the animal right hind paw of cuff groups was decreased compared to sham mice. After establishing the PWT, the mice were used for electrophysiological recordings.

*Interpretation-discussion:* The adult mice developed robust mechanical allodynia as previously observed in other experimental data set (Chapter 3).
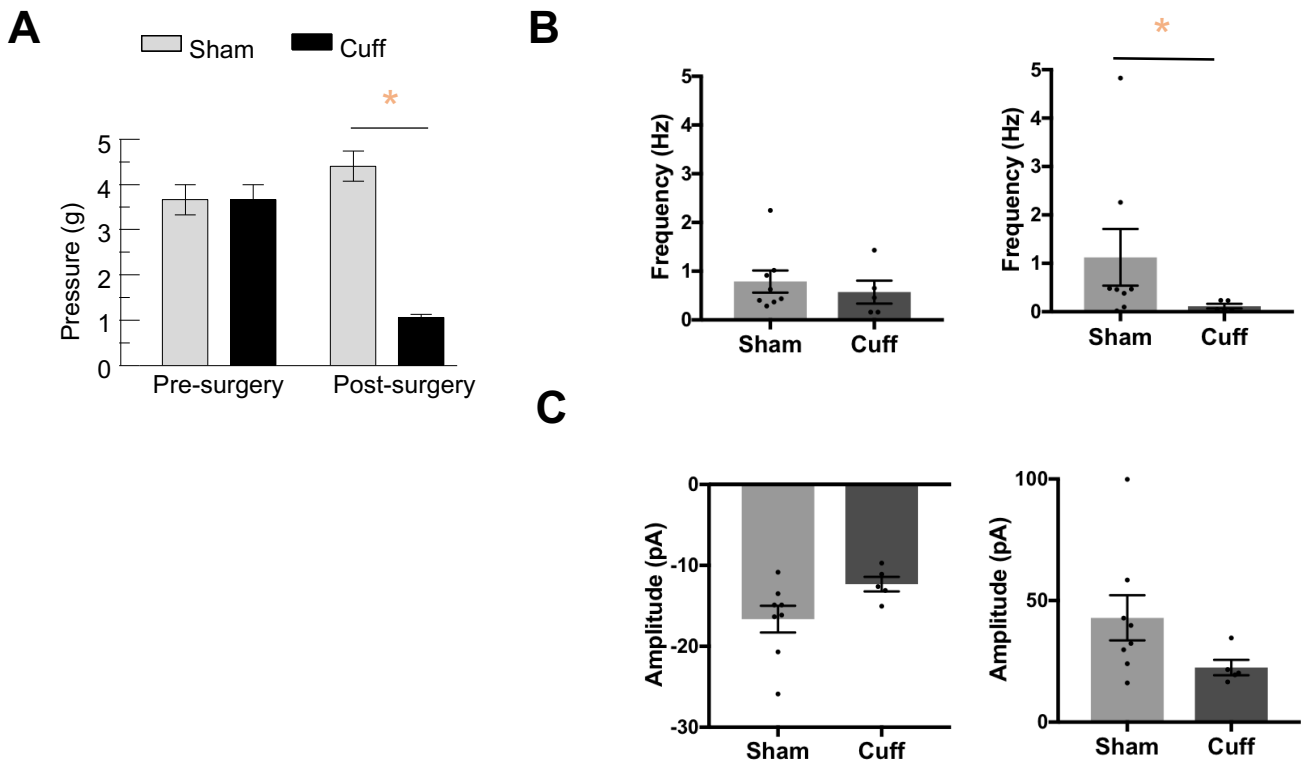
**Figure 5.1:** Behavioral and in vitro electrophysiological characterization of the cuff model. **5.1A:** Mechanical allodynia following peripheral nerve injury [Sham n = 8 and Cuff n = 5]. A reduction in the PWT is reduced in cuff group after surgery however, the PWT of sham controls is unchanged [T-test: $p < 0.01$] **5.1B:** Frequency changes in miniature excitatory (EPSC) and inhibitory (IPSC) post-synaptic currents recorded Lamina II cells. A reduction was observed in the frequency for miniature IPSCs (Right) but not EPSCs (Left) in cuff mice (Kolmogorov-Smirnov test, $p = 0.042$) *$p < 0.05$ – sham vs cuff. **5.1C:** Amplitude measurements from miniature EPSCs and IPSCs in LII neurons. No observable difference was detected in amplitude size.



EGFP      ChAT      Merged
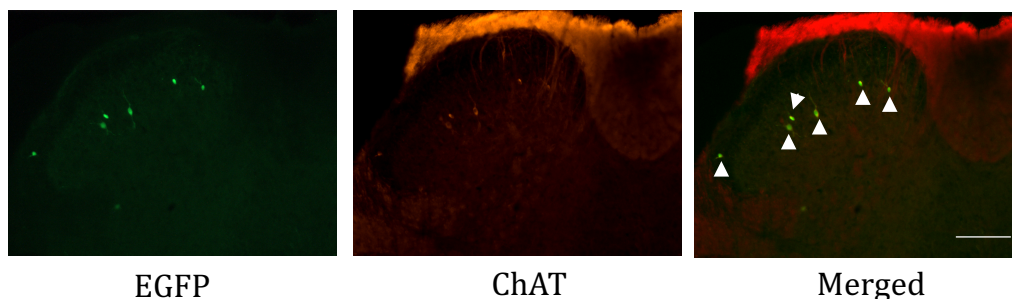
**Figure 5.2:** Distribution of DH cholinergic interneurons in sham and cuff adult ChAT::EGFP mice [N for Sham and Cuff = 2]. Comparable numbers of EGFP cells (green) colocalize with the ChAT antibodies (red) in both animal groups. Only Cuff RHS is shown here. The arrowhead denotes overlapping cells (Scale = 100 μm).

## 2.2.    *Electrophysiological characterization in LII neurons*

The cuff model of peripheral neuropathy has been well described in behavioral terms, but we were the first to analyze the plasticity occurring in the spinal cord with electrophysiology first in vivo (Medrano et al., 2016) and now in vitro. In order to put our findings in context with the literature, we first performed recordings in LII neurons located on the ipsilateral (to cuff insertion) DH in the presence of TTX 0.5 μM (Fig. 5.1B). The frequency of miniature IPSCs was lower in cuff mice compared to sham controls (Kolmogorov-Smirnov test, p = 0.042) whereas the frequency of miniature EPSCs was unchanged (Kolmogorov-Smirnov test, p = 0.586). However, the amplitudes for miniature EPSC and IPSCs remained similar for sham and cuff mice (Fig. 5.1C; un-paired t-test: mEPSC comparisons – p= 0.0782; mIPSC comparisons – p = 0.112).

*Interpretation-discussion:* We observed a reduction in the frequency of miniature IPSCs in LII from cuff mice compared to sham; we did not intend to differentiate GABAergic from glycinergic currents. This suggests that the plasticity occurring in LII in the cuff model is similar to the one observed in the Spared Nerve Injury (SNI) and Chronic constriction injury (CCI) models of neuropathy, where a reduction in the frequencies of miniature GABA-A currents is reported in LII. Like our observations, their amplitudes of miniature IPSC remained unchanged after injury (Moore et al., 2002; Iura et al., 2016).

We observe no difference in frequency for mEPSCs. In contrast, a study focusing on GABAergic interneurons in the CCI model reports a decrease in frequency of miniature EPSCs, although with unaltered amplitudes, in LII. They also observed an increased paired pulse ratio of Aδ- or C-fiber-evoked monosynaptic EPSCs, and suggested that these changes result from reduced neurotransmitter release from primary afferents (Leitner et al., 2013). It is not possible to say, at this stage, if such plasticity of excitatory currents in LII does not occur in the cuff model, or if we didn't observe it because we did not focus exclusively on GABAergic neurons but rather on identified LII neurons. Nevertheless, our recordings represent the first electrophysiological characterization of LII neurons in the cuff model for peripheral nerve injury.

# 3. Density of DH cholinergic neurons after cuff surgery

There is an on-going debate on whether there is a loss of neurons in the DH that would contribute to the development of hyperalgesia or allodynia following neuropathy. Therefore, we investigated whether DH cholinergic interneurons were affected. Following two weeks' post-surgery, the number of GFP+ were counted in the contralateral and ipsilateral DH of adult ChAT::EGFP+

**A**

| Firing patterns | Naive | | Sham | | Cuff | |
|---|---|---|---|---|---|---|
| | ChAT::EGFP | Non-ChAT | ChAT::EGFP | Non-ChAT | ChAT::EGFP | Non-ChAT |
| Tonic Firing | 85.7 | 87.5 | 83.3 | 71.4 | 75 | 66.7 |
| Single Firing | 0.0 | 0.0 | 16.7 | 0.0 | 12.5 | 16.7 |
| Initial burst Firing | 14.3 | 0.0 | 0.0 | 14.3 | 12.5 | 0.0 |
| Silent | 0.0 | 12.5 | 0.0 | 14.3 | 0.0 | 16.7 |
| Total N | 7 | 8 | 6 | 7 | 8 | 6 |

**Table 5.1:** Percentage of observed firing patterns in ChAT::EGFP and Non-ChAT cells in three animal types: naïve, sham and cuff mice.

**B**
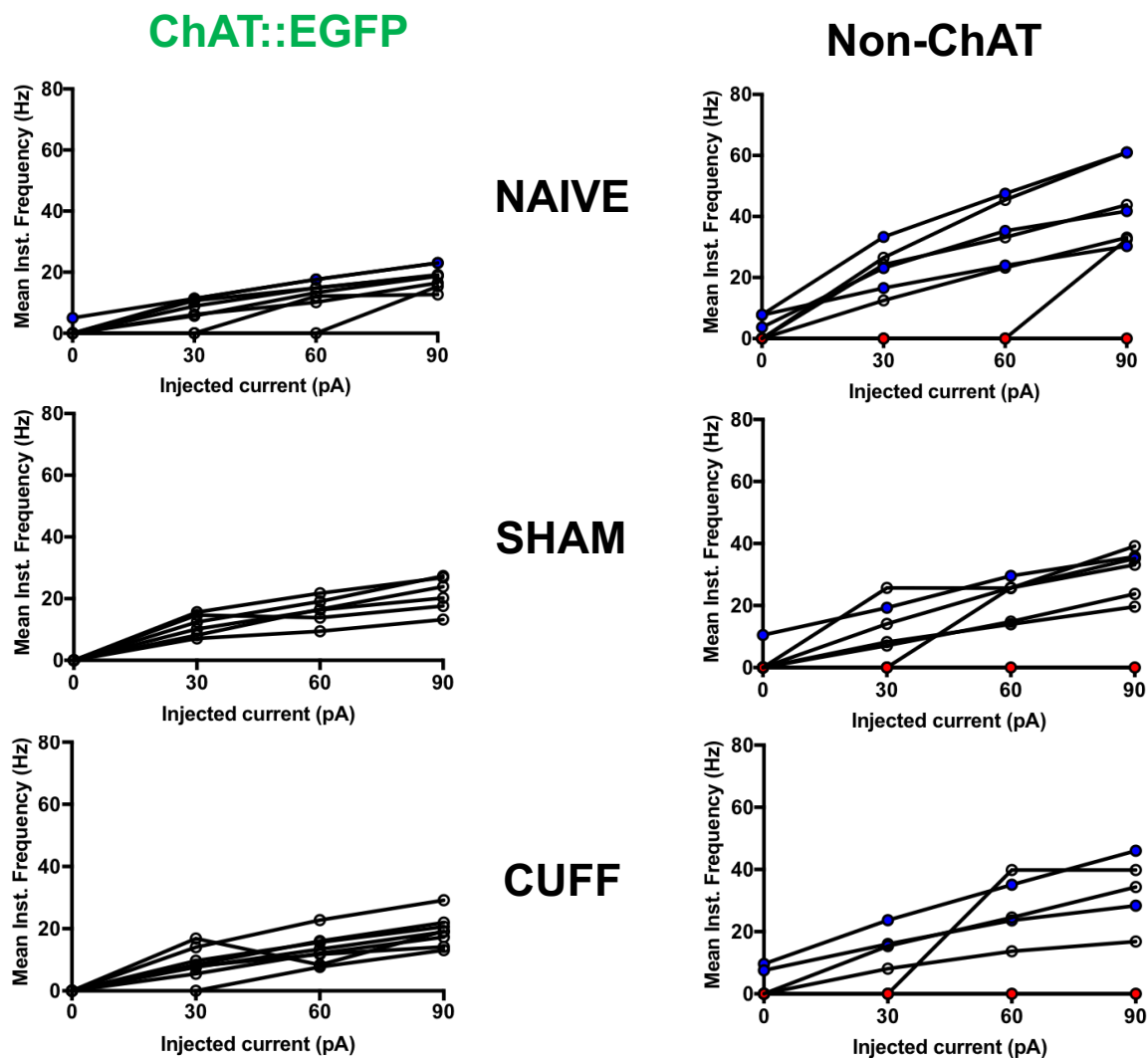


**Figure 5.3:** Mean Instantaneous frequencies for ChAT::EGFP+ and Non-ChAT cells in horizontal slices from naïve, sham and cuff adult mice. Spontaneously firing cells (blue dots) at rest are present in some naïve, sham and cuff cells. The reluctant firing cells (red dots) were present uniquely in Non-ChAT recorded cells.

mice. Only sections from L3 – L6 spinal segments were taken into account (Fig. 5.2). We confirmed by co-localization with ChAT antibodies that the vast majority (90%) of these neurons were ChAT-IR. For sham, we observed 2.13 ± 0.38 cholinergic neurons per 40 μm thick slices in the ipsilateral side of the DH. Similarly, 2.07± 0.38 co-localized ChAT and GFP+ cells in cuff animals were seen.

*Interpretation-discussion:* The number of cholinergic interneurons appeared to be unchanged following peripheral nerve injury. We described comparable cholinergic neuron counts as previously reported: 2.8 ± 0.3 neurons per 50 μm thick transverse section in naïve Cd1 mice (Mesnage et al., 2011).

# 4. Characterization of the spinal cholinergic DH neurons

## 4.1.    *Firing pattern*

We recorded from ChAT::EGFP and Non-ChAT neurons in horizontal spinal cord slices, from naïve, sham and cuff mice. A fraction of recorded neurons presented spontaneous ongoing firing at rest (Fig. 5.2): 1 from a total of 7 (14%) naïve cells, 2 out of 6 (33.3%) cholinergic neurons in sham mice, but none out of 8 (0%) in cuff. Among Non-ChAT neurons, 3 out of 8 (37.5%) for naive 1 out of 7 (14.2%) in sham mice, and 2 out 6 (33.3%) in cuff mice. There was no significant interaction between surgery (sham, cuff); type of neuron (ChAT::EGFP+, Non-ChAT) and presence of on-going firing (3x3x3 contingency table, p = 0.4479).

Analysis of the frequency of action potentials after injection of depolarizing currents (Fig. 5.3) enabled us to classify the neurons according to their firing pattern as previously presented for naïve mice (Chapter 4). The proportions of the different firing patterns are presented in Table 5.1. There was no statistical difference between ChAT::EGFP and Non-ChAT neurons concerning the proportion of the different firing patterns in three different animal groups (3x3x3 contingency tables, p = 0.131). There also was no statistical difference in the rheobase for these two populations (Table 5.2; Scheirer-Ray-Hare test, p = 0.157).

*Interpretation-discussion:* Mesnage and co-authors observed 67% of tonic firing pattern amongst ChAT::EGFP neurons (n=15), while 27% of neurons had ongoing firing activity. This is not significantly different from our proportions (chi-square test, p=0.35 for tonic firing pattern, p=0.52 for ongoing firing). Lamina III-IV had overall a similar distribution amongst firing pattern in naïve, sham and cuff animals, ruling out a massive plasticity in intrinsic neuronal properties. There was no specific feature to ChAT::EGFP neurons.
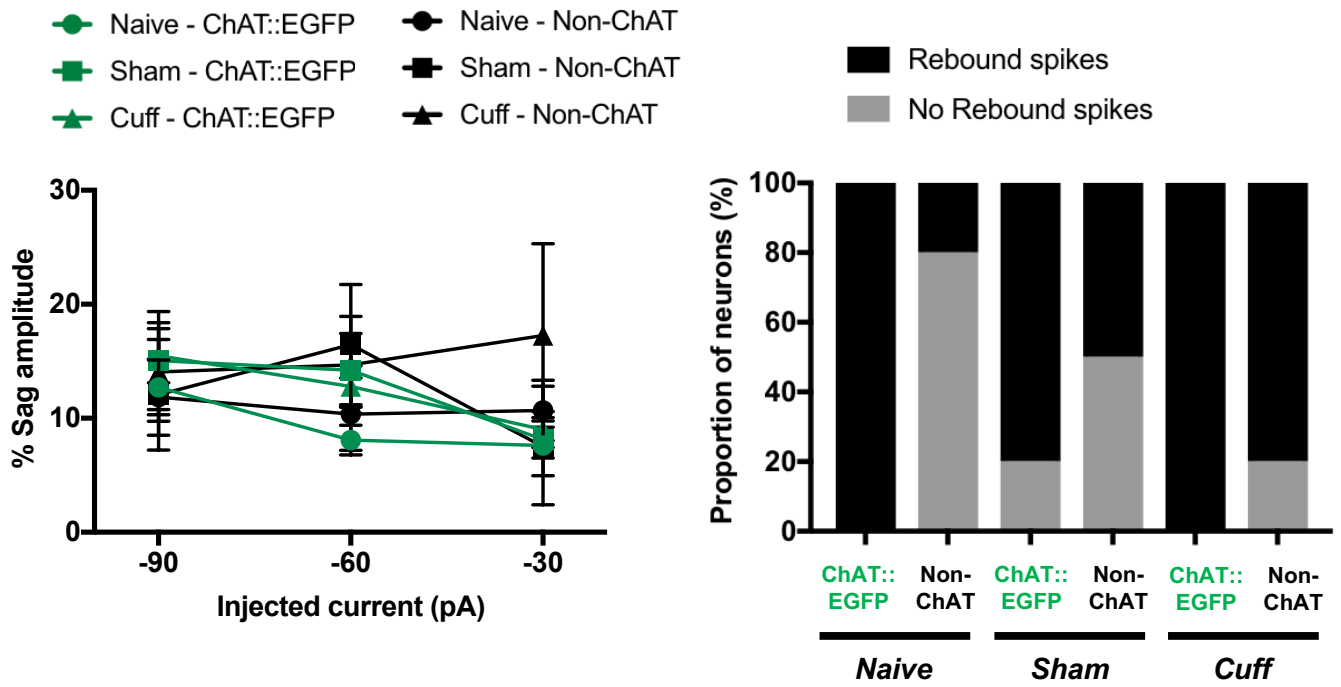
**Figure 5.4:** Electrophysiological properties of for ChAT::EGFP and Non-ChAT cells on horizontal slice in three animal types: naïve, sham and cuff mice. **Fig. 5.4A** % sag demonstrating concerning sag amplitude. There was no statistical differences between animals and neurons. **Fig. 5.4B** The proportion of cells demonstrating rebound spikes after hyperpolarization pulses.

| Animal | N | | RMP (mV) | | Input Resistance (TΩ) | | Capacitance (pF) | | Rheobase (pA) | |
| --- | --- | --- | --- | --- | --- | --- | --- | --- | --- | --- |
| | | | ChAT::EGFP | Non-ChAT | ChAT::EGFP | Non-ChAT | ChAT::EGFP | Non-ChAT | ChAT::EGFP | Non-ChAT |
| **Naïve** | ChAT::EGFP (7) | Mean | -50.84 | -57.85 | 0.74 | 0.77 | 87.89 * | 46.81 | 42.86 | 25.71 |
| | Non-ChAT (8) | SEM | 4.44 | 3.07 | 0.12 | 0.11 | 7.92 | 3.69 | 8.92 | 11.34 |
| **Sham** | ChAT::EGFP (6) | Mean | -49.27 | -49.89 | 0.58 | 0.58 | 81.68 | 89.81 # | 20.00 | 30.00 |
| | Non-ChAT (7) | SEM | 3.80 | 2.29 | 0.07 | 0.07 | 6.24 | 10.70 | 6.32 | 7.17 |
| **Cuff** | ChAT::EGFP (8) | Mean | -55.62 | -49.53 | 0.54 | 0.55 | 97.40 | 78.45 # | 33.75 | 24.00 |
| | Non-ChAT (6) | SEM | 2.07 | 3.93 | 0.05 | 0.09 | 5.68 | 8.34 | 3.75 | 10.25 |

**Table 5.2:** Electrophysiological properties of ChAT::EGFP and Non-ChAT cells in horizontal slices in naïve, sham and cuff mice. # $p < 0.05$ comparing capacitance of non-ChAT cells in sham and cuff vs naïve of; post-hoc: TukeyHSD * $p < 0.05$ comparing capacitance between ChAT::EGFP vs Non-ChAT in naive.

## 4.2.    *Passive properties*

The membrane properties of recorded neurons were investigated as in Result section 2. Similarly, the input resistance, the cell capacitance, and the amplitude of a (potential) sag current were assessed (Table 5.2). There was no difference in the resting potential (ANOVA, p = 0.1451), input resistance (ANOVA, p = 0.9769) or amplitude of a sag current (Fig. 5.4A; Scheirer- Ray-Hare test = 0.84373) between ChAT::EGFP or non-ChAT neurons or between animal groups (naïve, sham, cuff). For the cell capacitance, there was a significant interaction between type of neuron and animal group (Table 5.2; ANOVA, p = 0.007). As previously reported in naïve, GFP+ neurons had a statistically larger cell capacitance than non-ChAT neurons recorded in horizontal slices (TukeyHSD, p = 0.0026). Moreover, non-ChAT cells in naïve mice had significantly smaller cell capacitance compared to those recorded in sham and cuff (TukeyHSD, respectively p = 0.0015 and p = 0.045).

*Interpretation-discussion:* There was no passive property specific to ChAT::EGFP neurons. The fact that these neurons had a higher cell capacitance than non-ChAT cells could be explained by the morphology of their dendritic arbor: the team has indeed previously reported that cholinergic interneurons have a very extended dendritic arbor in the rostrocaudal direction, well preserved in these horizontal slices (Mesnage et al., 2011).

## 4.3.    *Rebound spiking*

The majority of ChAT::EGFP neurons presented a rebound spike upon the end of the hyperpolarizing pulse in naïve (100%), sham (80%) and cuff (100%) animals (Fig. 5.4B). In contrast, the proportion of Non-ChAT neurons presenting such a rebound spike appeared to differ depending on the animal group: 20% in naïve, 50% in sham and 80% in cuff mice. However there was a statistical difference between the two populations, when compared between the three animal groups, concerning this feature (3x3x3 Contingency table, p = 0.0029). The only significant difference in occurrence was between ChAT::EGFP+ and Non-ChAT cells in naïve animals (Fisher's exact test = 0.0101).

*Interpretation-discussion:* The team previously reported the existence of rebound spikes in half ChAT::EGFP neurons (Mesnage et al., 2011). We observed an even higher proportion of neurons producing rebound spikes in naïve mice, as well as in sham and cuff animals.

# 5. Spontaneous excitatory inputs onto DH LIII-IV neurons

## 5.1.  *Frequency of currents*

We recorded sEPSCs and mEPSCs from ChAT::EGFP and Non-ChAT neurons from sham and cuff mice, in transverse and horizontal slices. We also compared this data to the ones obtained in naïve animals. The individual and mean frequencies are illustrated in Fig. 5.5. We first performed a global analysis of the variance of all the data point obtained, in order to establish the validity of subsequent group comparisons (see Methods).

The data being non-normal, their log10 was taken to perform the ANOVA. There was a significant effect of the type of animals (Naïve, Sham, Cuff; p = 0.03), of type of currents (spontaneous vs. miniatures; p = 0.0006), of type of neuron (ChAT::EGFP vs. Non-ChAT; p = 5.5e-06) and the slice orientation (p = 9.3e-05). In addition, there was a significant association between the type of neurons and the slice orientation.

We simplified the model to take into account only those parameters that were proven meaningful, and then performed Tukey post-hoc tests. The difference between Naïve, Sham and Cuff proved non-significant. The frequency of miniatures (0.47 ± 0.05 Hz) was significantly lower than the frequency of spontaneous currents (0.89 ± 0.10 Hz) (TukeyHSD: p=0.0015). The frequency of excitatory currents in ChAT::EGFP neurons (0.47 ± 0.06 Hz) was significantly lower than in non-ChAT neurons (0.93 ± 0.10 Hz) (p=8e-06). Finally, the frequency of synaptic currents was significantly lower in transverse slices (0.47 ± 0.05 Hz) compared to horizontal slices (0.84 ± 0.11 Hz) (TukeyHSD: p=0.00016).

As for the interaction between the type of neurons and the slice orientation, ChAT::EGFP neurons received significantly lower excitatory synaptic inputs in transverse slices (0.17 ± 0.02 Hz) compared to horizontal (0.65 ± 0.13 Hz) (TukeyHSD: p=0.9e-0-4); and, in transverse slices, ChAT::EGFP neurons (0.17 ± 0.02 Hz) received significantly less excitatory synaptic inputs than non-ChAT neurons (0.71 ± 0.09 Hz) (TukeyHSD: p=0.59e-05).

*Interpretation-discussion:* We observed a small difference in the frequencies of excitatory currents depending on the animals groups (naïve/sham/cuff); however this difference was not due to a specific type of neuron, or slice or current, as there was no interaction between these parameters. In addition, this difference was not robust, as it was not confirmed by post-hoc testing of the
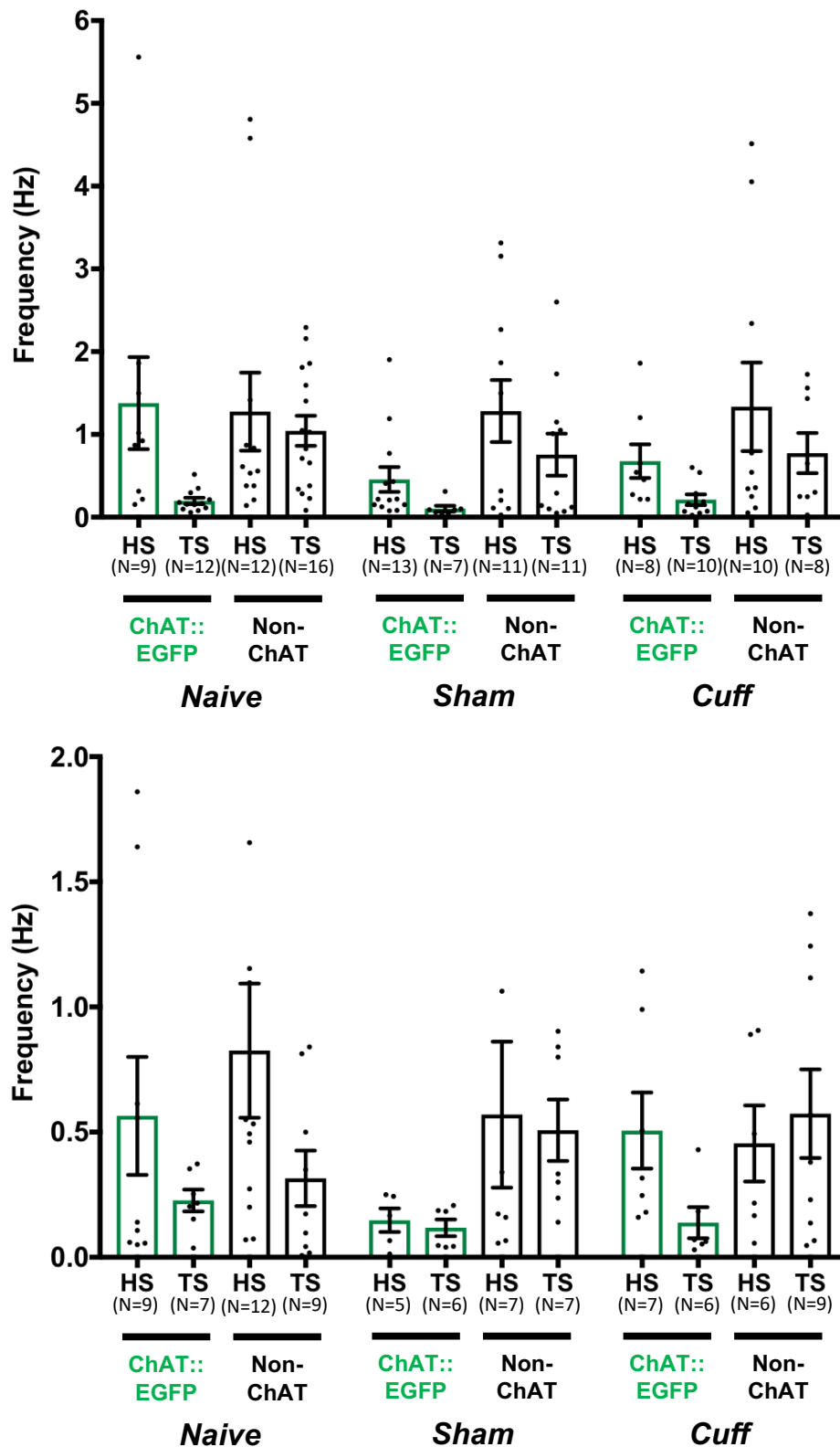
**Figure 5.5:** The frequencies of spontaneous (top) and miniature (bottom) excitatory post-synaptic currents (EPSC) of ChAT::EGFP and Non-ChAT cells in horizontal (HS) and transverse (TS) slices of naïve, sham and cuff mice. There were no significant interactions between neurons, animals, currents or slices

simplified model. Our data therefore fails to uncover a significant effect of the neuropathic surgery onto the frequency excitatory currents in lamina III-IV neurons.

Like naïve data, we observed a lower frequency of miniature compared to spontaneous currents; a lower frequency of currents in ChAT::EGFP with respect to Non-ChAT cells; and in transverse slices compared to horizontal slices. We also similarly observed lower EPSCs frequencies in ChAT::EGFP neurons on transverse than on horizontal slices, and, in transverse slices, lower EPSCs frequency in ChAT::EGFP neurons than in Non-ChAT neurons; however, these last differences were no longer unique to spontaneous events. All reported differences were conserved across all animal groups Result section 2.

## 5.2.    *Amplitude of currents*

We also compared the amplitude of mEPSCs in the different neurons, slice orientation and animals (Fig. 5.6). After normalization of the data (through log10), the ANOVA concluded on a significant interaction between the types of neurons (ChAT::EGFP, Non-ChAT) and the type of slice (horizontal, transverse) (p=0.0095) and between the type of animal(naïve, sham, cuff) and the slice orientation (p=0.0013). However, the post-hoc Tukey analysis did not confirm any of these associations.

*Interpretation-discussion:* There is no difference in the amplitude of mEPSCs linked to the neuropathy, regardless of the neurons studied.

# 6. Spontaneous inhibitory inputs onto DH LIII-IV neurons

## 6.1.    *Frequency of currents*

We recorded sIPSCs and mIPSCs from ChAT::EGFP and Non-ChAT neurons from sham and cuff mice, in transverse and horizontal slices. We also compared this data to the ones obtained in naïve animals. The individual and mean frequencies are illustrated in Fig. 5.7. We first performed a global analysis of the variance of all the data point obtained, in order to establish the validity of subsequent group comparisons.

The data being non-normal, their log10 was taken to perform the ANOVA. There was a significant effect of type of currents (spontaneous vs. miniatures; p=0.1e-06) and of type of neuron (ChAT::EGFP vs. Non-ChAT; p=1.85e-14). In addition, there was a significant association between the type of animals and types of neurons (p=0.025) as well as between types of animals and the slice orientation (p=0.022).
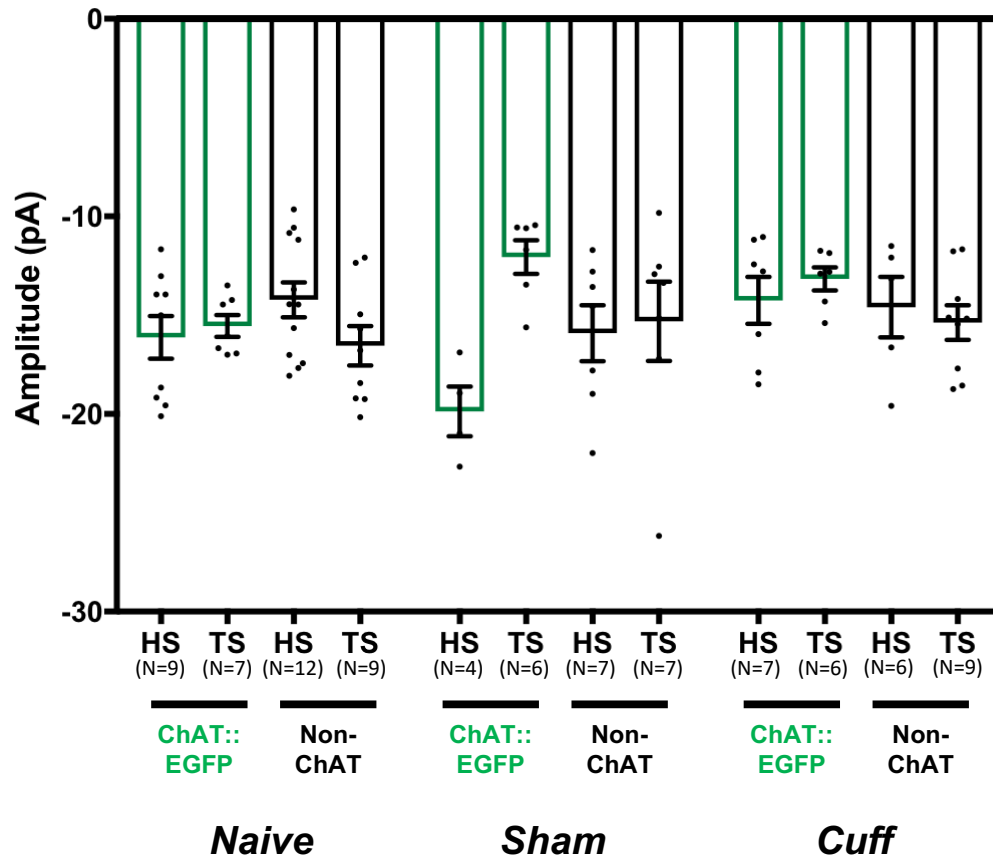
**Figure 5.6:** The amplitudes of miniature excitatory post-synaptic currents (EPSC) of ChAT::EGFP and Non-ChAT cells in horizontal (HS) and transverse (TS) slices of naïve, sham and cuff mice. The measured amplitudes remained unchanged across difference conditions.
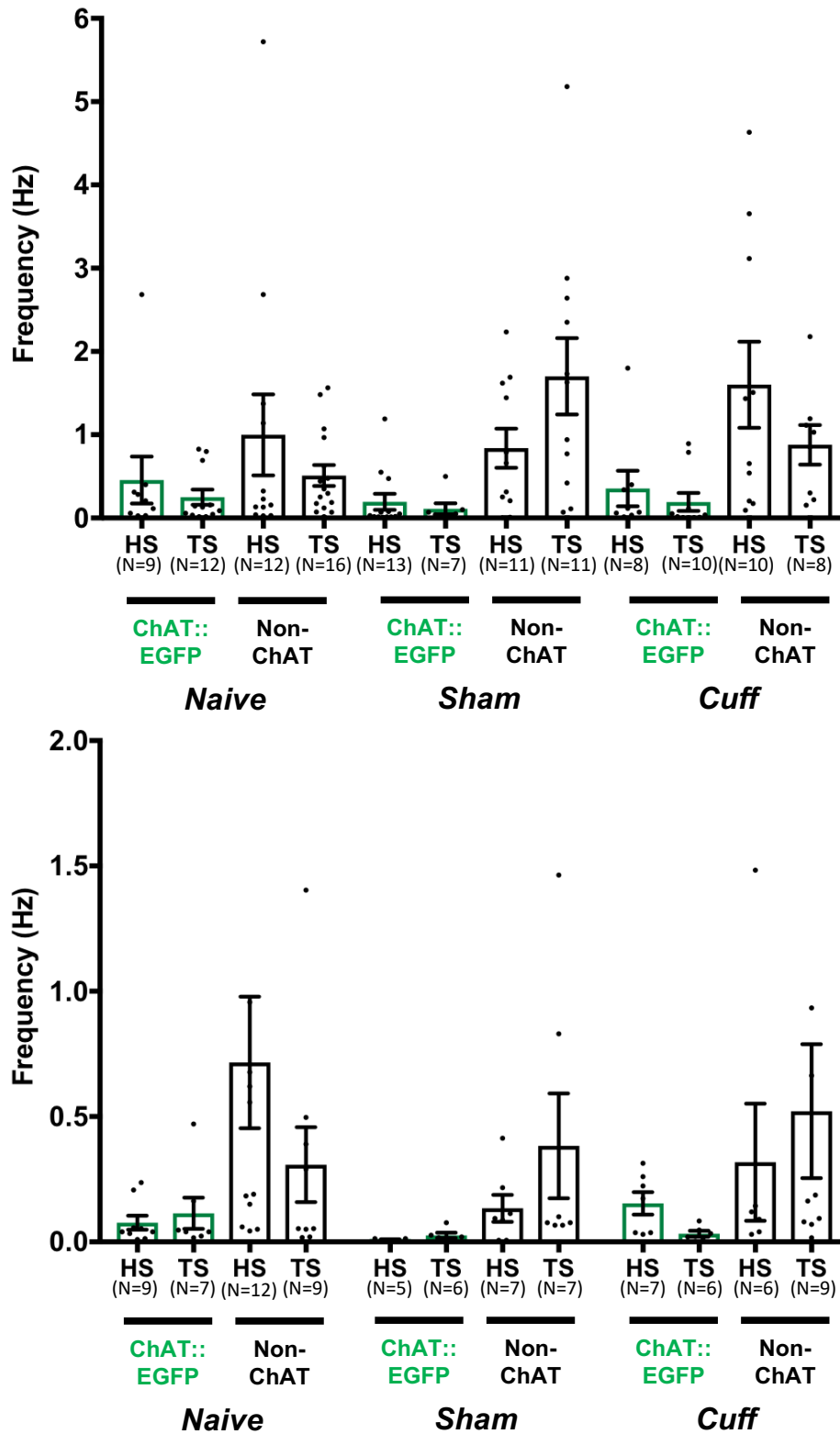
**Figure 5.7:** The frequencies of spontaneous (top) and miniature (bottom) inhibitory post-synaptic currents (IPSC) of ChAT::EGFP and Non-ChAT cells in horizontal (HS) and transverse (TS) slices of naïve, sham and cuff mice. The frequency of inhibitory currents (regardless of miniature or spontaneous) was significantly smaller in ChAT::EGFP than Non-ChAT cell (see text).

We simplified the model to take into account only those parameters that were proven meaningful, and then performed Tukey post-hoc tests. As expected, the frequency of mIPSCs (0.26 ± 0.05 Hz) was statistically lower than the frequency of sIPSCs (0.75 ± 0.10 Hz) (TukeyHSD: p = 1.18e-05). ChAT::EGFPs neurons (0.22 ± 0.05 Hz) had statistically lower frequency of inhibitory currents than Non-ChAT neurons (0.85 ± 0.11 Hz) (TukeyHSD: p = 8.20e-15) . As for the second order comparisons, there was a particularly highly significant difference between the frequency of IPSCs in ChAT::EGFP (Cuff: 0.19 ± 0.07 Hz; Sham: 0.11 ±0.04 Hz) vs Non-ChAT neurons (0.90 ± 0.2 Hz) in cuff mice (p=0.8e-5), as well as in sham mice (0.88 ± 0.19 Hz) (p<e-7). In addition, ChAT::EGFP neurons (Naïve: 0.29 ± 0.08 Hz) having a lower frequency;  was also the case in naïve mice (0.81 ±0.17) (although only with p=0.017). There was also a slight difference between sham and naïve mice for ChAT::EGFP mice (p=0.022), the frequency being smaller in sham mice.

The post-hoc analysis revealed no physiologically meaningful difference for the association of types of animals and slice orientation.

*Interpretation-discussion:* We observed a robust difference in the frequencies of inhibitory currents (independently of them being sIPSCs or mIPSCs) between ChAT::EGFP neurons and Non-ChAT neurons. In all groups of animals (naïve/sham/cuff), the frequencies recorded in ChAT::EGFP neurons were smaller. This confirms results of the previous study taking into account only naïve animals (but with slices of three orientations) and demonstrates that this unique feature of ChAT::EGFP neurons is maintained after neuropathy.

## 6.2.    *Amplitude of currents*

We compared with a similar approach the amplitude of mIPSCs in the different neurons, slice orientation and animals. After normalization of the data (through inversion), the ANOVA concluded on a significant effect of the "neurons" factor (p=0.0052). ChAT::EGFP neurons had mIPSCs of lower amplitude than Non-ChAT neurons (Fig. 5.8).

*Interpretation-discussion:* The mIPSCs recorded in ChAT::EGFP neurons were smaller than those in Non-ChAT neurons. Although these recordings were obtained both in transverse and horizontal slices, we can link this observation to the difference in capacitance that we reported (for horizontal slices) between ChAT::EGFP neurons and Non-ChAT neurons, the latter having a smaller capacitance (Result section 2). Indeed, a larger cell capacitance could explain smaller mIPSCs in ChAT::EGFP neurons.
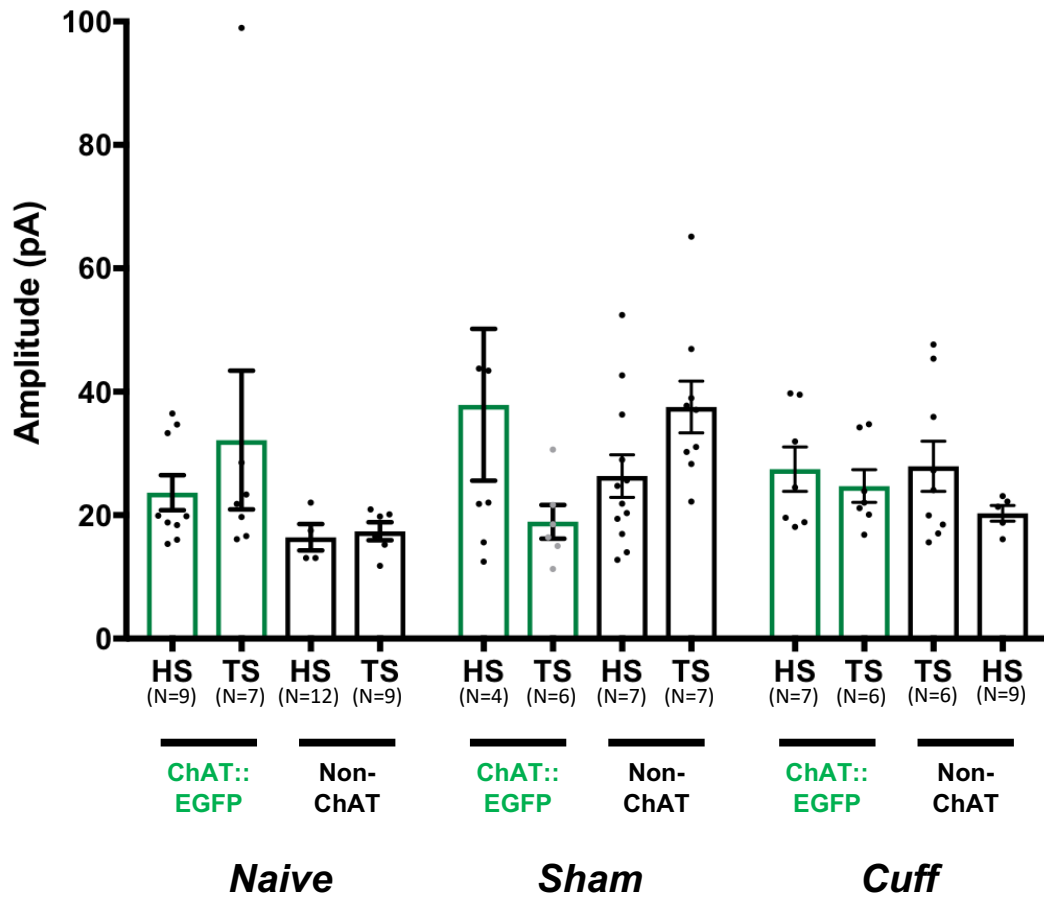
**Figure 5.8:** The amplitudes of miniature inhibitory post-synaptic currents (IPSC) of ChAT::EGFP and Non-ChAT cells in horizontal (HS) and transverse (TS) slices of naïve, sham and cuff mice. There were no observable link between each defined groups.

# 7. Excitatory/inhibitory ratio onto DH LIII-IV neurons

The frequencies of excitatory and inhibitory currents were analyzed separately in the previous sections, as we considered them to be two independent features of the recorded neurons (Fig. 5.9). However, because we actually have both excitatory and inhibitory currents recorded on each individual cell, we decided to analyze the ratio between their frequencies (E/I) in a separate analysis.

The E/I ratio was calculated in ChAT::EGFP and Non-ChAT neurons from naïve, sham and cuff mice, in transverse and horizontal slices; the log10 of the ratios was used to ensure normality of the data. We first performed a global analysis of the variance of all the data point obtained, in order to establish the validity of subsequent group comparisons.

There was a significant effect of the type of currents (spontaneous vs. miniatures; p=0.026), of type of neuron (ChAT::EGFP vs. Non-ChAT; p=8.2e-06) and the slice orientation (Horizontal vs Transverse; p=0.005). In addition, there was a significant association between the type of animal (naïve/sham/cuff) and the type of current.

We simplified the model to take into account only those parameters that were proven meaningful, and then performed Tukey post-hoc tests (Fig. 5.9). The difference between Naïve, Sham and Cuff proved non-significant. The E/I ratio was significantly higher from miniature currents (7.30 ± 2.7) compared to spontaneous currents (5.82 ± 2.41) (TukeyHSD: p=0.04). The E/I ratio in ChAT::EGFP neurons (8.45 ± 0.97) was significantly higher than in non-ChAT neurons (4.63 ± 0.60) (TukeyHSD: p=4e-06). The E/I ratio was lower in transverse slices (5.37 ± 0.89) compared to horizontal ones (7.12 ± 0.92) (Tukey HSD: p = 0.012).

As for the interaction between the type of animal and the type of current, the E/I ratio was significantly higher in miniature currents (10.27 ± 3.20) compared to spontaneous currents (4.94 ± 2.22) in Sham animals (TukeyHSD: p=0.023).

*Interpretation-discussion:* We observed a small difference in the E/I ratio depending on the animal groups (naïve/sham/cuff), as well as an interaction between this parameter with the type of currents (miniatures / spontaneous). However this difference in animals was not robust, as it was not confirmed by post-hoc testing of the simplified model. In addition, post-hoc testing of the interaction between types of animals and currents only demonstrated a difference between the E/I ratio of spontaneous and miniature currents, within sham animals. When analyzing only the naïve dataset, we had already observed a difference in the E/I ratio between ChAT:: EGFP and Non-
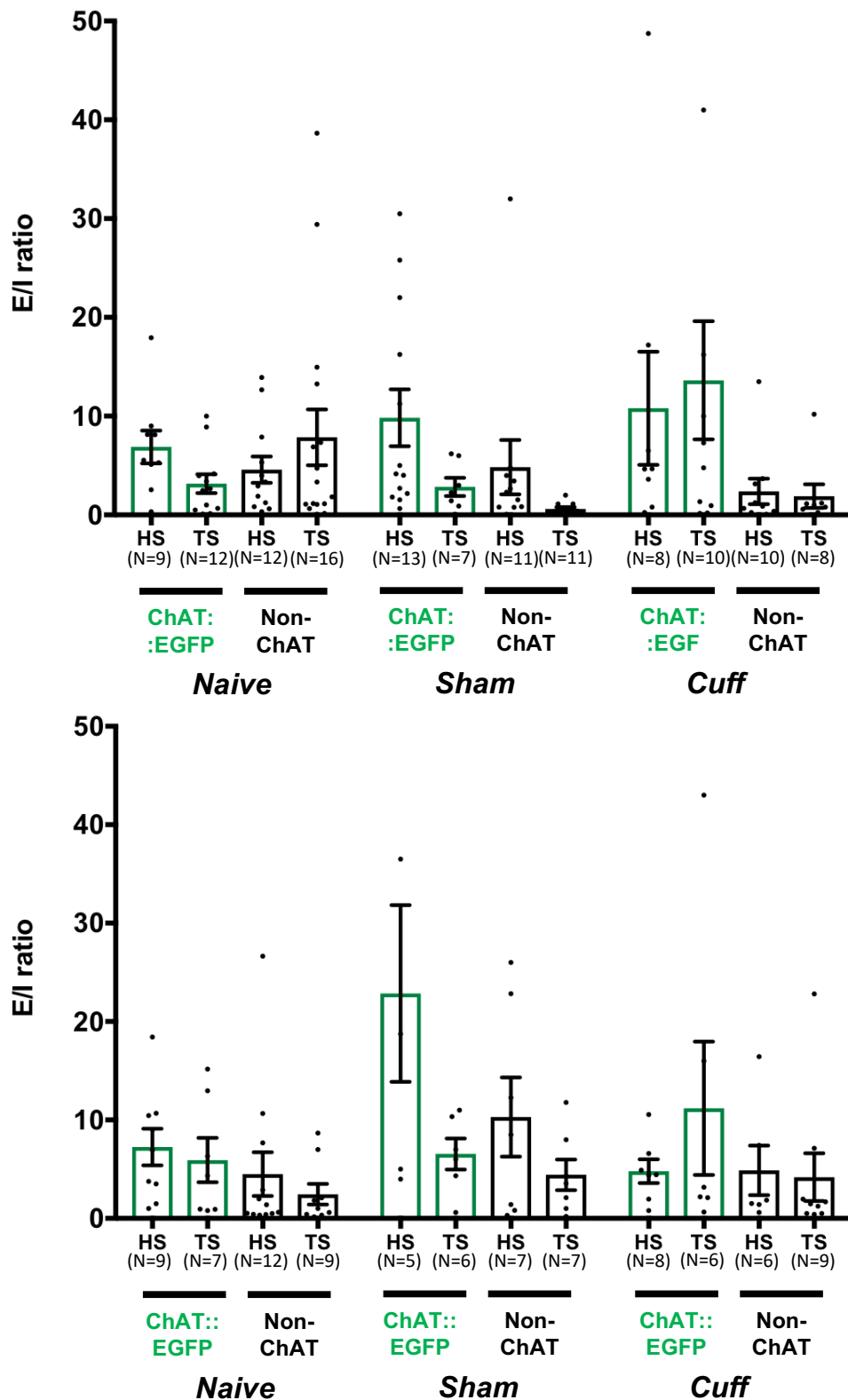
**Figure 5.9:** The ratio between the frequency (f) of spontaneous (top) and miniature (bottom) excitatory (EPSC) over inhibitory (IPSC) post-synaptic currents (f.EPSC/f.IPSC) of ChAT::EGFP and Non-ChAT cells in horizontal (HS) and transverse (TS) slices of naïve, sham and cuff mice. No significant differences were detected at interactions between the Animal (Naïve, Sham, Cuff) * Neuron (ChAT::EGFP or Non-ChAT) * Slice (HS or TS) * Current (Spontaneous or Miniature). However, there were detectable differences observed with fewer interactions (see text).

ChAT, which was confirmed here. Our data therefore fails to uncover a significant effect of the neuropathic surgery onto the E/I ratio in lamina III-IV neurons.

# 8. Discussion

We have characterized ChAT::EGFP and Non-ChAT neurons in naïve, sham and cuff adult mice. In general, the properties and inputs to LIII/IV neurons remains unchanged following peripheral nerve injury.

## 8.1.    *DH cholinergic interneurons during neuropathy*

We have reported a smaller frequency in both excitatory and inhibitory inputs to ChAT::EGFP compared to Non-ChAT cells for all animal groups. This informs us that the general activity of upstream cells remains unaltered even after peripheral neuropathy. Moreover, the reduced frequency of excitatory inputs to ChAT cells in transverse slices compared to horizontal slices confirms the possibility that their excitatory drivers are present in distal regions. Finally, the elevated E/I ratio in cholinergic interneurons compared to Non-ChAT cells reaffirms that this cholinergic population receives a greater excitatory input compared to inhibitory ones, as reported in naïve mice.

The number of ChAT::EGFP neurons, a sub-population of GABAergic neurons, remained unchanged following neuropathy. The existence of GABAerigc cell death after peripheral neuropathy and its contribution to mechanical allodynia is controversially debated (Polgar et al., 2004; Scholz et al., 2005). Nevertheless, other morphological alteration may contribute to these pathological behaviors, as has been suggested for parvalbumin –PV) interneurons (Petitjean et al., 2015). PV neurons provide feed-forward inhibition onto PKC gamma neurons thus 'gating' the transmission of non-noxious information into nociceptive circuits. Their number remains unchanged from 3 – 8 weeks' post-surgery in SNI mice. However, the number PV+ appositions on PKC-gamma cell bodies are reduced following injury, which has been proposed to lead to mechanical allodynia (Petitjean et al., 2015).

For the behavior output of cholinergic interneurons after peripheral injury; the intrathecal injection of cholino-toxin, AF64A, in neuropathic rats did not exacerbated the mechanical allodynia. However, after the highest dose of AF64A (15 nmol), the analgesic effect of clonidine (15μg) was lost. The effect absence is correlated to the reduced numbers of DH cholinergic cells (Paqueron et al., 2001). This indicates that the action of clonidine involves cholinergic interneurons within the spinal pathway during neuropathic conditions.

## 8.2.     *Cellular changes in the network after neuropathy*

We have reported a smaller capacitance in naïve compared to sham and cuff mice. Our initial hypothesis was an age difference between groups: the naïve group had animals starting from P21 whereas the youngest animals in sham and cuff groups were P28. However, we performed a linear regression analysis between age and cell capacitance and found no correlation ($R^2 = 0.30118$). This goes in the same direction as a study showing that cell capacitance of superficial DH cells is similar for P24 -45 adult mice (Tadros et al., 2012). An alternative hypothesis is that this difference could be due to a sampling bias. Slices obtained from older animals and/or neuropathic conditions are probably more prone to death, and this possibly concerns different subpopulation differentially. As the experiments were performed on horizontal slices, the dorsal superficial white matter partially blocks the light illumination pathway. The increased myelination in older animals could decrease visibility and perhaps contribute to a selection bias. In order to explain different probabilities of finding connected pairs between LI-III in two of their own studies, the group of B. Safronov alluded to poorer optics in one of them (Santos et al., 2007; Santos et al., 2009)

Other passive properties and firing patterns appeared to be similar between ChAT::EGFP and Non-ChAT neurons, in different states. This is not completely unexpected as observed for other studies on neuronal subpopulations in the DH. A study looking, in LIII, at GAD67::EGFP and non-EGFP+ cells found no differences in passive membrane properties (RMP, Capacitance, Input resistance) as well as firing patterns between the SNL and control groups. The most common firing pattern was tonic firing in both states (Gassner et al., 2013). Similarly, electrophysiological properties in LII GABAergic neurons were unchanged after peripheral neuropathy (Schoffnegger et al., 2006). Altogether, this suggests that changed membrane excitability or altered firing patterns in LIII/IV of the spinal cord dorsal horn are unlikely causes for alterations underlying neuropathic pain.

## 8.3.     *General overview of changes occurring during neuropathy*

Between naive and neuropathic states, there was no difference between the frequencies or amplitudes in excitatory and inhibitory currents irrespective of neuron type. Moreover, the E/I ratio was shown to be also unchanged. This suggests that the inputs into LIII/IV have not been altered. Surprisingly, the balance between excitation and inhibition is known to be dysregulated after neuropathy. Moreover, the downregulation of chloride transporter KCC2 has been reported in superficial laminae in rodents following neuropathy (Coull et al., 2005; Doyon et al., 2016; Kahle

et al., 2016). The lower chloride extrusion capacity is expected to lead to disinhibition of spinal circuits, but we did not observe such effect in our measured variables on LIII/IV neurons.

Furthermore, we observed no differences in spontaneous activity (i.e. when no current injected) in recorded cells between all conditions (Naïve – 26%; Sham – 23% and Cuff – 14%). Ectopic discharge of primary afferents is known to drive central sensitization after peripheral nerve damage (Latremoliere and Woolf, 2009). Moreover, in vivo recording demonstrated increased ongoing activity in DH neurons following neuropathy (Medrano et al., 2016).The absence of difference in the occurrence of spontaneous activity in slices could be due to the isolation of the spinal cord during in vitro electrophysiology and thus removing components such as PNS, descending controls and/or absent spinal segments/circuits required for such activity.

Altogether, the absence of effects in our dataset does not imply that LIII/IV circuits are unaltered during neuropathy. In naïve animals, the importance of LIII cells are demonstrated by their role in feed-forward inhibition which prevents transmission of non-noxious information from reaching LI projection neurons, providing substrate for mechanical allodynia (Torsney and MacDermott, 2006; Miraucourt et al., 2009; Lu et al., 2013; Duan et al., 2014). Importantly, these studies recorded evoked measures (currents or potentials), while although we have recorded the spontaneous and miniature synaptic currents of LIII/IV cells in naïve and neuropathic animals. This could imply that LIII/IV circuit remains unfazed until challenged by incoming stimuli during injured states.

In summary, we have observed that morphology, membrane properties and incoming synaptic inputs to DH cholinergic interneurons and Non-ChAT remain similar to naïve states after peripheral nerve injury. Thus, these variables do not underlie the changes following sciatic nerve injury.

# Chapter 6: Global discussion and perspectives

In this thesis, our main objective was to understand the role of the spinal cholinergic system in the nociceptive information processing in naïve and neuropathic states. Therefore, we have studied: (1) the spinal cholinergic system modulating noxious mechanical information transmission in vivo, and (2) the spinal dorsal Horn (DH) cholinergic interneurons in vitro. These objectives are ultimately two parts of a whole, as our working hypothesis is that the DH cholinergic interneurons are contributing to the spinal cholinergic tone modulating nociceptive spinal circuits.

**Role of the spinal cholinergic system in pain**

We have demonstrated that a spinal cholinergic tone contributes to mechanical noxious information modulation in naïve mice. The modulatory role of cholinergic agonists onto nociceptive processing has long been described. Interestingly, nicotinic agonists are known to have pro-nociceptive and anti-nociceptive effects (Khan et al., 1998). This can be due to the widespread expression of nAChRs along the nociceptive pathway. Expression of nAChRs, as well as of mAChRs has been reported in primary afferents (Zhang et al., 2007a; Chen et al., 2014b); descending fibers (Cordero-Erausquin and Changeux, 2001), neurons terminals (Marubio et al., 1999; Genzen and McGehee, 2003; Takeda et al., 2003; Jeong et al., 2013) and postsynaptic DH neurons (Baba et al., 1998; Genzen and McGehee, 2005). In our hands, the cholinergic system demonstrated only an anti-nociceptive effect, as its inhibition produced a decrease in the threshold for behavioral withdrawal to a nociceptive stimulus, or increased response (in terms of action potentials) in DH neurons to such stimuli. Admittedly, we have manipulated the endogenous cholinergic tone, while exogenous applications of (nicotinic) agonists might have overstimulated this endogenous system, and/or differentially activated receptors compared to endogenous stimulation. This could explain a difference in net effect of these two manipulations.

The spinal cholinergic system is also known to be crucially involved in the analgesic effect of common analgesics such as clonidine and morphine (Pan et al., 1999; Chen and Pan, 2001). In clinics, inhibitors of AChE have been used as a co-adjuvant to reduce overall drug consumption (Eisenach, 2009). Both clonidine and morphine have been shown to increased spinal acetylcholine levels (Gage et al., 2001; Abelson and Hoglund, 2004). Nevertheless, the clinical application for cholinergic drugs is limited due to side effects (Eisenach, 2009). The improved understanding of the spinal cholinergic system may pave way for therapeutics.

**The mode of action of cholinergic interneurons**

Our in vivo recordings demonstrate that the modulatory effect of the endogenous cholinergic system involves an effect via nAChR and mAChR on the processing of incoming peripheral signals, both low and high threshold (respectively touch and pinch). This effect, recorded in a random DH neuron, also involves an inhibitory interneuron (I′) downstream to the cholino-responsive neuron. We have not yet completed the elucidation of the cholinergic source contributing to this effect, but DH cholinergic interneurons are very likely candidates.

These interneurons have been shown to have large dendritic and axonal aborization spreading several segments (Mesnage et al., 2011). We have demonstrated that they receive inputs from both excitatory and inhibitory neurons from the network, but also following activation of peripheral fibers. Our collaborator's preliminary data has demonstrated ChAT::EGFP are also interconnected. Therefore, they could potentially modulate different circuits present at different spinal segments through themselves, thus having a major effect on the spinal network in spite of their scarcity. This would be reminiscent of scarce, but highly connected, GABAergic interneurons in the developing mammalian hippocampus, which can powerfully modulate the network activity patterns (Witten et al., 2010). Cholinergic interneurons are also presynaptic to LII cells, and these, as well as the post-synaptic LIII/IV ChAT, could represent the I' neuron revealed in vivo.

A peculiar feature of DH cholinergic interneurons is indeed that they also express GABA, and even Glycine. The combination of these neurotransmitter proves interesting as it potentially involves both excitation and inhibition, as has been reported in hippocampus (involving GABA and Glutamate) (Gutierrez, 2000). Co-release of acetylcholine with another neurotransmitter has also been previously reported (Omalley and Masland, 1989; Manns et al., 2001). In the CNS, acetylcholine seems to have a greater role in neuro-modulation as opposed to acting as a fast neurotransmitter at the neuromuscular junction (Picciotto et al., 2012). As observed on motor neurons, M2 receptors can change neuronal excitability (Wilson et al., 2004). Potentially, the co-release of GABA/Glycine could be potentiated by acetylcholine. More generally, cholinergic terminals have been observed on primary afferent fiber endings in LII (Ribeiro-da-Silva and Cuello, 1990). This indicates that cholinergic interneurons could modulate incoming information by inducing primary afferent depolarization via GABA or even ACh (Hochman et al., 2010).

An ongoing question in the field of cholinergic physiology, is the exact nature of transmission: synaptic vs volumic. In supra-spinal structures, both traditional and extra-synaptic transmission

have been reported. The arguments supporting extra-synaptic transmission are the presence of cholinergic receptors on non-cholinergic synapses and increased extracellular ACh levels supports this notion (Sarter et al., 2009). Extra-synaptic GABA receptors have also been described, and implicated in neuropathic and inflammatory pain states (Iura et al., 2016; Perez-Sanchez et al., 2017). Whether such link exists between the mode of cholinergic transmission and the behavior remains to be demonstrated.

**Spinal cholinergic circuit in neuropathic mice**

After peripheral neuropathy, the spinal cholinergic tone appears to have undergone changes. This was already reported in the literature, as previous reports even claimed a loss of the cholinergic tone after neuropathy (Rashid and Ueda, 2002) or a plasticity in the effect of drugs (clonidine) acting through the spinal cholinergic system (Pan et al., 1999). At the behavioral level, we still observed the presence of a cholinergic tone acting on nAChR and, to a certain extent, mAChR. In vivo recordings confirmed that the plasticity of the tone was differential, affecting more the nociceptive pathway. Although plasticity in the cholinergic system has occurred, our in vitro recordings fail to uncover alterations in the basal inputs and passive properties of DH cholinergic interneurons. Such discrepancies may be explained by technical limitations due to slices or the inappropriate measured variables.

We also observed no difference in the density of ChAT interneurons after neuropathy. However, other cholinergic elements could change such as the appositions of ChAT boutons on targets, decreased levels of ACh (downregulation of ChAT), altered AChR receptor expression/localization/efficacy or AChE distribution/activity. Nevertheless, preliminary data suggest that AChE activity was unchanged after neuropathy (collaboration with E. Krejci, Paris University, unpublished observations). The exact nature of the changes impacting the spinal cholinergic system thus remains to be elucidated.

**Perspectives**

All behavior literature has been working on measures following evoked stimulation. This makes it difficult to study the "basal" state and role of the cholinergic system. In order to address this point, we could set a conditional place preference paradigm with intrathecal injection of cholinergic drugs to see relative contributions of different receptors.

Identifying the source of ACh involved in the observed behavior is an objective that we expect to reach in the coming weeks. However the DREADD experiments described in Results section 1

do not enable to identify the exact contribution of the cholinergic component (vs. the GABA and/or glycine one). To specifically address this point, we have designed a virus with a floxed construct encoding an inducible form of si-RNA against ChAT. With this tool, the strategy is to silence ChAT exclusively in ChAT neurons (due to the cre-dependence and the use of ChAT-Cre mice) at a chosen time (to avoid developmental effects). The vector is under production and should enable to refine our conclusions on the mode of action of these neurons.

Finally, we have been trying to record from DH cholinergic interneurons in vivo. This has proven difficult, due to their low density, even with tools such as optrode developed by our collaborators in Québec (LeChasseur et al., 2011). We will yet pursue our endeavor, as studying the natural stimulus in an intact animal is the best way to understand the activators to this population. Moreover, following their activity can be an indicator as to how the cholinergic tone and acetylcholine levels evolve in vivo.

# Bibliography

Abelson KSP, Hoglund AU (2004) The effects of the alpha(2)-adrenergic receptor Agonists clonidine and rilmenidine, and antagonists yohimbine and efaroxan, on the spinal cholinergic receptor system in the rat. Basic Clin Pharmacol Toxicol 94:153-160.

Abraira VE, Ginty DD (2013) The Sensory Neurons of Touch. Neuron 79:618-639.

Al Ghamdi KS, Polgar E, Todd AJ (2009) Soma size distinguishes projection neurons from neurokinin 1 receptor-expressing interneurons in lamina I of the rat lumbar spinal dorsal horn. Neuroscience 164:1794-1804.

Al-Khater KM, Todd AJ (2009) Collateral Projections of Neurons in Laminae I, III, and IV of Rat Spinal Cord to Thalamus, Periaqueductal Gray Matter, and Lateral Parabrachial Area. Journal of Comparative Neurology 515:629-646.

Almarestani L, Waters SM, Krause JE, Bennett GJ, Ribeiro-Da-Silva A (2007) Morphological characterization of spinal cord dorsal horn lamina I neurons projecting to the parabrachial nucleus in the rat. Journal of Comparative Neurology 504:287-297.

Almeida TF, Roizenblatt S, Tufik S (2004) Afferent pain pathways: a neuroanatomical review. Brain Research 1000:40-56.

Alvarez FJ, Villalba RM, Zerda R, Schneider SP (2004) Vesicular glutamate transporters in the spinal cord, with special reference to sensory primary afferent synapses. Journal of Comparative Neurology 472:257-280.

Amir R, Kocsis JD, Devor M (2005) Multiple interacting sites of ectopic spike electrogenesis in primary sensory neurons. Journal of Neuroscience 25:2576-2585.

Anglade P, Larabi-Godinot Y (2010) Historical landmarks in the histochemistry of the cholinergic synapse: perspectives for future researches. Biomedical Research-Tokyo 31:1-12.

Antal M, Petko M, Polgar E, Heizmann CW, StormMathisen J (1996) Direct evidence of an extensive GABAergic innervation of the spinal dorsal horn by fibres descending from the rostral ventromedial medulla. Neuroscience 73:509-518.

Attal N, Fermanian C, Fermanian J, Lanteri-Minet M, Alchaar H, Bouhassira D (2008) Neuropathic pain: Are there distinct subtypes depending on the aetiology or anatomical lesion? Pain 138:343-353.

Baba H, Kohno T, Okamoto M, Goldstein PA, Shimoji K, Yoshimura M (1998) Muscarinic facilitation of GABA release in substantia gelatinosa of the rat spinal dorsal horn. Journal of Physiology-London 508:83-93.

Baba H, Ji RR, Kohno T, Moore KA, Ataka T, Wakai A, Okamoto M, Woolf CJ (2003) Removal of GABAergic inhibition facilitates polysynaptic A fiber-mediated excitatory transmission to the superficial spinal dorsal horn. Molecular and Cellular Neuroscience 24:818-830.

Barber RP, Phelps PE, Houser CR, Crawford GD, Salvaterra PM, Vaughn JE (1984) The morphology and distribution of neurons containing choline-acetyltransferase in the adult-rat spinal-cord - an immunocytochemical study. J Comp Neurol 229:329-346.

Bardoni R (2013) Role of Presynaptic Glutamate Receptors in Pain Transmission at the Spinal Cord Level. Current Neuropharmacology 11:477-483.

Barrot M (2012) Tests and models of nociception and pain in rodents. Neuroscience 211:39-50.

Basbaum AI, Bautista DM, Scherrer G, Julius D (2009) Cellular and Molecular Mechanisms of Pain. Cell 139:267-284.

Bellier JP, Kimura H (2011) Peripheral type of choline acetyltransferase: Biological and evolutionary implications for novel mechanisms in cholinergic system. Journal of Chemical Neuroanatomy 42:225-235.

Benbouzid M, Choucair-Jaafar N, Yalcin I, Waltisperger E, Muller A, Freund-Mercier MJ, Barrot M (2008a) Chronic, but not acute, tricyclic antidepressant treatment alleviates neuropathic allodynia after sciatic nerve cuffing in mice. European Journal of Pain 12:1008-1017.

Benbouzid M, Pallage V, Rajalu M, Waltisperger E, Doridot S, Poisbeau P, Freund-Mercier MJ, Barrot M (2008b) Sciatic nerve cuffing in mice: A model of sustained neuropathic pain. European Journal of Pain 12:591-599.

Benbouzid M, Gaveriaux-Ruff C, Yalcin I, Waltisperger E, Tessier LH, Muller A, Kieffer BL, Freund-Mercier MJ, Barrot M (2008c) Delta-opioid receptors are critical for tricyclic antidepressant treatment of neuropathic allodynia. Biological Psychiatry 63:633-636.

Bennett GJ, Xie YK (1988) A peripheral mononeuropathy in rat that produces disorders of pain sensation like those seen in man. Pain 33:87-107.

Bernardini N, Sauer SK, Haberberger R, Fischer MJM, Reeh PW (2001) Excitatory nicotinic and desensitizing muscarinic (M2) effects on C-nociceptors in isolated rat skin. Journal of Neuroscience 21:3295-3302.

Bernardini N, Roza C, Sauer SK, Gomeza J, Wess J, Reeh PW (2002) Muscarinic M2 receptors on peripheral nerve endings: A molecular target of antinociception. Journal of Neuroscience 22.

Berthele A, Boxall SJ, Urban A, Anneser JMH, Zieglgansberger W, Urban L, Tolle TR (1999) Distribution and developmental changes in metabotropic glutamate receptor messenger RNA expression in the rat lumbar spinal cord. Developmental Brain Research 112:39-53.

Bessou P, Perl E (1969) Response of cutaneous sensory units with unmyelinated fibers to noxious stimuli. Journal of neurophysiology.

Betley JN, Wright CVE, Kawaguchi Y, Erdelyi F, Szabo G, Jessell TM, Kaltschmidt JA (2009) Stringent Specificity in the Construction of a GABAergic Presynaptic Inhibitory Circuit. Cell 139:161-174.

Biella G, Riva L, Sotgiu ML (1997) Interaction between neurons in different laminae of the dorsal horn of the spinal cord. A correlation study in normal and neuropathic rats. European Journal of Neuroscience 9:1017-1025.

Bohlhalter S, Mohler H, Fritschy JM (1994) Inhibitory neurotransmission in rat spinal cord: co-localization of glycine- and GABA A -receptors at GABAergic synaptic contacts demonstrated by triple immunofluorescence staining. Brain Research 642:59-69.

Bohlhalter S, Weinmann O, Mohler H, Fritschy JM (1996) Laminar compartmentalization of GABA(A)-receptor subtypes in the spinal cord: An immunohistochemical study. Journal of Neuroscience 16:283-297.

Borges LF, Iversen SD (1986) Topography of choline acetyltransferase immunoreactive neurons and fibers in the rat spinal cord. Brain Research 362:140-148.

Bouhassira D, Villanueva L, Bing Z, Lebars D (1992) Involvement of the subnucleus reticularis dorsalis in diffuse noxious inhibitory controls in the rat. Brain Research 595:353-357.

Bourquin AF, Suveges M, Pertin M, Gilliard N, Sardy S, Davison AC, Spahn DR, Decosterd I (2006) Assessment and analysis of mechanical allodynia-like behavior induced by spared nerve injury (SNI) in the mouse. Pain 122:14-16.

Braz JM, Nassar MA, Wood JN, Basbaum AI (2005) Parallel "pain" pathways arise from subpopulation of primary afferent nociceptor. Neuron 47:787-793.

Breivik H, Eisenberg E, O'Brien T, Openminds (2013) The individual and societal burden of chronic pain in Europe: the case for strategic prioritisation and action to improve knowledge and availability of appropriate care. Bmc Public Health 13.

Breivik H, Collett B, Ventafridda V, Cohen R, Gallacher D (2006) Survey of chronic pain in Europe: Prevalence, impact on daily life, and treatment. Eur J Pain 10:287-333.

Bridges D, Thompson SWN, Rice ASC (2001) Mechanisms of neuropathic pain. 87 1:12 - 26.

Brown AG (1982) The dorsal horn of the Spinal-cord. Quarterly Journal of Experimental Physiology and Cognate Medical Sciences 67:193-212.

Brown DA (2010) Muscarinic Acetylcholine Receptors (mAChRs) in the Nervous System: Some Functions and Mechanisms. Journal of Molecular Neuroscience 41:340-346.

Bruinstroop E, Cano G, Vanderhorst V, Cavalcante JC, Wirth J, Sena-Esteves M, Saper CB (2012) Spinal projections of the A5, A6 (locus coeruleus), and A7 noradrenergic cell groups in rats. Journal of Comparative Neurology 520:1985-2001.

Buckley N, Bonner T, Buckley C, Brann M (1989) Antagonist binding properties of five cloned muscarinic receptors expressed in CHO-K1 cells. Molecular pharmacology 35:469 - 476.

Butler RK, Finn DP (2009) Stress-induced analgesia. Progress in Neurobiology 88:184-202.

Cai YQ, Chen SR, Han HD, Sood AK, Lopez-Berestein G, Pan HL (2009) Role of M-2, M-3, and M-4 muscarinic receptor subtypes in the spinal cholinergic control of nociception revealed using siRNA in rats. Journal of Neurochemistry 111:1000-1010.

Callahan BL, Gil ASC, Levesque A, Mogil JS (2008) Modulation of mechanical and thermal nociceptive sensitivity in the laboratory mouse by behavioral state. Journal of Pain 9:174-184.

Carlton SM, Dougherty PM, Pover CM, Coggeshall RE (1991) Neuroma formation and numbers of axons in a rat model of experimental peripheral neuropathy. Neuroscience Letters 131:88-92.

Castrolopes JM, Tavares I, Coimbra A (1993) GABA decreases in the spinal cord dorsal horn after peripheral neurectomy. Brain Research 620:287-291.

Castrolopes JM, Tolle TR, Pan B, Zieglgansberger W (1994) Expression of GAD mRNA in spinal cord neurons of normal and monoarthritic rats. Molecular Brain Research 26:169-176.

Caterina MJ, Leffler A, Malmberg AB, Martin WJ, Trafton J, Petersen-Zeitz KR, Koltzenburg M, Basbaum AI, Julius D (2000) Impaired nociception and pain sensation in mice lacking the capsaicin receptor. Science 288:306-313.

Cavanaugh DJ, Chesler AT, Braz JM, Shah NM, Julius D, Basbaum AI (2011) Restriction of Transient Receptor Potential Vanilloid-1 to the Peptidergic Subset of Primary Afferent Neurons Follows Its Developmental Downregulation in Nonpeptidergic Neurons. Journal of Neuroscience 31:10119-10127.

Cervero F (2009) Visceral versus Somatic Pain: Similarities and Differences. Digestive Diseases 27:3-10.

Chaplan SR, Guo HQ, Lee DH, Luo L, Liu CL, Kuei C, Velumian AA, Butler MP, Brown SM, Dubin AE (2003) Neuronal hyperpolarization-activated pacemaker channels drive neuropathic pain. Journal of Neuroscience 23:1169-1178.

Chen JTC, Guo D, Campanelli D, Frattini F, Mayer F, Zhou LM, Kuner R, Heppenstall PA, Knipper M, Hu J (2014a) Presynaptic GABAergic inhibition regulated by BDNF contributes to neuropathic pain induction. Nature Communications 5.

Chen SR, Pan HL (2001) Spinal endogenous acetylcholine contributes to the analgesic effect of systemic morphine in rats. Anesthesiology 95:525-530.

Chen SR, Pan HL (2003) Spinal GABA(B) receptors mediate antinociceptive actions of cholinergic agents in normal and diabetic rats. Brain Research 965:67-74.

Chen SR, Pan HL (2004) Activation of muscarinic receptors inhibits spinal dorsal horn projection neurons: Role of GABA(B) receptors. Neuroscience 125:141-148.

Chen SR, Chen H, Yuan WX, Wess J, Pan HL (2010) Dynamic Control of Glutamatergic Synaptic Input in the Spinal Cord by Muscarinic Receptor Subtypes Defined Using Knockout Mice. Journal of Biological Chemistry 285:40427-40437.

Chen SR, Chen H, Yuan WX, Wess J, Pan HL (2014b) Differential Regulation of Primary Afferent Input to Spinal Cord by Muscarinic Receptor Subtypes Delineated Using Knockout Mice. Journal of Biological Chemistry 289:14321-14330.

Cheng LP, Arata A, Mizuguchi R, Qian Y, Karunaratne A, Gray PA, Arata S, Shirasawa S, Bouchard M, Luo P, Chen CL, Busslinger M, Goulding M, Onimaru H, Ma QF (2004) Tlx3 and Tlx1 are post-mitotic selector genes determining glutamatergic over GABAergic cell fates. Nature Neuroscience 7:510-517.

Chery N, De Koninck Y (1999) Junctional versus extrajunctional glycine and GABA(A) receptor-mediated IPSCs in identified lamina I neurons of the adult rat spinal cord. Journal of Neuroscience 19:7342-7355.

Chiari A, Tobin JR, Pan HL, Hood DD, Eisenach JC (1999) Sex differences in cholinergic analgesia I - A supplemental nicotinic mechanism in normal females. Anesthesiology 91:1447-1454.

Cizkova D, Marsala J, Lukacova N, Marsala M, Jergova S, Orendacova J, Yaksh TL (2002) Localization of N-type Ca2+ channels in the rat spinal cord following chronic constrictive nerve injury. Experimental Brain Research 147:456-463.

Clayton BA, Hayashida K, Childers SR, Xiao RY, Eisenach JC (2007) Oral donepezil reduces hypersensitivity after nerve injury by a spinal muscarinic receptor mechanism. Anesthesiology 106:1019-1025.

Coggeshall RE, Carlton SM (1997) Receptor localization in the mammalian dorsal horn and primary afferent neurons. Brain Research Reviews 24:28-66.

Cohen SP, Mao JR (2014) Neuropathic pain: mechanisms and their clinical implications. Bmj-British Medical Journal 348.

Colleoni M, Sacerdote P (2010) Murine models of human neuropathic pain. Biochimica Et Biophysica Acta-Molecular Basis of Disease 1802:924-933.

Colloca L, Ludman T, Bouhassira D, Baron R, Dickenson A, Yarnitsky D, Freeman R, Truini A, Attal N, Finnerup NB, Eccleston C, Kalso E, Bennett DL, Dworkin R, Raja SN (2017) Neuropathic pain. Nature Reviews Disease Primers 3.

Cook AJ, Woolf CJ, Wall PD, McMahon SB (1987) Dynamic receptive field plasticity in rat spinal cord dorsal horn following C-primary afferent input. Nature 325:151-153.

Corallo C, Whitfield A, Wu A (2009) Anticholinergic syndrome following an unintentional overdose of scopolamine. Therapeutics and clinical risk management 5:719–723.

Cordero-Erausquin M, Changeux JP (2001) Tonic nicotinic modulation of serotoninergic transmission in the spinal cord. Proceedings of the National Academy of Sciences of the United States of America 98:2803-2807.

Cordero-Erausquin M, Pons S, Faure P, Changeux JP (2004) Nicotine differentially activates inhibitory and excitatory neurons in the dorsal spinal cord. Pain 109:308-318.

Cordero-Erausquin M, Inquimbert P, Schlichter R, Hugel S (2016) NEURONAL NETWORKS AND NOCICEPTIVE PROCESSING IN THE DORSAL HORN OF THE SPINAL CORD. Neuroscience 338:230-247.

Cordero-Erausquin M, Allard S, Dolique T, Bachand K, Ribeiro-da-Silva A, De Koninck Y (2009) Dorsal Horn Neurons Presynaptic to Lamina I Spinoparabrachial Neurons Revealed by Transynaptic Labeling. Journal of Comparative Neurology 517:601-615.

Corthay J, Dunant Y, Eder L, Loctin F (1985) Incorporation of acetate into acetylcholine, acetylcarnitine, and amino acids in the Torpedo electric organ. Journal of Neurochemistry 45:1809-1819.

Costigan M, Scholz J, Woolf CJ (2009) Neuropathic Pain: A Maladaptive Response of the Nervous System to Damage. Annual Review of Neuroscience 32:1-32.

Coull JAM, Boudreau D, Bachand K, Prescott SA, Nault F, Sik A, De Koninck P, De Koninck Y (2003) Trans-synaptic shift in anion gradient in spinal lamina I neurons as a mechanism of neuropathic pain. Nature 424:938-942.

Coull JAM, Beggs S, Boudreau D, Boivin D, Tsuda M, Inoue K, Gravel C, Salter MW, De Koninck Y (2005) BDNF from microglia causes the shift in neuronal anion gradient underlying neuropathic pain. Nature 438:1017-1021.

Crespo L, Wecker L, Dunaway G, Faingold C, Watts S (2010) Brody's Human Pharmacology - 5th edition: Mosby Elsevier.

Dani JA (2015) Neuronal Nicotinic Acetylcholine Receptor Structure and Function and Response to Nicotine. Nicotine Use in Mental Illness and Neurological Disorders 124:3-19.

Daniele CA, MacDermott AB (2009) Low-Threshold Primary Afferent Drive onto GABAergic Interneurons in the Superficial Dorsal Horn of the Mouse. J Neurosci 29:686-695.

De Vry J, Kuhl E, Franken-Kunkel P, Eckel G (2004) Pharmacological characterization of the chronic constriction injury model of neuropathic pain. European Journal of Pharmacology 491:137-148.

Decosterd I, Woolf CJ (2000) Spared nerve injury: an animal model of persistent peripheral neuropathic pain. Pain 87:149-158.

DeKock M, Meert TF (1997) alpha(2)-adrenoceptor agonists and stress-induced analgesia in rats: Influence of stressors and methods of analysis. Pharmacology Biochemistry and Behavior 58:109-117.

DeKock M, Eisenach J, Tong C, Schmitz AL, Scholtes JL (1997) Analgesic doses of intrathecal but not intravenous clonidine increase acetylcholine in cerebrospinal fluid in humans. Anesth Analg 84:800-803.

Derjean D, Bertrand S, Le Masson G, Landry M, Morisset V, Nagy F (2003) Dynamic balance of metabotropic inputs causes dorsal horn neurons to switch functional states. Nature Neuroscience 6:274-281.

Detweiler DJ, Eisenach JC, Tong CY, Jackson C (1993) A cholinergic interaction in Alpha(2) adrenoceptor-mediated antinociception in sheep. J Pharmacol Exp Ther 265:536-542.

Dhaka A, Earley TJ, Watson J, Patapoutian A (2008) Visualizing cold spots: TRPM8-expressing sensory neurons and their projections. Journal of Neuroscience 28:566-575.

Dickenson A (2010) The neurobiology of chronic pain states. Anesthesia and intensive care medicine 12.

Dietz V (2002) Proprioception and locomotor disorders. Nature Reviews Neuroscience 3:781-790.

Djouhri L (2016) A delta-fiber low threshold mechanoreceptors innervating mammalian. hairy skin: A review of their receptive, electrophysiological and cytochemical properties in relation to A delta-fiber high threshold mechanoreceptors. Neuroscience and Biobehavioral Reviews 61:225-238.

Djouhri L, Lawson SN (2004) A beta-fiber nociceptive primary afferent neurons: a review of incidence and properties in relation to other afferent A-fiber neurons in mammals. Brain Research Reviews 46:131-145.

Dong XW, Goregoaker S, Engler H, Zhou X, Mark L, Crona J, Terry R, Hunter J, Priestley T (2007) Small interfering RNA-mediated selective knockdown of Na(v)1.8 tetrodotoxin-resistent sodium channel reverses mechanical allodynia in neuropathic rats. Neuroscience 146:812-821.

Dowdall T, Robinson I, Meert TF (2005) Comparison of five different rat models of peripheral nerve injury. Pharmacology Biochemistry and Behavior 80:93-108.

Doyon N, Vinay L, Prescott SA, De Koninck Y (2016) Chloride Regulation: A Dynamic Equilibrium Crucial for Synaptic Inhibition. Neuron 89:1157-1172.

Duan B, Cheng LZ, Bourane S, Britz O, Padilla C, Garcia-Campmany L, Krashes M, Knowlton W, Velasquez T, Ren XY, Ross SE, Lowell BB, Wang Y, Goulding M, Ma QF (2014) Identification of Spinal Circuits Transmitting and Gating Mechanical Pain. Cell 159:1417-1432.

Dubin AE, Patapoutian A (2010) Nociceptors: the sensors of the pain pathway. Journal of Clinical Investigation 120:3760-3772.

Dussor GO, Jones DJ, Hulsebosch CE, Edell TA, Flores CM (2005) The effects of chemical or surgical deafferentation on H-3 -acetylcholine release from rat spinal cord. Neuroscience 135:1269-1276.

Dworkin RH et al. (2003) Advances in neuropathic pain - Diagnosis, mechanisms, and treatment recommendations. Archives of Neurology 60:1524-1534.

Echeverry S, Shi XQ, Yang M, Huang H, Wu YC, Lorenzo LE, Perez-Sanchez J, Bonin RP, De Koninck Y, Zhang J (2017) Spinal microglia are required for long-term maintenance of neuropathic pain. Pain 158:1792-1801.

Eckert WA, McNaughton KK, Light AR (2003) Morphology and axonal arborization of rat spinal inner lamina II neurons hyperpolarized by mu-opioid-selective agonists. Journal of Comparative Neurology 458:240-256.

Eglen R, Michel A, Cornett C, Kunysz E, Whiting R (1989 ) The interaction of hexamethonium with muscarinic receptor subtypes in vitro. British Journal of Pharmacology 98:499–506

Eiden LE (1998) The cholinergic gene locus. Journal of Neurochemistry 70:2227-2240.

Eisenach JC (2009) Epidural Neostigmine: Will It Replace Lipid Soluble Opioids for Postoperative and Labor Analgesia? Anesth Analg 109:293-295.

Eisenach JC, Detweiler DJ, Tong CY, Dangelo R, Hood DD (1996) Cerebrospinal fluid norepinephrine and acetylcholine concentrations during acute pain. Anesth Analg 82:621-626.

Eliava M et al. (2016) A New Population of Parvocellular Oxytocin Neurons Controlling Magnocellular Neuron Activity and Inflammatory Pain Processing. Neuron 89:1291-1304.

Erickson JD, Varoqui H, Schafer MKH, Modi W, Diebler MF, Weihe E, Rand J, Eiden LE, Bonner TI, Usdin TB (1994) Functional identification of a vesicular acetylcholine transporter and its expression from a "cholinergic" gene locus. Journal of Biological Chemistry 269:21929-21932.

Everdingen M, De Rijke JM, Kessel AG, Schouten HC, Van Kleef M, Patijn J (2007) Prevalence of pain in patients with cancer: a systematic review of the past 40 years. Annals of Oncology 18:1437-1449.

Fang FG, Haws CM, Drasner K, Williamson A, Fields HL (1989) Opioid peptides (DAGO-enkephalin, dynorphin A(1–13), BAM 22P) microinjected into the rat brainstem: comparison of their antinociceptive effect and their effect on neuronal firing in the rostral ventromedial medulla. Brain Research 501:116-128.

Ferguson SM, Blakely RD (2004) The choline transporter resurfaces: New roles for synaptic vesicles? Molecular Interventions 4:22-37.

Fields HL, Bry J, Hentall I, Zorman G (1983) The activity of neurons in the rostral medulla of the rat during withdrawal from noxious heat. Journal of Neuroscience 3:2545-2552.

Flynn JR, Brichta AM, Galea MP, Callister RJ, Graham BA (2011) A horizontal slice preparation for examining the functional connectivity of dorsal column fibres in mouse spinal cord. Journal of Neuroscience Methods 200:113-120.

Foster E, Wildner H, Tudeau L, Haueter S, Ralvenius WT, Jegen M, Johannssen H, Hosli L, Haenraets K, Ghanem A, Conzelmann KK, Bosl M, Zeilhofer HU (2015) Targeted Ablation, Silencing, and Activation Establish Glycinergic Dorsal Horn Neurons as Key Components of a Spinal Gate for Pain and Itch. Neuron 85:1289-1304.

Francois A, Low SA, Sypek EI, Christensen AJ, Sotoudeh C, Beier KT, Ramakrishnan C, Ritola KD, Sharif-Naeini R, Deisseroth K, Delp SL, Malenka RC, Luo LQ, Hantman AW, Scherrer G (2017) A Brainstem-Spinal Cord Inhibitory Circuit for Mechanical Pain Modulation by GABA and Enkephalins. Neuron 93:822-+.

Fucile S, Sucapane A, Eusebi F (2005) Ca2+ permeability of nicotinic acetylcholine receptors from rat dorsal root ganglion neurones. Journal of Physiology-London 565:219-228.

Fundytus ME, Yashpal K, Chabot JG, Osborne MG, Lefebvre CD, Dray A, Henry JL, Coderre TJ (2001) Knockdown of spinal metabotropic glutamate receptor 1 (mGluR(1)) alleviates pain and restores opioid efficacy after nerve injury in rats. British Journal of Pharmacology 132:354-367.

Gabay E, Tal M (2004) Pain behavior and nerve electrophysiology in the CCI model of neuropathic pain. Pain 110:354-360.

Gabrielle P, Jeana M, Lorenza EC (2003) Cytosolic choline acetyltransferase binds specifically to cholinergic plasma membrane of rat brain synaptosomes to generate membrane-bound enzyme. Neurochemical Research 28:543-549.

Gage HD, Gage JC, Tobin JR, Chiari A, Tong CY, Xu ZM, Mach RH, Efange SMN, Ehrenkaufer RLE, Eisenach JC (2001) Morphine-induced spinal cholinergic activation: in vivo imaging with positron emission tomography. Pain 91:139-145.

Ganley RP, Iwagaki N, del Rio P, Baseer N, Dickie AC, Boyle KA, Polgar E, Watanabe M, Abraira VE, Zimmerman A, Riddell JS, Todd AJ (2015) Inhibitory Interneurons That Express GFP in the PrP-GFP Mouse Spinal Cord Are Morphologically Heterogeneous, Innervated by Several Classes of Primary Afferent and Include Lamina I Projection Neurons among Their Postsynaptic Targets. Journal of Neuroscience 35:7626-7642.

Gao BX et al. (2010) Pharmacological effects of nonselective and subtype-selective nicotinic acetylcholine receptor agonists in animal models of persistent pain. Pain 149:33-49.

Garland EL (2012) Pain Processing in the Human Nervous System A Selective Review of Nociceptive and Biobehavioral Pathways. Primary Care 39:561-+.

Gassner M, Leitner J, Gruber-Schoffnegger D, Forsthuber L, Sandkuhler J (2013) Properties of spinal lamina III GABAergic neurons in naive and in neuropathic mice. European Journal of Pain 17:1168-1179.

Gatchel RJ, Peng YB, Peters ML, Fuchs PN, Turk DC (2007) The biopsychosocial approach to chronic pain: Scientific advances and future directions. Psychological Bulletin 133:581-624.

Gauriau C, Bernard JF (2002) Pain pathways and parabrachial circuits in the rat. Experimental Physiology 87:251-258.

Genzen JR, McGehee DS (2003) Short- and long-term enhancement of excitatory transmission in the spinal cord dorsal horn by nicotinic acetylcholine receptors. Proceedings of the National Academy of Sciences of the United States of America 100:6807-6812.

Genzen JR, McGehee DS (2005) Nicotinic modulation of GABAergic synaptic transmission in the spinal cord dorsal horn. Brain Research 1031:229-237.

Genzen JR, Van Cleve W, McGehee DS (2001) Dorsal root ganglion neurons express multiple nicotinic acetylcholine receptor subtypes. Journal of Neurophysiology 86:1773-1782.

Gomez JL, Bonaventura J, Lesniak W, Mathews WB, Sysa-Shah P, Rodriguez LA, Ellis RJ, Richie CT, Harvey BK, Dannals RF, Pomper MG, Bonci A, Michaelides M (2017) Chemogenetics revealed: DREADD occupancy and activation via converted clozapine. Science 357:503-+.

Grudt TJ, Perl ER (2002) Correlations between neuronal morphology and electrophysiological features in the rodent superficial dorsal horn. Journal of Physiology-London 540:189-207.

Guo A, Vulchanova L, Wang J, Li X, Elde R (1999) Immunocytochemical localization of the vanilloid receptor 1 (VR1): relationship to neuropeptides, the P2X(3) purinoceptor and IB4 binding sites. European Journal of Neuroscience 11:946-958.

Guo D, Hu J (2014) Spinal presynaptic inhibition in pain control. Neuroscience 283:95-106.

Gutierrez R (2000) Seizures induce simultaneous GABAergic and glutamatergic transmission in the dentate Gyrus-CA3 system. Journal of Neurophysiology 84:3088-3090.

Gutierrez-Mecinas M, Furuta T, Watanabe M, Todd AJ (2016) A quantitative study of neurochemically defined excitatory interneuron populations in laminae I-III of the mouse spinal cord. Molecular Pain 12.

Haberberger RV, Henrich M, Lips KS, Kummer W (2003) Nicotinic receptor alpha7-subunits are coupled to the stimulation of nitric oxide synthase in rat dorsal root ganglion neurons. Histochemistry and Cell Biology 120:173-181.

Hahn M, Hahn SL, Stone DM, Joh TH (1992) Cloning of the rat gene encoding choline acetyltransferase, a cholinergic neuron-specific marker. Proceedings of the National Academy of Sciences of the United States of America 89:4387-4391.

Hama A, Menzaghi F (2001) Antagonist of nicotinic acetylcholine receptors (nAChR) enhances formalin-induced nociception in rats: tonic role of nAChRs in the control of pain following injury. Brain Res 888:102-106.

Han ZS, Zhang ET, Craig AD (1998) Nociceptive and thermoreceptive lamina I neurons are anatomically distinct. Nature Neuroscience 1:218-225.

Hanz S, Perlson E, Willis D, Zheng JQ, Massarwa R, Huerta JJ, Koltzenburg M, Kohler M, van-Minnen J, Twiss JL, Fainzilber M (2003) Axoplasmic importins enable retrograde injury signaling in lesioned nerve. Neuron 40:1095-1104.

Hartvig P, Gillberg PG, Gordh T, Post C (1989) Cholinergic mechanisms in pain and analgesia. Trends Pharmacol Sci 10(Suppl):75-79.

He XH, Zang Y, Chen X, Pang RP, Xu JT, Zhou XA, Wei XH, Li YY, Xin WJ, Qin ZH, Liu XG (2010) TNF-alpha contributes to up-regulation of Nav1.3 and Nav1.8 in DRG neurons following motor fiber injury. Pain 151:266-279.

Heinricher MM, Barbaro NM, Fields HL (1989) Putative nociceptive modulating neurons in the rostral ventromedial medulla of the rat: firing of on- and off-cells is related to nociceptive responsiveness. Somatosensory and Motor Research 6:427-439.

Heinricher MM, Tavares I, Leith JL, Lumb BM (2009) Descending control of nociception: Specificity, recruitment and plasticity. Brain Research Reviews 60:214-225.

Hendrich J, Van Minh AT, Heblich F, Nieto-Rostro M, Watschinger K, Striessnig J, Wratten J, Davies A, Dolphin AC (2008) Pharmacological disruption of calcium channel trafficking by the alpha(2)delta ligand gabapentin. Proceedings of the National Academy of Sciences of the United States of America 105:3628-3633.

Henschke N, Kamper SJ, Maher CG (2015) The Epidemiology and Economic Consequences of Pain. Mayo Clinic Proceedings 90:139-147.

Hochman S, Shreckengost J, Kimura H, Quevedo J (2010) Presynaptic inhibition of primary afferents by depolarization: observations supporting nontraditional mechanisms. Neurons and Networks in the Spinal Cord 1198:140-152.

Hoglund AU, Baghdoyan HA (1997) M2, M3 and M4, but not M1, muscarinic receptor subtypes are present in rat spinal cord. J Pharmacol Exp Ther 281:470-477.

Hoglund AU, Hamilton C, Lindblom L (2000) Effects of microdialyzed oxotremorine, carbachol, epibatidine, and scopolamine on intraspinal release of acetylcholine in the rat. Journal of Pharmacology and Experimental Therapeutics 295:100-104.

Honda K, Koga K, Moriyama T, Koguchi M, Takano Y, Kamiya H (2002) Intrathecal alpha(2) adrenoceptor agonist clonidine inhibits mechanical transmission in mouse spinal cord via activation of muscarinic M-1 receptors. Neurosci Lett 322:161-164.

Hossaini M, Duraku LS, Sarac C, Jongen JLM, Holstege JC (2010) Differential distribution of activated spinal neurons containing glycine and/or GABA and expressing c-fos in acute and chronic pain models. Pain 151:356-365.

Howe JR, Wang JY, Yaksh TL (1983) Selective antagonism of the antinociceptive effect of intrathecally applied alpha adrenergic agonists by intrathecal prazosin and intrathecal yohimbine. Journal of Pharmacology and Experimental Therapeutics 224:552-558.

Huang F, Buchwald P, Browne CE, Farag HH, Wu WM, Ji FB, Hochhaus G, Bodor N (2001) Receptor binding studies of soft anticholinergic agents. Aaps Pharmsci 3.

Huang MG, Huang TW, Xiang Y, Xie ZQ, Chen Y, Yan R, Xu JY, Cheng LP (2008) Ptf1a, Lbx1 and Pax2 coordinate glycinergic and peptidergic transmitter phenotypes in dorsal spinal inhibitory neurons. Developmental Biology 322:394-405.

Hughes DI, Scott DT, Todd AJ, Riddell JS (2003) Lack of evidence for sprouting of A beta afferents into the superficial laminas of the spinal cord dorsal horn after nerve section. Journal of Neuroscience 23:9491-9499.

Hunt SP, Mantyh PW (2001) The molecular dynamics of pain control. Nature Reviews Neuroscience 2:83-91.

Hwang JH, Hwang KS, Leem JK, Park PH, Han SM, Lee DM (1999) The antiallodynic effects of intrathecal cholinesterase inhibitors in a rat model of neuropathic pain. Anesthesiology 90:492-499.

Hwang JH, Hwang KS, Choi Y, Park PH, Han SM, Lee DM (2000) An analysis of drug interaction between morphine and neostigmine in rats with nerve-ligation injury. Anesthesia and Analgesia 90:421-426.

Hylden JLK, Anton F, Nahin RL (1989) Spinal lamina I projection neurons in the rat: Collateral innervation of parabrachial area and thalamus. Neuroscience 28:27-37.

Ibuki T, Hama AT, Wang XT, Pappas GD, Sagen J (1997) Loss of GABA-immunoreactivity in the spinal dorsal horn of rats with peripheral nerve injury and promotion of recovery by adrenal medullary grafts. Neuroscience 76:845-858.

Inquimbert P, Rodeau JL, Schlichter R (2007) Differential contribution of GABAergic and glycinergic components to inhibitory synaptic transmission in lamina II and laminae III-IV of the young rat spinal cord. European Journal of Neuroscience 26:2940-2949.

Iura A, Takahashi A, Hakata S, Mashimo T, Fujino Y (2016) Reductions in tonic GABAergic current in substantia gelatinosa neurons and GABA(A) receptor subunit expression after chronic constriction injury of the sciatic nerve in mice. European Journal of Pain 20:1678-1688.

Jaggi AS, Jain V, Singh N (2011) Animal models of neuropathic pain. Fundamental & Clinical Pharmacology 25:1-28.

Jensen TS, Baron R, Haanpaa M, Kalso E, Loeser JD, Rice ASC, Treede RD (2011) A new definition of neuropathic pain. Pain 152:2204-2205.

Jeong SG, Choi IS, Cho JH, Jang IS (2013) Cholinergic modulation of primary afferent glutamatergic transmission in rat medullary dorsal horn neurons. Neuropharmacology 75:295-303.

Jones CK, Byun N, Bubser M (2012) Muscarinic and Nicotinic Acetylcholine Receptor Agonists and Allosteric Modulators for the Treatment of Schizophrenia. Neuropsychopharmacology 37:16-42.

Julius D, Basbaum AI (2001) Molecular mechanisms of nociception. Nature 413:203-210.

Kahle KT et al. (2016) Inhibition of the kinase WNK1/HSN2 ameliorates neuropathic pain by restoring GABA inhibition. Science Signaling 9.

Kanazawa I, Sutoo D, Oshima I, Saito S (1979) Effect of transfection on Choline-acetyltransferase, Thyrotropin releasing hormone and Substance-P in the cat cervical spinal-cord. Neurosci Lett 13:325-330.

Kardon AP, Polgar E, Hachisuka J, Snyder LM, Cameron D, Savage S, Cai XY, Karnup S, Fan CR, Hemenway GM, Bernard CS, Schwartz ES, Nagase H, Schwarzer C, Watanabe M, Furuta T, Kaneko T, Koerber HR, Todd AJ, Ross SE (2014) Dynorphin Acts as a Neuromodulator to Inhibit Itch in the Dorsal Horn of the Spinal Cord. Neuron 82:573-586.

Kashiwadani H, Kanmura Y, Kuwaki T (2017) Application of calibrated forceps for assessing mechanical nociception with high time resolution in mice. Plos One 12.

Kato G, Kosugi M, Mizuno M, Strassman AM (2013) Three-dimensional organization of local excitatory and inhibitory inputs to neurons in laminae III-IV of the spinal dorsal horn. Journal of Physiology-London 591:5645-5660.

Kato G, Kawasaki Y, Koga K, Uta D, Kosugi M, Yasaka T, Yoshimura M, Ji RR, Strassman AM (2009) Organization of Intralaminar and Translaminar Neuronal Connectivity in the Superficial Spinal Dorsal Horn. Journal of Neuroscience 29:5088-5099.

Kauppila T, Kontinen VK, Pertovaara A (1998) Influence of spinalization on spinal withdrawal reflex responses varies depending on the submodality of the test stimulus and the experimental pathophysiological condition in the rat. Brain Research 797:234-242.

Keller AF, Beggs S, Salter MW, De Koninck Y (2007) Transformation of the output of spinal lamina I neurons after nerve injury and microglia stimulation underlying neuropathic pain. Molecular Pain 3.

Keller AF, Coull JA, Chery N, Poisbeau P, De Koninck Y (2001) Region-specific developmental specialization of GABA-glycine cosynapses in laminas I-II of the rat spinal dorsal horn. Journal of Neuroscience 21:7871-7880.

Khan I, Osaka H, Stanislaus S, Calvo RM, Deerinck T, Yaksh TL, Taylor P (2003) Nicotinic acetylcholine receptor distribution in relation to spinal neurotransmission pathways. J Comp Neurol 467:44-59.

Khan IM, Buerkle H, Taylor P, Yaksh TL (1998) Nociceptive and antinociceptive responses to intrathecally administered nicotinic agonists. Neuropharmacology 37:1515-1525.

Kim YH, Back SK, Davies AJ, Jeong H, Jo HJ, Chung G, Na HS, Bae YC, Kim SJ, Kim JS, Jung SJ, Oh SB (2012) TRPV1 in GABAergic Interneurons Mediates Neuropathic Mechanical Allodynia and Disinhibition of the Nociceptive Circuitry in the Spinal Cord. Neuron 74:640-647.

Kimura M, Hayashida K, Eisenach JC, Saito S, Obata H (2013) Relief of Hypersensitivity after Nerve Injury from Systemic Donepezil Involves Spinal Cholinergic and gamma-Aminobutyric Acid Mechanisms. Anesthesiology 118:173-180.

Kiyosawa A, Katsurabayashi S, Akaike N, Pang ZP (2001) Nicotine facilitates glycine release in the rat spinal dorsal horn. Journal of Physiology-London 536:101-110.

Kobayashi K, Fukuoka T, Obata K, Yamanaka H, Dai Y, Tokunaga A, Noguchi K (2005) Distinct expression of TRPM8, TRPA1, and TRPV1 mRNAs in rat primary afferent neurons with A delta/C-fibers and colocalization with trk receptors. Journal of Comparative Neurology 493:596-606.

Koga K, Honda K, Ando S, Harasawa I, Kamiya H, Takano Y (2004) Intrathecal clonidine inhibits mechanical allodynia via activation of the spinal muscarinic M-1 receptor in streptozotocin-induced diabetic mice. European Journal of Pharmacology 505:75-82.

Kovelowski CJ, Ossipov MH, Sun H, Lai J, Malan TP, Porreca F (2000) Supraspinal cholecystokinin may drive tonic descending facilitation mechanisms to maintain neuropathic pain in the rat. Pain 87:265-273.

Kremer M, Yalcin I, Nexon L, Wurtz X, Ceredig RA, Daniel D, Hawkes RA, Salvat E, Barrot M (2016) The antiallodynic action of pregabalin in neuropathic pain is independent from the opioid system. Molecular Pain 12.

Kuner R (2010) Central mechanisms of pathological pain. Nat Med 16:1258-1266.

Kwiat GC, Basbaum AI (1992) The origin of brainstem noradrenergic and serotonergic projections to the spinal cord dorsal horn in the rat. Somatosensory and Motor Research 9:157-173.

Labrakakis C, MacDermott AB (2003) Neurokinin receptor 1-expressing spinal cord neurons in lamina I and III/IV of postnatal rats receive inputs from capsaicin sensitive fibers. Neuroscience Letters 352:121-124.

Laing I, Todd AJ, Heizmann CW, Schmidt H (1994) Subpopulations of GABAergic neurons in laminae I-III of rat spinal dorsal horn defined by coexistence with classical transmitters, peptides, nitric oxide synthase or parvalbumin. Neuroscience 61:123-132.

Lallemend F, Ernfors P (2012) Molecular interactions underlying the specification of sensory neurons. Trends in Neurosciences 35:373-381.

Landry M, Bouali-Benazzouz R, El Mestikawy S, Ravassard P, Nagy F (2004) Expression of vesicular glutamate transporters in rat lumbar spinal cord, with a note on dorsal root ganglia. Journal of Comparative Neurology 468:380-394.

Lang PM, Burgstahler R, Sippel W, Irnich D, Schlotter-Weigel B, Grafe P (2003) Characterization of neuronal nicotinic acetylcholine receptors in the membrane of unmyelinated human C-fiber axons by in vitro studies. Journal of Neurophysiology 90:3295-3303.

Larsson M (2017) Pax2 is persistently expressed by GABAergic neurons throughout the adult rat dorsal horn. Neuroscience Letters 638:96-101.

Latremoliere A, Woolf CJ (2009) Central Sensitization: A Generator of Pain Hypersensitivity by Central Neural Plasticity. Journal of Pain 10:895-926.

Lavand'homme P, Pan H, Eisenach J (1998) Intrathecal neostigmine, but not sympathectomy, relieves mechanical allodynia in a rat model of neuropathic pain. Anesthesiology 89:493-499.

Lavand'homme PM, Eisenach JC (1999) Sex differences in cholinergic analgesia II - Differing mechanisms in two models of allodynia. Anesthesiology 91:1455-1461.

Lavertu G, Cote SL, De Koninck Y (2014) Enhancing K-Cl co-transport restores normal spinothalamic sensory coding in a neuropathic pain model. Brain 137:724-738.

Lawson SN, Waddell PJ (1991) Soma neurofilament immunoreactivity is related to cell size and fibre conduction velocity in rat primary sensory neurons. Journal of Physiology-London 435:41-63.

Le Bars D (2002) The whole body receptive field of dorsal horn multireceptive neurones. Brain Research Reviews 40:29-44.

Le Bars D, Dickenson A, Besson J (1979a) Diffuse noxious inhibitory controls (DNIC). I. Effects on dorsal horn convergent neurones in the rat. Pain 6:283-304.

Le Bars D, Dickenson, Besson J (1979b) Diffuse noxious inhibitory controls (DNIC). II. Lack of effect on non-convergent neurones, supraspinal involvement and theoretical implications. Pain 6:305-327.

Le Pichon CE, Chesler AT (2014) The functional and anatomical dissection of somatosensory subpopulations using mouse genetics. Frontiers in Neuroanatomy 8.

LeChasseur Y, Dufour S, Lavertu G, Bories C, Deschenes M, Vallee R, De Koninck Y (2011) A microprobe for parallel optical and electrical recordings from single neurons in vivo. Nature Methods 8:319-U363.

Lee CJ, Labrakakis C, Joseph DJ, MacDermott AB (2004) Functional similarities and differences of AMPA and kainate receptors expressed by cultured rat sensory neurons. Neuroscience 129:35-48.

Leitner J, Westerholz S, Heinke B, Forsthuber L, Wunderbaldinger G, Jager T, Gruber-Schoffnegger D, Braun K, Sandkuhler J (2013) Impaired Excitatory Drive to Spinal Gabaergic Neurons of Neuropathic Mice. Plos One 8.

Lever I, Cunningham J, Grist J, Yip PK, Malcangio M (2003) Release of BDNF and GABA in the dorsal horn of neuropathic rats. European Journal of Neuroscience 18:1169-1174.

Li DP, Chen SR, Pan YZ, Levey AI, Pan HL (2002) Role of presynaptic muscarinic and GABA(B) receptors in spinal glutamate release and cholinergic analgesia in rats. Journal of Physiology-London 543:807-818.

Li LS, Rutlin M, Abraira VE, Cassidy C, Kus L, Gong SC, Jankowski MP, Luo WQ, Heintz N, Koerber HR, Woodbury CJ, Ginty DD (2011) The Functional Organization of Cutaneous Low-Threshold Mechanosensory Neurons. Cell 147:1615-1627.

Light AR, Perl ER (1979) Spinal termination of functionally identified primary afferent neurons with slowly conducting myelinated fibers. Journal of Comparative Neurology 186:133-150.

Light AR, Kavookjian AM (1988) Morphology and ultrastructure of physiologically identified substantia gelatinosa (lamina II) neurons with axons that terminate in deeper dorsal horn laminae (III–V). Journal of Comparative Neurology 267:172-189.

Lima D, Coimbra A (1986) A Golgi study of the neuronal population of the marginal zone (lamina I) of the rat spinal cord. Journal of Comparative Neurology 244:53-71.

Littlewood NK, Todd AJ, Spike RC, Watt C, Shehab SAS (1995) The types of neuron in spinal dorsal horn which possess neurokinin-1 receptors. Neuroscience 66:597-608.

Liu FY, Qu XX, Cai J, Wang FT, Xing GG, Wan Y (2011) Electrophysiological properties of spinal wide dynamic range neurons in neuropathic pain rats following spinal nerve ligation. Neuroscience Bulletin 27:1-8.

Liu Q, Vrontou S, Rice FL, Zylka MJ, Dong XZ, Anderson DJ (2007) Molecular genetic visualization of a rare subset of unmyelinated sensory neurons that may detect gentle touch. Nature Neuroscience 10:946-948.

Llorca-Torralba M, Borges G, Neto F, Mico JA, Berrocoso E (2016) Noradrenergic Locus Coeruleus pathways in pain modulation. Neuroscience 338:93-113.

Lochner M, Thompson AJ (2016) The muscarinic antagonists scopolamine and atropine are competitive antagonists at 5-HT3 receptors. Neuropharmacology 108:220-228.

Loeser JD, Melzack R (1999) Pain: an overview. Lancet 353:1607-1609.

Loewi O (1921) Uber humorale ubertragbarkeit der hirzenwickung. Pflugers Arch 189:239-242.

Lorenzo LE, Magnussen C, Bailey AL, St Louis M, De Koninck Y, Ribeiro-da-Silva A (2014) Spatial and temporal pattern of changes in the number of GAD65-immunoreactive inhibitory terminals in the rat superficial dorsal horn following peripheral nerve injury. Molecular Pain 10.

Lu GW, Willis WD (1999) Branching and/or collateral projections of spinal dorsal horn neurons. Brain Research Reviews 29:50-82.

Lu Y, Perl ER (2003) A specific inhibitory pathway between substantia gelatinosa neurons receiving direct C-fiber input. Journal of Neuroscience 23:8752-8758.

Lu Y, Perl ER (2005) Modular organization of excitatory circuits between neurons of the spinal superficial dorsal horn (laminae I and II). Journal of Neuroscience 25:3900-3907.

Lu Y, Dong HL, Gan YD, Gong YY, Ren YN, Gu N, Zhou SD, Xia N, Sun YY, Ji RR, Xiong LZ (2013) A feed-forward spinal cord glycinergic neural circuit gates mechanical allodynia. Journal of Clinical Investigation 123:4050-4062.

Luccarini P, Sessle BJ, Woda A (2001) Superficial and deep convergent nociceptive neurons are differentially affected by N-methyl-D-aspartate applied on the brainstem surface of the rat medullary dorsal horn. Neuroscience 107:311-316.

Luis-Delgado OE, Barrot M, Rodeau JL, Schott G, Benbouzid M, Poisbeau P, Freund-Mercier MJ, Lasbennes F (2006) Calibrated forceps: A sensitive and reliable tool for pain and analgesia studies. Journal of Pain 7:32-39.

Luo L, Chang L, Brown SM, Ao H, Lee DH, Higuera ES, Dubin AE, Chaplan SR (2007) Role of peripheral hyperpolarization-activated cyclic nucleotide-modulated channel pacemaker channels in acute and chronic pain models in the rat. Neuroscience 144:1477-1485.

Luz LL, Szucs P, Safronov BV (2014) Peripherally driven low-threshold inhibitory inputs to lamina I local-circuit and projection neurones: a new circuit for gating pain responses. Journal of Physiology-London 592:1519-1534.

Luz LL, Szucs P, Pinho R, Safronov BV (2010) Monosynaptic excitatory inputs to spinal lamina I anterolateral-tract-projecting neurons from neighbouring lamina I neurons. Journal of Physiology-London 588:4489-4505.

Mackie M, Hughes DI, Maxwell DJ, Tillakaratne NJK, Todd AJ (2003) Distribution and colocalisation of glutamate decarboxylase isoforms in the rat spinal cord. Neuroscience 119:461-472.

Manns ID, Mainville L, Jones BE (2001) Evidence for glutamate, in addition to acetylcholine and GABA, neurotransmitter synthesis in basal forebrain neurons projecting to the entorhinal cortex. Neuroscience 107:249-263.

Mansikka H, Pertovaara A (1995) The role of α 2 -adrenoceptors of the medullary lateral reticular nucleus in spinal antinociception in rats. Brain Research Bulletin 37:633-638.

Mapplebeck JCS, Beggs S, Salter MW (2016) Sex differences in pain: a tale of two immune cells. Pain 157:S2-S6.

Maricich SM, Morrison KM, Mathes EL, Brewer BM (2012) Rodents Rely on Merkel Cells for Texture Discrimination Tasks. Journal of Neuroscience 32:3296-3300.

Marubio LM, Arroyo-Jimenez MD, Cordero-Erausquin M, Lena C, Le Novere N, d'Exaerde AD, Huchet M, Damaj MI, Changeux JP (1999) Reduced antinociception in mice lacking neuronal nicotinic receptor subunits. Nature 398:805-810.

Massoulie J (2002) The origin of the molecular diversity and functional anchoring of cholinesterases. Neurosignals 11:130-143.

Matsumoto M, Xie WJ, Inoue M, Ueda H (2007) Evidence for the tonic inhibition of spinal pain by nicotinic cholinergic transmission through primary afferents. Mol Pain 3:41.

Maxwell DJ, Fyffe REW, Rethelyi M (1983) Morphological properties of physiologically characterized lamina III neurones in the cat spinal cord. Neuroscience 10:1-22.

Maxwell DJ, Belle MD, Cheunsuang O, Stewart A, Morris R (2007) Morphology of inhibitory and excitatory interneurons in superficial laminae of the rat dorsal horn. Journal of Physiology-London 584:521-533.

McCormick DA (1989) Acetylcholine: distribution, receptors and actions. Semin Neurosci 1:91-101.

McCoy ES, Taylor-Blake B, Street SE, Pribisko AL, Zheng JH, Zylka MJ (2013) Peptidergic CGRP alpha Primary Sensory Neurons Encode Heat and Itch and Tonically Suppress Sensitivity to Cold. Neuron 78:138-151.

Medrano MC, Dhanasobhon D, Yalcin I, Schlichter R, Cordero-Erausquin M (2016) Loss of inhibitory tone on spinal cord dorsal horn spontaneously and nonspontaneously active neurons in a mouse model of neuropathic pain. Pain 157:1432-1442.

Meisner JG, Marsh AD, Marsh DR (2010) Loss of GABAergic Interneurons in Laminae I-III of the Spinal Cord Dorsal Horn Contributes to Reduced GABAergic Tone and Neuropathic Pain after Spinal Cord Injury. Journal of Neurotrauma 27:729-737.

Mendell LM (2014) Constructing and deconstructing the gate theory of pain. Pain 155:210-216.

Merskey H, Bogduk N (1994) Classification of chronic pain: descriptions of chronic pain syndromes and definitions of pain terms. 2nd ed Seattle: International Association for the Study of Pain.

Mesnage B, Gaillard S, Godin AG, Rodeau JL, Hammer M, Von Engelhardt J, Wiseman PW, De Koninck Y, Schlichter R, Cordero-Erausquin M (2011) Morphological and Functional Characterization of Cholinergic Interneurons in the Dorsal Horn of the Mouse Spinal Cord. J Comp Neurol 519:3139-3158.

Michaelevski I, Segal-Ruder Y, Rozenbaum M, Medzihradszky KF, Shalem O, Coppola G, Horn-Saban S, Ben-Yaakov K, Dagan SY, Rishal I, Geschwind DH, Pilpel Y, Burlingame AL, Fainzilber M (2010) Signaling to Transcription Networks in the Neuronal Retrograde Injury Response. Science Signaling 3.

Mika J, Zychowska M, Popiolek-Barczyk K, Rojewska E, Przewlocka B (2013) Importance of glial activation in neuropathic pain. European Journal of Pharmacology 716:106-119.

Millan MJ (1999) The induction of pain: An integrative review. Progress in Neurobiology 57:1-164.

Millan MJ (2002) Descending control of pain. Progress in Neurobiology 66:355-474.

Miranda HF, Sierralta F, Pinardi G (2002) Neostigmine interactions with non steroidal anti-inflammatory drugs. British Journal of Pharmacology 135:1591-1597.

Miraucourt LS, Dallel R, Voisin DL (2007) Glycine Inhibitory Dysfunction Turns Touch into Pain through PKCgamma Interneurons. Plos One 2.

Miraucourt LS, Moisset X, Dallel R, Voisin DL (2009) Glycine Inhibitory Dysfunction Induces a Selectively Dynamic, Morphine-Resistant, and Neurokinin 1 Receptor-Independent Mechanical Allodynia. Journal of Neuroscience 29:2519-2527.

Mishra SK, Tisel SM, Orestes P, Bhangoo SK, Hoon MA (2011) TRPV1-lineage neurons are required for thermal sensation. Embo Journal 30:582-593.

Miwa JM, Freedman R, Lester HA (2011) Neural Systems Governed by Nicotinic Acetylcholine Receptors: Emerging Hypotheses. Neuron 70:20-33.

Modol L, Cobianchi S, Navarro X (2014) Prevention of NKCC1 phosphorylation avoids downregulation of KCC2 in central sensory pathways and reduces neuropathic pain after peripheral nerve injury. Pain 155:1577-1590.

Moore KA, Kohno T, Karchewski LA, Scholz J, Baba H, Woolf CJ (2002) Partial peripheral nerve injury promotes a selective loss of GABAergic inhibition in the superficial dorsal horn of the spinal cord. Journal of Neuroscience 22:6724-6731.

Morgan MM, Fields HL (1994) Pronounced changes in the activity of nociceptive modulatory neurons in the rostral ventromedial medulla in response to prolonged thermal noxious stimuli. Journal of Neurophysiology 72:1161-1170.

Mosconi T, Kruger L (1996) Fixed-diameter polyethylene cuffs applied to the rat sciatic nerve induce a painful neuropathy: Ultrastructural morphometric analysis of axonal alterations. Pain 64:37-57.

Moser N, Mechawar N, Jones I, Gochberg-Sarver A, Orr-Utreger A, Plomann M, Salas R, Molles B, Marubio L, Roth U, Maskos U, Winzer-Serhan U, Bourgeois JP, Le Sourd AM, De Biasi M, Schroder H, Lindstrom J, Maelicke A, Changeux JP, Wevers A (2007) Evaluating the suitability of nicotinic acetylcholine receptor antibodies for standard immunodetection procedures. Journal of Neurochemistry 102:479-492.

Nachmansohn D, Machado A (1943) The formation of acetylcholine. A new enzyme choline acetylase. J Neurophysiol 6:397–403

Naguib M, Yaksh TL (1994) Antinociceptive effects of spinal cholinesterase inhibition and isobolographic analysis of the interaction with mu-receptor and alpha-2-receptor systems. Anesthesiology 80:1338-1348.

Naim M, Spike RC, Watt C, Shehab SAS, Todd AJ (1997) Cells in laminae III and IV of the rat spinal cord that possess the neurokinin-1 receptor and have dorsally directed dendrites receive a major synaptic input from tachykinin-containing primary afferents. Journal of Neuroscience 17:5536-5548.

Nakamura M, Jang IS (2010) Presynaptic nicotinic acetylcholine receptors enhance GABAergic synaptic transmission in rat periaqueductal gray neurons. European Journal of Pharmacology 640:178-184.

Nakatsuka T, Furue H, Yoshimura M, Gu JGG (2002) Activation of central terminal vanilloid receptor-1 receptors and alpha beta-methylene-ATP-sensitive P2X receptors reveals a converged synaptic activity onto the deep dorsal horn neurons of the spinal cord. Journal of Neuroscience 22:1228-1237.

Nakatsuka T, Park JS, Kumamoto E, Tamaki T, Yoshimura M (1999) Plastic changes in sensory inputs to rat substantia gelatinosa neurons following peripheral inflammation. Pain 82:39-47.

Naser P, Kuner R (2017) Molecular, cellular and circuit basis of cholinergic modulation of pain. Neuroscience.

Nassar MA, Levato A, Stirling LC, Wood JN (2005) Neuropathic pain develops normally in mice lacking both Na(v)1.7 and Na(v)1.8. Molecular Pain 1.

Nassar MA, Baker MD, Levato A, Ingram R, Mallucci G, McMahon SB, Wood JN (2006) Nerve injury induces robust allodynia and ectopic discharges in Na(v)1.3 null mutant mice. Molecular Pain 2.

Newton RA, Bingham S, Case PC, Sanger GJ, Lawson SN (2001) Dorsal root ganglion neurons show increased expression of the calcium channel alpha 2 delta-1 subunit following partial sciatic nerve injury. Molecular Brain Research 95:1-8.

Niu JW, Ding L, Li JJ, Kim H, Liu JK, Li HP, Moberly A, Badea TC, Duncan ID, Son YJ, Scherer SS, Luo WQ (2013) Modality-Based Organization of Ascending Somatosensory Axons in the Direct Dorsal Column Pathway. Journal of Neuroscience 33:17691-17709.

Noguchi K, Gel YR, Brunner E, Konietschke F (2012) nparLD: An R Software Package for the Nonparametric Analysis of Longitudinal Data in Factorial Experiments. J Stat Softw 50:1-23.

Oda Y (1999) Choline acetyltransferase: The structure, distribution and pathologic changes in the central nervous system. Pathology International 49:921-937.

Olave MJ, Puri N, Kerr R, Maxwell DJ (2002) Myelinated and unmyelinated primary afferent axons form contacts with cholinergic interneurons in the spinal dorsal horn. Exp Brain Res 145:448-456.

Olson W, Dong P, Fleming M, Luo WQ (2016) The specification and wiring of mammalian cutaneous low-threshold mechanoreceptors. Wiley Interdisciplinary Reviews-Developmental Biology 5:389-404.

Omalley DM, Masland RH (1989) Co-release of acetylcholine and gamma-aminobutyric acid by a retinal neuron. Proceedings of the National Academy of Sciences of the United States of America 86:3414-3418.

Pan HL, Chen SR, Eisenach JC (1999) Intrathecal clonidine alleviates allodynia in neuropathic rats - Interaction with spinal muscarinic and nicotinic receptors. Anesthesiology 90:509-514.

Pan HL, Wu ZZ, Zhou HY, Chen SR, Zhang HM, Li DP (2008) Modulation of pain transmission by G-protein-coupled receptors. Pharmacology & Therapeutics 117:141-161.

Paqueron X, Conklin D, Eisenach JC (2003) Plasticity in action of intrathecal clonidine to mechanical but not thermal nociception after peripheral nerve injury. Anesthesiology 99:199-204.

Paqueron X, Li XH, Bantel C, Tobin JR, Voytko ML, Eisenach JC (2001) An obligatory role for spinal cholinergic neurons in the antiallodynic effects of clonidine after peripheral nerve injury. Anesthesiology 94:1074-1081.

Park JH, Kim SK, Kim HN, Sun B, Koo S, Choi SM, Bae H, Min BI (2009) Spinal cholinergic mechanism of the relieving effects of electroacupuncture on cold and warm allodynia in a rat model of neuropathic pain. Journal of Physiological Sciences 59:291-298.

Pawlowski SA, Gaillard S, Ghorayeb I, Ribeiro-da-Silva A, Schlichter R, Cordero-Erausquin M (2013a) A Novel Population of Cholinergic Neurons in the Macaque Spinal Dorsal Horn of Potential Clinical Relevance for Pain Therapy. Journal of Neuroscience 33:3727-+.

Pawlowski SA, Gaillard S, Ghorayeb I, Ribeiro-da-Silva A, Schlichter R, Cordero-Erausquin M (2013b) A Novel Population of Cholinergic Neurons in the Macaque Spinal Dorsal Horn of Potential Clinical Relevance for Pain Therapy. J Neurosci 33:3727-3737.

Peirs C, Williams SPG, Zhao XY, Walsh CE, Gedeon JY, Cagle NE, Goldring AC, Hioki H, Liu Z, Marell PS, Seal RP (2015) Dorsal Horn Circuits for Persistent Mechanical Pain. Neuron 87:797-812.

Peralta E, Ashkenazi A, Winslow J, Smith D, Ramachandran J, Capon D (1987) Distinct primary structures, ligand-binding properties and tissue-specific expression of four human muscarinic acetylcholine receptors. The EMBO journal 6:3923 - 3929.

Perez-Sanchez J, Lorenzo LE, Lecker I, Zurek AA, Labrakakis C, Bridgwater EM, Orser BA, De Koninck Y, Bonin RP (2017) alpha 5GABA(A) Receptors Mediate Tonic Inhibition in the Spinal Cord Dorsal Horn and Contribute to the Resolution Of Hyperalgesia. Journal of Neuroscience Research 95:1307-1318.

Perl ER (2011) Pain mechanisms: A commentary on concepts and issues. Progress in Neurobiology 94:20-38.

Pertovaara A, Almeida A (2006) Descending Inhibitory Systems: Elsevier.

Petitjean H, Rodeau JL, Schlichter R (2012) Interactions between superficial and deep dorsal horn spinal cord neurons in the processing of nociceptive information. European Journal of Neuroscience 36:3500-3508.

Petitjean H, Pawlowski SA, Fraine SL, Sharif B, Hamad D, Fatima T, Berg J, Brown CM, Jan LY, Ribeiro-da-Silva A, Braz JM, Basbaum AI, Sharif-Naeini R (2015) Dorsal Horn Parvalbumin Neurons Are Gate-Keepers of Touch-Evoked Pain after Nerve Injury. Cell Reports 13:1246-1257.

Petko M, Antal M (2012) Propriospinal pathways in the dorsal horn (laminae I-IV) of the rat lumbar spinal cord. Brain Research Bulletin 89:41-49.

Phillips C (2009) The cost and burden of chronic pain. Reviews in pain 3.

Picciotto MR, Higley MJ, Mineur YS (2012) Acetylcholine as a Neuromodulator: Cholinergic Signaling Shapes Nervous System Function and Behavior. Neuron 76:116-129.

Pieraut S, Laurent-Matha VR, Sar C, Hubert T, Mechaly I, Hilaire C, Mersel M, Delpire E, Valmier J, Scamps F (2007) NKCC1 phosphorylation stimulates neurite growth of injured adult sensory neurons. Journal of Neuroscience 27:6751-6759.

Pillai A, Mansouri A, Behringer R, Westphal H, Goulding M (2007) Lhx1 and Lhx5 maintain the inhibitory-neurotransmitter status of interneurons in the dorsal spinal cord. Development 134:357-366.

Pitcher GM, Ritchie J, Henry JL (1999) Nerve constriction in the rat: model of neuropathic, surgical and central pain. Pain 83:37-46.

Pogorzala LA, Mishra SK, Hoon MA (2013) The Cellular Code for Mammalian Thermosensation. Journal of Neuroscience 33:5533-5541.

Polgar E, Todd AJ (2008) Tactile allodynia can occur in the spared nerve injury model in the rat without selective loss of GABA or GABA(A) receptors from synapses in laminae I-II of the ipsilateral spinal dorsal horn. Neuroscience 156:193-202.

Polgar E, Shehab SAS, Watt C, Todd AJ (1999) GABAergic neurons that contain neuropeptide Y selectively target cells with the neurokinin 1 receptor in laminae III and IV of the rat spinal cord. Journal of Neuroscience 19:2637-2646.

Polgar E, Gray S, Riddell JS, Todd AJ (2004) Lack of evidence for significant neuronal loss in laminae I-III of the spinal dorsal horn of the rat in the chronic constriction injury model. Pain 111:144-150.

Polgar E, Hughes DI, Arham AZ, Todd AJ (2005) Loss of neurons from laminas I-III of the spinal dorsal horn is not required for development of tactile allodynia in the spared nerve injury model of neuropathic pain. The Journal of Neuroscience 25:6658-6666.

Polgar E, Durrieux C, Hughes DI, Todd AJ (2013a) A Quantitative Study of Inhibitory Interneurons in Laminae I-III of the Mouse Spinal Dorsal Horn. Plos One 8.

Polgar E, Hughes DI, Riddell JS, Maxwell DJ, Puskar Z, Todd AJ (2003) Selective loss of spinal GABAergic or glycinergic neurons is not necessary for development of thermal hyperalgesia in the chronic constriction injury model of neuropathic pain. Pain 104:229-239.

Polgar E, Sardella TCP, Tiong SYX, Locke S, Watanabe M, Todd AJ (2013b) Functional differences between neurochemically defined populations of inhibitory interneurons in the rat spinal dorsal horn. Pain 154:2606-2615.

Potrebic SB, Mason P, Fields HL (1995) The density and distribution of serotonergic appositions onto identified neurons in the rat rostral ventromedial medulla. Journal of Neuroscience 15:3273-3283.

Prescott SA, De Koninck Y (2002) Four cell types with distinctive membrane properties and morphologies in lamina I of the spinal dorsal horn of the adult rat. Journal of Physiology-London 539:817-836.

Price DD, Greenspan JD, Dubner R (2003) Neurons involved in the exteroceptive function of pain. Pain 106:215-219.

Price GW, Kelly JS, Bowery NG (1987) The location of GABA B receptor binding sites in mammalian spinal cord. Synapse 1:530-538.

Randall L, Selitto J (1957) A method for measurement of analgesic activity on inflamed tissue. Archives internationales de pharmacodynamie et de thérapie 11:409 - 419

Rashid MH, Ueda H (2002) Neuropathy-specitic analgesic action of intrathecal nicotinic agonists and its spinal GABA-mediated mechanism. Brain Res 953:53-62.

Rashid MH, Furue H, Yoshimura M, Ueda H (2006) Tonic inhibitory role of alpha 4 beta 2 subtype of nicotinic acetylcholine receptors on nociceptive transmission in the spinal cord in mice. Pain 125:125-135.

Rau KK, Johnson RD, Cooper BY (2005) Nicotinic AChR in subclassified capsaicin-sensitive and -insensitive Nociceptors of the rat DRG. Journal of Neurophysiology 93:1358-1371.

Ren J, Qin C, Hu F, Tan J, Qiu L, Zhao SL, Feng GP, Luo MM (2011) Habenula "Cholinergic" Neurons Corelease Glutamate and Acetylcholine and Activate Postsynaptic Neurons via Distinct Transmission Modes. Neuron 69:445-452.

Ribeiro-da-Silva A, Cuello AC (1990) Choline acetyltransferase-immunoreactive profiles are presynaptic to primary sensory fibers in the rat superficial dorsal horn. J Comp Neurol 295:370-384.

Ribeiro-da-Silva A, De Koninck Y (2008) Morphological and Neurochemical Organization of the Spinal Dorsal Horn.

Ritz LA, Greenspan JD (1985) Morphological features of lamina V neurons receiving nociceptive input in cat sacrocaudal spinal cord. Journal of Comparative Neurology 238:440-452.

Rueter LE, Meyer MD, Decker MW (2000) Spinal mechanisms underlying A-85380-induced effects on acute thermal pain. Brain Res 872:93-101.

Sacerdote P, Franchi S, Trovato AE, Valsecchi AE, Panerai AE, Colleoni M (2008) Transient early expression of TNF-alpha in sciatic nerve and dorsal root ganglia in a mouse model of painful peripheral neuropathy. Neuroscience Letters 436:210-213.

Saegusa H, Kurihara T, Zong S, Kazuno A, Matsuda Y, Nonaka T, Han W, Toriyama H, Tanabe T (2001) Suppression of inflammatory and neuropathic pain symptoms in mice lacking the N-type Ca2+ channel. Embo Journal 20:2349-2356.

Sandkuhler J, Stelzer B, Fu QG (1993) Characteristics of propriospinal modulation of nociceptive lumbar spinal dorsal horn neurons in the cat. Neuroscience 54:957-967.

Santos SFA, Rebelo S, Derkach VA, Safronov BV (2007) Excitatory interneurons dominate sensory processing in the spinal substantia gelatinosa of rat. Journal of Physiology-London 581:241-254.

Santos SFA, Luz LL, Szucs P, Lima D, Derkach VA, Safronov BV (2009) Transmission Efficacy and Plasticity in Glutamatergic Synapses Formed by Excitatory Interneurons of the Substantia Gelatinosa in the Rat Spinal Cord. Plos One 4.

Sarter M, Parikh V, Howe WM (2009) Phasic acetylcholine release and the volume transmission hypothesis: time to move on. Nature Reviews Neuroscience 10:383-U386.

Satoh O, Omote K (1996) Roles of monoaminergic, glycinergic and GABAergic inhibitory systems in the spinal cord in rats with peripheral mononeuropathy. Brain Research 728:27-36.

Schmalhofer WA, Calhoun J, Burrows R, Bailey T, Kohler MG, Weinglass AB, Kaczorowski GJ, Garcia ML, Koltzenburg M, Priest BT (2008) ProTx-II, a Selective Inhibitor of Na(v)1.7 Sodium Channels, Blocks Action Potential Propagation in Nociceptors. Molecular Pharmacology 74:1476-1484.

Schneider SP (1992) Functional properties and axon terminations of interneurons in laminae III-V of the mammalian spinal dorsal horn in vitro. Journal of Neurophysiology 68:1746-1759.

Schneider SP (2003) Spike frequency adaptation and signaling properties of identified neurons in rodent deep spinal dorsal horn. Journal of Neurophysiology 90:245-258.

Schneider SP (2008) Local circuit connections between hamster laminae III and IV dorsal horn neurons. Journal of Neurophysiology 99:1306-1318.

Schneider SP, Lopez M (2002) Immunocytochemical localization of glutamic acid decarboxylase in physiologically identified interneurons of hamster spinal laminae III-V. Neuroscience 115:627-636.

Schneider SP, Walker TM (2007) Morphology and electrophysiological properties of hamster spinal dorsal horn neurons that express VGLUT2 and enkephalin. Journal of Comparative Neurology 501:790-809.

Schoffnegger D, Ruscheweyh R, Sandkuhler J (2008) Spread of excitation across modality borders in spinal dorsal horn of neuropathic rats. Pain 135:300-310.

Schoffnegger D, Heinke B, Sommer C, Sandkuhler J (2006) Physiological properties of spinal lamina II GABAergic neurons in mice following peripheral nerve injury. Journal of Physiology-London 577:869-878.

Scholz J, Woolf CJ (2002) Can we conquer pain? Nat Neurosci 5:1062-1067.

Scholz J, Broom DC, Youn DH, Mills CD, Kohno T, Suter MR, Moore KA, Decosterd I, Coggeshall RE, Woolf CJ (2005) Blocking caspase activity prevents transsynaptic neuronal apoptosis and the loss of inhibition in lamina II of the dorsal horn after peripheral nerve injury. Journal of Neuroscience 25:7317-7323.

Seal RP, Wang XD, Guan Y, Raja SN, Woodbury CJ, Basbaum AI, Edwards RH (2009) Injury-induced mechanical hypersensitivity requires C-low threshold mechanoreceptors. Nature 462:651-655.

Seguela P, Wadiche J, Dineleymiller K, Dani JA, Patrick JW (1993) Molecular cloning, functional properties, and distribution of rat brain alpha 7: a nicotinic cation channel highly permeable to calcium. Journal of Neuroscience 13:596-604.

Seibt F, Schlichter R (2015) Noradrenaline-mediated facilitation of inhibitory synaptic transmission in the dorsal horn of the rat spinal cord involves interlaminar communications. European Journal of Neuroscience 42:2654-2665.

Seijffers R, Allchorne AJ, Woolf CJ (2006) The transcription factor ATF-3 promotes neurite outgrowth. Molecular and Cellular Neuroscience 32:143-154.

Semba K, Masarachia P, Malamed S, Jacquin M, Harris S, Egger MD (1984) Ultrastructure of Pacinian corpuscle primary afferent terminals in the cat spinal cord. Brain Research 302:135-150.

Shehab SAS, Spike RC, Todd AJ (2003) Evidence against cholera toxin B subunit as a reliable tracer for sprouting of primary afferents following peripheral nerve injury. Brain Research 964:218-227.

Shelukhina IV, Kryukova EV, Lips KS, Tsetlin VI, Kummer W (2009) Presence of alpha 7 nicotinic acetylcholine receptors on dorsal root ganglion neurons proved using knockout mice and selective alpha-neurotoxins in histochemistry. Journal of Neurochemistry 109:1087-1095.

Sherriff FE, Henderson Z, Morrison JFB (1991) Further evidence for the absence of a descending cholinergic projection from the brain-stem to the spinal-cord in the rat. Neurosci Lett 128:52-56.

Shields SD, Eckert WA, Basbaum AI (2003) Spared nerve injury model of neuropathic pain in the mouse: A behavioral and anatomic analysis. Journal of Pain 4:465-470.

Shortland P, Woolf CJ (1993) Morphology and somatotopy of the central arborizations of rapidly adapting glabrous skin afferents in the rat lumbar spinal cord. Journal of Comparative Neurology 329:491-511.

Shreckengost J, Calvo J, Quevedo J, Hochman S (2010) Bicuculline-Sensitive Primary Afferent Depolarization Remains after Greatly Restricting Synaptic Transmission in the Mammalian Spinal Cord. Journal of Neuroscience 30:5283-5288.

Singer E, Placheta P (1980) Reduction of [ 3 H]muscimol binding sites in rat dorsal spinal cord after neonatal capsaicin treatment. Brain Research 202:484-487.

Smith NJ, Hone AJ, Memon T, Bossi S, Smith TE, McIntosh JM, Olivera BM, Teichert RW (2013) Comparative functional expression of nAChR subtypes in rodent DRG neurons. Frontiers in Cellular Neuroscience 7.

Spike RC, Watt C, Zafra F, Todd AJ (1997) An ultrastructural study of the glycine transporter GLYT2 and its association with glycine in the superficial laminae of the rat spinal dorsal horn. Neuroscience 77:543-551.

Staley KJ, Mody I (1991) Integrity of perforant path fibers and the frequency of action potential independent excitatory and inhibitory synaptic events in dentate gyrus granule cells. Synapse 9:219-224.

Stornetta RL, Macon CJ, Nguyen TM, Coates MB, Guyenet PG (2013) Cholinergic neurons in the mouse rostral ventrolateral medulla target sensory afferent areas. Brain Structure & Function 218:455-475.

Story GM, Peier AM, Reeve AJ, Eid SR, Mosbacher J, Hricik TR, Earley TJ, Hergarden AC, Andersson DA, Hwang SW, McIntyre P, Jegla T, Bevan S, Patapoutian A (2003) ANKTM1, a TRP-like channel expressed in nociceptive neurons, is activated by cold temperatures. Cell 112:819-829.

Suzuki R, Rygh LJ, Dickenson AH (2004a) Bad news from the brain: descending 5-HT pathways that control spinal pain processing. Trends in Pharmacological Sciences 25:613-617.

Suzuki R, Rahman W, Hunt SP, Dickenson AH (2004b) Descending facilitatory control of mechanically evoked responses is enhanced in deep dorsal horn neurones following peripheral nerve injury. Brain Research 1019:68-76.

Suzuki R, Rahman W, Rygh LJ, Webber M, Hunt SP, Dickenson AH (2005) Spinal-supraspinal serotonergic circuits regulating neuropathic pain and its treatment with gabapentin. Pain 117:292-303.

Szucs P, Luz LL, Pinho R, Aguiar P, Antal Z, Tiong SYX, Todd AJ, Safronov BV (2013) Axon diversity of lamina I local-circuit neurons in the lumbar spinal cord. Journal of Comparative Neurology 521:2719-2741.

Tadros MA, Harris BM, Anderson WB, Brichta AM, Graham BA, Callister RJ (2012) Are all spinal segments equal: intrinsic membrane properties of superficial dorsal horn neurons in the developing and mature mouse spinal cord. Journal of Physiology-London 590:2409-2425.

Takeda D, Nakatsuka T, Papke R, Gu JG (2003) Modulation of inhibitory synaptic activity by a non-alpha 4 beta 2, non-alpha 7 subtype of nicotinic receptors in the substantia gelatinosa of adult rat spinal cord. Pain 101:13-23.

Takeda D, Nakatsuka T, Gu JG, Yoshida M (2007) The activation of nicotinic acetylcholine receptors enhances the inhibitory synaptic transmission in the deep dorsal horn neurons of the adult rat spinal cord. Molecular Pain 3.

Tamamaki N, Yanagawa Y, Tomioka R, Miyazaki JI, Obata K, Kaneko T (2003) Green fluorescent protein expression and colocalization with calretinin, parvalbumin, and somatostatin in the GAD67-GFP knock-in mouse. Journal of Comparative Neurology 467:60-79.

Tan AM, Chang YW, Zhao P, Hains BC, Waxman SG (2011) Rac1-regulated dendritic spine remodeling contributes to neuropathic pain after peripheral nerve injury. Experimental Neurology 232:222-233.

Tesfaye S, Selvarajah D (2012) Advances in the epidemiology, pathogenesis and management of diabetic peripheral neuropathy. Diabetes-Metabolism Research and Reviews 28:8-14.

Thacker MA, Clark AK, Bishop T, Grist J, Yip PK, Moon LDF, Thompson SWN, Marchand F, McMahon SB (2009) CCL2 is a key mediator of microglia activation in neuropathic pain states. European Journal of Pain 13:263-272.

Todd AJ (1991) Immunohistochemical evidence that acetylcholine and glycine exist in different populations of GABAergic neurons in lamina III of rat spinal dorsal horn. Neuroscience 44:741-746.

Todd AJ (2010) Neuronal circuitry for pain processing in the dorsal horn. Nat Rev Neurosci 11:823-836.

Todd AJ, Sullivan AC (1990) Light microscope study of the coexistence of GABA-like and glycine-like immunoreactivities in the spinal cord of the rat. Journal of Comparative Neurology 296:496-505.

Todd AJ, Spike RC, Chong D, Neilson M (1995) The relationship between glycine and gephyrin in synapses of the rat spinal cord. European Journal of Neuroscience 7:1-11.

Todd AJ, Watt C, Spike RC, Sieghart W (1996) Colocalization of GABA, glycine, and their receptors at synapses in the rat spinal cord. Journal of Neuroscience 16:974-982.

Todd AJ, Hughes DI, Polgar E, Nagy GG, Mackie M, Ottersen OP, Maxwell DJ (2003) The expression of vesicular glutamate transporters VGLUT1 and VGLUT2 in neurochemically defined axonal populations in the rat spinal cord with emphasis on the dorsal horn. European Journal of Neuroscience 17:13-27.

Tolle TR, Berthele A, Zieglgansberger W, Seeburg PH, Wisden W (1993) The differential expression of 16 NMDA and non-NMDA receptor subunits in the rat spinal cord and in periaqueductal gray. Journal of Neuroscience 13:5009-5028.

Torsney C, MacDermott AB (2006) Disinhibition opens the gate to pathological pain signaling in superficial neurokinin 1 receptor-expressing neurons in rat spinal cord. Journal of Neuroscience 26:1833-1843.

Tripathi A, Srivastava U (2010) Acetylcholinesterase: a versatile enzyme of nervous system. Annals of Neurosciences 15.

Truini A, Garcia-Larrea L, Cruccu G (2013) Reappraising neuropathic pain in humans-how symptoms help disclose mechanisms. Nature Reviews Neurology 9:572-582.

Tsuda M, Shigemoto-Mogami Y, Koizumi S, Mizokoshi A, Kohsaka S, Salter MW, Inoue K (2003) P2X4 receptors induced in spinal microglia gate tactile allodynia after nerve injury. Nature 424:778-783

Tsujino H, Kondo E, Fukuoka T, Dai Y, Tokunaga A, Miki K, Yonenobu K, Ochi T, Noguchi K (2000) Activating transcription factor 3 (ATF3) induction by axotomy in sensory and

motoneurons: A novel neuronal marker of nerve injury. Molecular and Cellular Neuroscience 15:170-182.

Umana I, Daniele C, Miller B, Gallagher K, Brown M, Abbur i C, Mason P, McGehee D (2017) Nicotinic Modulation of Descending Pain Control Circuitry. Pain 158:1938 - 1950.

Urban MO, Gebhart GF (1999) Supraspinal contributions to hyperalgesia. Proceedings of the National Academy of Sciences of the United States of America 96:7687-7692.

Vera-Portocarrero LP, Zhang ET, Ossipov MH, Xie JY, King T, Lai J, Porreca F (2006) Descending facilitation from the rostral ventromedial medulla maintains nerve injury-induced central sensitization. Neuroscience 140:1311-1320.

Villanueva L, Lopez-Avila A, Monconduit L (2006) Ascending nociceptive pathways: Elsevier B.V.

Vincler MA, Eisenach JC (2005) Knock down of the alpha 5 nicotinic acetylcholine receptor in spinal nerve-ligated rats alleviates mechanical allodynia. Pharmacology Biochemistry and Behavior 80:135-143.

von Engelhardt J, Eliava M, Meyer AH, Rozov A, Monyer H (2007) Functional characterization of intrinsic cholinergic interneurons in the cortex. J Neurosci 27:5633-5642.

Vrontou S, Wong AM, Rau KK, Koerber HR, Anderson DJ (2013) Genetic identification of C fibres that detect massage-like stroking of hairy skin in vivo. Nature 493:669-+.

Wada E, McKinnon D, Heinemann S, Patrick J, Swanson L (1990) The distribution of mRNA encoded by a new member of the neuronal nicotinic acetylcholine receptor gene family (alpha 5) in the rat central nervous system. Brain research 526:45-53.

Wada E, Wada K, Boulter J, Deneris E, Heinemann S, Patrick J, Swanson L (1989) Distribution of alpha 2, alpha 3, alpha 4, and beta 2 neuronal nicotinic receptor subunit mRNAs in the central nervous system: a hybridization histochemical study in the rat. The Journal of comparative neurology 284:314-335.

Wall P, Waxman S, Basbaum A (1974) Ongoing activity in peripheral nerve: injury discharge. Experimental neurology 45:576-589.

Wang XL, Zhang HM, Li DP, Chen SR, Pan HL (2006) Dynamic regulation of glycinergic input to spinal dorsal horn neurones by muscarinic receptor subtypes in rats. Journal of Physiology-London 571:403-413.

Wei B, Kumada T, Furukawa T, Inoue K, Watanabe M, Sato K, Fukuda A (2013) Pre- and post-synaptic switches of GABA actions associated with Cl- homeostatic changes are induced in the spinal nucleus of the trigeminal nerve in a rat model of trigeminal neuropathic pain. Neuroscience 228:334-348.

Wei J, Walton EA, Milici A, Buccafusco JJ (1994) m1-m5 muscarinic receptor distribution in rat CNS by RT-PCR and HPLC. Journal of Neurochemistry 63:815-821.

Wieskopf JS et al. (2015) The nicotinic alpha 6 subunit gene determines variability in chronic pain sensitivity via cross-inhibition of P2X2/3 receptors. Science Translational Medicine 7.

Williams ACD, Craig KD (2016) Updating the definition of pain. Pain 157:2420-2423.

Willis W, Coggeshall R (1978) Sensory Mechanisms of the Spinal Cord: Springer Science & Business Media.

Wilson JM, Rempel J, Brownstone RM (2004) Postnatal development of cholinergic synapses on mouse spinal motoneurons. Journal of Comparative Neurology 474:13-23.

Winkler CW, Hermes SM, Chavkin CI, Drake CT, Morrison SF, Aicher SA (2006) Kappa opioid receptor (KOR) and GAD67 immunoreactivity are found in OFF and NEUTRAL cells in the rostral ventromedial medulla. Journal of Neurophysiology 96:3465-3473.

Witten IB, Lin S-C, Brodsky M, Prakash R, Diester I, Anikeeva P, Gradinaru V, Ramakrishnan C, Deisseroth K (2010) Cholinergic Interneurons Control Local Circuit Activity and Cocaine Conditioning. Science 330:1677-1681.

Wolff M, Heugel P, Hempelmann G, Scholz A, Muhling J, Olschewski A (2007) Clonidine reduces the excitability of spinal dorsal horn neurones. British Journal of Anaesthesia 98:353-361.

Woodbury CJ, Ritter AM, Koerber HR (2001) Central anatomy of individual rapidly adapting low-threshold mechanoreceptors innervating the "hairy" skin of newborn mice: Early maturation of hair follicle afferents. Journal of Comparative Neurology 436:304-323.

Woodbury CJ, Kullmann FA, McIlwrath SL, Koerber HR (2008) Identity of myelinated cutaneous sensory neurons projecting to nocireceptive laminae following nerve injury in adult mice. Journal of Comparative Neurology 508:500-509.

Woolf CJ (1983) Evidence for a central component of post-injury pain hypersensitivity. Nature 306:686-688.

Woolf CJ, Salter MW (2000) Neuroscience - Neuronal plasticity: Increasing the gain in pain. Science 288:1765-1768.

Woolf CJ, Ma QF (2007) Nociceptors-noxious stimulus detectors. Neuron 55:353-364.

Woolf CJ, Shortland P, Coggeshall RE (1992) Peripheral nerve injury triggers central sprouting of myelinated afferents. Nature 355:75-78.

Woolf NJ (1991) Cholinergic systems in mammalian brain and spinal cord. Progress in Neurobiology 37:475-524.

Wrigley PJ, Jeong HJ, Vaughan CW (2009) Primary afferents with TRPM8 and TRPA1 profiles target distinct subpopulations of rat superficial dorsal horn neurones. British Journal of Pharmacology 157:371-380.

Wu G, Ringkamp M, Murinson BB, Pogatzki EM, Hartke TV, Weerahandi HM, Campbell JN, Griffin JW, Meyer RA (2002) Degeneration of myelinated efferent fibers induces spontaneous activity in uninjured C-fiber afferents. Journal of Neuroscience 22:7746-7753.

Wu J, Lukas RJ (2011) Naturally-expressed nicotinic acetylcholine receptor subtypes. Biochemical Pharmacology 82:800-807.

Xie WR, Strong JA, Li HQ, Zhang JM (2007) Sympathetic sprouting near sensory neurons after nerve injury occurs preferentially on spontaneously active cells and is reduced by early nerve block. Journal of Neurophysiology 97:492-502.

Xu QH, Yaksh TL (2011) A brief comparison of the pathophysiology of inflammatory versus neuropathic pain. Current Opinion in Anesthesiology 24:400-407.

Yalcin I, Megat S, Barthas F, Waltisperger E, Kremer M, Salvat E, Barrot M (2014) The Sciatic Nerve Cuffing Model of Neuropathic Pain in Mice. Jove-Journal of Visualized Experiments.

Yalcin I, Charlet A, Cordero-Erausquin M, Tessier LH, Picciotto MR, Schlichter R, Poisbeau P, Freund-Mercier MJ, Barrot M (2011) Nociceptive thresholds are controlled through spinal beta(2)-subunit-containing nicotinic acetylcholine receptors. Pain 152:2131-2137.

Yasaka T, Tiong SYX, Hughes DI, Riddell JS, Todd AJ (2010) Populations of inhibitory and excitatory interneurons in lamina II of the adult rat spinal dorsal horn revealed by a combined electrophysiological and anatomical approach. Pain 151:475-488.

Yasaka T, Tiong SYX, Polgar E, Watanabe M, Kumamoto E, Riddell JS, Todd AJ (2014) A putative relay circuit providing low-threshold mechanoreceptive input to lamina I projection neurons via vertical cells in lamina II of the rat dorsal horn. Molecular Pain 10.

Yasaka T, Kato G, Furue H, Rashid MH, Sonohata M, Tamae A, Murata Y, Masuko S, Yoshimura M (2007) Cell-type-specific excitatory and inhibitory circuits involving primary afferents in the substantia gelatinosa of the rat spinal dorsal horn in vitro. Journal of Physiology-London 581:603-618.

Yoon MH, Choi JI, Jeong SW (2003) Antinociception of intrathecal cholinesterase inhibitors and cholinergic receptors in rats. Acta Anaesthesiol Scand 47:1079-1084.

Yoon SY, Kwon YB, Kim HW, Roh DH, Kang SY, Kim CY, Han HJ, Kim KW, Yang IS, Beitz AJ, Lee JH (2005) Intrathecal neostigmine reduces the zymosan-induced inflammatory response in a mouse air pouch model via adrenomedullary activity: Involvement of spinal muscarinic type 2 receptors. Neuropharmacology 49:275-282.

Young T, Wittenauer S, Parker R, Vincler M (2008a) Peripheral nerve injury alters spinal nicotinic acetylcholine receptor pharmacology. European Journal of Pharmacology 590:163-169.

Young T, Wittenauer S, McIntosh JM, Vincler M (2008b) Spinal alpha 3 beta 2* nicotinic acetylcholine receptors tonically inhibit the transmission of nociceptive mechanical stimuli. Brain Research 1229:118-124.

Yu XH, Da Silva AR, De Koninck Y (2005) Morphology and neurokinin 1 receptor expression of spinothalamic lamina I neurons in the rat spinal cord. Journal of Comparative Neurology 491:56-68.

Zeilhofer HU, Wildner H, Yevenes GE (2012) Fast synaptic inhibition in spinal sensory processing and pain control. Physiological Reviews 92:193-235.

Zeilhofer HU, Studler B, Arabadzisz D, Schweizer C, Ahmadi S, Layh B, Bosl MR, Fritschy JM (2005) Glycinergic neurons expressing enhanced green fluorescent protein in bacterial artificial chromosome transgenic mice. Journal of Comparative Neurology 482:123-141.

Zhang ET, Craig AD (1997) Morphology and distribution of spinothalamic lamina I neurons in the monkey. Journal of Neuroscience 17:3274-3284.

Zhang HM, Chen SR, Pan HL (2007a) Regulation of glutamate release from primary afferents and interneurons in the spinal cord by muscarinic receptor subtypes. Journal of Neurophysiology 97:102-109.

Zhang HM, Li DP, Chen SR, Pan HL (2005) M-2, M-3, and M-4 receptor subtypes contribute to muscarinic potentiation of GABAergic inputs to spinal dorsal horn neurons. Journal of Pharmacology and Experimental Therapeutics 313:697-704.

Zhang HM, Chen SR, Matsui M, Gautam D, Wess J, Pan HL (2006) Opposing functions of spinal M-2, M-3, and M-4 receptor subtypes in regulation of GABAergic inputs to dorsal horn neurons revealed by muscarinic receptor knockout mice. Molecular Pharmacology 69:1048-1055.

Zhang HM, Zhou HY, Chen SR, Gautam D, Wess J, Pan HL (2007b) Control of Glycinergic input to spinal dorsal horn neurons by distinct muscarinic receptor subtypes revealed using knockout mice. Journal of Pharmacology and Experimental Therapeutics 323:963-971.

Zhang J, De Koninck Y (2006) Spatial and temporal relationship between monocyte chemoattractant protein-1 expression and spinal glial activation following peripheral nerve injury. Journal of Neurochemistry 97:772-783.

Zhu Z, Bowman HR, Baghdoyan HA, Lydic R (2008) Morphine Increases Acetylcholine Release in the Trigeminal Nuclear Complex. Sleep 31:1629-1637.

Zhuo M, Gebhart GF (1991) Tonic cholinergic inhibition of spinal mechanical transmission. Pain 46:211-222.

Zrouri H, Le Goascogne C, Li WW, Pierre M, Courtin F (2004) The role of MAP kinases in rapid gene induction after lesioning of the rat sciatic nerve. European Journal of Neuroscience 20:1811-1818.

Zwart R, Vijverberg HPM (1997) Potentiation and inhibition of neuronal nicotinic receptors by atropine: Competitive and noncompetitive effects. Mol Pharmacol 52:886-895.

Zylka MJ, Rice FL, Anderson DJ (2005) Topographically distinct epidermal nociceptive circuits revealed by axonal tracers targeted to Mrgprd. Neuron 45:17-25.

Appendix A: Loss of inhibitory tone on spinal cord dorsal horn spontaneously and non-spontaneously active neurons in a mouse model of neuropathic pain

# PAIN®

# Loss of inhibitory tone on spinal cord dorsal horn spontaneously and nonspontaneously active neurons in a mouse model of neuropathic pain

Maria Carmen Medrano[a], Dhanasak Dhanasobhon[a,b], Ipek Yalcin[a], Rémy Schlichter[a,b], Matilde Cordero-Erausquin[a,c,*]

**Abstract**

Plasticity of inhibitory transmission in the spinal dorsal horn (SDH) is believed to be a key mechanism responsible for pain hypersensitivity in neuropathic pain syndromes. We evaluated this plasticity by recording responses to mechanical stimuli in silent neurons (nonspontaneously active [NSA]) and neurons showing ongoing activity (spontaneously active [SA]) in the SDH of control and nerve-injured mice (cuff model). The SA and NSA neurons represented 59% and 41% of recorded neurons, respectively, and were predominantly wide dynamic range (WDR) in naive mice. Nerve-injured mice displayed a marked decrease in the mechanical threshold of the injured paw. After nerve injury, the proportion of SA neurons was increased to 78%, which suggests that some NSA neurons became SA. In addition, the response to touch (but not pinch) was dramatically increased in SA neurons, and high-threshold (nociceptive specific) neurons were no longer observed. Pharmacological blockade of spinal inhibition with a mixture of GABA$_A$ and glycine receptor antagonists significantly increased responses to innocuous mechanical stimuli in SA and NSA neurons from sham animals, but had no effect in sciatic nerve-injured animals, revealing a dramatic loss of spinal inhibitory tone in this situation. Moreover, in nerve-injured mice, local spinal administration of acetazolamide, a carbonic anhydrase inhibitor, restored responses to touch similar to those observed in naive or sham mice. These results suggest that a shift in the reversal potential for anions is an important component of the abnormal mechanical responses and of the loss of inhibitory tone recorded in a model of nerve injury-induced neuropathic pain.

**Keywords:** Dorsal horn, Electrophysiology, Spinal cord, Mice, Mechanical stimuli, Spike, Spontaneous activity, Disinhibition, Neuropathic pain

## 1. Introduction

Chronic pain continues to be the most common cause of disability that impairs quality of life, accruing enormous socio-economic costs. In particular, neuropathic pain, caused by a lesion or disease of the somatosensory nervous system, lacks optimal treatment, often leading to unsatisfactory pain management. This may be due to incomplete understanding of the neuronal circuits involved in nociceptive processing and their plasticity in pain conditions.[41]

Spinal dorsal horn (SDH) neurons integrate sensory, nociceptive or innocuous, information, and relay it to the brain through projection neurons.[39–41] Plasticity of the inhibitory transmission in the SDH is believed to be a key mechanism responsible for the hypersensitivity occurring during neuropathy.[27,28,31,41,43] In rats,

a reduction of GABA release and a decrease in the expression of GABA-synthesizing enzymes has been observed in different models of nerve injury.[19,21] A change in chloride homeostasis leading to disinhibition of SDH neurons has also been extensively characterized in neuropathic rats.[9,10,27] Because GABA$_A$ and glycine receptors are permeable to both chloride and bicarbonate (usually in opposite directions), it has been suggested that reducing the bicarbonate depolarizing driving force could mitigate the disinhibition due to a collapse in chloride gradient.[1,2,17] However in vivo recordings performed in rats have provided controversial data concerning the plasticity of inhibitory transmission in neuropathic models, arguing for either a decrease or an increase of GABAergic tone.[7,15] Both studies have focused on SDH neurons responding to natural peripheral stimulations but showing no spontaneous ongoing activity between stimuli (nonspontaneously active [NSA] neurons). However, some SDH neurons display considerable ongoing activity in the absence of experimentally applied stimuli (SA neurons).[32,36,37] Interestingly, an increased level of spontaneous activity has been reported in animal models of neuropathic pain.[12,14,16,38] This implies that some NSA neurons may become SA after neuropathy, blurring the borders between NSA and SA populations, and biasing studies focusing on only one of these populations.

In this study, we systematically analyzed both SA and NSA neurons to provide an exhaustive characterization of the neurons involved in sensory processing of mechanical information and their plasticity after nerve injury in mice. With this approach, we

aimed at assessing whether an inhibitory tone can be detected in the mouse SDH, and whether this tone undergoes plasticity in a model of neuropathy. To evaluate whether this plasticity is related to reduced activation of GABA$_A$ and/or glycine receptors, or from altered reversal potential of the ions flowing through these receptors, we tested the consequences of manipulating bicarbonate homeostasis in the SDH.[17] We used the sciatic nerve cuffing model that has been broadly used to decipher the neurobiological mechanisms leading to neuropathic pain in rats,[14,16,25] and has more recently been adapted to the adapted to the mouse (or) adapted to mice.[45] We provide the first electrophysiological characterization of this mouse model and the first evaluation of disinhibition in the mouse SDH after neuropathy.

## 2. Materials and methods

### 2.1. Animals

A total of 96 male CD1 mice, aged 6 to 8 weeks were used for this study. They were housed 4 or 5 per cage in a facility maintained at constant temperature (23°C) with a 12-hour light–dark cycle and food and water ad libitum. The animal facilities are legally registered for animal experimentation under Animal House Agreement A67-2018-38, and scientists in charge of the experiments possess the certificate authorizing experimentation on living animals, delivered by the governmental veterinary office. All procedures were performed in accordance with the local animal care and use committee as well as with European Communities Council Directive 86/609/EEC.

### 2.2. Peripheral nerve injury and behavioral testing

The peripheral nerve injury was induced by cuffing the main branch of the right sciatic nerve.[3] Surgeries were performed under ketamine (17 mg/mL)/xylazine (2.5 mg/mL) anesthesia (intraperitoneally [i.p.], 4 mL/kg) (Centravet, Taden, France). The common branch of the right sciatic nerve was exposed and a 2-mm section of split PE-20 polyethylene tubing (Harvard Apparatus, Les Ulis, France) was placed around it (cuff group). The shaved skin was closed using suture. Sham-operated mice underwent the same surgical procedure without implantation of the cuff (sham group). Sham and cuff animals were allowed to recover for at least 1 week after surgery. After this, mechanical allodynia was tested using von Frey filaments (Bioseb, Vitrolles, France), which were applied to the plantar surface of each hind paw (ipsilateral and contralateral to the cuff) until a slight bent was observed, in a series of ascending forces up to the mechanical threshold. Each filament was tested 5 times per paw, and the threshold was defined as the lower one of 2 consecutive filaments for which 3 or more withdrawals out of the 5 trials were observed.[5]

### 2.3. In vivo electrophysiology

#### 2.3.1. Animal preparation

Animals were anesthetized with urethane (2.5 g/kg, i.p.), and the trachea was cannulated. Laminectomy was performed on naive, sham, and cuff animals to expose L3 to L5 segments of the spinal cord. Rectal temperature was continuously monitored, and the animal was maintained at 35.5°C using a heating pad (TC-1000; Bioseb). The mouse was placed in a stereotaxic and spinal frame with 2 clamps fixed on its vertebra to immobilize the spinal cord. Around the exposed lumbar spinal cord, a small chamber (approximately 0.1 mL) was created with 2% agar. After removal of the dura, the spinal cord was covered with saline (NaCl 0.9%).

#### 2.3.2. Single-unit extracellular recordings

Single-unit extracellular recordings were made from SDH neurons responding to mechanical stimulation of the right hind paw, ie, from the side ipsilateral to the surgery in sham and cuff animals. Recordings were made with a glass electrode (Harvard Apparatus, Holliston, MA) filled with 0.5 M CH$_3$COOK (resistance: 15-25 MΩ). A motorized micromanipulator (Narishige, Tokyo, Japan) was used to gradually descend the electrode with 4-μm steps until the single-unit activity of an SDH neuron was recorded. The recording electrode was inserted at depths ≤500 μm from the surface of the spinal cord (corresponding to lamina I to V). The signal was amplified (IR-183; Cygnus Technology, Delaware Water Gap, PA), filtered at 0.3 to 3 kHz (Brownlee amplifier; AutoMate Scientific, Berkeley, CA), and digitized at 20 kHz with a MICRO3-1401 (CED, Cambridge, United Kingdom). Data were analyzed offline with Spike 2 software (CED). The cutaneous receptive field of the recorded neuron was identified by touching the ipsilateral hind paw. The response to a nonnociceptive mechanical stimulus, touch, and to a nociceptive one, pinch, was determined as described by others.[6] The touch stimulus was applied by brushing the skin with a camel's hair brush for 10 seconds (8-10 times). The pinch stimulus was applied by means of small serrated forceps (Graefe forceps; Fine Scientific Tools, Vancouver, Canada) for 10 seconds. Three types of neurons could be distinguished based on their differential response to touch vs pinch: (1) low-threshold (LT) neurons responded equally or more to nonnoxious touch than to noxious pinch; (2) wide-dynamic-range (WDR) neurons responded more to pinch than to touch; and (3) high-threshold (HT) neurons responded only to pinch, or at least 10 times more to pinch than to touch.

### 2.4. Drugs

Drugs were applied directly at the surface of the SDH using the agar chamber described above. The following drugs were purchased from Sigma (St Louis, MO): acetazolamide (ACTZ, a carbonic anhydrase inhibitor), bicuculline (a γ-aminobutyric acid [GABA$_A$] receptor antagonist), phenylbenzene ω-phosphono-α-amino acid (PMBA), a glycine receptor antagonist,[30] and D(−)-2-amino-5-phosphonopentanoic acid (D-AP5, an N-methyl-D-aspartate [NMDA] receptor antagonist). 6-cyano-7-nitroquinoxaline-2,3-dione (CNQX, a non-NMDA ionotropic glutamate receptor [iGluR] antagonist), was purchased from Tocris Bioscience (Bristol, United Kingdom). Stock solutions were first prepared in water at 100× their final concentration, stored at −20°C and, on the day of the experiment, diluted in saline to their final concentration. Acetazolamide was prepared as previously described.[17] All solutions were applied at 34°C to 35°C.

### 2.5. Data analysis

Putative single-unit activity was isolated online with template matching (Spike 2). Data are shown as mean ± SEM. The baseline ongoing activity (or firing rate [FR]) of SDH neurons is an average of the number of spikes during the first 2 minutes of recordings. The same period was used to calculate the coefficient of variation (CV) of the interspike interval, a value used widely as an indicator of regularity (the lower the CV value, the more regular the unit activity). The CV was calculated using the Spike 2 toolboxes and the script Meanix (CED). To measure the action potential widths or spike duration, the time between the first peak and trough of the action potential was measured, regardless of the order in which they occurred.[20] This analysis was performed using the Spike 2 toolboxes and the script PTA-analysis version

1.01 (Sylvain Côté, Laval University, Québec). This script also provided the measurement of the amplitude of the spike (from peak to trough).

The responses evoked by the mechanical stimuli were quantified as the mean discharge rate over the duration of the stimulus (10 seconds) after subtracting the background ongoing activity recorded for 1 minute before applying the stimulus.[6] In each neuron, touch and pinch were applied 3 times to confirm the reproducibility of these stimuli. We calculated and then averaged the effects elicited by the consecutive applications of each stimulus. We waited at least 60 seconds between application of 2 consecutive stimuli to avoid the development of sensitization. Postdischarge (PD) was calculated for each neuron as the cumulative number of action potentials during the 10 seconds (short PD) or 1 minute (long PD) after the end of the stimulus using a custom-made LabVIEW program. The results were analyzed with GraphPad Prism (version 5.0 for Windows; GraphPad Software, Inc, San Diego, CA) and Microsoft Excel (2010). Statistical evaluation was performed with nonparametric tests because most of the data did not show a normal distribution (Shapiro–Wilk normality test). The paired-samples Wilcoxon signed-rank test was performed to compare the effects before and after drug application within the same cell. The 2-sample Wilcoxon–Mann–Whitney rank-sum test was performed to compare independent groups. The Fisher exact test was used to compare proportion of SA vs NSA neurons and the proportion of LT, WDR, and HT in SA and NSA neurons. The level of significance was set at $P = 0.05$.

## 3. Results

### 3.1. Quantitative comparison of spontaneously active and nonspontaneously active neurons in spinal dorsal horn of naive animals

We recorded single-unit activity from a total of 96 SDH neurons from 42 naive mice. All of them responded to mechanical stimulation of the ipsilateral paw. Fifty-seven of those neurons (59%) showed sustained continuous ongoing activity (the FR ranging from 0.1 to 9.8 Hz; mean basal FR: 4.1 ± 0.6 Hz, **Fig. 1A**), whereas 39 (41%) were silent and only fired when the stimuli were applied (**Fig. 1A**). Therefore, those neurons were respectively named spontaneously active (SA) and non-spontaneously active

(NSA) neurons. We tested whether pharmacological blockade of fast inhibitory and excitatory synaptic transmission abolished ongoing activity of SA neurons in naive animals. For this, we used a cocktail of saturating doses of GABA$_A$, glycine, and glutamate receptors antagonists (bicuculline, PMBA, D-AP5, and CNQX, all at 100 μM). The antagonists had no effect on the ongoing activity (result not shown, $P = 0.4375$, paired-samples Wilcoxon test, n = 6), which suggests that the ongoing firing activity of SA neurons represents an intrinsic property of these neurons.

To better define SA and NSA neurons, we first compared their location. Although both types of neurons could be found throughout the first 5 dorsal laminae (**Fig. 1B**), SDH SA neurons were distributed significantly deeper in the spinal cord than NSA neurons (359 ± 18 μm, n = 57, vs 268 ± 25 μm, n = 39, $P = 0.0054$, 2-sample Wilcoxon test) (**Figs. 1B and C**; **Table 1**). Taking this into account, we tested other electrophysiological parameters that might be useful in further distinguishing SA and NSA neurons. Although yet unexploited in the spinal cord, analysis of action potential waveform is classically used in the brain to characterize and distinguish neuronal types.[4,24,33] Spike duration in SA neurons was on average 0.49 ± 0.04 milliseconds, which was not different from that in NSA neurons: 0.48 ± 0.06 milliseconds. However, we found that the spike amplitude was significantly larger in NSA than in SA neurons (**Table 1**). These differences suggest that SA and NSA might represent different types of neurons.

Having established the fundamental electrophysiological properties of both types of cells, we quantified the responses of identified SDH SA and NSA neurons to mechanical stimulation in naive mice. Two types of mechanical stimuli were applied to the ipsilateral hind paw: nonnoxious touch using a brush (dynamic touch) and noxious pinch using serrated forceps (see Material and methods). In SA neurons, the increase in firing frequency induced by touch was 2.3 ± 0.5 Hz, whereas the increase in the FR induced by pinch was significantly larger, 4.0 ± 0.5 Hz (n = 57 in both, $P < 0.00001$, paired-samples Wilcoxon test, **Fig. 2A**). In NSA neurons, the effect of pinch was also significantly larger than that of touch: 4.1 ± 0.4 vs 1.6 ± 0.3 Hz, respectively (n = 40 in both, $P < 0.00001$, paired-samples Wilcoxon test, **Fig. 2A**). There was no significant difference between SA and NSA neurons of the naive group in their responses to touch or pinch (2-sample Wilcoxon test).
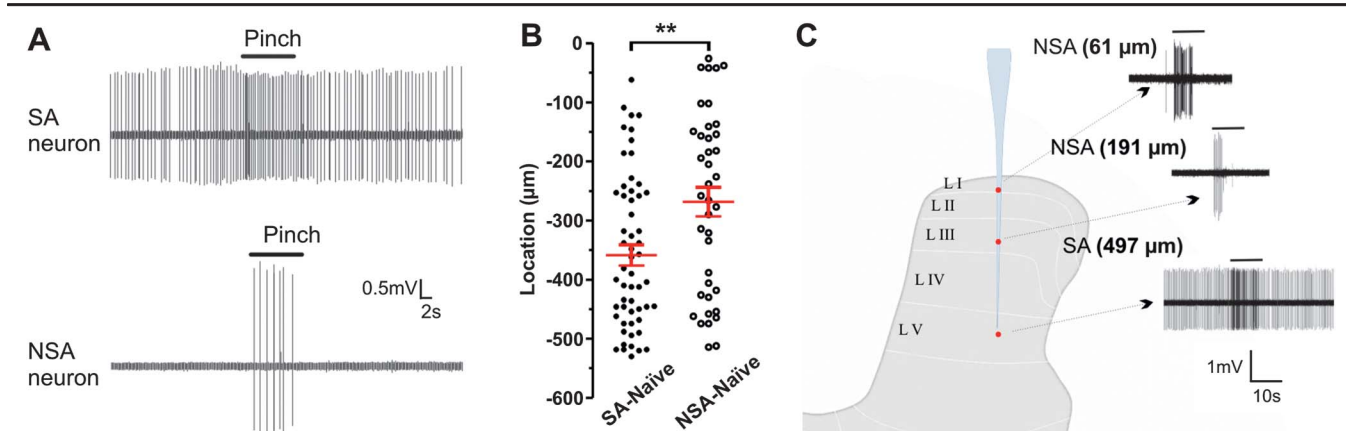


**Figure 1.** Distinguishing features of spontaneously active (SA) and nonspontaneously active (NSA) neurons in naive mice. (A) Representative examples of extracellular recordings of a spinal dorsal horn (SDH) SA (top) and an NSA (bottom) neuron showing the effect induced by pinch in the ipsilateral paw (10-second stimulus, solid line). (B) Location of the recorded SA and NSA neurons. Symbols are the individual cells, and red lines are mean ± SEM of each group of cells. **$P <$ 0.01, SA vs NSA (2-sample Wilcoxon test). (C) Recordings obtained from 3 different neurons (2 NSA and 1 SA) in the same pipette descent and schematic representation of their position in the SDH. The solid lines represent the pinch stimulus (10 seconds). Note that the NSA neurons are more superficial than the SA.

**Table 1**

**Electrophysiological properties of mouse spinal cord dorsal horn neurons.**

| | Spontaneously active (SA) | | | Nonspontaneously active (NSA) | | |
|---|---|---|---|---|---|---|
| | Naive | Sham | Cuff | Naive | Sham | Cuff |
| Location (μm) | 359 ± 18 | 400 ± 21 | 368 ± 18 | 268 ± 24* | 305 ± 15† | 297 ± 28‡ |
| Firing rate (Hz) | 4.1 ± 0.6 | 3.5 ± 0.5 | 4.0 ± 0.4 | — | — | — |
| CV (%) | 66.3 ± 4.0 (57) | 61.1 ± 5.1 (41) | 63.3 ± 4.2 (71) | — (39) | — (39) | — (20) |
| Spike duration (ms) | 0.49 ± 0.04 | 0.54 ± 0.05 | 0.59 ± 0.07 | 0.47 ± 0.06 | 0.51 ± 0.06 | 0.50 ± 0.06 |
| Peak to trough spike amplitude (mV) | 1.6 ± 0.2 (21) | 1.1 ± 0.2 (25) | 1.4 ± 0.1 (36) | 3.3 ± 0.4† (21) | 1.7 ± 0.2* (29) | 1.8 ± 0.2 (17) |

Mean ± SEM of different electrophysiological parameters defining SA and NSA neurons in the different groups.
\* $P < 0.01$.
† $P < 0.001$ NSA vs SA (2-samples Wilcoxon test; the number of neurons analyzed is given in parentheses).
‡ $P < 0.05$.
CV = coefficient of variation.

Based on their responses to touch and pinch, SA and NSA neurons were classified as LT, wide dynamic range (WDR), or high threshold (HT) (see Materials and methods). In both populations, the majority of recorded neurons were WDR, responding more to pinch than to touch (respectively 75% and 62% of SA and NSA neurons, **Fig. 2B**). The percentage of HT neurons was 11% in SA neurons and 28% in NSA. Finally, 14% of SA, and 10% of NSA neurons were classified as LT. There was no difference in the distribution of SA vs NSA neurons in these 3 categories.

Previous reports have mentioned that some neurons continue firing after the cessation of the stimulus, a property called post-discharge (PD)[26]; this has been proposed to have a peripheral origin, involving a continuous release of neurotransmitters (glutamate and substance P) by primary afferents outlasting the end of the stimulus. We have therefore evaluated whether NSA and SA neurons could be differentiated by the existence or absence of a PD. Indeed in NSA neurons, the mean number of events 60 seconds after touch or pinch was significantly higher than that recorded 60 seconds before the stimulus: the average number of spikes during 1 minute before and after touch was 0.0 ± 0.0 spikes and 3.4 ± 0.7 spikes, respectively ($P = 0.0014$, paired-samples Wilcoxon test), and before vs after pinch 0.0 ± 0.0 spikes vs 14.3 ± 2.6 spikes ($P = 0.001$, paired-samples Wilcoxon test). The PD induced by the noxious stimuli was larger than that induced by touch ($P = 0.0003$, paired-samples Wilcoxon test, **Fig. 2C**). In contrast, SA neurons did not display a similar "long" PD, nor a shorter one over 10 seconds. Indeed, in SA neurons, the mean number of events during 60 seconds before and after touch and pinch was: pretouch: 176.2 ± 25.5 vs posttouch: 178.4 ± 28.4 spikes; prepinch: 195.1 ± 34.8 vs postpinch: 192.4 ± 35.1 spikes (**Fig. 2C**). This difference in the presence of a PD suggests that SA and NSA neurons differentially process mechanical stimuli.
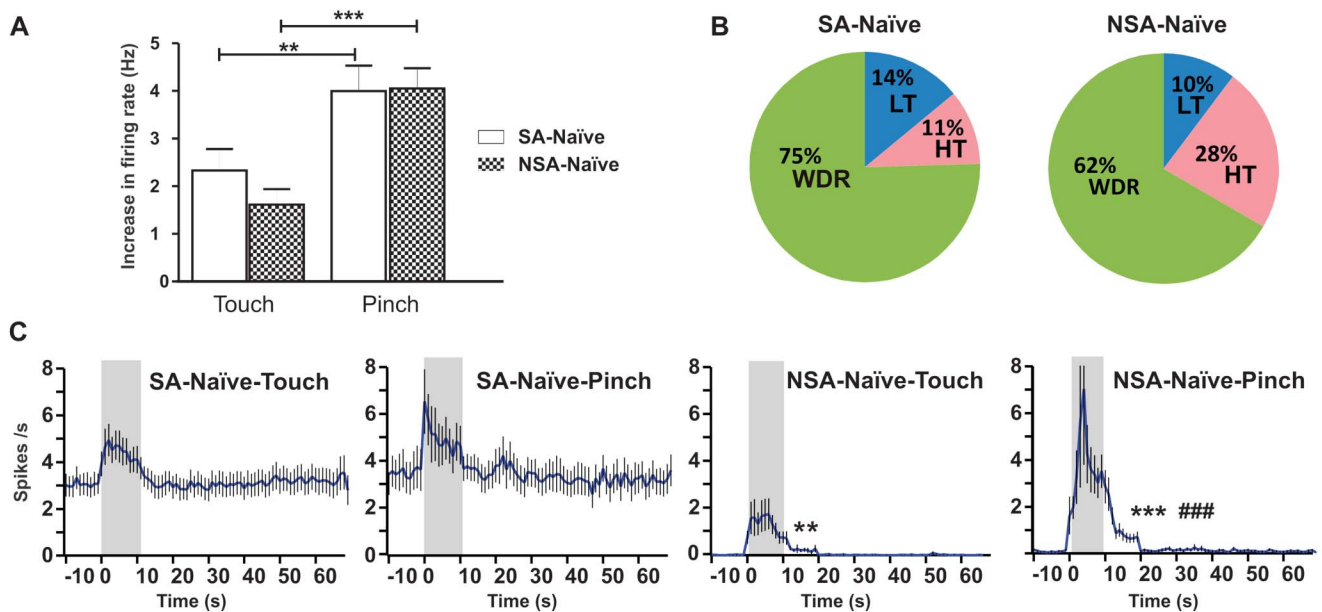


**Figure 2.** Effect induced by touch and pinch on spontaneously active (SA) and nonspontaneously active (NSA) neurons in naive mice. (A) Increase of the firing rate induced by touch and pinch. Bars represent mean ± SEM of the increase of the firing rate during touch and pinch application (10 seconds); \*\*$P < 0.01$, \*\*\*$P < 0.001$ touch vs pinch (paired-samples Wilcoxon test). (B) Percentages of low-threshold (LT), wide dynamic range (WDR), and high-threshold (HT) neurons. Spontaneously active and NSA neurons were classified into 3 types: LT, WDR, and HT based on the ratio between the effect of touch and pinch. (C) Analysis of postdischarge (PD) induced by touch and pinch in SA and NSA neurons. The blue line represents the mean number of spikes per second, for all analyzed neurons (n = 57 SA neurons, n = 40 NSA neurons). The vertical bars are the SEM. The gray bars represent the application of the stimuli. The PD was considered as the number of spikes for 60 seconds after the stimuli. \*\*$P < 0.01$, \*\*\*$P < 0.001$ PD vs basal (paired-samples Wilcoxon test); ###$P < 0.005$, pinch vs touch (paired-samples Wilcoxon test).

### 3.2. Adaptation of spontaneously and nonspontaneously active neurons after nerve injury

To study the plasticity induced by nerve injury, we performed in vivo electrophysiological recordings from SDH neurons in sham and cuff mice in the second and third weeks after surgery. Before starting the recording sessions, sham and cuff mice were tested for the presence of mechanical allodynia using von Frey hairs. As expected, the cuff group showed a significant reduction in the mechanical threshold of the hind paw ipsilateral to the surgery in comparison with the ipsilateral paw in sham (1.05 ± 0.10 g, n = 20 mice vs 3.91 ± 0.21 g, n = 21 mice, respectively, $P = 0.001$, Mann–Whitney test, **Fig. 3A**). These data confirmed the development of mechanical allodynia in cuff but not sham mice.

We recorded single-unit activity from a total of 80 SDH neurons from 21 sham mice and 91 SDH neurons from 23 cuff mice. The proportions of SA sham and NSA sham neurons were 51% and 49%, respectively, (n = 41 SA sham neurons, and n = 39 NSA sham neurons), which was not significantly different from the proportions in naive mice ($P = 0.2907$, Fisher exact test). Interestingly, the proportion of SA and NSA neurons was significantly different in cuff vs sham mice: we observed 78% of SA cuff neurons and 22% of NSA cuff neurons (n = 71 and n = 20, respectively, $P = 0.0003$, Fisher exact test, cuff vs sham; **Fig. 3B**). The distribution of the basal FR of SA sham neurons was not different from that of SA cuff neurons: mean basal FR 3.5 ± 0.5 Hz (ranging from 0.1 to 12.7 Hz, n = 41) in SA sham vs 4.0 ± 0.4 Hz (ranging from 0.3 to 15.7 Hz, n = 71) in SA cuff ($P = 0.3398$, Wilcoxon rank-sum test).

To further characterize SA and NSA neuronal properties after nerve injury, we analyzed their recording location in sham and cuff animals. Consistent with the results obtained in naive animals, recorded SA sham neurons were located significantly deeper than NSA sham neurons (400 ± 21 μm, n = 41, vs 305 ± 15 μm, n = 39, respectively, $P = 0.0005$, 2-sample Wilcoxon test,

**Fig. 3C**). Similarly, in cuff mice, SA neurons were recorded at significantly deeper locations than silent cells (368 ± 18 μm, n = 71, vs 297 ± 28 μm, n = 20; $P = 0.04725$, 2-sample Wilcoxon test, **Fig. 3C**). There was no difference in the location of SA or NSA neurons in sham vs cuff.

To better understand the changes occurring in SA and NSA neurons during neuropathy, the electrophysiological parameters related to the spike waveform were analyzed in neurons from sham and cuff animals. Overall, there was no difference in the spike duration between SA and NSA neurons from sham and cuff (**Table 1**). As in neurons from naive mice, the amplitude of the spike of SA sham neurons was significantly smaller than that of NSA sham neurons ($P = 0.0014$, 2-sample Wilcoxon test, **Table 1**). Interestingly, in cuff animals, we did not find any statistical difference in spike amplitude between SA cuff and NSA cuff neurons (**Table 1**).

We next explored the responses of SA and NSA neurons to mechanical stimuli in control and neuropathic mice. First, as seen in naive animals, there was no significant difference between NSA sham and SA sham neurons in their response to the stimuli ($P = 0.3188$ for touch, $P = 0.5601$ for pinch). Also, the response induced by pinch was significantly larger than the response induced by touch in both SA and NSA neurons recorded from sham animals ($P = 0.0010$ and $P = 0.0003$, respectively, paired-samples Wilcoxon test, **Fig. 4A**). However, this was not the case in cuff animals, in which the response to touch was not significantly different from the one to pinch in SA cuff neurons ($P = 0.060$), or was even significantly larger than the one to pinch in NSA cuff neurons ($P = 0.0192$, paired-sample Wilcoxon test, **Fig. 4A**). This was due to a very large increase of the response to touch (accompanied by a decrease in the response to pinch) observed in NSA cuff neurons compared with that in NSA sham neurons (4.9 ± 1.2 Hz vs 2.1 ± 0.3 Hz for touch, 1.9 ± 0.5 Hz vs 3.8 ± 0.4 Hz for pinch, respectively; $P = 0.0159$ and $P = 0.0026$, 2-sample Wilcoxon test, **Fig. 4A**). The decrease in the average
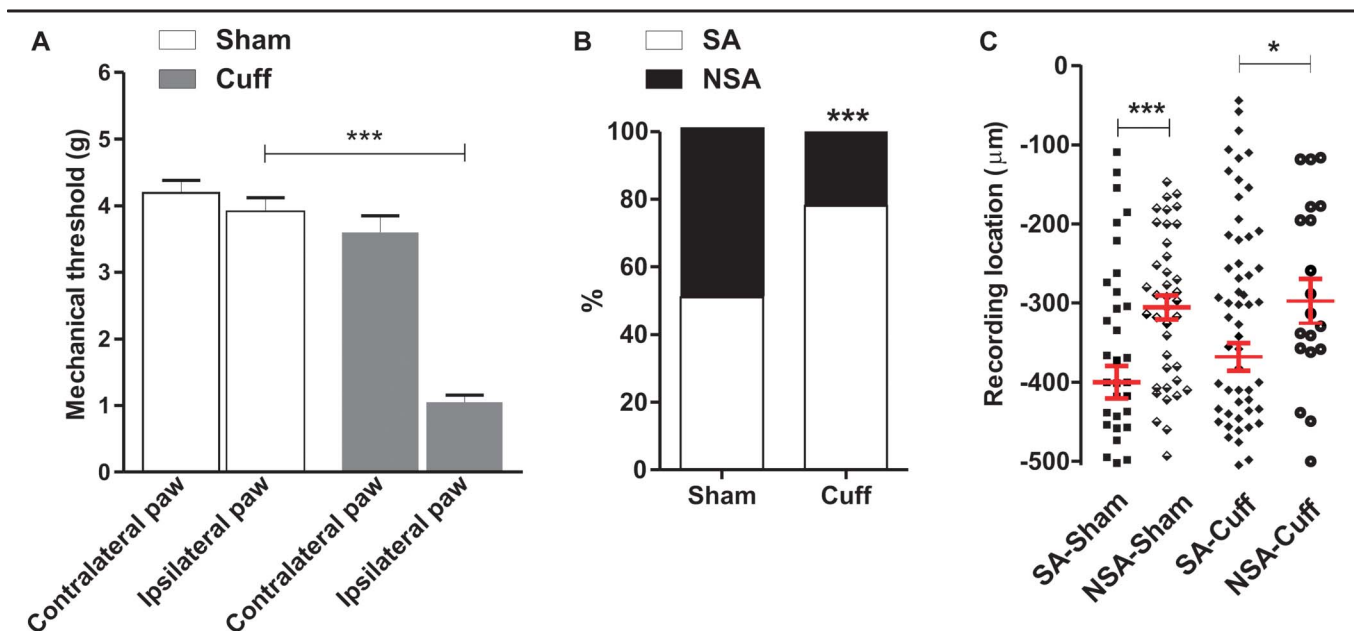


**Figure 3.** Behavioral assessment of sham and cuff mice, and distribution of spontaneously active (SA) and nonspontaneously active (NSA) neurons in these mice. (A) Mechanical threshold assessed with von Frey filaments on the hind paw contralateral and ipsilateral to the injury in control (sham) and neuropathic (cuff) animals. Bars are mean ± SEM of the mechanical pressure (in grams) yielding to paw withdrawal in each condition. ***$P < 0.001$, 2-sample Wilcoxon test. (B) Percentage of SA and NSA neurons recorded in sham and cuff mice (respectively n = 80 and n = 91 total neurons). ***$P < 0.001$, Fisher exact test. (C) Location of the recorded SA and NSA neurons in sham and cuff animals. Symbols are the individual cells, and horizontal lines are mean ± SEM of each group of cells. *$P < 0.05$, ***$P < 0.001$, 2-sample Wilcoxon test.
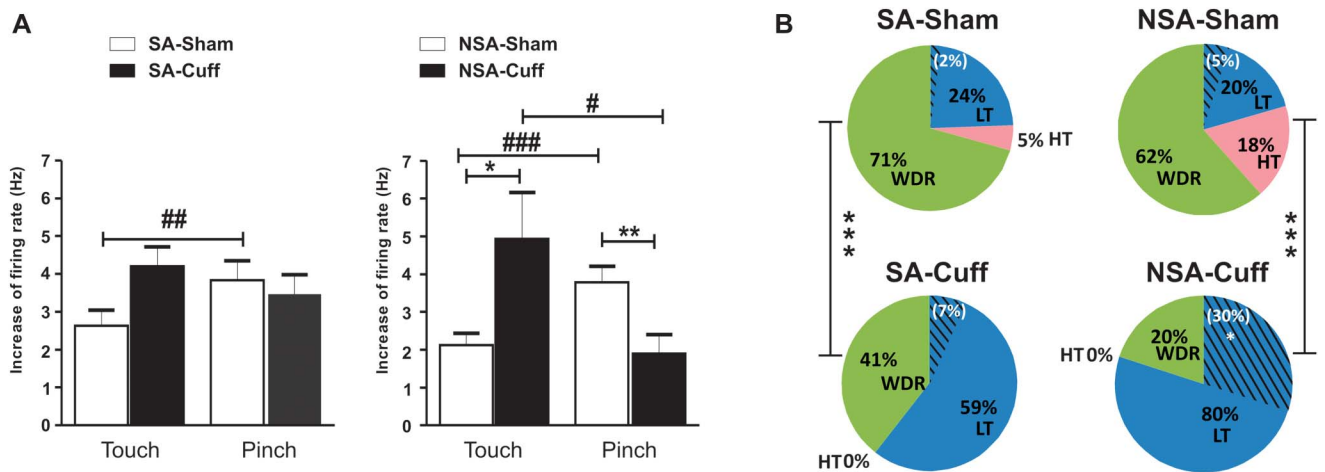
**Figure 4.** Effect of touch and pinch in spontaneously active (SA) and nonspontaneously active (NSA) neurons recorded from sham and cuff animals. (A) Increase of the firing rate induced by touch and pinch in SA (left) and NSA (right) neurons from sham (white) and cuff (black) animals. Bars represent mean ± SEM of the increase of the firing rate during touch and pinch application (10 seconds). Note that in NSA cuff, the effect induced by touch was larger than that in NSA sham, whereas the effect induced by pinch was smaller (*P < 0.05, **P < 0.01, 2-sample Wilcoxon test). In sham (control) mice, the effect of pinch was significantly greater than the effect of touch for both groups of neurons (##P < 0.01, ###P < 0.001, paired-samples Wilcoxon test). However, in NSA cuff neurons, the effect of pinch was smaller than the effect induced by touch (#P < 0.05, paired-samples Wilcoxon test). In SA cuff neurons, the effect induced by touch is not different from that induced by pinch. (B) Percentages of low-threshold (LT), wide dynamic range (WDR), and high-threshold (HT) neurons form sham and cuff animals. Spontaneously active and NSA neurons were classified into 3 types: LT, WDR, and HT based on the ratio between the effect of touch and pinch. Note that in both SA and NSA, the percentage of LT neurons increased considerably after nerve injury. ***P < 0.001 SA vs NSA (Fisher exact test). Some LT neurons did not show any response to pinch (hatched bars, % in white). Note that this percentage was significantly larger in NSA cuff neurons (in comparison with NSA sham neurons, *P < 0.05, Fisher exact test).

response to pinch in NSA cuff neurons could be linked to an overrepresentation of neurons displaying no response at all to pinch in this group: indeed, although nonresponders to pinch represented 5% of NSA sham neurons (2 of 39 neurons), they represented 30% of NSA cuff neurons (6 of 20 neurons, P = 0.0144, Fisher exact test). The overall proportion of neurons not responding to pinch in sham vs cuff mice was unchanged (5% vs 12%, respectively, 4 of 80 neurons in sham and 11 of 91 neurons in cuff, P = 0.1138, Fisher exact test). This indicated that the enrichment of nonresponders to pinch observed in NSA cuff was specific to this group. Our data suggest that, although many silent neurons become SA in cuff mice (leading to an increase in the proportion of SA neurons from 51% to 78% in sham vs cuff, **Fig. 3B**), nonnociceptive neurons (nonresponders to pinch) preferentially remain silent (NSA) after nerve injury.

The increased proportion of neurons with ongoing activity, as well as the large increase in the response to the low threshold mechanical stimulation showed that there was neuronal hypersensitivity to nonnoxious stimuli in the SDH after cuffing the sciatic nerve, consistent with the behavioral allodynia found in cuff animals (**Fig. 3A**). To understand the encoding properties of SA and NSA neurons, it is important to compare the response of individual neurons with different types of peripheral stimuli. We therefore analyzed the impact of nerve injury on the proportion of LT, WDR, and HT neurons within SA and NSA populations. Like in naive animals, we found the 3 types of neurons in sham mice, with WDR being the predominant population (**Fig. 4B**). However, after nerve injury, a similar analysis revealed only 2 types of neurons: WDR and LT. We could not record HT neurons in cuff animals. More specifically, SA sham cells were 71% WDR, 24% LT, and 5% HT, respectively. This was significantly different from SA cuff neurons: 41% WDR and 59% of LT (P = 0.0003, Fisher exact test, **Fig. 4B**). Regarding the NSA neurons, this change was even more striking. Indeed, in NSA sham, we found 62% of WDR, 20% of LT, and 18% HT, whereas in NSA cuff, only 20% of the neurons

were WDR and the other 80% were classified as LT (P = 0.0009, Fisher exact test, **Fig. 4B**). These results show that after nerve injury, in both SA and NSA neurons, there is a decrease of WDR and HT in favor of LT neurons. It should be noted that the majority of LT neurons recorded in cuff also responded to the noxious stimulation (pinch) and should therefore not be considered as nonnociceptive. These results are consistent with the behavior of cuff mice that experience a marked decrease in the mechanical threshold of the injured paw. Finally, all of these data suggest that both SA and NSA neurons are involved in the plasticity induced by the peripheral nerve injury in the ipsilateral SDH.

The analysis of the PD showed that, as observed in naive mice, NSA sham neurons showed a significant long PD after both touch (pretouch: 0.0 ± 0.0 vs posttouch: 2.7 ± 0.6 spikes over 1 minute, P = 0.0003, paired-samples Wilcoxon test) and pinch (prepinch: 0.0 ± 0.0 vs postpinch: 18.4 ± 4.5 spikes over 1 minute, P = 0.0001, paired-samples Wilcoxon test, **Fig. 5A**). In NSA sham neurons the PD induced by the noxious stimuli was larger than the one induced by touch (P = 0.0001, paired-samples Wilcoxon test, **Fig. 5A**). In cuff mice, NSA neurons also showed long PD after touch (pretouch: 0.0 ± 0.0 vs posttouch: 16.3 ± 5.5 spikes over 1 minute, P = 0.0003, paired-samples Wilcoxon test) and pinch (prepinch: 0.0 ± 0.0 vs postpinch: 29.9 ± 12.4 spikes over 1 minute, P = 0.0001, paired-samples Wilcoxon test, **Fig. 5B**); the PD observed in NSA cuff was significantly larger than that in NSA sham neurons (P = 0.0001 in both groups, touch and pinch, **Figs. 5A and B**). Although SA sham neurons did not show any PD after touching or pinching (**Fig. 5A**), as observed in naive mice, SA cuff neurons showed a short-term PD in the first 10 seconds after both touch and pinch: (pretouch: 27.4 ± 4.2 vs posttouch: 37.2 ± 5.0 spikes over 10 seconds, P = 0.0001, paired-samples Wilcoxon test; prepinch: 25.3 ± 4.5 vs postpinch: 35.9 ± 5.0 spikes over 10 seconds, P < 0.01, unpaired t test, **Fig. 5B**). No significant difference was found in the PD induced by touch and the one induced by pinch in neurons from cuff animals.
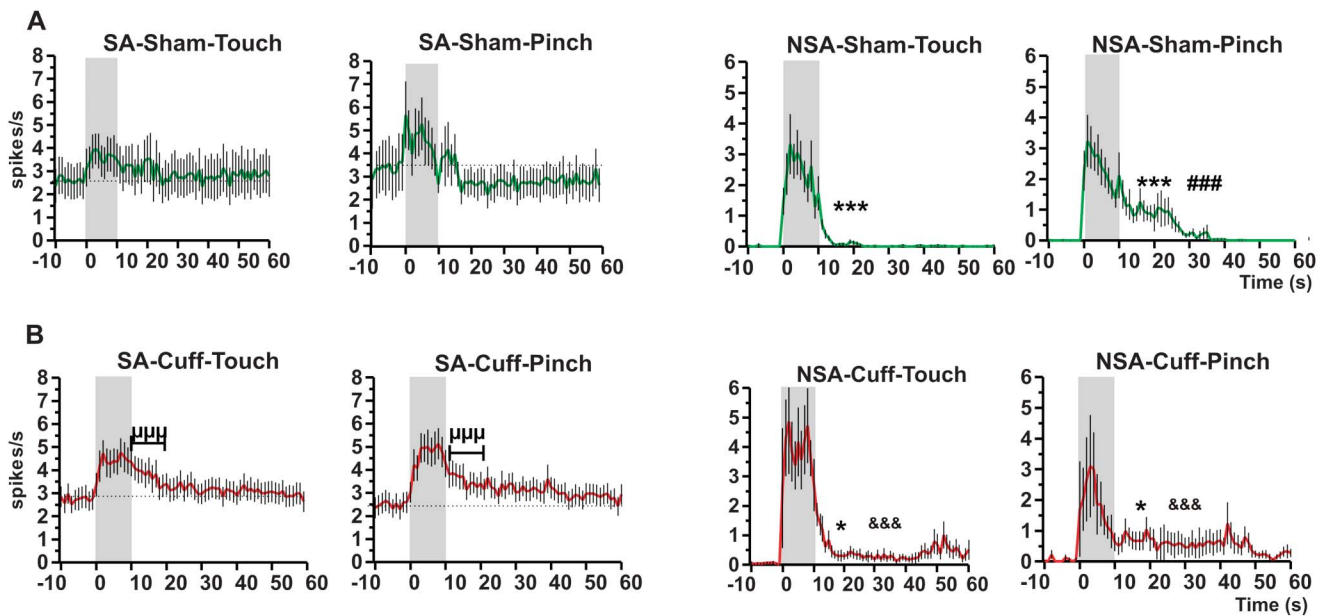
**Figure 5.** Postdischarge (PD) induced by touch and pinch of spontaneously active (SA) and nonspontaneously active (NSA) neurons in sham and cuff animals. The green (sham) and red (cuff) lines and the vertical bars represent mean ± SEM of the number of spikes per second, respectively. The gray bars represent the application of the stimuli. (A) Long PD (measured over 1 minute) induced by touch and pinch in neurons recorded from sham animals. Note that in NSA sham neurons, touch and pinch induce a PD, which is greater after pinching. (B) PD induced by touch and pinch in neurons recorded from cuff animals. Note that in SA cuff neurons, both touch and pinch induce a short-term PD. In NSA cuff neurons, the PD is greater than in NSA sham cells. $*P < 0.05$, $***P < 0.001$ PD vs basal (paired-samples Wilcoxon test). $###P < 0.001$ touch vs pinch (paired-samples Wilcoxon test); $\mu\mu\mu P < 0.001$, short-term PD vs basal (paired-samples Wilcoxon test); $\&\&\& P < 0.001$ sham vs cuff (2-sample Wilcoxon test).

### 3.3. Plasticity of the inhibition in spontaneously and nonspontaneously active neurons of the spinal dorsal horn after nerve injury

Previous reports have suggested that spinal disinhibition may be a substrate for the behavioral hypersensitivity observed after nerve injury.[7,16,32] To address this question in our model, we tested the effect of the blockade of fast synaptic spinal inhibition with a mixture of the GABA$_A$ antagonist, bicuculline, and the glycinergic antagonist, PMBA, in both sham and cuff mice. Combined blockade of GABA$_A$ and glycine receptors induced an increase in the response to touch and pinch in SA sham neurons ($P = 0.0206$ and $P = 0.0313$, respectively; n = 8 in both, paired-samples Wilcoxon test, **Fig. 6A**). In addition, the ongoing activity of SA sham neurons significantly increased after application of the antagonists ($P = 0.0137$, paired-samples Wilcoxon test, **Fig. 6A**). Likewise, in NSA sham cells, the effect of touch and pinch was significantly larger after the application of the GABA$_A$ and glycine receptors antagonists ($P = 0.0025$ and $P = 0.0010$, paired-samples Wilcoxon test, n = 12 in both, **Fig. 6A**). Interestingly, 8 of 12 NSA sham neurons developed ongoing activity after the application of bicuculline and PMBA, leading to an average FR of 0.4 ± 0.3 Hz (vs 0.0 ± 0.0 Hz before drug, $P = 0.0142$, paired-samples Wilcoxon test, **Fig. 6A**). These results demonstrate the importance of the GABAergic and glycinergic systems in the control of spinal responses to mechanical inputs. Importantly, in both SA and NSA neurons, the effect of pinch increased significantly after blocking spinal inhibition (**Fig. 6A**).

Because of this increase in the responses to pinch, the effect of blocking spinal inhibition seemed different from the plasticity observed after nerve injury (where the response to pinch was unchanged, in SA neurons, or even reduced, in NSA neurons, **Fig. 4A**). However, a direct comparison was hampered by the fact that some of the NSA neurons developed ongoing activity after bicuculline and PMBA (**Fig. 6A**). These could therefore not be directly compared with the neurons classified as NSA in cuff mice. For this specific comparison, we pooled SA and NSA neurons. In this total population of neurons, we observed that the response to pinch was reduced in cuff mice vs sham mice (n = 91 and n = 80, respectively, $P = 0.0079$), whereas the response to pinch recorded in the presence of bicuculline and PMBA was increased compared with the control situation (before the drug, n = 20, $P = 0.0003$, results not shown). These data demonstrate that, although blocking spinal inhibition and nerve injury similarly increase responses of SDH neurons to innocuous stimuli, they induce opposite effects on their response to noxious stimuli. This suggests that the underlying mechanisms of these 2 plasticities are distinct.

Interestingly, bicuculline and PMBA showed no effectiveness in neurons recorded from cuff animals. Indeed, in silent neurons and neurons with ongoing activity recorded from cuff mice, application of the inhibitory antagonists modified neither the ongoing activity nor the response to stimuli (**Fig. 6B**). These results suggest that during neuropathy, the local spinal inhibition induced by GABA and glycine has no net effect on the control of responses to mechanical inputs or the ongoing activity of SA neurons.

GABA$_A$ and glycine receptors are permeable to both chloride and bicarbonate, usually in opposite directions (chloride flowing in and bicarbonate flowing out). If the disinhibition reported here is due to a collapse in chloride gradient, it could be mitigated by reducing the bicarbonate driving force. For this reason, we performed a group of experiments in which we used the carbonic anhydrase inhibitor acetazolamide (ACTZ) thus limiting the production of bicarbonate.[17] We compared the effects induced by touch and pinch when saline or ACTZ (10 mM) was topically applied on the exposed spinal cord of sham or cuff mice. In sham mice, as previously reported,[17] there was no difference in the responses to touch (or pinch) in neurons after topical application of saline or ACTZ (2-sample Mann–Whitney test, n = 6 with 4
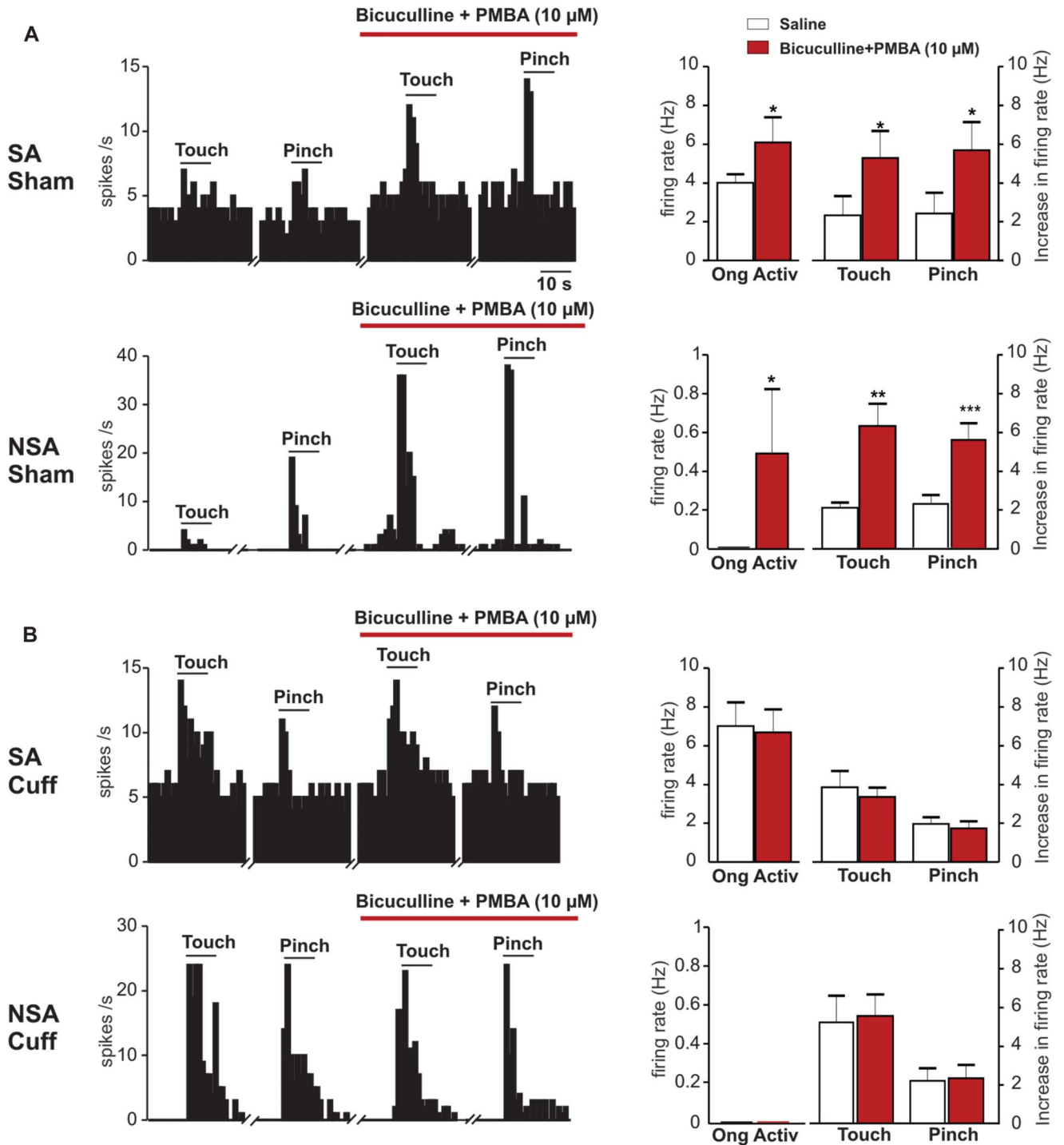
**Figure 6.** Pharmacologically induced disinhibition in spontaneously active (SA) and nonspontaneously active (NSA) neurons of the spinal dorsal horn. (A) Data from sham mice. On the left, representative examples of the firing rate from 1 SA (top) and 1 NSA (bottom) neurons recorded in sham animals showing the effect induced by the mechanical stimuli (touch and pinch) in control conditions (saline) and during the application of the inhibitory antagonists. The vertical bars represent the firing rate (spikes/s). Touch and pinch were applied for the period indicated by the horizontal bars (10 seconds). On the right, bars represent mean ± SEM of the ongoing activity and the increase of firing rate induced by touch and pinch in SA (n = 8) and NSA (n = 12) neurons from sham mice. (B) Data from cuff mice. On the left, representative examples of the firing rate from 1 SA (top) and 1 NSA (bottom) neuron recorded from cuff animals showing the effect induced by the mechanical stimuli (touch and pinch) in control conditions (saline) and during the application of the inhibitory antagonists. The vertical bars represent the firing rate (spikes/s). Touch and pinch were applied for the period indicated by the horizontal bars (10 seconds). On the right, bars represent mean ± SEM of the ongoing activity and the increase of firing rate induced by touch and pinch in SA (n = 8) and NSA (n = 9) neurons from cuff mice. Note the difference in scale for the Y-axis of ongoing activity graphs in SA vs NSA neurons. Pharmacological disinhibition enhances the ongoing activity and the responses to the stimuli in sham animals, but it did not have any effect in neurons recorded from cuff mice ($*P < 0.05$, $**P < 0.01$, $***P < 0.001$, compared with the control, paired-samples Wilcoxon test).

NSA and 2 SA neurons in the saline group, and n = 6 with 3 NSA and 3 SA neurons in the ACTZ group; **Fig. 7A**). In contrast, in cuff mice, responses to touch were considerably diminished in the presence of ACTZ compared with those obtained in saline (P = 0.0037, 2-sample Mann–Whitney test, n = 14 with 3 NSA and 11 SA neurons in the saline group, and n = 14 with 5 NSA and 9 SA neurons in the ACTZ group, **Fig. 7A**). A consequence of this reduced response to touch in the presence of ACTZ was that, although in control conditions (saline), cuff neurons showed a significantly larger response to touch than to pinch (P = 0.0059, paired-samples Wilcoxon test, **Fig. 7A**), this was normalized in the presence of ACTZ. Indeed, after ACTZ, the response to touch became again significantly smaller than the response to pinch (P = 0.0238, paired-samples Wilcoxon test, n = 14, **Fig. 7A**), as observed in naive or sham mice (cf. **Fig. 2** or **Fig. 4**). In this cuff sample (n = 14), 86% of recorded neurons were LT and 14% WDR; however, among neurons (also n = 14) recorded in the same mice but in the presence of ACTZ, the proportion of LT neurons was reduced to 21%, whereas 79% were WDR (P = 0.0018, Fisher exact test, saline vs ACTZ, **Fig. 7B**). Importantly, among the 14 recordings obtained in saline conditions (cuff mice), 10 of them were also recorded for a sufficiently long period after ACTZ, enabling direct paired analysis of the ACTZ effect. Only 1 neuron was classified as WDR, whereas the other 9 were classified as LT when recorded under saline. After ACTZ application, 6 of the 9 LT neurons were switched to WDR, the other 3 remaining classified as LT (and the WDR neuron remained WDR). This phenotypical switch was statistically significant (P = 0.0198, Fisher exact test). These results suggest that reducing bicarbonate efflux by blocking carbonic anhydrase can counter-act the phenotypical switch in neuronal responses observed in cuff animals.

## 4. Discussion

In this study, we propose that 2 different categories of neurons can be distinguished in the SDH based on their ongoing activity: SA and NSA neurons. We demonstrate that both types of neurons contribute to the processing of mechanical inputs and are under the control of an inhibitory tone in naive animals.

Although NSA neurons could still be recorded after nerve injury, our results strongly suggest that some previously silent neurons developed spontaneous activity in cuff mice. Interestingly, neither SA nor NSA neurons seem to be placed under a tonic inhibitory tone in neuropathic conditions, in line with the common hypothesis of reduced inhibition in this condition (see below). The fact that some neurons switched from NSA to SA implies that it is important to proceed to the simultaneous study of both types of neurons to fully elucidate the alterations occurring in the spinal cord during neuropathic pain.

Spontaneous activity has been observed in injured primary sensory and SDH neurons, in animal models and patients.[41] Spinal dorsal horn neurons with spontaneous activity have also been sporadically reported in naive rats,[32] cats,[20,34,35] and monkeys.[46] It has been suggested that they may provide a basal level of activity that can be adjusted by intraspinal and descending inputs[20]; however, their function is still unclear. Their properties had never been systematically compared with those of non-spontaneous activity neurons until now. We observed that SA neurons are on average located deeper than NSA neurons. This is consistent with the results of Sandkühler and Eblen-Zajjur[32] who reported that, for some groups of neurons, the deeper they are, the more rhythmicity they show. They also observed spontane-ous, or background, activity in the 3 types of neurons recorded in the rat dorsal horn: LT, WDR, and HT, with proportions comparable to those we observed in mice. There was no difference in the effect induced by the mechanical stimuli between the 2 categories of neurons, SA and NSA. Altogether, these results suggest that both SA and NSA neurons are involved in the processing of innocuous and noxious mechanical inputs.

It is interesting to note that, when projection neurons are specifically targeted for in vivo electrophysiological recordings, they are always described as silent in control conditions.[6,7,14,16] However, studies reporting neurons with background activity, including ours, have not tested the possibility of a supraspinal projection site.[12,20,25,32] It is therefore tempting to suggest, although it remains to be demonstrated, that SA neurons correspond to interneurons that only project locally. They might be part of the spontaneously synchronizing system described in the SDH of rats, cats, and macaques that has been suggested
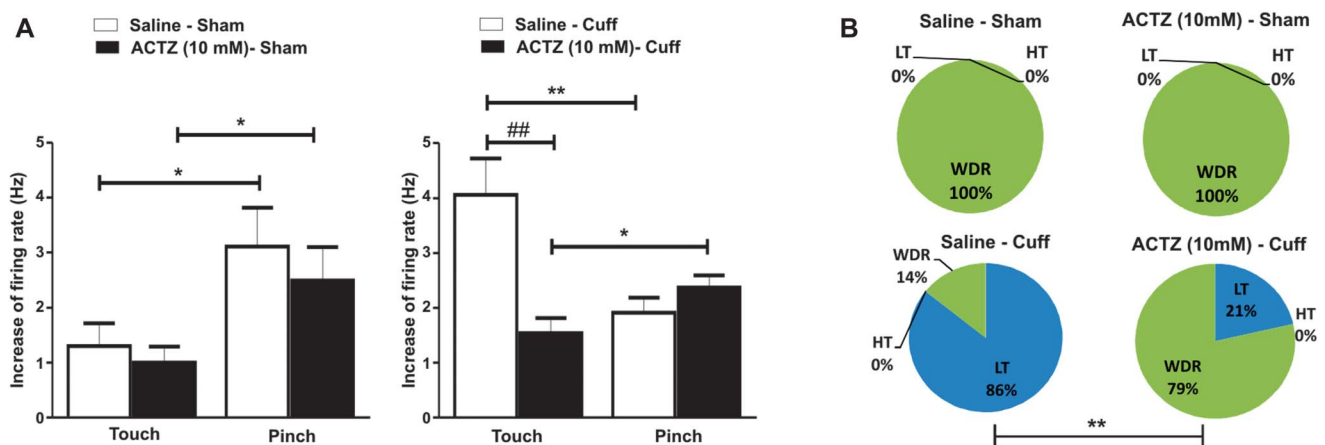


**Figure 7.** Effect of the carbonic anhydrase inhibitor acetazolamide (ACTZ 10 mM) on the effect induced by touch and pinch in neurons recorded from sham and cuff animals. (A) Increase of the firing rate induced by touch and pinch in neurons from sham (left) and cuff (right) animals. Bars represent the mean of the effect induced by touch and pinch. Note that in cuff neurons in the control situation, the effect induced by touch was larger than the effect induced by pinch (*P < 0.01, paired-samples Wilcoxon test). However, after ACTZ application, the effect of touch was smaller than the effect induced by pinch (*P < 0.05, paired-samples Wilcoxon test). (B) Percentages of low-threshold (LT), wide dynamic range (WDR), and high-threshold (HT) neurons form sham and cuff animals before and after the application of ACTZ (10 mM). Note that the percentage of LT neurons recorded in cuff animals decreased considerably after ACTZ application (**P < 0.01, Fisher exact test).

to provide a basal level of activity in sensory and motor pathways.[18,20,32,42]

Previous reports suggest that neurons in nerve-injured rodents are characterized by an increased level of spontaneous activity.[12,14,16,38] Our data similarly demonstrate an increased proportion of SA neurons after neuropathy (78% in cuff vs 51% in sham). The average FR of SA cuff neurons did not differ from the one of SA sham neurons; this observation does not exclude the possibility that neurons that were already SA in the control situation displayed an increased ongoing FR after nerve injury. Indeed, the SA cuff population is also formed of formerly NSA neurons in control conditions that developed ongoing activity, and whose low FR could balance the increased FR of formerly SA neurons, therefore leading to an unchanged FR of SA cuff vs SA sham at the population level.

One of the objectives of our study was to elucidate the contribution of SA and NSA neurons to the processing of mechanical inputs. To gain more insight into the sensory modality preferentially encoded by the recorded neurons, we analyzed the ratio between their responses to light touch vs pinch. This enabled us to classify the neurons as LT, WDR, and HT, as previously described. However, although previous studies focus on a single neuronal type, typically WDR or HT neurons,[7,13,15,23,25,32] we systematically studied all 3 types of neurons. To our knowledge, this is the first study in which the properties of LT, WDR, and HT neurons are compared in control and neuropathic mice. This not only enabled to analyze the changes in the proportions of these 3 categories in neuropathic mice, but also to compare their distribution in SA vs NSA neurons.

Importantly, both SA and NSA neurons can still be observed after neuropathy, ruling out the idea that all SDH neurons would be SA in this condition. Both populations were subject to an important plasticity, impacting in particular the ratio of their response to touch vs pinch. The increase in the response to touch was such, in nerve-injured mice, that the increase in the FR induced by touch in NSA neurons was significantly larger than the one induced by pinch. Accordingly, most neurons recorded in cuff animals were classified as LT, a smaller proportion of WDR, and we observed no HT cells. The increase in the proportion of LT neurons was also most noticeable among NSA neurons, as they represented only 18% of NSA sham neurons, compared with 80% of NSA cuff neurons. It should be noted that although according to the classical classification, the majority of neurons were assigned to the LT category, the majority still responded to pinch, ie, processed nociceptive information. They should therefore not be considered as "nonnociceptive." The number of neurons truly nonresponsive to pinch was unchanged in cuff vs sham mice (combined NSA and SA neurons); however, these neurons were enriched in NSA cuff (compared with SA cuff), which suggests that nonnociceptive neurons are less prone to develop ongoing activity after nerve injury.

The cuff model of neuropathic pain has first been developed for rats[22] and used to explore the cellular changes occurring in the SDH during neuropathy.[14,16,25,26] This model was more recently adapted for mice[3] and, to our knowledge, our study is the first to characterize the electrophysiological properties of SDH neurons in vivo in cuff mice. It is important to mention that all of our experiments were made during the second and third weeks after surgery, once the behavioral allodynia was stably established.[44] Within this time frame, the animals do not present anxiodepressive-like behaviors that characterize later stages of the neuropathy.[3,44]

The plasticity of spinal inhibitory transmission occurring after nerve injury is believed to be a key mechanism responsible for allodynia.[27] Yet previous in vivo recordings in the rat SDH provided controversial data, supporting either a decrease or an increase in the GABAergic (but not glycinergic) tone in neuropathic rats.[7,15] In our hands, blocking GABAergic and glycinergic receptors with bicuculline and PMBA, respectively, had no effect on the peripherally driven responses in the neuropathic SDH. This indicates that the inhibitory tone is either absent, or has lost its net effect on SDH neurons after nerve injury. This could be due to chloride homeostasis dysregulation elevating the reversal potential for anions ($E_{anion}$) close to the neurons resting potential and therefore leading to the absence of net effect of GABAergic signaling.[11] Indeed, hyperpolarizing $E_{anion}$ by inhibiting carbonic anhydrase (with acetazolamide) reversed the exacerbated neuronal responses to light touch that were observed in cuff mice. By disrupting bicarbonate homeostasis, ACTZ is also expected to limit the emergence of a depolarizing phase in GABAergic currents, in situations in which chloride extrusion capacities are highly compromised.[8,29] Interestingly, ACTZ has been shown to reduce neuropathic allodynia in different models and tests.[1,2]

However, our data argue against reduced inhibitory receptor expression (or activation) as the main contributor to SDH disinhibition, in agreement with a recent study by Lee and Prescott.[17] Indeed, pharmacological reduction of inhibition (in control mice) only partially recapitulated the neuronal phenotype observed in cuff animals. As previously described in naive rats and cats, inhibition of GABA_A and/or glycine receptors induced an increased response to both low- and high-intensity mechanical stimulation (see Refs. 7,17,34,35, but see also Ref. 15). Interestingly, we demonstrate that in cuff mice, only the responses to touch are markedly increased, whereas those to pinch are reduced compared with sham animals. Our recordings therefore demonstrate that the dramatic loss of general impact of inhibitory transmission (ie, disinhibition) occurring in neuropathic mice cannot be fully accounted for by reduced inhibitory receptor expression or activation.

In summary, in this study, we have demonstrated that we can distinguish 2 categories of SDH neurons involved in the processing of mechanical information. By recording them under the same conditions, we could compare their properties and demonstrate that both silent neurons and neurons with background activity experience essential modifications after nerve injury. Although previous studies predominantly focus on silent spinal neurons, our study demonstrates that neurons with spontaneous activity should not be neglected to gain a full understanding of the spinal nociceptive network in control conditions and during neuropathy. Our findings demonstrate a dramatic loss of spinal inhibitory transmission in nerve injury–induced neuropathic pain.

## Conflict of interest statement

The authors have no conflicts of interest to declare.

## Acknowledgements

## References

[1] Asiedu M, Ossipov MH, Kaila K, Price TJ. Acetazolamide and midazolam act synergistically to inhibit neuropathic pain. PAIN 2010;148:302–8.

[2] Asiedu MN, Mejia GL, Hubner CA, Kaila K, Price TJ. Inhibition of carbonic anhydrase augments GABAA receptor-mediated analgesia via a spinal mechanism of action. J Pain 2014;15:395–406.

[3] Benbouzid M, Pallage V, Rajalu M, Waltisperger E, Doridot S, Poisbeau P, Freund-Mercier MJ, Barrot M. Sciatic nerve cuffing in mice: a model of sustained neuropathic pain. Eur J Pain 2008;12:591–9.

[4] Bienvenu TC, Busti D, Micklem BR, Mansouri M, Magill PJ, Ferraguti F, Capogna M. Large intercalated neurons of amygdala relay noxious sensory information. J Neurosci 2015;35:2044–57.

[5] Bohren Y, Tessier LH, Megat S, Petitjean H, Hugel S, Daniel D, Kremer M, Fournel S, Hein L, Schlichter R, Freund-Mercier MJ, Yalcin I, Barrot M. Antidepressants suppress neuropathic pain by a peripheral beta2-adrenoceptor mediated anti-TNFalpha mechanism. Neurobiol Dis 2013; 60:39–50.

[6] Chen SR, Pan HL. Activation of muscarinic receptors inhibits spinal dorsal horn projection neurons: role of GABAB receptors. Neuroscience 2004; 125:141–8.

[7] Chen YP, Chen SR, Pan HL. Effect of morphine on deep dorsal horn projection neurons depends on spinal GABAergic and glycinergic tone: implications for reduced opioid effect in neuropathic pain. J Pharmacol Exp Ther 2005;315:696–703.

[8] Cordero-Erausquin M, Coull JA, Boudreau D, Rolland M, De Koninck Y. Differential maturation of GABA action and anion reversal potential in spinal lamina I neurons: impact of chloride extrusion capacity. J Neurosci 2005;25:9613–23.

[9] Coull JA, Beggs S, Boudreau D, Boivin D, Tsuda M, Inoue K, Gravel C, Salter MW, De Koninck Y. BDNF from microglia causes the shift in neuronal anion gradient underlying neuropathic pain. Nature 2005;438: 1017–21.

[10] Coull JA, Boudreau D, Bachand K, Prescott SA, Nault F, Sik A, De Koninck P, De Koninck Y. Trans-synaptic shift in anion gradient in spinal lamina I neurons as a mechanism of neuropathic pain. Nature 2003;424: 938–42.

[11] De Koninck Y. Altered chloride homeostasis in neurological disorders: a new target. Curr Opin Pharmacol 2007;7:93–9.

[12] Hao JX, Kupers RC, Xu XJ. Response characteristics of spinal cord dorsal horn neurons in chronic allodynic rats after spinal cord injury. J Neurophysiol 2004;92:1391–9.

[13] Hirsch SJ, Dickenson AH. Morphine sensitivity of spinal neurons in the chronic constriction injury neuropathic rat pain model. Neurosci Lett 2014;562:97–101.

[14] Keller AF, Beggs S, Salter MW, De Koninck Y. Transformation of the output of spinal lamina I neurons after nerve injury and microglia stimulation underlying neuropathic pain. Mol Pain 2007;3:27.

[15] Kontinen VK, Stanfa LC, Basu A, Dickenson AH. Electrophysiologic evidence for increased endogenous gabaergic but not glycinergic inhibitory tone in the rat spinal nerve ligation model of neuropathy. Anesthesiology 2001;94:333–9.

[16] Lavertu G, Cote SL, De Koninck Y. Enhancing K-Cl co-transport restores normal spinothalamic sensory coding in a neuropathic pain model. Brain 2014;137(Pt 3):724–38.

[17] Lee KY, Prescott SA. Chloride dysregulation and inhibitory receptor blockade yield equivalent disinhibition of spinal neurons yet are differentially reversed by carbonic anhydrase blockade. PAIN 2015;156:2431–7.

[18] Lidierth M, Wall PD. Synchronous inherent oscillations of potentials within the rat lumbar spinal cord. Neurosci Lett 1996;220:25–8.

[19] Lorenzo LE, Magnussen C, Bailey AL, St Louis M, De Koninck Y, Ribeiro-da-Silva A. Spatial and temporal pattern of changes in the number of GAD65-immunoreactive inhibitory terminals in the rat superficial dorsal horn following peripheral nerve injury. Mol Pain 2014;10:57.

[20] Manjarrez E, Rojas-Piloni JG, Jimenez I, Rudomin P. Modulation of synaptic transmission from segmental afferents by spontaneous activity of dorsal horn spinal neurones in the cat. J Physiol 2000;529(Pt 2):445–60.

[21] Moore KA, Kohno T, Karchewski LA, Scholz J, Baba H, Woolf CJ. Partial peripheral nerve injury promotes a selective loss of GABAergic inhibition in the superficial dorsal horn of the spinal cord. J Neurosci 2002;22: 6724–31.

[22] Mosconi T, Kruger L. Fixed-diameter polyethylene cuffs applied to the rat sciatic nerve induce a painful neuropathy: ultrastructural morphometric analysis of axonal alterations. PAIN 1996;64:37–57.

[23] Omori Y, Kagaya K, Enomoto R, Sasaki A, Andoh T, Nojima H, Takahata H, Kuraishi Y. A mouse model of sural nerve injury-induced neuropathy: gabapentin inhibits pain-related behaviors and the hyperactivity of wide-dynamic range neurons in the dorsal horn. J Pharmacol Sci 2009;109: 532–9.

[24] Parr-Brownlie LC, Poloskey SL, Flanagan KK, Eisenhofer G, Bergstrom DA, Walters JR. Dopamine lesion-induced changes in subthalamic nucleus activity are not associated with alterations in firing rate or pattern in layer V neurons of the anterior cingulate cortex in anesthetized rats. Eur J Neurosci 2007;26:1925–39.

[25] Pitcher GM, Henry JL. Nociceptive response to innocuous mechanical stimulation is mediated via myelinated afferents and NK-1 receptor activation in a rat model of neuropathic pain. Exp Neurol 2004;186: 173–97.

[26] Pitcher GM, Henry JL. Governing role of primary afferent drive in increased excitation of spinal nociceptive neurons in a model of sciatic neuropathy. Exp Neurol 2008;214:219–28.

[27] Prescott SA. Synaptic inhibition and disinhibition in the spinal dorsal horn. Prog Mol Biol Transl Sci 2015;131:359–83.

[28] Price TJ, Cervero F, de Koninck Y. Role of cation-chloride-cotransporters (CCC) in pain and hyperalgesia. Curr Top Med Chem 2005;5:547–55.

[29] Price TJ, Cervero F, Gold MS, Hammond DL, Prescott SA. Chloride regulation in the pain pathway. Brain Res Rev 2009;60:149–70.

[30] Saitoh T, Ishida M, Maruyama M, Shinozaki H. A novel antagonist, phenylbenzene omega-phosphono-alpha-amino acid, for strychnine-sensitive glycine receptors in the rat spinal cord. Br J Pharmacol 1994; 113:165–70.

[31] Sandkuhler J. Models and mechanisms of hyperalgesia and allodynia. Physiol Rev 2009;89:707–58.

[32] Sandkuhler J, Eblen-Zajjur AA. Identification and characterization of rhythmic nociceptive and non-nociceptive spinal dorsal horn neurons in the rat. Neuroscience 1994;61:991–1006.

[33] Sharott A, Doig NM, Mallet N, Magill PJ. Relationships between the firing of identified striatal interneurons and spontaneous and driven cortical activities in vivo. J Neurosci 2012;32:13221–36.

[34] Sorkin LS, Puig S. Neuronal model of tactile allodynia produced by spinal strychnine: effects of excitatory amino acid receptor antagonists and a mu-opiate receptor agonist. PAIN 1996;68:283–92.

[35] Sorkin LS, Puig S, Jones DL. Spinal bicuculline produces hypersensitivity of dorsal horn neurons: effects of excitatory amino acid antagonists. PAIN 1998;77:181–90.

[36] Steedman WM, Zachary S. Characteristics of background and evoked discharges of multireceptive neurons in lumbar spinal cord of cat. J Neurophysiol 1990;63:1–15.

[37] Surmeier DJ, Honda CN, Willis WD. Patterns of spontaneous discharge in primate spinothalamic neurons. J Neurophysiol 1989;61:106–15.

[38] Suzuki R, Dickenson AH. Differential pharmacological modulation of the spontaneous stimulus-independent activity in the rat spinal cord following peripheral nerve injury. Exp Neurol 2006;198:72–80.

[39] Takazawa T, MacDermott AB. Synaptic pathways and inhibitory gates in the spinal cord dorsal horn. Ann N Y Acad Sci 2010;1198:153–8.

[40] Todd AJ. Neuronal circuitry for pain processing in the dorsal horn. Nat Rev Neurosci 2010;11:823–36.

[41] West SJ, Bannister K, Dickenson AH, Bennett DL. Circuitry and plasticity of the dorsal horn—toward a better understanding of neuropathic pain. Neuroscience 2015;300:254–75.

[42] Williams ER, Soteropoulos DS, Baker SN. Spinal interneuron circuits reduce approximately 10-Hz movement discontinuities by phase cancellation. Proc Natl Acad Sci U S A 2010;107:11098–103.

[43] Yaksh TL. Behavioral and autonomic correlates of the tactile evoked allodynia produced by spinal glycine inhibition: effects of modulatory receptor systems and excitatory amino acid antagonists. PAIN 1989;37: 111–23.

[44] Yalcin I, Bohren Y, Waltisperger E, Sage-Ciocca D, Yin JC, Freund-Mercier MJ, Barrot M. A time-dependent history of mood disorders in a murine model of neuropathic pain. Biol Psychiatry 2011;70:946–53.

[45] Yalcin I, Megat S, Barthas F, Waltisperger E, Kremer M, Salvat E, Barrot M. The sciatic nerve cuffing model of neuropathic pain in mice. J Vis Exp 2014;89:e51608.

[46] Yezierski RP, Sorkin LS, Willis WD. Response properties of spinal neurons projecting to midbrain or midbrain-thalamus in the monkey. Brain Res 1987;437:165–70.

# Appendix B: Résume de la thèse (prolongé) et résumé grand public

# Résume de la thèse (Prolongé)

## Introduction :

L'Acétylcholine (ACh) endogène est un important modulateur des processus sensoriels nociceptifs dans la moelle épinière. L'administration péridurale de néostigmine (un inhibiteur de l'acétylcholine estérase) empêche la dégradation de l'acétylcholine et de ce fait en augmente la concentration. Cette administration permettant de soulager la douleur est utilisée en clinique, lors des accouchements et dans le cadre post-opératoire (Eisenach, 2009). Il a été démontré que l'effet de certains analgésiques couramment utilisés, tels que la clonidine et la morphine, passe par l'augmentation de la concentration d'ACh (Pan et al., 1999; Chen and Pan, 2001). Chez le rongeur, antagoniser les récepteurs cholinergiques nicotiniques et muscariniques dans la moelle épinière provoque une hyperalgésie et/ou une allodynie, c'est-à-dire respectivement une réaction accrue à une stimulation nociceptive (douloureuse) et/ou une réponse nociceptive à une stimulation habituellement non-nociceptive(Honda et al., 2002; Rashid et al., 2006). Cela suggère l'existence d'un « tonus » basal d'ACh dans la moelle épinière modulant le seuil de réponse aux signaux nociceptifs. De façon intéressante, ce « tonus » est modifié à la suite d'une neuropathie (Rashid and Ueda, 2002). Cependant, les mécanismes précis de la plasticité des systèmes cholinergiques spinaux observée dans le cadre neuropathique ne sont pas encore bien compris.

Bien que les preuves de l'existence du « tonus » cholinergique soient bien documentées, il reste encore des controverses au sujet de la source de l'ACh libérée dans ce contexte. Trois structures possèdent des neurones exprimant la Choline Acétyltransférase (ChAT) et des terminaisons au niveau de la Corne Dorsale de la Moelle Épinière (CDME). Il s'agit des ganglions rachidiens (DRG) (Matsumoto et al., 2007), de la Médulla Ventromédiale Rostrale (RVM) (Stornetta et al., 2013) et enfin, de la moelle épinière. Cette dernière structure possède une source potentielle locale, constituée d'une population d'interneurones située dans la corne dorsale, décrite chez le rat par Barber et ses collaborateurs (Barber et al., 1984).

Cette population éparse d'interneurones cholinergiques a récemment été caractérisée par notre équipe dans la CDME des souris et des primates (Mesnage et al., 2011; Pawlowski et al., 2013). Un plexus dense de fibres cholinergiques a été décrit dans les couches II-III de la moelle épinière (Barber et al., 1984; Olave et al., 2002). Ces fibres ChAT contenant dendrites et axones, forment des synapses et interagissent de manière réciproque avec les terminaisons des afférences somatosensorielles. En effet, les axones cholinergiques réalisent des connections présynaptiques

avec des fibres afférentes primaires de bas seuil et non myélinisées qui en retour, contactent des dendrites cholinergiques (Ribeiro-da-Silva and Cuello, 1990). Ainsi, l'interaction entre les neurones ChAT et les fibres afférentes primaires semble être le substrat le plus probable sous-tendant l'analgésie cholinergique. Ces quelques interneurones ont des corps cellulaires localisés dans les couches LIII et IV. Ils possèdent des territoires dendritiques et axonaux très étendus, orientés dorsalement et participant ainsi au plexus cholinergique (Mesnage et al., 2011). Ces données suggèrent que ces interneurones joueraient un rôle dans la modulation de l'information sensorielle. De ce fait, notre objectif est d'identifier les paramètres qui permettraient à cette population de neurones d'effectuer ce contrôle majeur qui à été constaté sur les processus douloureux, en élucidant les mécanismes d'interactions entre les interneurones cholinergiques de la corne dorsale et le réseau nociceptif avoisinant.

## Méthodes et Résultats :

**Résultats 1 : Plasticity of the spinal cholinergic tone after neuropathy**

Nous avons évalué le rôle de la modulation cholinergique spinale sur la transmission nociceptive mécanique chez des souris Cd1 naïves et neuropathiques. Pour induire une douleur neuropathique chez la souris, nous avons utilisé le model du « cuff » (Benbouzid et al., 2008). Le seuil mécanique de retrait des pates arrières a été déterminé grâce à l'utilisation de filaments de von Frey. Après l'établissement des seuils de base, des injections intrathécales ont étés réalisées, suivies de tests de von Frey exécutés à des temps fixes après injection.

Chez les animaux naïfs, nous avons confirmé la présence d'un « tonus » cholinergique endogène et spinal modulant les seuils nociceptifs mécaniques, impliquant les récepteurs nicotiniques (nAChR) et muscariniques (mAChR). Suite à la neuropathie, le « tonus » cholinergique est altéré, et agit la aussi à travers les nAChRs et les mAChRs. Enfin, pour contrôler la spécificité de la dose la plus élevée de mécamylamine (antagoniste des nAChR) utilisée, nous avons confirmé que chez des souris transgéniques chez lesquelles la sous unité $\beta_2$ nicotinique est absente cet antagoniste n'avait pas d'effet.

Dans un contexte in vivo, le taux de décharge des neurones de la CDME à été enregistré en réponse à des stimulations de type non-nociceptives (toucher) et nociceptives (pincement). En présence d'antagonistes des AChRs nicotiniques et muscariniques, la réponse des neurones de la CDME était augmentée pour les deux types de stimulations, dans les animaux sham et naïfs. Chez les souris cuff par contre, les réponses aux deux types de stimulations n'étaient plus modifiées par des

antagonistes des AChRs, à l'exception des réponses au toucher lors de l'application des antagonistes des nAChRs. Ainsi, nous avons mis en évidence la présence d'un "tonus" cholinergique impliquant les nAChRs et mAChRs chez les sham et naifs qui subit des changements à la suite de neuropathie. De façon intéressante, l'action de ce système cholinergique sur les sensations du toucher et de pincement est sous contrôle d'autres "tonus" inhibiteurs (GABAergiques ou glycinergiques) dans les conditions naives, sham et cuff.

Pour clarifier la contribution des populations cholinergiques des DRG, de la RVM et de la moelle épinière dans le « tonus » cholinergique spinal impliqué dans la transmission nociceptive mécanique, nous avons utilisé l'approche du DREADD (Designer Receptor Exclusively Activated by Designer Drugs). Pour cela, nous avons effectué des injections de virus recombinant adéno associé (rAAV) codant pour une construction cre-dépendante dans des souris ChAT::Cre. Cela a permis l'infection des neurones cholinergiques au niveau spinal L3-L4, dans la RVM et, grâce à des injections dans les pattes arrières de souriceaux, dans les ganglions rachidiens. Trois semaines après une telle infection, les neurones exprimaient le récepteur hDMi4, que nous avons activé par l'injection de son agoniste, la clozapine-N-oxide, en i.p.. Nous avons ensuite réalisé les tests de von Frey afin d'évaluer un changement comportemental suite à l'inhibition de différentes populations cholinergiques infectées.

## Résultats 2: Dorsal horn cholinergic interneurons: the dual language of a minority population

Nous avons cherché à élucider la nature des contacts reçus par les interneurones cholinergiques d'intérêt provenant du réseau de la corne dorsale, mais aussi de la périphérie. Pour cela, nous sommes passés par une approche in vitro. En effet, nous avons réalisé des tranches aigues de moelle épinière de souris transgéniques exprimant la protéine fluorescente EGFP (enhanced Green Fluorescent Protein) uniquement dans les neurones cholinergiques. Nous avons alors enregistré ces neurones fluorescents par la technique du Patch-Clamp en configuration cellule entière afin d'analyser les courants spontanés post-synaptiques excitateurs (sCPSE) et inhibiteurs (sCPSI) qu'ils reçoivent, et ceci sur des tranches de trois orientations différentes (horizontales, parasagitales et transverses).

Chez les animaux naïfs, nos données suggèrent que les interneurones cholinergiques de la corne dorsale spinale reçoivent sCPSE et sCPSI. Il semblerait qu'ils reçoivent des sCPSE à une fréquence plus basse sur des tranches transversales en comparaison des deux autres types de tranches. De ce fait, il se pourrait que la source des informations excitatrices reçues par cette population soit

localisée sur des segments plus distants. De façon intéressante, nous avons constaté une fréquence plus faible de sCPSI dans nos neurones d'intérêts par rapport aux neurones Non-ChAT, toutes tranches confondues. Afin d'étudier plus en détail la localisation des cellules présynaptique aux neurones ChAT, nous avons réalisé des enregistrements en présence de tetrodotoxine (TTX). Cette drogue a pour effet de bloquer l'initialisation et la propagation des potentiels d'action, par conséquent, cela nous à permis de détecter des courants post-synaptiques miniatures excitateurs (mCPSE) et inhibiteurs (mCPSI). Cependant, nous n'avons pas pu en conclure la localisation des neurones présynaptiques car il n'y avait pas de différence significative dans la fréquence de mCPSE (ou mCPSI) en fonction des différentes orientations de tranches.

Dans la mesure où les courants excitateurs et inhibiteurs étaient enregistrés dans les mêmes cellules, nous avons décidé d'analyser le ratio de fréquence des CPSE/CPSI pour les neurones ChAT::EGFP et Non-ChAT. Ce ratio était plus élevé chez les neurones cholinergiques de la CDME, suggérant que les entrées inhibitrices étaient plus basses comparées aux entrées excitatrices.

Afin d'étudier les proprieties membranaires passives des neurones (résistance d'entrée, potentiel de repos, amplitude du "sag"), et leur patron de décharge, nous avons appliqué des sauts de courant dépolarisants et hyperpolarisants. Nous n'avons pas observé de différences dans les patrons de décharge et la plupart des propriétés membranaires passives entre neurones ChAT::EGFP et non-ChAT. Toutefois, les neurones cholinergiques avaient une capacité membranaire plus grande dans les tranches horizontales par rapport aux tranches parasagittales ou transverses. Cela peut être dû à la grande étendue de l'arbre axo-dendritique de ces neurones dans l'axe rostro-caudal, mieux conservé dans les tranches horizontales que dans les autres. De plus, la présence de potentiel d'action rebond à la fin d'un saut hyperpolarisant semble être une caractéristique des neurones ChAT::EGFP chez les animaux naïfs.

Pour mieux comprendre l'identité des afférences reçues par les interneurones cholinergiques, nous avons utilisé une approche pharmacologique dans le but d'activer les fibres qui les contactent. Nous avons donc appliqué, sur des tranches horizontales, un bain de Capsaïcine, agoniste des récepteurs TRPV1 que l'on retrouve sur certaines des fibres nociceptives. Cette drogue a eu pour effet d'augmenter la fréquence des sCPSE ainsi que des sCPSI enregistrés dans la population qui nous intéresse. En vue de localiser les récepteurs TRPV1, nous avons testé l'effet de la capsaïcine en présence de TTX. Nous n'avons pas observé de changement de la fréquence des mCPSE dans ces conditions, ce qui a permis de conclure que nos interneurones reçoivent uniquement des contacts indirects provenant des fibres afférentes primaires sensibles à la capsaïcine. Par contre, le menthol,

agoniste du récepteur TRPM8 et l'huile de moutarde, agoniste du récepteur TRPA1, n'ont pas altéré les fréquences des sCPSE ou sCPSI au niveau des cellules ChAT. Ces données suggèrent que ces interneurones ne reçoivent pas de contacts provenant des fibres afférentes primaires exprimant TRPA1 ou TRPM8. Nous avons également étudié les afférences périphériques des neurones cholinergiques en stimulant électriquement les racines dorsales sur des tranches de moelle épinière. Nous avons démontré que les interneurones cholinergiques étaient en aval des fibres afférentes via un réseau d'interneurones excitateurs et inhibiteurs. Le seuil de stimulation de ces réponses implique que des fibres de bas seuil et de haut seuil sont en amont des interneurones cholinergiques. Une analyse plus approfondie devrait permettre de déterminer la connectivité exacte (mono- ou poly-synaptique) et la nature (A-beta; A-delta ou C) de ces fibres.

Afin d'étudier le réseau en aval des interneurones cholinergiques, nous avons injecté un rAAV exprimant la Lectine du blé ou Wheat Germ Agglutinin (WGA) dans des souris ChAT::Cre. Cette lectine permet un marquage trans-synaptique antérograde, et permet ainsi d'identifier les cibles post- synaptiques des neurones infectés, et de cette manière d'obtenir des informations sur leur localisation et leurs propriétés neurochimiques.

**Résultats 3: Characterization of the DH cholinergic interneurons following peripheral nerve injury**

Dans les neurones de la laminae II, nous avons observé une réduction au niveau de la fréquence des mCPSI chez les animaux « Cuff » par rapport aux animaux « Sham », ce qui nous à permis de vérifier que notre modèle « Cuff » présentait des changements électrophysiologiques similaires à ceux observés dans les autres modèles établis de neuropathie.

Dans des conditions de neuropathie, nous avons tenté d'élucider les changements plastiques qui ont lieu au niveau des interneurones cholinergiques. Le nombre de cellules cholinergiques observé dans les souris ChAT::EGFP ne diffère pas entre les conditions « Sham » et « Cuff ».

Après comparaison des données recueillies concernant les profils de décharge, les propriétés passives des membranes et courants entrant des animaux naïfs, sham et cuff, nous avons constaté que plusieurs profils de décharge et propriétés passives sont resté inchangés à la suite d'une lésion nerveuse périphérique. De façon surprenante, nous avons noté que la proportion des cellules non ChAT présentant un potentiel d'action "rebond" augmente dans les groupes sham et cuff. Au sujet des afférences de la corne dorsale, nous avons là aussi étudié les fréquences de courants spontanés et miniatures excitateurs et inhibiteurs des neurones ChAT dans les orientations horizontales et

transverses, mais n'avons constaté aucune différence entre les deux conditions. En conclusion, nous n'avons observé aucune différence au niveau des courants entrants des neurones des laminae III et IV, dans les conditions sham et cuff.

## Conclusions :

Notre étude apporte une nouvelle vision du système cholinergique spinal. Nous avons démontré que le « tonus » cholinergique endogène de la moelle épinière a pour rôle de définir un seuil nociceptif mécanique dans les conditions normales et dans les conditions neuropathiques. Nous poursuivons actuellement notre investigation de la contribution des différentes sources cholinergiques dans la modulation des informations nociceptives mécaniques.

Les interneurones cholinergiques sont bien intégrés dans le réseau de la corne dorsale, et reçoivent des informations excitatrices et inhibitrices provenant vraisemblablement d'autres segments spinaux. De surcroît, cette population reçoit des messages indirects provenant de fibres afférentes primaires exprimant le récepteur TRPV1. En outre, de toute les propriétés membranaires passives mesurées, nous avons observé que les neurones cholinergiques ont une large capacitance. Cette notion est renforcée par leur morphologie comportant de larges prolongements axonaux et dendritiques.

Dans des conditions neuropathiques, la quantité d'interneurones cholinergiques et les courants spontanés qu'ils reçoivent semblent inchangés. De plus, nous avons montré que les propriétés actives et passives des membranes des neurones ChAT n'ont pas changé à la suite d'une lésion. Une meilleure compréhension du système cholinergique spinal pourrait ouvrir une voie vers des alternatives dans les traitements de la douleur.

# Bibliographie

Barber RP, Phelps PE, Houser CR, Crawford GD, Salvaterra PM, Vaughn JE (1984) The morphology and distribution of neurons containing choline-acetyltransferase in the adult-rat spinal-cord - an immunocytochemical study. J Comp Neurol 229:329-346.

Benbouzid M, Choucair-Jaafar N, Yalcin I, Waltisperger E, Muller A, Freund-Mercier MJ, Barrot M (2008) Chronic, but not acute, tricyclic antidepressant treatment alleviates neuropathic allodynia after sciatic nerve cuffing in mice. European Journal of Pain 12:1008-1017.

Chen SR, Pan HL (2001) Spinal endogenous acetylcholine contributes to the analgesic effect of systemic morphine in rats. Anesthesiology 95:525-530.

Eisenach JC (2009) Epidural Neostigmine: Will It Replace Lipid Soluble Opioids for Postoperative and Labor Analgesia? Anesth Analg 109:293-295.

Honda K, Koga K, Moriyama T, Koguchi M, Takano Y, Kamiya H (2002) Intrathecal alpha(2) adrenoceptor agonist clonidine inhibits mechanical transmission in mouse spinal cord via activation of muscarinic M-1 receptors. Neurosci Lett 322:161-164.

Matsumoto M, Xie WJ, Inoue M, Ueda H (2007) Evidence for the tonic inhibition of spinal pain by nicotinic cholinergic transmission through primary afferents. Mol Pain 3:41.

Mesnage B, Gaillard S, Godin AG, Rodeau JL, Hammer M, Von Engelhardt J, Wiseman PW, De Koninck Y, Schlichter R, Cordero-Erausquin M (2011) Morphological and Functional Characterization of Cholinergic Interneurons in the Dorsal Horn of the Mouse Spinal Cord. J Comp Neurol 519:3139-3158.

Olave MJ, Puri N, Kerr R, Maxwell DJ (2002) Myelinated and unmyelinated primary afferent axons form contacts with cholinergic interneurons in the spinal dorsal horn. Exp Brain Res 145:448-456.

Pan HL, Chen SR, Eisenach JC (1999) Intrathecal clonidine alleviates allodynia in neuropathic rats - Interaction with spinal muscarinic and nicotinic receptors. Anesthesiology 90:509-514.

Pawlowski SA, Gaillard S, Ghorayeb I, Ribeiro-da-Silva A, Schlichter R, Cordero-Erausquin M (2013) A Novel Population of Cholinergic Neurons in the Macaque Spinal Dorsal Horn of Potential Clinical Relevance for Pain Therapy. Journal of Neuroscience 33:3727-+.

Rashid MH, Ueda H (2002) Neuropathy-specitic analgesic action of intrathecal nicotinic agonists and its spinal GABA-mediated mechanism. Brain Res 953:53-62.

Rashid MH, Furue H, Yoshimura M, Ueda H (2006) Tonic inhibitory role of alpha 4 beta 2 subtype of nicotinic acetylcholine receptors on nociceptive transmission in the spinal cord in mice. Pain 125:125-135.

Ribeiro-da-Silva A, Cuello AC (1990) Choline acetyltransferase-immunoreactive profiles are presynaptic to primary sensory fibers in the rat superficial dorsal horn. J Comp Neurol 295:370-384.

Stornetta RL, Macon CJ, Nguyen TM, Coates MB, Guyenet PG (2013) Cholinergic neurons in the mouse rostral ventrolateral medulla target sensory afferent areas. Brain Structure & Function 218:455-475.

# Résumé Grand Public

L'objectif général du projet est d'identifier de nouvelles cibles thérapeutiques pour le traitement de la douleur. Pour ce faire, nous nous intéressons à une population de neurones présents dans la moelle épinière, qui ont la particularité de moduler les influx nerveux signalant la douleur.

Nous travaillons sur la moelle épinière car c'est par là que l'information douloureuse transite (et est intégrée) avant d'être relayée vers le cerveau. Les neurones qui nous intéressent sont ceux qui libèrent un neurotransmetteur appelé acétylcholine (ACh). Des expériences précédentes ont montré que ces neurones sont également impliqués dans les effets d'analgésiques utilises en clinique tels que la morphine et la clonidine. Nous avons récemment démontré que cette population de neurones, qu'on appelle « cholinergiques », se retrouvait aussi dans la moelle épinière des singes macaques, avec une densité similaire à celle observée chez la souris, ce qui valide notre modelé murin. Ces neurones sont la source probable d'ACh impliquée dans les propriétés d'analgésiques utilisés en clinique en injection péridurale (les inhibiteurs d'acétylcholinestérase).

Nous étudions le mécanisme d'action analgésique de l'ACh spinale, grâce à des expériences de comportement, et des enregistrements électrophysiologiques in vitro et in vivo. Nous utilisons également un modele de douleur neuropathique afin d'étudier la plasticité du système cholinergique dans cette situation, et les possibilités de le stimuler pour soulager les douleurs. Allant au de delà de l'amélioration de notre compréhension de l'analgésie cholinergique, notre projet contribue à l'élucidation d'une partie de la micro-circuiterie neuronale de la moelle épinière, et apporte une nouvelle lumière sur le mode d'action d'analgésiques classiques. Notre étude contribue ainsi à l'identification de nouvelles cibles thérapeutiques pour le traitement de la douleur chronique.

# Dhanasak DHANASOBHON
# Spinal cholinergic system and chronic pain

UNIVERSITÉ DE STRASBOURG

École Doctorale
des Sciences de la Vie
et de la Santé
STRASBOURG

## Résumé

Chez les rongeurs et humains, un « tonus » cholinergique spinal endogène modulant les comportements nociceptifs (douloureux) a été décrit. Une source potentielle de cette acétylcholine sont les interneurones cholinergiques de la corne dorsale (CD) de la moelle épinière. Nos objectifs étaient les suivants : (1) caractériser le « tonus » cholinergique spinal responsable de l'établissement des seuils mécaniques nociceptifs et (2) élucider le rôle des neurones cholinergiques CD dans la modulation de l'information sensorielle chez des animaux naïfs et neuropathiques. Nous avons confirmé la présence d'un « tonus » cholinergique qui module les seuils mécaniques et démontré qu'il est encore présent, bien qu'il soit modifié, après une neuropathie. Les interneurones cholinergiques reçoivent des entrées excitatrices localisées sur des segments plus distants et reçoivent généralement une faible fréquence d'entrées inhibitrices. De plus, ils sont indirectement reliés par des afférences primaires nociceptives qui expriment TRPV1, ce qui démontre leur implication dans le circuit nociceptif. Dans les conditions neuropathiques, les entrées des neurones LIII / IV ne sont pas affectées après une lésion du nerf périphérique. Une meilleure compréhension du système cholinergique spinal peut ouvrir la voie à une thérapie alternative contre la douleur.

Mot clés : Moelle épinière ; Corne Dorsale ; Neuropathique ; Douleur chronique ; Acétylcholine ; Seuils mécanique ; transmission synaptique

## Résumé en anglais

An endogenous spinal cholinergic tone modulating nociceptive (pain-like) behaviors has been demonstrated in rodents and humans. One potential source of this acetylcholine is the spinal Dorsal Horn (DH) cholinergic interneurons. Our objectives were to: (1) characterize the spinal cholinergic tone establishing mechanical nociceptive thresholds and (2) to elucidate the role of DH cholinergic neurons in the modulation of sensory information of naïve and neuropathic animals. We have confirmed the presence of a cholinergic tone modulating mechanical thresholds and demonstrated that it is still present, although altered, after neuropathy. The DH cholinergic interneurons receive excitatory inputs from distant spinal segments and generally receive lower inhibitory inputs. In addition, they are indirectly connected by a subset of nociceptive primary afferents expressing TRPV1, demonstrating their involvement in nociceptive processing. In neuropathic spinal circuits, the inputs to LIII/IV neurons appears to be unaffected after injury. Better understanding the spinal cholinergic system can pave way to alternative pain therapy.

Key words: Spinal cord; Dorsal Horn; Neuropathy; Chronic pain; Acetylcholine; Mechanical thresholds; synaptic transmission